UNIVERSITA' DELLA CALABRIA

Dipartimento di Farmacia e Scienze della Salute e della Nutrizione

Dottorato di Ricerca in

Biochimica Cellulare ed Attività dei Farmaci in Oncologia

Con il contributo di FSE-Regione Calabria

CICLO XXVIII

The Role of Intrinsic and Extrinsic Signals in the Regulation of Breast Cancer Stem Cell Activity

Settore Scientifico Disciplinare MED/05

Coordinatore: Ch.mo Prof. **Diego Sisci**

Tutor: Ch.ma Prof.ssa **Stefania Catalano**

Dottorando: Dott.ssa **Francesca Chemi**

"La presente tesi è cofinanziata con il sostegno della Commissione Europea, Fondo Sociale Europeo e della Regione Calabria. L'autore è il solo responsabile di questa tesi e la Commissione Europea e la Regione Calabria declinano ogni responsabilità sull'uso che potrà essere fatto delle informazioni in essa contenute".

Table of Contents

Introduction

Breast cancer is the most common malignancy and the leading cause of cancer-related death in women worldwide (Jemal A. *et al*., **2010**). Approximately 75% of primary breast cancers are estrogen receptor (ER) positive and endocrine therapies such as selective estrogen receptor (ER) modulators (SERMs; e.g., tamoxifen), selective ER downregulators (SERDs; e.g., fulvestrant), and the aromatase inhibitors are the standard treatment options for estrogen receptor-positive breast cancer patients. However, the effectiveness of these agents is limited by the development of the novo or acquired resistance that limits the success of this therapeutic strategy. Indeed, resistance to hormonal therapy is seen in 50%–60% of early breast cancer (BC) cases and develops in almost all patients with advanced disease (Davies C *et al*., **2011**; Palmieri C *et al*., **2014**).

In the last years, several studies have been supported the hypothesis that cancers are maintained and re-populated by stem-like cells within the tumor, termed cancer stem cells (CSCs). CSCs, first identified in Al-Hajj work using cells isolated from pleural effusions and primary tumors of breast cancer patients (Al-Hajj M *et al*., **2003**), were characterized on the basis of their expression profile of specific cell surface markers, including EpCAM+, CD24- and CD44+, and by their ability to undergo self-renewal, a process that drives tumorigenesis, or to differentiate into the non-self-renewing cells forming the tumor bulk (Visvader JE *et al*., **2008**) (Figure 1).

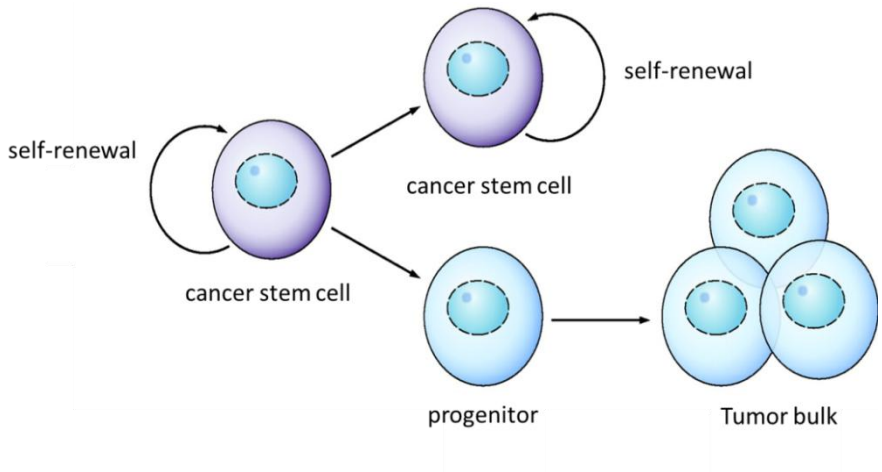

Figure 1: The cancer stem cell model. Cancer stem cells retain the ability to self-renew and are able to produce daughter cells, through multiple asymmetric cell divisions, that may form the tumor bulk.

From a clinical point of view, the main concern with CSCs is related to their ability to evade the effects of conventional therapies (e.g. endocrine, chemo- and radiotherapy), and thereby repopulate the tumour following treatment (Li X *et al*., **2008**; Phillips TM *et al*., **2006**; Kakarala M *et al*., **2008**).

Similar to embryonic and somatic stem cells, the self-renewal and differentiation of CSCs are regulated by both intrinsic and extrinsic pathways whose dysregulation may be a key event initiating carcinogenesis. Among the intrinsic pathways, an important role is displayed by developmental signals such as Wnt, Hedgehog, Janus kinase 2-signal transducer and activator of transcription 3 (JAK2-STAT3) and Notch pathways that are frequently deranged in cancers (Liu S *et al*., **2005**) (Figure 2).

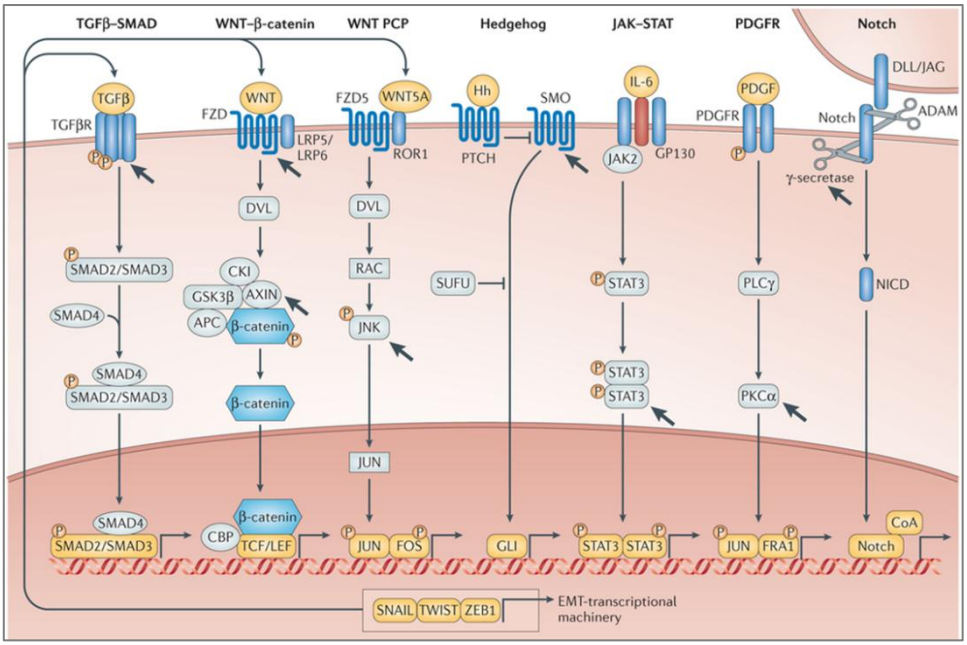

Figure 2*: *Intrinsic signals regulating cancer stem cells. Cancer stem cells, like the normal stem cells, are finely regulated by the classical embryonic signals shown in the figure.

In particular, it has been shown that aberrant Notch activation transforms normal breast cells, is found in pre-invasive and invasive human BCs, and correlates with early recurrence (Stylianou S *et al*., **2006**; Farnie G *et al*., **2007**). Moreover, Harrison et al. reported that, inhibition of Notch signaling, particularly NOTCH4 receptor, reduced breast CSC activity (BCSC) (Harrison H *et al*., **2010**).

CSCs also rely on a specific tumor microenvironment, termed as cancer stem niche, that provides paracrine and juxtacrine signals for maintaining CSC properties.

The cancer stem niche contains a number of cell types, including mesenchymal stem cells (MSCs), cancer-associated fibroblasts (CAFs), adipocytes, endothelial and immune cells, all of which, through networks of cytokines and growth factors, have been shown to influence tumor growth and metastasis (Korkaya H. *et al*., **2011**) (Figure 3).

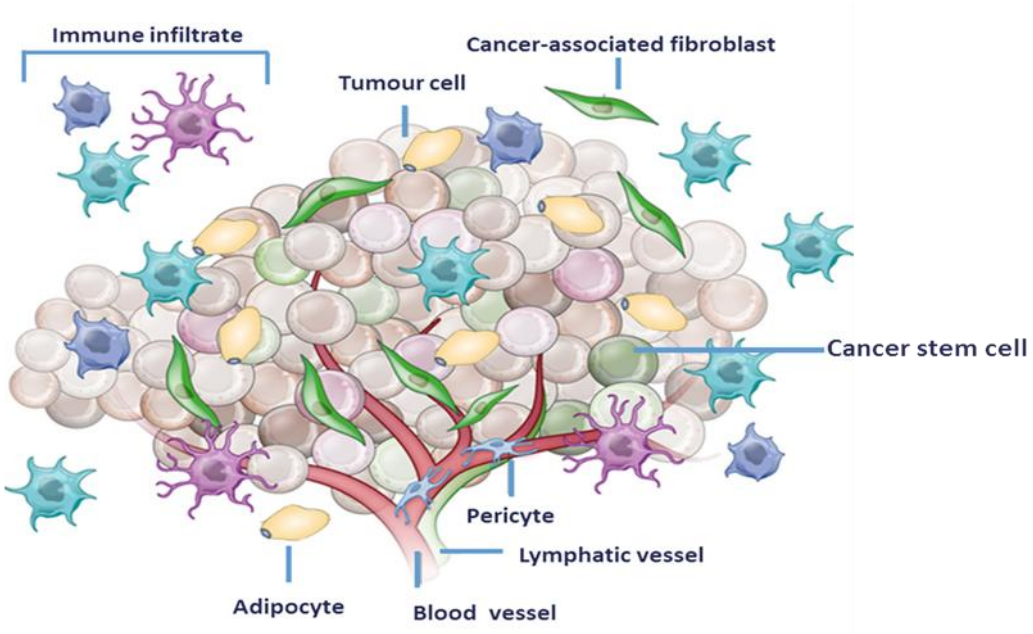

Figure 3: Schematic representation of tumor microenvironment.

Adipocytes and CAFs are the major components in breast cancer microenvironment, and along with their secreted factors represent key players in stroma-epithelial cell interactions. As an important paracrine mediator, the adipocyte-derived cytokine leptin, that we have recently demonstrated to be also secreted by CAFs (Barone I *et al*., **2012**), has been correlated with breast cancer occurrence. Leptin exerts its biologic function through binding to its receptor (OBR) which activates multiple downstream signaling pathways such as those involving JAK2-STAT3, mitogen-activated protein kinase (MAPK), and phosphatidylinositol 3-kinase/protein kinase B (PI3K/AKT)(Cirillo D *et al*., **2008**) (Figure 4). Leptin and both short and long OBR isoforms are overexpressed in breast cancer, especially in higher grade tumors and are associated with distant metastases (Ishikawa M *et al*., **2004**; Miyoshi Y *et al*., **2006**).

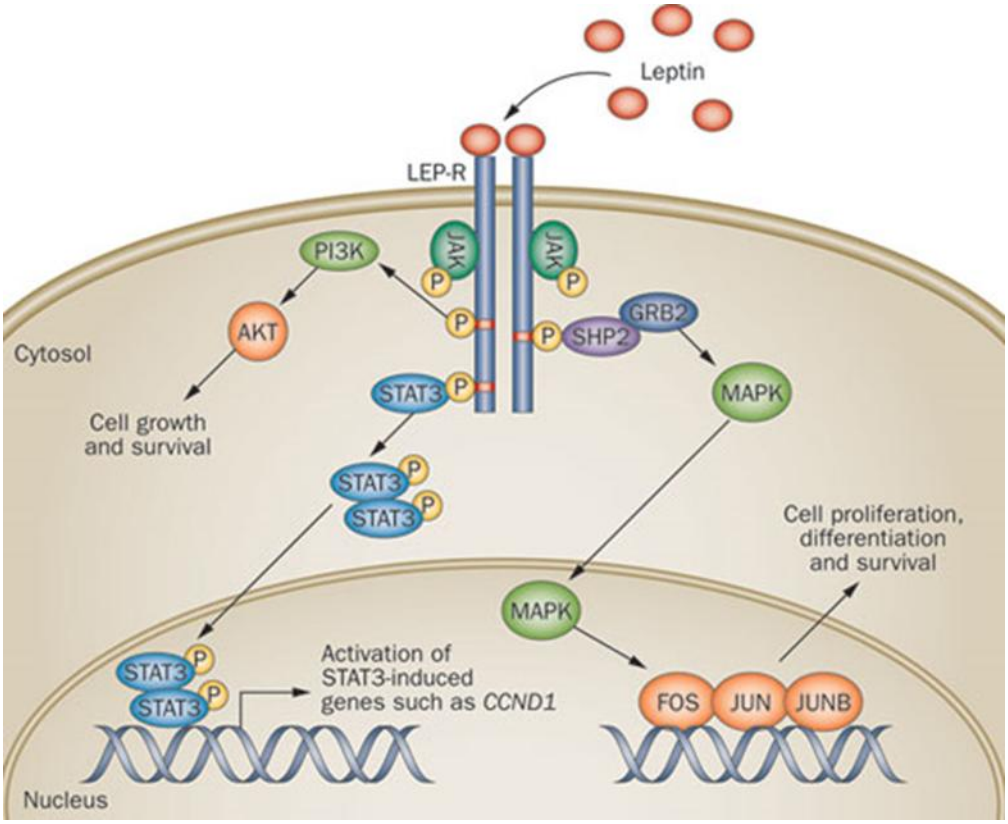

Figure 4: Leptin signaling. Binding of leptin to its receptor, LEP-R, results in the activation of its downstream pathways such as JAK2-STAT3, mitogen-activated protein kinase (MAPK), and phosphatidylinositol 3-kinase/protein kinase B (PI3K/AKT).

It has been extensively demonstrated using both *in vitro* and *in vivo* experimental models, that leptin modulates many aspects of breast cancer biology: e.g., increases cell proliferation and transformation, induces the expression of several cell cycle modulators, exerts anti-apoptotic effects, reduces efficacy of breast cancer treatment, influences cancer initiation processes (Table 1). Moreover, leptin is able to shape the tumor microenvironment within the mammary gland by inducing multiple concurrent events: potentiated migration of endothelial cells, promotion of angiogenesis and sustained recruitment of macrophages and monocytes (Andò S *et al*., **2014**; Saxena NK *et al*., **2013**; Newman G *et al*., **2014**).

Experimental Models	Findings	References
In vitro		
MCF-7, T47D, ZR75-1 MDA-B-361, SKBR3 MDA-MB-231	Increased cell proliferation and transformation	Barone, et al. 2012, Catalano, et al. 2003, Catalano, et al. 2011, Dieudonne, et al. 2002, Garofalo, et al. 2004, Giordano, et al. 2013, Hu, et al. 2002, Laud, et al. 2002, Okumura, et al. 2002, Ray, et al. 2007, Saxena, et al. 2007, Soma, et al. 2008, Somasundar, et al. 2003, Yin, et al. 2004.
MCF-7, T47D, ZR75-1	Up-regulation of cdk2, cyclin D1, hyperphosphorylation of pRb, activation of estrogen receptor, induced expression of c-myc	Catalano, et al. 2004, Chen, et al. 2006, Garofalo, et al. 2004, Hu, et al. 2002, Mauro, et al. 2007, Okumura, et al. 2002, Saxena, et al. 2007, Yin, et al. 2004.
MCF-7, ZR75-1	Anti-apoptotic effect	Chen, et al. 2006; Jiang et al. 2008; Perera et al. 2008.
MCF-7	Reduced efficacy of breast cancer treatment	Garofalo ,et al. 2004, Giordano, et al. 2013.
In vivo		
Obese Zucker rats	Small percentage of carcinoma developed in obese compared with lean rats	Lee, et al. 2001.
MMTV/TGF-a $Lep^{ob/ob}$ MMTV/TGF-a $Lep^{db/db}$	No transgene-induced mammary tumors development	Cleary, et al. 2003, Cleary, et al. 2004.
MMTV/PyMT-a $db/db^{NSE/NSE}$	Reduced mammary tumor growth and progression. Enhanced mitochondrial β-oxidation.	Park, et al. 2010.
Clinical Studies		
Breast Cancer	Overexpression of Leptin and its receptor in breast cancer and its association with distant metastasis and poor prognosis	Garofalo, et al. 2006, Ishikawa et al. 2004; Jordè et al. 2008, Miyoshi et al. 2006; Revillon at al. 2006.

Table 1. ***Overview of current knowledge about the involvement of leptin in the pathogenesis and progression of breast cancer***.

Recent studies have also reported that leptin signaling may be involved in the promotion of CSC phenotype. In particular, it has been reported that leptin is able to regulate several signaling pathways and oncogenes, such as HER2, and AKT as well as transcription factors, such as STAT3 and NF-kB, that it is known are implicated in BCSCs (Guo S *et al*., **2012**). In addition, leptin also activates the Notch signaling pathway (Guo S *et al*., **2011**; Knight BB *et al*., **2011**) and induces the expression of CD44 and ALDH1 which have been found to be important mediators of BCSCs biology. Interestingly, Zheng et al. have reported a decreased tumor outgrowth and a functional depletion of BCSCs in obese leptin-deficient mice transplanted with murine mammary tumor virus (MMTV)-Wnt-1 tumor cells, showing that leptin signaling plays an important role in tumor cell growth and stem-cell survival (Zheng Q *et al*., **2011**). More recently, it has been shown that the leptin receptor is necessary for maintaining CSC-like and metastatic properties in triple-negative breast cancer cells (Zheng Q *et al*., **2013**) , and that inhibition of STAT3 suppresses leptin-induced CSCs and cancer progression in diet-induced obese rats (Chang CC *et al*., **2015**).

On the basis of the above observations, the aims of the current study were:

1. ***To evaluate the role of leptin, as a mediator of the tumor-stroma interaction, in regulating BCSC activity using breast cancer cell lines and patient-derived breast cancer cells isolated from metastatic ascites and pleural effusions.*** Particularly, we investigated: *i*) the impact of CAFs and adipocytes isolated from stromal breast tissues on mammosphere formation and self-renewal in breast cancer cells; *ii*) the specific role of leptin and its receptor in influencing BCSC phenotype in the context of the tumor microenvironment; *iii*) the effect of inhibiting leptin signaling as potential therapeutic target to reduce BCSC activity in *in vitro* and *ex vivo* models.
2. ***To investigate the role of NOTCH4 signaling in breast cancer stem cell activity induced by Tamoxifen and Fulvestrant treatments.*** In particular, we evaluated: *i)* the effect of the anti-estrogen Tamoxifen and Fulvestrant on BCSC activity using patient-derived ER+ tumor cells and early and metastatic ER+ patients derived xenografts (PDX); *ii*) the expression and activity of Notch4 signaling in breast cancer cell lines and BC PDX tumors; *iii*) the effects of anti-estrogens administered in the presence of the gamma-secretase inhibitor (GSI) RO4929097, which targets NOTCH4 signaling, on BCSC activity in ER+ PDX tumors.

Materials and Methods

Cell culture

Human MCF-7, MDA-MB-231, T47D and ZR-75-1 breast cancer epithelial cells were authenticated, cultured according to supplier's instructions, and used within 4 months after frozen aliquots recovery. Breast subcutaneous human female preadipocytes (Lot. #:BR071812B; BR070810) were from Zen-Bio. Adipocytes, obtained following differentiation procedure, were routinely maintained in Adipocyte maintenance medium (Zen-Bio). Every 4 months, cells were authenticated by single tandem repeat analysis at our Sequencing Core; morphology, doubling times, estrogen sensitivity, and mycoplasma negativity were tested (MycoAlert, Lonza).

MCF-7, T47D and ZR-75-1 cells were treated for 6 days with ethanol (control), 10^{-6}M 4-OH-tamoxifen or 10^{-7}M fulvestrant.

MCF7 Tamoxifen- and Fulvestrant-resistant cell lines were generated by Dr Julia Gee (University of Cardiff, Wales) and were cultured in phenol red-free DMEM/F12 media with LGlutamine (Gibco) supplemented with 5% charcoal stripped serum and in the presence of 10^{-7}M 4-OH-tamoxifen or 10^{-7}M fulvestrant, respectively . MCF7 resistant cell lines were authenticated by comparative karyotyping to ATCC derived MCF7.

Cancer Associated Fibroblast (CAF) isolation

Human breast cancer specimens were collected in 2011 from primary tumors of patients who signed informed consent. Following tumor excision, small pieces were digested (500 IU collagenase in Hank's balanced salt solution; Sigma; 37C for 2 hours). After differential centrifugation (90 g for 2 minutes), the supernatant containing CAFs was centrifuged (500 g for 8 minutes), resuspended, and cultured in RPMI-1640 medium supplemented with 15% FBS and antibiotics. CAFs between 4 and 10 passages were used, tested by mycoplasma presence, and authenticated by morphology and expression of fibroblast activation protein (FAP), Vimentin and α-smooth muscle actin (α-SMA).

Immunofluorescence

Cells were fixed with 4% paraformaldehyde, permeabilized with PBS 0.2% Triton X-100 followed by blocking with 5% bovine serum albumin (1 hour at room temperature), and incubated with anti-α-SMA (Sigma) and anti-ER-α (Santa Cruz) (4C, overnight) and with fluorescein isothiocyanate–conjugated secondary antibody (30 minutes at room temperature). IgG primary antibody was used as negative control. 40, 6-Diamidino-2-phenylindole (DAPI; Sigma) staining was used for nuclei detection. Fluorescence was photographed with OLYMPUS BX51 microscope, 20X objective.

Conditioned medium (CM) and Leptin-immunodepleted CM

CAFs and Adipocytes were incubated with regular full media (48–72 hours). Conditioned media were collected, centrifuged to remove cellular debris, and used in respective experiments. Protein G-agarose (Santa Cruz) beads were incubated with anti-leptin (Santa Cruz) or IgG antibodies. Antibody–beads complexes were incubated with CAF and Adipocytes conditioned media and centrifuged. Leptin immunodepletion was verified by ELISA (LDN).

Patient-derived Samples

Early BC samples were collected in RPMI (GIBCO), dissected into 1- to 2-mm^3 cubes and digested with the Human Tumor Dissociation Kit (Miltenyi Biotec) for 2 hr at 37°C. Digested tissue was filtered sequentially through 100- and 40-mmcell strainers, then centrifuged at 300 g for 5 min and washed in PBS.

Pleural effusion and ascites samples were obtained from patients with metastatic breast cancer undergoing palliative drainage at The Christie Hospital NHS Foundation Trust Manchester (UK). Metastatic breast sample details in Table 1. Ascites and pleural effusions were centrifuged at 1000 g for 10 min at 4°C and suspended in PBS. Erythrocytes and leucocytes were removed by centrifugation through Lymphoprep solution (Axis Shield), followed by removal of CD45-positive cells using anti-CD45 magnetic beads (Miltenyi Biotec). Single cell suspension of breast cancer epithelial cells was then used to perform mammosphere assay.

Mammosphere culture

MCF-7 and MDA-MB-231 monolayer cells were enzymatically and manually disaggregated to obtain single-cells suspension. Single cells were plated in ultralow attachment plates (Corning) at a density of 500 cells/cm2 in a serum-free Human mammary epithelial cell growth medium (HUMEC), supplemented with B27, 20ng/mL human epidermal growth factor (EGF), 4µg/mL heparin, 5µg/ml insulin, 1ng/ml hydrocortisone, 1mg/ml penicillin-streptomycin and 0,25µg/ml amphotericin B (Life Technologies). Growth factors and treatments (leptin, Life Technologies; AG490 Sigma; PD98059/LY294002 Calbiochem) were added to the mammosphere cultures every 3 days. After 7 days mammospheres >50µm (primary mammospheres-M1) were counted using a microscope (x40 magnification), collected, enzymatically dissociated, plated at the same seeding density used in the primary generation to obtain secondary mammospheres-M2. Mammospheres forming efficiency (MFE) was calculated as number of mammospheres per well/number of cells seeded per well and reported as fold versus control.

Flow cytometry

Mammospheres were dispersed to obtain single-cell suspension. Cells were washed in PBS with 2,5% BSA and stained with FITC anti-human CD44 and PE anti-human CD24 (BD Biosciences,), according to the supplier's protocol. Flow cytometric analysis was performed on a FACScan and acquisition was performed with WinDI software (Becton Dickinson).

Reverse transcription and real-time reverse transcriptase PCR assays

Total RNA was extracted from cells using TRIzol reagent and the PPARγ, OB, FAP, 36B4 gene expression was performed by the reverse transcription-PCR method using a RETROscript kit (Applied Biosystem). Analysis gene expression of the other genes used in this study was performed by Real-time reverse transcription–PCR. Total RNA (2µg) was reverse transcribed with the RETROscript kit; cDNA was diluted 1:2 in nuclease-free water and 5µl were analysed in triplicates by real-time PCR in an iCycler iQ Detection System (Bio-Rad, USA) using SYBR Green Universal PCR Master Mix with 0.1

mmol/l of each primer in a total volume of 30 µl reaction mixture following the manufacturer's recommendations. Negative control contained water instead of first strand cDNA was used. Each sample was normalized on its GAPDH mRNA content. The relative gene expression levels were normalized to a calibrator that was chosen to be the basal, untreated sample. Final results were expressed as n-fold differences in gene expression relative to GAPDH mRNA and calibrator, calculated using the ΔCt method as follows: n-fold=2- (ΔCtsample–ΔCtcalibrator) where ΔCt values of the sample and calibrator were determined by subtracting the average Ct value of the GAPDH mRNA reference gene from the average Ct value of the gene analysed.

Primers used for the amplification were reported in Table 2.

Table2. Sequences of primers and probes.

Gene Symbol	Gene Name	Primer Sequences
PPARγ	Peroxisome Proliferator-Activated Receptor gamma	For 5'-GAGTTCATGCTTGTCAAGGATGC- 3' Rev 5'-CGATATCACTGGAGATCTCGCC-3'
OB	Leptin	For 5' -GAGACCTCCTCCATGTGCTG-3' Rev 5'- TGAGCTCAGATATCGGGCTGAAC-3'
FAP	Fibroblast activation protein	For 5'-AGAAAGCAGAACTGGATGG-3' Rev 5'-ACACACTTCTTGCTTGGAGGAT-3'
36B4	36B4	For 5'-CTCAACATCTCCCCCTTCTC-3' Rev 5'- CAAATCCCATATCCTCGT -3'
GAPDH	glyceraldehyde-3-phosphate dehydrogenase	For 5'- CCCACTCCTCCACCTTTGAC-3' Rev 5'- TGTTGCTGTAGCCAAATTCGTT-3'
OBRL	Leptin Receptor Long Isoform	For 5'-GATAGAGGCCCAGGCATTTTTTA-3' Rev 5'- CACCACTCTCTCTCTTTTTGATTGA-3'
OBRS	Leptin Receptor Short Isoform	For 5'-ATTGTGCCAGTAATTATTTCCTCTTCC-3' Rev 5'-CCACCATATGTTAACTCTCAGAAGTTCA-3'
CD44	CD44 molecule	For 5'- CCTTTGATGGACCAATTACCATAAC-3' Rev 5'- TCAGGATTCGTTCTGTATTCTCCTT-3'
OCT4	POU class 5 homeobox 1 (POU5F1)	For 5'- AGCGACTATGCACAACGAGA- 3' Rev 5'- CCATAGCCTGGGTACCAAA- 3'
N-CAD	N-cadherin	For 5'- ACAGTGGCCACCTACAAAGG-3' Rev 5'- CCGAGATGGGGTTGATAATG-3'
NOTCH1	Notch 1	For 5'-GTGACTGCTCCCTCAACTTCAAT- 3' Rev 5'-CTGTCACAGTGGCCGTCACT- 3'
SMO	Smoothened, frizzled family receptor	For 5'- CACCCTGGCCACATTCGT- 3' Rev 5'- CGCATTGACGTAGAAGAGAATAACA- 3'
BMI1	Polycomb ring finger oncogene	For 5'- GTGCTTTGTGGAGGGTACTTCAT- 3' Rev 5'-TACACGTTTTACAGAAGGAATGTAGAC-3'
SUZ12	SUZ12 polycomb repressive complex 2 subunit	For 5'- AGCTTACGTTTACTGGTTTCTTCCA- 3' Rev 5'- GCAAACTTTCACAAGCAGGACTT- 3'
BMP7	Bone morphogenetic protein 7	For 5'-GGGAACGCTTCGACAATGAG- 3' Rev 5'- CGATTCCCTGCCCAAGTG- 3'
BMPR2	Bone morphogenetic protein receptor, type II	For 5'- GCCTTTGGGAGAAATCAAAAGGGG- 3' Rev 5'- CATTCTGAATTGAGGGAGGAGTGG- 3'

YES1	v-yes-1 Yamaguchi sarcoma viral oncogene homolog 1	For 5'- CCTCGAGAATCTTTGCGACTAGA- 3' Rev 5'-CCATTCCATGTTCCCATCCA- 3'
SMAD4	SMAD family member 4	For 5'-GGAGCTCATCCTAGTAAATG-3' Rev 5'-GACGGGCATAGATCACATGA-3'
SOX4	SRY (sex determining region Y)-box 4	For 5'- GGCCTCGAGCTGGGAATCGC-3' Rev 5'- GCCCACTCGGGGTCTTGCAC-3'
MAPK6	Mitogen-activated protein kinase 6	For 5'-GTCGGAGAAGTCCCGTTGTATC- 3' Rev 5'-TCCAGCTCACCACAATCACAAT- 3'
SKT36	Serine/threonine kinase 36	For 5'- CGCATCCTACACCGAGATATGA- 3' Rev 5'- GCAAATCCAAAGTCACAGAGCTT- 3'
BIRC6	Baculoviral IAP repeat-containing protein 6	For 5'- GGACCACCGCATCTCTACAT -3' Rev 5'- GCAGTGGATGAAGCCAGCCT- 3'
HSPA1A	Heat shock 70kDa protein 1A	For 5'- CCTGTGTTTGCAATGTTGAAATTT -3' Rev 5'- CTCTGCATGTAGAAACCGGAAA- 3'
HSPD1	Heat shock 60kDa protein 1 (chaperonin)	For 5'-GATGTTGATGGAGAAGCTCTAAGTACA-3' Rev 5'-TGCCACAACCTGAAGACCAA-3'
HSPH1	Heat shock 105kDa/110kDa protein 1	For 5'-AAATCAGCAAATCACTCATGCAA-3' Rev 5'-ATGCTCGGCCATGAAATCTT-3'
HSP90AA1	Heat shock protein 90kDa alpha, class A member 1	For 5'-ATTGCCCAGTTGATGTCATTGA-3' Rev 5'-ATGCATCTGATGAATTTGAAATGAG-3
HEY1	Hes-Related Family BHLH Transcription Factor With YRPW Motif 1	For 5'- CGAGCTGGACGAGACCAT-3' Rev 5'-GAGCCGAACTCAAGTTTCCA-3'
HES1	Hes Family BHLH Transcription Factor 1	For 5'- GAAGCACCTCCGGAACCT-3' Rev 5'-GTCACCTCGTTCATGCACTC-3'

Protein expression analysis using western-blot

Proteins were extracted with Protein Lysis Buffer (25mM HEPES, 50mM NaCl, 30mM NaPP, 50mM NaF, 1% Triton-X-100, 10% Glycerol, 5mM EDTA, Protease Inhibitor cocktail, 1µM PMSF). Lysates were placed on a rotator for 1 hour at 4°C, then were centrifuged at 10000g at 4°C for 10min, and supernatants were collected. Protein concentrations were assessed using the BCA Protein Assay Kit (Thermo Scientific). Proteins were separated on a 10% gel (Biorad) by SDS-PAGE at 200V for 1 hour, and then were transferred on polyvinylidene difluoride (PVDF) membranes (BioRad) at 25 V/1,300 mA for 15 min using a Trans Blot Turbo (BioRad). Membranes were blocked in a solution of PBS containing 0,05% Tween-20 and 5% skimmed milk (Marvel) for 1h at room temperature and primary antibodies were incubated overnight at 4°C. Primary antibodies used were anti-ERα(Santa Cruz), anti-Vimentin (Santa Cruz), anti-pan-Cytokeratin (Santa Cruz), anti-p-STAT3 (Santa Cruz), anti-p-AKT (Santa Cruz), anti-p42/44 MAPK (Cell Signalling), anti-HSP90 (Santa Cruz), anti- NOTCH1 (Rockland), anti-NOTCH2 (Cell Signalling), anti-NOTCH3 (Santa Cruz), anti-NOTCH4 (Abcam), anti-HES1

(Millipore), anti-JAG1 (Santa Cruz), anti-DLL1 (Abcam), anti-DLL4 (Abcam), anti-GAPDH (Santa Cruz) and anti-β-actin (Sigma). Horseradish peroxidase-conjugated secondary antibodies (Dako) were incubated for 1h at room temperature. Proteins were visualized with Luminata Classico or Luminata Forte (Millipore) by exposing the membranes to X-ray films (HyperfilmTM MP, Amersham).

Transmigration assays

Mammosphere derived MCF-7, treated with or without leptin, were placed in the upper compartments of Boyden chamber (8-µm membranes/Corning Costar. Bottom well contained regular full media. After 24 hours, migrated cells were fixed and stained with Coomassie brilliant blue. Migration was quantified by viewing 5 separate fields per membrane at 20 magnification and expressed as the mean number of migrated cells. Data represent 3 independent experiments, assayed in triplicate.

Lentiviral and Retroviral transfection

We established stable OBR sh MCF-7 cell line using the lentiviral expression system (GeneCopoeia; lentiviral plasmid sh-clone #HSH010584). 48h after transfection with packaging plasmids and pLentiviral plasmids of target gene in HEK293 cells, supernatants containing lentiviral particles were filtered (0.45µm PES), mixed with polybrene (8µg/ml) and used to infect MCF-7 cells. 24h after infection, cells were selected with 2µg/mL puromycin overtime to eliminate un-infected cells. OBR mRNA in stable MCF-7 clones was confirmed by real-time RT-PCR.

Overexpression of Notch IntraCellular Domain 4 (NICD4) or Jagged 1 ligand (JAG1) in MCF-7 cells was carried out by lenti- and retro-viral transduction, respectively. Lentiviruses were produced by co-transfection of pPsPax2, pMD2.G vectors and the relevant pCDH lentiviral vector (containing NICD4 or empty vector) in HEK293T cells using polyethylenimine (Millipore). Virus-containing supernatant was collected after 48h. Full length human JAG1 cDNA cloned into the retroviral vector LZRSpBMN-linker-IRES GFP was kindly provided by ML Toribio (CBMSO, Madrid). To obtain retroviral particles, the retroviral vectors (hJAG1-expressing vector or the empty vector) were co-transfected with pMD2.G (envelope system) into PhoenixGP packaging cells following

the calcium phosphate method (CalPhos Mammalian Transfection kit, Clontech Laboratories). Retroviruses-containing supernatants were harvested 24, 48 and 72h post-transfection. Once virus-containing supernatants were collected, they were centrifuged at 400 g for 5min and filtered through 0.45 µm filter to remove cell debris. The viral supernatants were concentrated by ultracentrifugation using an AH-629 rotor (Sorvall Ultra Pro80, Sorvall) at 20000 rpm for 2h at 4°C. The viral pellets were resuspended in PBS and aliquots were stored at -80°C. MCF-7 cells were transduced with either lenti- or retro-viral particles in the presence of 8 µg/ml polybrene (Sigma). Stable transduced MCF-7 cells were selected by FACS based on GFP expression.

Microarray and data analysis

Microarray analyses were carried out on total RNA from MCF-7-M2 mammosphere-derived cells treated with CAF-CM, Adipocyte-CM or Leptin by pooling equal amounts of nucleic acids extracted from three independent cell cultures. Gene expression profiling was performed in triplicate using 500ng of each RNA pool as described (Nassa G *et al*., **2014**), cRNAs were hybridized for 18h at 55°C on Illumina HumanHT-12 v4.0 BeadChips (Illumina Inc.) and scanned with an Illumina iSCAN. Data analyses were performed with GenomeStudio software version 2011.1 (Illumina Inc.). Data were normalized with the quantile algorithm and genes were considered if the detection p-value was <0.01. Statistical significance was calculated with the Illumina DiffScore, a proprietary algorithm that uses the bead standard deviation to build an error model. Transcripts showing a DiffScore ≤−30 and ≥30, corresponding to a p-value of 0.001 and significant fold change in treated vs untreated≥1.5 were considered. Venn diagram was generated using Venny 2.0 software. Heat-maps were generated with the Multiexperiment Viewer 4.9 software after performing one way hierarchical clustering of transcripts with the average linkage method and Euclidian distance.

Raw microarray data have been deposited, in a format complying with the Minimum Information About a Microarray Gene Experiment (MIAME) guidelines of the Microarray Gene Expression Data Society (MGED), in the EBI ArrayExpress database (http://www.ebi.ac.uk/ arrayexpress) with Accession Number: E-MTAB-3641.

Total RNA from 8 different metastatic breast cancer samples was extracted using the RNeasy Plus Mini Kit (QIAGEN). The Exon Gene Array ST1 platform (Affimetrix) was used to assess gene expression. Data obtained were analysed using Bioconductor R Software. The mean of log2 gene expression values was calculated across all 8 patient derived samples for each individual gene.

Construction of RNA-seq database

RNA-seq data was obtained from the TCGA depository. We transferred the pre-processed level 3 data generated by the Illumina HiSeq 2000 RNA Sequencing Version 2 platform. Expression levels for these samples were computed using a combination of MapSplice and RSEM. Individual patient files were merged into a single database using the plyr R package (Wickham **2011**).

Patient derived xenografts and in vivo experiments

Mouse studies commenced in 8- to 12-week-old female mice and were conducted in accordance with the UK Home Office Animals (Scientific Procedures) Act 1986, using NSG (NOD.Cg-Prkdcscid Il2rgtm1Wjl/SzJ) mice. All *in vivo* work was performed with a minimum of n = 4 mice per condition. Serial passaging of the PDX was carried out by implanting small fragments of the tumor subcutaneously into dorsal flanks of NSG mice. Early (HBCx34) and metastatic (BB3RC31) BC estrogen-dependent PDXs were administered with 8 mg/ml of 17-beta estradiol in drinking water at all times and were treated with drugs when tumors reached 200–300 mm^3. Experiments were performed using PDX tumors between passages 5 and 8. Animal weight and tumor size was measured bi-dimensionally using callipers twice a week. Tamoxifen citrate (Sigma, 10 mg/kg/day) and RO4929097 (Cellagen Technology, 3 mg/kg/day) were administered by oral gavage (0.1 ml per dose) on a basis of 5 days out of 7 (weekends excluded) for 14 days. Tamoxifen citrate and RO4929097 were prepared in 1% carboxymethylcellulose (Sigma) dissolved in distilled water. Fulvestrant (kindly provided by AstraZeneca, 200 mg/kg/week) was administered by subcutaneous injection (0.1 ml per dose) on a weekly basis for 14 days.

To determine tumor initiation capacity of metastatic (BB3RC31) PDX cells treated *in vivo*, respectively, NSG mice were injected subcutaneously with cells in mammosphere media mixed 1:1 with Matrigel. 90-day slow release estrogen pellets were implanted sub-cutaneously into mice two days before cell injection (0.72 mg, Innovative Research of America). Positive tumor growth was assessed at day 60 or 90 after cell injection by determining the mice bearing a tumor greater than 100 mm^3 and is represented as mice positive for growth/mice tested (n=4 per condition in all experiments). p values were calculated with Chisquared test.

Aldefluor assay (Stemcell Technologies)

Dissociated single cells were suspended in Aldefluor assay buffer containing an ALDH substrate, bodipyaminoacetaldehyde (BAAA) at 1.5 mM, and incubated for 45 min at 37ºC. To distinguish between ALDH-positive and -negative cells, a fraction of cells was incubated under identical conditions in the presence of a 2-fold molar excess of the ALDH inhibitor, diethylaminobenzaldehyde (DEAB). Mouse cells were excluded from the FACS analysis with anti-mouse MHC Class I (H-2Kd) antibody conjugated with Pacific Blue (BioLegend). 7-aminoactinomycin D (7AAD, BD) was added for dead cell exclusion. Data were acquired on a LSR II (BD) flow cytometer and analysed using the BD FACSDiva™ software.

Notch transcriptional assay

To measure the activation of Notch dependent transcription, cells were transfected with CBF1 firefly luciferase reporter (containing 10 copies of a CBF1 consensus sequence) and CMV-Renilla luciferase reporter. Plasmids were incubated with X-tremegene (Roche) in a ratio of 3:1 (µl of X-tremegene: µg of DNA) in OptiMEM (Life Technologies) for 15 minutes, before addition to the culture media. After 48 hours cells were lysed with 1x Passive lysis buffer (5x, Promega), put on the rocker for 15 minutes and luminescence was assayed with the Dual-Glo Luciferase assay system (Promega) following manufacturer's instructions. Luciferase activity was measured using a luminometer (Promega, Glomax Multi+ Detection System with Instinct

Software). Luminescence of the firefly luciferase was normalised to that of the renilla luciferase.

NOTCH4 targeting using CRISPR-Cas9n technology

To generate MCF-7 clones with genomic alterations in NOTCH4, a double-nickase approach was used by expressing a D10A mutant version of Cas9 (Cas9 nickase) together with a pair of sgRNAs complementary to opposite strands of the targeted genomic locus. sgRNA oligo sequences (sgRNA-A, 5'-ACCTGCCTGAGCCTGTCTCT-3'; sgRNA-B, 3'-TCTTGGGACACGGTTACCT-5') targeting exon 2 of NOTCH4 gene were designed using the CRISPR design tool (http://crispr.mit.edu/) - Figure S2D. sgRNA-coding sequences were cloned into pSpCas9n (BB)-2A-GFP (Addgene, PX461) vector. MCF-7 cells were co-transfected with PX461-sgRNA-A and PX461-sgRNA-B plasmids using X-tremeGENE Transfection reagent (Roche, 06366244001). Two days post-transfection, GFP-positive cells were directly FACS sorted as single cells into 96-well plates. After 14 days in culture, clones were screened for CRISPR-mediated indels. Genomic DNA was extracted using the Wizard Genomic DNA Purification Kit (Promega, A1120) and genotyping PCR was performed using a set of primers flanking the CRISPR target site (forward 5'-GGGTACCATGTGGAGAGTGG-3'; reverse 5'-CACAAGAAGCTGGGTGTCAA-3'). PCR products purified with QIAquick PCR Purification Kit (Qiagen) were cloned into pGEM-T Easy vector and then Sanger sequenced using T7 sequencing primer. Absence of wild-type alleles was confirmed by using a specific restriction enzyme for target sequence (BanI, Biolabs). Proteins were extracted and separated on 10% SDS-PAGE gel. Membranes were incubated with anti-NOTCH4 (Santa Cruz) and anti-β-actin (Sigma) antibodies.

Growth assay (SRB assay)

6000 cells were seeded per well in a 96 well-plate at least in triplicate for each condition used. Plates were incubated in a humidified incubator at 37°C with 5% CO2 and an SRB assay was performed at different time points to assess cellularity. Briefly, cells were fixed with 25µl/well of 50% (w/v) trichloroacetic (TCA) and incubated at 4°C for a minimum of 1hour. Fixed cells were washed 5 times with water and left to air dry.

Cells were then stained with 100µl/well of 0.4% (w/v) Sulforhodamine B (SRB) dissolved in 1% acetic acid for 30 minutes at room temperature. Residual SRB was washed away with 3 washes of 1% acetic acid and plates were left to air dry. Finally, SRB was solubilized with 100µl/well of 10mM Tris-base (pH 10.5) for 20 minutes at room temperature and absorbance was measured at 490 nm with an automated plate reader(BioTek ELx800).

Statistical analyses

Each datum point represents the mean±s.d. of three different experiments. Data were analyzed by Student's t test using the GraphPad Prism 4 software. $P<0.05$ was considered as statistically significant. Pearson correlation coefficient (r) was used to measure the correlation between OBR or Heat Shock Protein 90 (HSP90) gene expression of 8 metastatic breast cancer samples and mean MFE; a 2-tailed $p \leq 0.05$ was considered statistically significant.

Kaplan-Meier analysis was performed as described (Gyorffy B et al., **2010**). Kaplan-Meier survival graph, and hazard ratio with 95% confidence intervals and logrank P value were calculated and plotted in R using Bioconductor packages.

AIM 1

Evaluation of the role of leptin, as a mediator of the tumor-stroma interaction, in regulating breast CSC activity

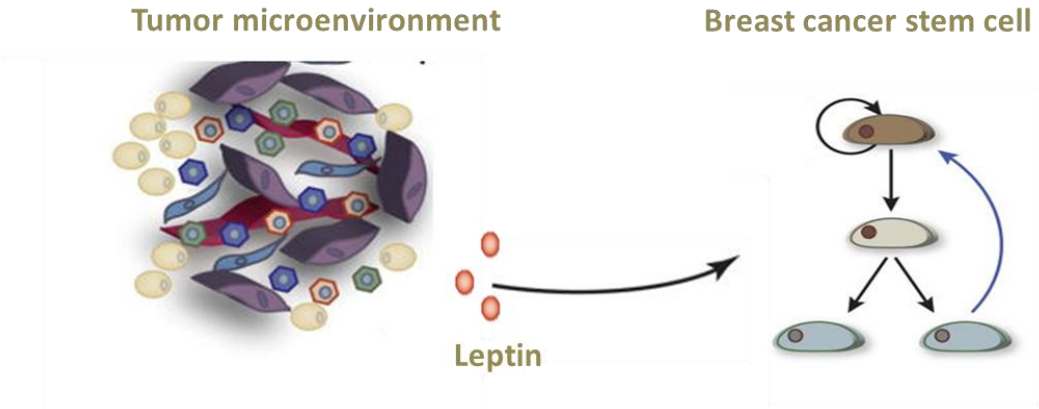

Results

CAFs and adipocytes induce mammosphere formation in breast cancer cells through leptin secretion

To assess the ability of stromal cells to affect CSC activity in breast cancer cells we performed co-culture experiments. As experimental models for breast CSCs (BCSCs), we used estrogen receptor (ER)-α-positive MCF-7 cells grown as mammospheres. This culture system has been used to characterize, enrich and propagate breast cancer cells with stem-like phenotype, relying on the feature of stem cells to escape anoikis and grow as spheroids in anchorage-independent conditions (Dontu G *et al*., **2003**). MCF-7 mammosphere cells were characterized by flow cytometric analysis that revealed an enrichment of CD44+ / CD24− subpopulation compared to MCF-7 monolayer cells (Figure 5A). In addition, real-time PCR further revealed that genes associated with stem cell phenotype, including OCT4, N-CAD, BMI1, SOX4, were expressed in mammosphere cells at higher levels than in monolayer cells (Figure 5B). Moreover, MCF-7 mammosphere cells were also analyzed for the expression of ERα (Figure 5C and 5D).

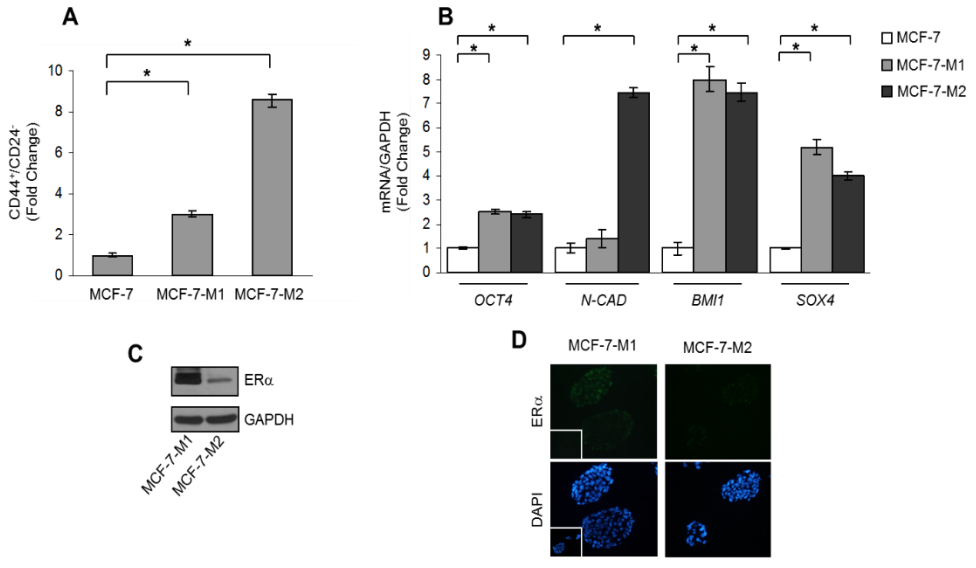

Figure 5: Characterization of MCF-7 cells grown as mammospheres: A) Flow cytometric analysis of CD44+ /CD24− phenotype in MCF-7 monolayer cells, and in MCF-7 cells grown as primary (MCF-7-M1) and secondary-mammospheres (MCF-7-M2). B) OCT4, N-CAD, BMI1 and SOX4 mRNA content evaluated by real-time RT–PCR in MCF-7, MCF-7-M1 and MCF-7-M2 cells.

Each sample was normalized to its GAPDH mRNA content. The values represent the means ± s.d. of three different experiments each performed in triplicate. *p < 0.05. C) Immunoblotting for estrogen receptor (ER)-α in MCF-7-M1 and MCF-7-M2 cells. GAPDH as loading control. D) Immunofluorescence of ERα and DAPI staining (for nuclei detection) in MCF-7-M1 and MCF-7-M2 cells. Small squares, negative control.

As stromal cells, we used either CAFs isolated from biopsies of primary breast tumors or human breast adipocytes obtained after preadipocyte differentiation. CAFs possessed the basic fibroblast characteristics with long and spindle-shaped morphology and highly expressed alpha-smooth muscle actin (α-SMA), vimentin, and fibroblast activation protein (FAP) (Figure 6A and 6B). Adipocytes displayed a classical morphological phenotype characterized by accumulation of lipid droplets associated with the expression of specific markers as PPARγ and leptin (OB) (Figure 6C).

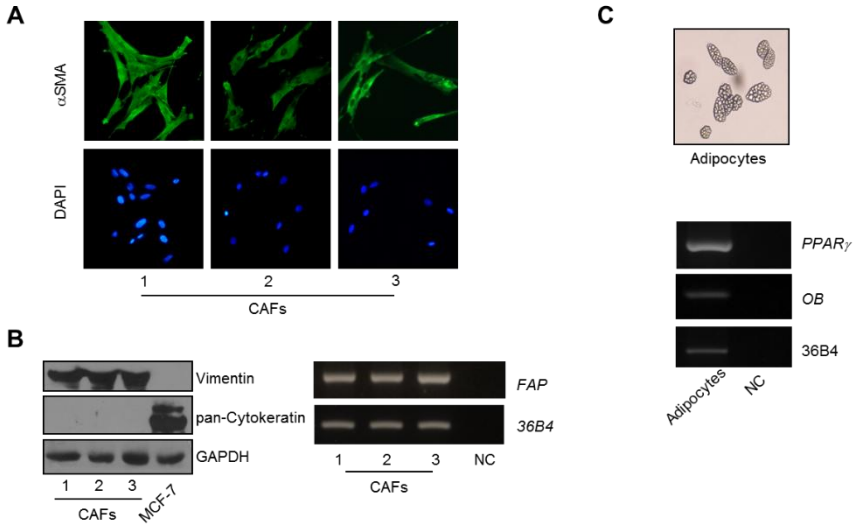

Figure 6**: **Characterization of stromal cells used in this study. A) Cancer Associated Fibroblasts (CAFs) were isolated from primary breast tumour biopsies by collagenase digestion. Immunofluorescence of alpha-smooth muscle actin (α-SMA) and DAPI staining (for nuclei detection). B) Left panel, immunoblotting of Vimentin and pan-Cytokeratin protein expression, GAPDH as loading control. Rigth panel, RT-PCR analysis of Fibroblast Activation Protein (FAP) mRNA levels. C) Subcutaneous preadipocytes from breast tissues were stimulated to differentiate into mature adipocytes. Upper panel, a typical bright-field picture of adipocytes characterized by accumulation of lipid droplets; lower panel, RT-PCR analysis, for expression of the specific adipocyte markers PPARγ and leptin (OB). 36B4 (internal standard). NC, negative control.

Using co-culture experiments, we examined mammosphere formation from MCF-7 cells in the presence or absence of conditioned media (CM) harvested from CAFs and adipocytes. Compared to the cells cultured alone, MCF-7 cells co-cultured with CAF- or adipocyte-derived CM showed a significant enhancement in mammosphere forming efficiency (MFE) (Figure 7A). Stem cells are maintained in the primary mammospheres through self-renewal, and are able to give rise to secondary mammospheres when cells from the primary spheres are dissociated and allowed to grow in anchorage-independent conditions. Therefore, we carried out secondary mammosphere cultures to examine the effects of CM on BCSC self-renewal. Our experiments demonstrated an increased self-renewal in MCF-7 cells treated with CAF- and adipocyte-derived CM in the first generation compared with the untreated spheres (Figure 7B and 7C). These data suggest that BCSC activity is influenced by soluble factors secreted from stromal cells. Thus, given the role of leptin as an important cytokine secreted by both CAFs and adipocytes, we assessed the impact of leptin in the context of the heterotypic signaling working in BCSC–stromal interactions. First, ELISA measurement in CM from stromal cells showed that leptin levels were 2,4 ± 0,12 ng/mg protein and 20,32 ± 2 ng/mg protein in CAF and adipocyte-derived CM, respectively. Leptin was then immunodepleted from CAF- and adipocyte-derived CM using a specific leptin antibody, and resulting media were tested for the ability to induce mammosphere formation in breast cancer cells. AS shown in Figure 7D and 7E, leptin depletion significantly decreased the MFE/self-renewal promoted by stromal cell-derived CM.

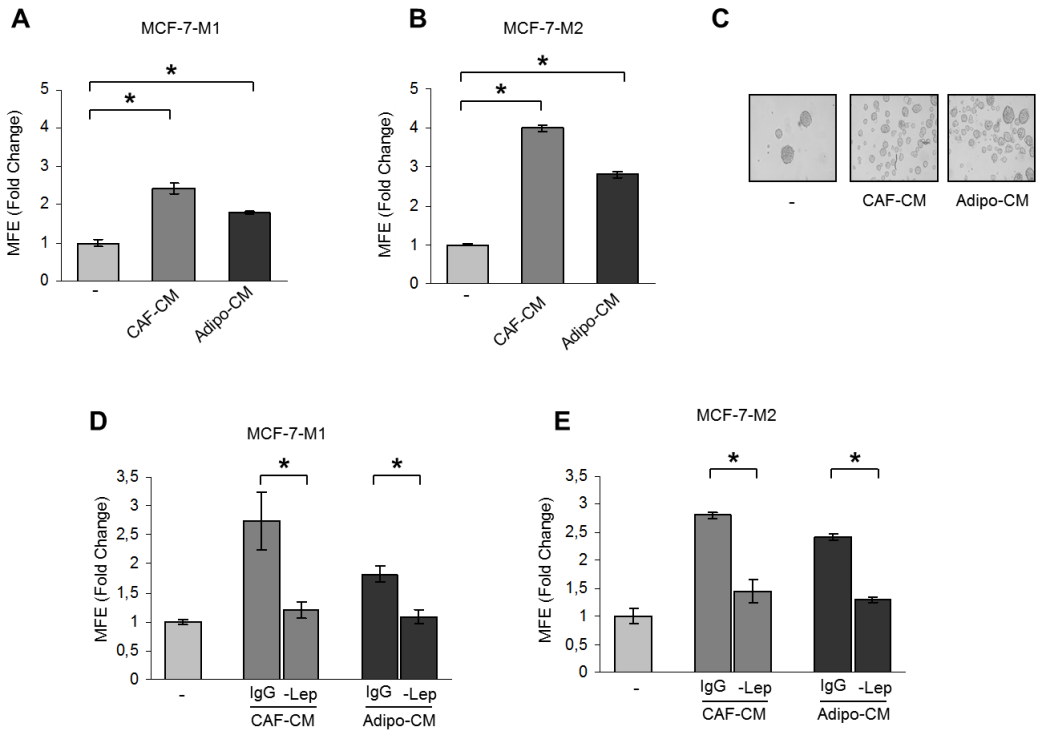

Figure 7: Leptin mediates the effects of stromal cell-CM on breast cancer cell mammosphere formation. A) Mammosphere Forming Efficiency (MFE) evaluated in MCF-7-M1 and MCF-7-M2 (B) in the presence or absence (−) of CAF- and Adipocyte-derived Conditioned Media (CAF-CM and Adipo-CM, respectively). MFE was calculated by dividing the number of mammospheres (colonies >50 µm) formed by the number of the cells plated and expressed as fold change compared to untreated cells (−). C) Representative phase-contrast images of mammospheres treated as in panel (B) are shown. MFE evaluated in MCF-7-M1 (D) and MCF-7-M2 (E) in the presence or absence (−) of leptin-immunodepleted CAF-CM and Adipo-CM (-Lep). IgG: CM immunodepleted with nonspecific antibody. The values represent the means ± s.d. of three different experiments each performed in triplicate. *$p < 0.05$.

Targeting leptin signaling reduces stem cell activity mediated by stromal cells

Our previous experiments indicate that leptin may represent an important paracrine molecule that mediates the interaction between stromal cells and BCSCs. To support this observation, we tested the effect of a full leptin receptor antagonist, peptide LDFI, on BCSC activity. We have previously shown that this peptide inhibits leptin induced breast cancer growth *in vitro* and exhibits antineoplastic activities *in vivo* (Catalano S *et al.*, **2015**). Our data demonstrated that treatment with peptide LDFI significantly reduced MFE/self-renewal promoted by stromal cell-derived CM in MCF-7 cells (Figure 8A). To extend the results obtained, we have grown the ERα-negative MDA-MB-231

breast cancer cells as mammospheres and evaluated the effects of CAF- or adipocyte-CM in the presence or absence of peptide LDFI. Treatment of MDA-MB-231 mammosphere cultures with CAF- or adipocyte-derived CM significantly increased MFE/self-renewal and the addition of the OBR antagonist LDFI strongly reduced these effects (Figure 8B), confirming that leptin/leptin receptor may play a crucial role in maintaining the BCSC traits mediated by stromal cells in different cellular backgrounds.

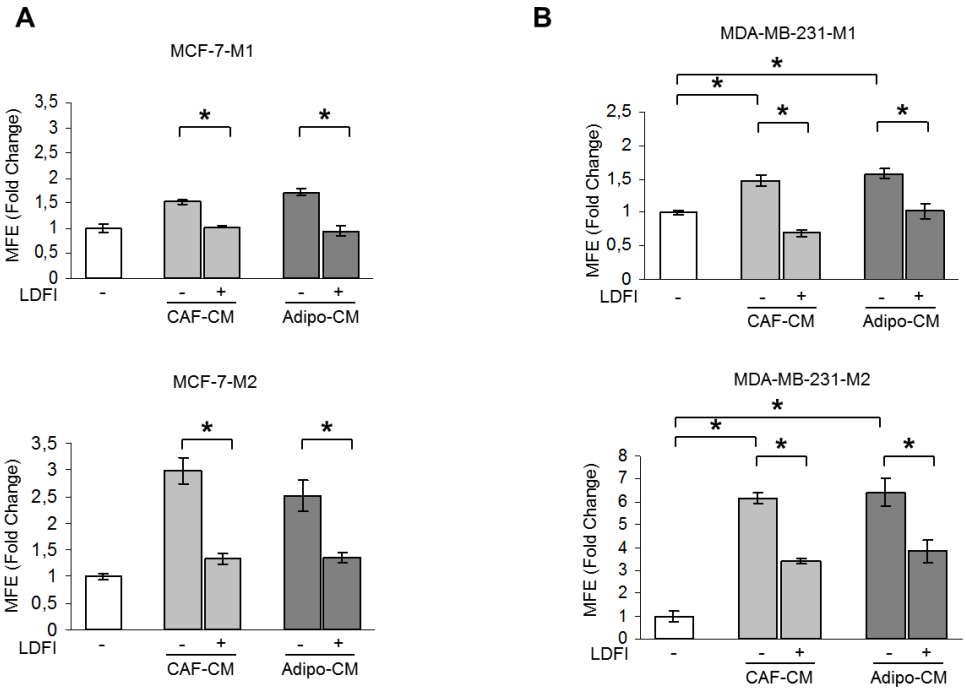

Figure 8: Effects of a selective leptin receptor antagonist on breast cancer stem cell activity. MFE evaluated in MCF-7-M1 and MCF-7-M2 (A) and in MDA-MB-231-M1 and MDA-MB-231-M2 (B) treated with CAF-CM and Adipo-CM with/without peptide LDFI (1 µg/ml). The values represent the means ± s.d. of three different experiments each performed in triplicate. *p < 0.05.

Leptin signaling regulates mammosphere formation/self-renewal activity of breast cancer cells

Having shown that stromal cells regulate BCSC activity through secretion of leptin, we next investigated the direct involvement of this cytokine in the regulation of mammosphere formation/self-renewal in MCF-7 cells. In agreement with previous data demonstrating that leptin receptor plays a crucial role in maintaining cancers in a stem cell-like state (Feldman DE *et al*., **2012**; Zheng Q *et al*., **2011** & **2013**; Chang CC *et al*., **2015**), we found that MCF-7 mammosphere cultures exhibited increased OBR mRNA expression and in a greater extent the long isoform, compared to monolayer cells (Figure 9A). Leptin treatment of mammosphere cultures resulted in a significant increase in MFE/self-renewal and in an enhanced percentage of CD44+/CD24− population compared with untreated cells (Figure 9B, 9C and 9D).

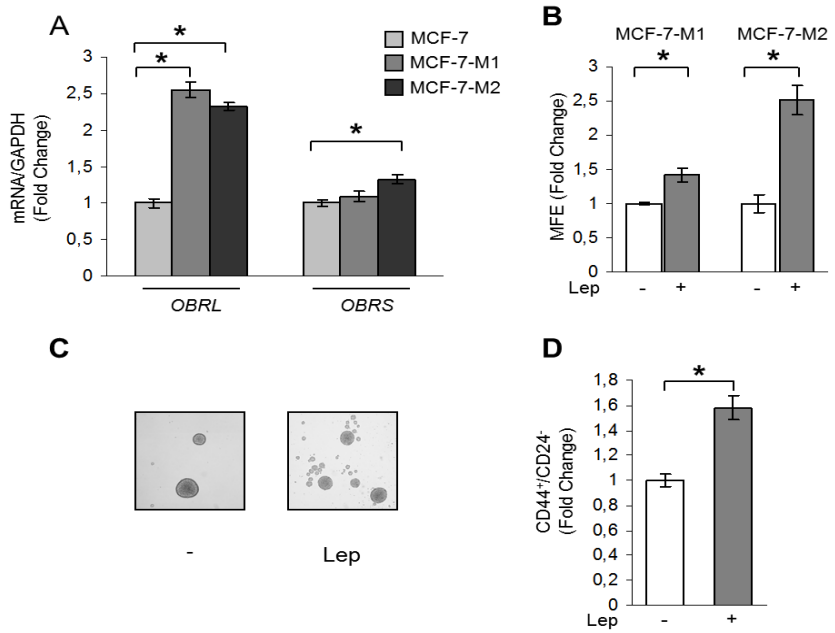

Figure 9: Leptin induces MFE in breast cancer cells. A) Leptin receptor long (OBRL) and short (OBRS) isoform mRNA levels, evaluated by real time RT-PCR, in MCF-7, MCF-7-M1 and MCF-7-M2 cells. Each sample was normalized to its GAPDH mRNA content. B) MFE in MCF-7-M1 and MCF-7-M2 in the presence or absence (−) of leptin 500 ng/ml (Lep). C) Representative phase-contrast images of mammospheres treated as in panel (B) are shown. D) CD44+/CD24− population in MCF-7-M2 cells treated or not (−) with Lep. The values represent the means ± s.d. of three different experiments each performed in triplicate. *p < 0.05.

Accordingly, in MDA-MB-231 mammosphere cultures, we observed a significant increase in the long isoform of OBR mRNA expression compared to monolayer cells (Figure 10A), and an enhanced MFE/self-renewal after leptin exposure (Figure 10B), demonstrating that this cytokine can directly regulate BCSC activity.

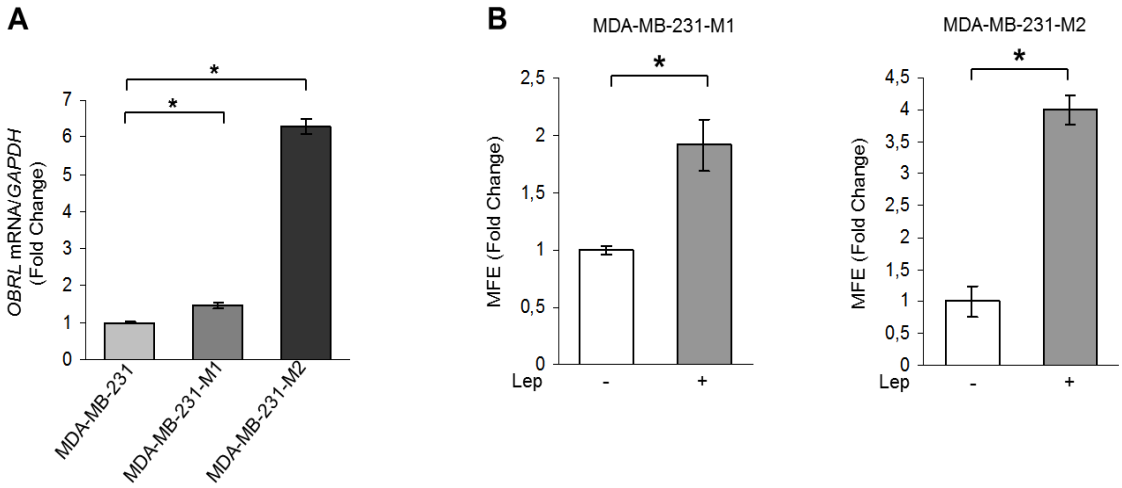

Figure 10. Leptin induces MFE in ER- breast cancer MDA-MB-231 cells. A) Leptin receptor long (OBRL) mRNA content evaluated by real-time RT–PCR in MDA-MB-231, MDA-MB-231-M1 and MDA-MB-231-M2 cells. Each sample was normalized to its GAPDH mRNA content. B) MFE evaluated in MDA-MB-231-M1 and MDA-MB-231-M2 cells (C) in the presence or absence (−) of leptin 500 ng/ml (Lep) in the mammosphere culture media. The values represent the means ± s.d. of three different experiments each performed in triplicate. *p < 0.05.

Since BCSCs display increased cell motility and invasion, we tested the effects of leptin on the migratory potential of MCF-7 mammospheres. Our data clearly showed that leptin exposure increased the number of migrated cells suggesting that this cytokine can facilitate the invasive behavior of BCSCs (Figure 11A). Next, OBR expression was stably knocked-down using lentiviral delivered short hairpin RNA (OBR sh) in MCF-7 cells (Figure 11B left panel). Suppression of OBR expression led to a significant inhibition of MFE (Figure 11B right panel), implying that this gene is necessary for maintaining cancer stem-like properties in breast cancer cells. In addition, we observed that leptin treatment induced the phosphorylation of specific OBR downstream signaling molecules such as STAT3, Akt and p42/44 MAPK (Figure 11C). As expected, the increase in MFE induced by leptin was reversed by the JAK2-STAT3 inhibitor AG490, the MEK1 inhibitor PD98059 and the PI3K/AKT inhibitor LY294002 (Figure 11D), suggesting that leptin promotes stem cell properties via activation of classical leptin

signaling pathways. In agreement with these observations, we also found an up-regulation of well-known leptin target genes as ObR and the heat shockp rotein 90 (HSP90) (Giordano C *et al*., **2013**) in MCF-7 cells treated with leptin (Figure 11E and 11F).

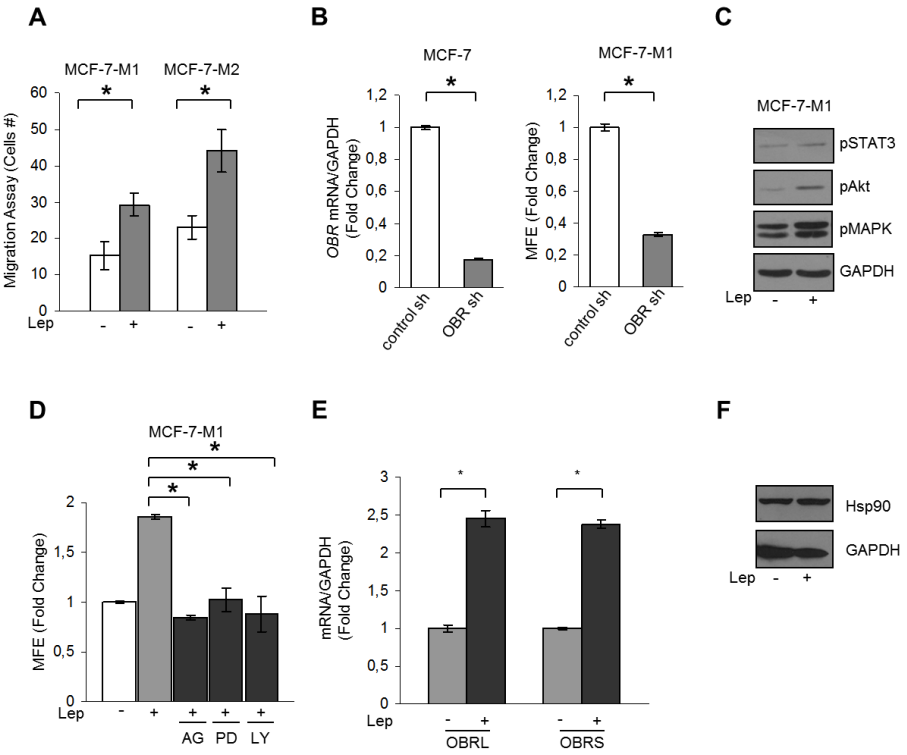

Figure 11: Leptin signaling directly induces BCSC activity in breast cancer cells. A) Transmigration assays in MCF-7-M1 and MCF-7-M2-derived cells treated or not (−) with Lep. B) MCF-7 cells were stably transfected with either a scrambled shRNA (control-sh) or OBR shRNA (OBR-sh). OBRL mRNA content was evaluated by real time RT-PCR (left panel). Each sample was normalized to its GAPDH mRNA content. MFE in MCF-7-M1 derived from either control-sh or OBR-sh clones (right panel). C) Immunoblotting of phosphorylated (p), STAT3 (Tyr705), Akt (Ser473), and MAPK (Thr202/Tyr204) at the indicated residues measured in cellular extracts from MCF-7- M1 cells treated or not (−) with Lep. GAPDH, loading control. D) MFE in MCF-7-M1 treated with Lep and AG490 (AG-20 µmol/L), PD98059 (PD-10 µmol/L) or LY294002 (LY-10 µmol/L). E) Leptin receptor long (OBRL) and short (OBRS) mRNA content evaluated by real-time RT–PCR in MCF-7-M1 cells in the presence or absence (−) of leptin 500 ng/ml (Lep). Each sample was normalized to its GAPDH mRNA content. F) Immunoblotting analysis of HSP90 levels in total protein extracts from MCF-7-M1 cells in the presence or absence (−) of leptin 500 ng/ml (Lep) in the mammosphere culture media. GAPDH was used as loading control.The values represent the means ± s.d. of three different experiments each performed in triplicate. *$p < 0.05$.

Gene expression profiling in leptin or stromal CM-treated mammosphere-derived cells

To determine whether leptin, CAF- and adipocyteCM may similarly affect gene expression profile in mammosphere-derived cells, we performed gene expression profiling analysis on total RNA extracted from the second generation spheres. Microarray results highlighted several RNAs differentially expressed in treated vs untreated MCF-7 mammospheres. Venn diagram analysis was used to compare the gene lists and to identify those genes that are unique and in common among the three treatments (Figure 12A). A total of 2270 transcripts were commonly regulated in all treated samples (808 up- and 1462 down-regulated transcripts, respectively). It should be noted that the global overlap among genes expressed in treated samples includes a number of genes known to play a role in stem cell biology such as BMI1, SUZ12, YES1, SOX4 (Figure 12B, left panel, Table 3). Similar trends were also observed for the expression of other genes involved in cell cycle control (Figure 12B, middle panel, Table 4). Moreover, treated samples displayed up-regulation of some transcripts related to the heat shock protein family, that recently have been suggested to be crucial in sustaining proliferation and self-renewal of stem cells (Isolani ME *et al*., **2012**), (Figure 12B, right panel, Table 5). To validate our microarray study MCF-7 mammospheres treated with leptin were evaluated for the expression of a panel of genes by using real-time PCR (Figure 12C). Taken together, gene expression profile analyses strongly support the role of leptin as a crucial paracrine molecule able to mediate the microenvironment effects on BCSC activity.

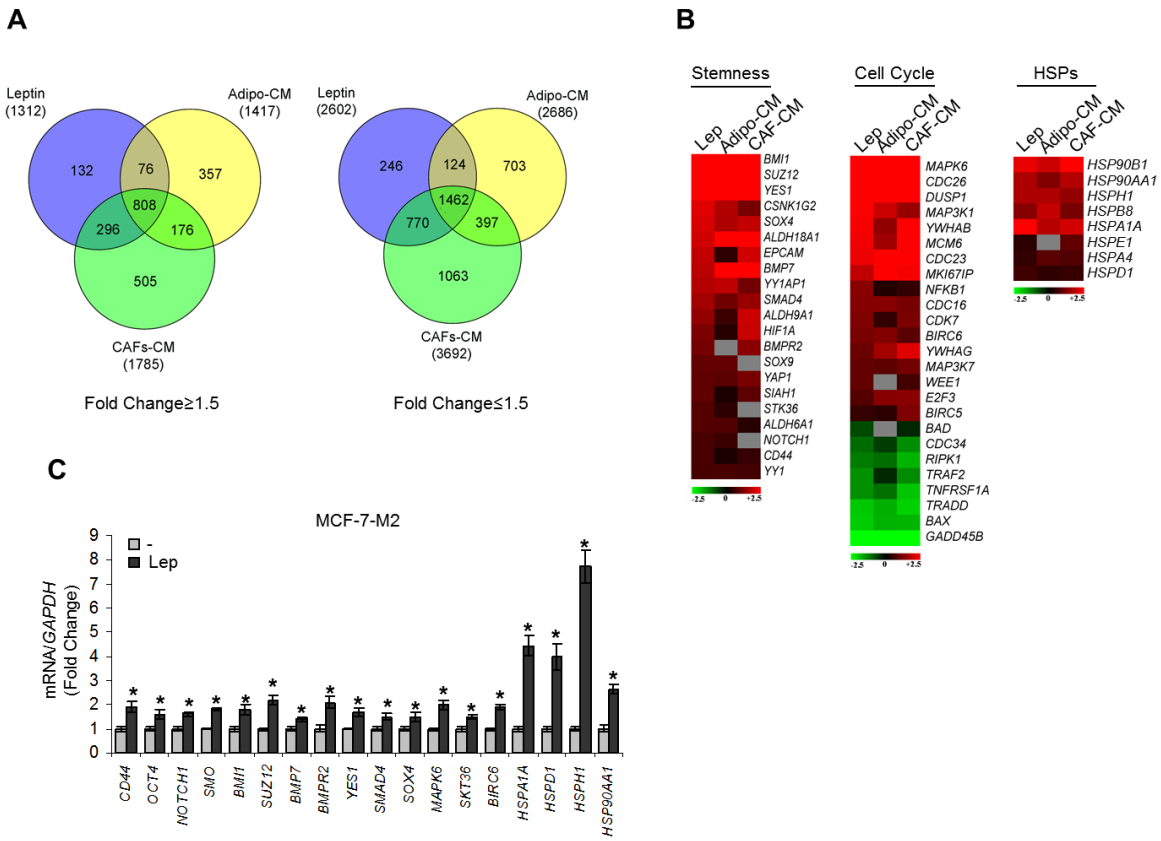

Figure 12: Gene expression profiling in mammosphere cultures treated with stromal cell-CM or leptin. A) Venn diagram of up-(left panel) and down-(right panel) regulated transcript identified by microarray analysis in MCF-7-M2 cells treated with CAF-CM, Adipo-CM or Lep compared to untreated samples. B) Heat-maps of stemness related-genes, cell cycle related-genes and HSP family genes from microarray data. Gene expression changes were calculated in treated cells with respect to the untreated controls. Transcript showing a DiffScore ≤ − 30 and ≥ 30, corresponding to a p-value of 0.001, and significant fold change in treated vs untreated ≥ 1.5 were considered. C) Real-time RT-PCR validation of a subset of genes in MCF-7-M2 cells treated or not (−) with Lep. Each sample was normalized to its GAPDH mRNA content. The values represent the means ± s.d. of three different experiments each performed in triplicate. *$p < 0.05$ vs untreated (−) sample.

Table 3. *Selection of relevant modulated genes involved in stem cell biology in MCF-7 M2 derived cells.*

Gene Symbol	Gene Name	Lep	Adipo-CM	CAF-CM
BMI1	Polycomb ring finger oncogene	+4.10	+3.63	+5.23
SUZ12	SUZ12 polycomb repressive complex 2 subunit	+3.43	+3.25	+3.73
YES1	v-yes-1 Yamaguchi sarcoma viral oncogene homolog 1	+3.04	+3.34	+3.51
CSNK1G2	Casein kinase 1, gamma 2	+2.32	+2.05	+1.70
SOX4	SRY (sex determining region Y)-box 4	+2.28	+2.03	+2.15
ALDH18A1	Aldehyde dehydrogenase 18 family, member A1	+2.24	+2.51	+3.24
EPCAM	Epithelial cell adhesion molecule	+2,15	+1,28	+2.23
BMP7	Bone morphogenetic protein 7	+2.10	+3.11	+3.26
YY1AP1	YY1 associated protein 1	+2.07	+2.12	+1.68
SMAD4	SMAD family member 4	+1.97	+1.67	+1.9
ALDH9A1	Aldehyde dehydrogenase 9 family, member A1	+1.88	+1.36	+2.20
HIF1A	Hypoxia-inducible Factor 1, alpha subunit	+1,74	+1.23	+2.18
BMPR2	Bone morphogenetic protein receptor, type II	+1.69	ns	+1.82
SOX9	SRY (sex determining region Y)-box 9	+1.59	+1.59	ns
YAP1	Yes-associated protein 1	+1.58	+1.54	+1.72
SIAH1	Siah E3 ubiquitin protein ligase 1	+1.58	+1.17	+1.55
STK36	Serine/threonine kinase 36	+1.50	+1.27	ns
ALDH6A1	Aldehyde dehydrogenase 6 family, member A1	+1.50	+1.48	+1.24
NOTCH1	Notch 1	+1.44	+1.35	ns
CD44	CD44 molecule (Indian blood group)	+1.44	+1.16	+1.33
YY1	YY1 transcription factor	+1.42	+1.43	+1.40

Numbers represent the ratio of the values of treated compared with untreated MCF-7 M2 spheres obtained by microarray data analysis. Statistical significance was calculated with the Illumina DiffScore, only genes with a DiffScore ≤−30 and ≥30, corresponding to a *p*-value of 0.001, were considered as statistically significant. ns: non significant.

Table 4. *Selection of relevant modulated genes involved in cell cycle control in MCF-7 M2 derived cells.*

Gene Symbol	Gene Name	Lep	Adipo-CM	CAF-CM
MAPK6	Mitogen-activated protein kinase 6	+6.27	+6.27	+7.90
CDC26	Cell division cycle 26 homolog (S. cerevisiae)	+3.85	+5	+4.8
DUSP1	Dual specificity protein phosphatase 1	+2.74	+2.71	+2.5
MAP3K1	Mitogen-activated protein kinase kinase kinase 1	+2.55	+2.19	+1.9
YWHAB	Tyrosine 3-monooxygenase/tryptophan 5-monooxygenase act pro, b	+2.46	+1,86	+2.67
MCM6	Michromosome maintance complex componeny 6	+2,42	+1.95	+3.44
CDC23	Cell division cycle 23 homolog (S. cerevisiae)	+2.41	+2.77	+3.64
MKI67IP	MKI67 (FHA domain) interacting nucleolar phosphoprotein	+2.14	+1.69	+2.46
NFKB1	Nuclear factor of kappa light polypeptide gene enhancer in B-cells 1	+1.81	+1.21	+1.31
CDC16	Cell division cycle 16 homolog (S. cerevisiae)	+1,79	+1.8	+1.7
CDK7	Cyclin-dependent kinase 7	+1.75	+1.3	+1.74
BIRC6	Baculoviral IAP repeat-containing protein 6	+1.72	+1.78	+1.53
YWHAG	Tyrosine 3-monooxygenase/tryptophan 5-monooxygenase act pro, g	+1.64	+1.97	+2.33
MAP3K7	Mitogen-activated protein kinase kinase kinase 7	+1.59	+1.55	+1.68
WEE1	WEE1 homolog (S. pombe)	+1.59	ns	+1.41
E2F3	Transcription factor	+1.50	+1.8	+1.82
BIRC5	Baculoviral IAP repeat-containing protein 5	+1.32	+1.27	+1.75
BAD	BCL2-antagonist of cell death	-1.44	ns	-1.23
CDC34	Cell division cycle 34 homolog (S. cerevisiae)	-1.64	-1.36	-1.84
RIPK1	Receptor (TNFRSF)-interacting serine-threonine kinase 1	-1.73	-1.65	-2.06
TRAF2	TNF receptor-associated factor 2	-1.85	-1.24	-1.82
TNFRSF1A	Tumor necrosis factor receptor superfamily, member 1A	-1.85	-1.67	-2.16
TRADD	TNFRSF1A-associated via death domain	-2.18	-2.04	-2.24
BAX	BCL2-associated X protein	-2.21	-2.05	-2.07
GADD45B	Growth arrest and DNA-damage-inducible beta	-2.29	-2.05	-2.69

Numbers represent the ratio of the values of treated compared with untreated MCF-7 M2 spheres obtained by microarray data analysis. Statistical significance was calculated with the Illumina DiffScore, only genes with a DiffScore ≤−30 and ≥30, corresponding to a *p*-value of 0.001, were considered as statistically significant. ns: non significant.

Table 5. *Expression profile of Heat shock protein family related genes in MCF-7 M2 derived cells.*

Gene Symbol	Gene Name	Lep	AAdipo-CM	CAF-CM
HSP90B1	Heat shock protein 90kDa beta, member 1	+2.38	+2.20	+2.7
HSP90AA1	Heat shock protein 90kDa alpha, class A member 1	+2.02	+1.76	+2.07
HSPH1	Heat shock 105kDa/110kDa protein 1	+2.02	+2.04	+1.88
HSPB8	Heat shock 22kDa protein 8	+1.80	+2.17	+1.71
HSPA1A	Heat shock 70kDa protein 1A	+2.74	+2.08	+2.25
HSPE1	Heat shock 10kDa protein 1	+1.26	ns	+1.58
HSPA4	Heat shock 70kDa protein 4	+1.30	+1.54	+1.48
HSPD1	Heat shock 60kDa protein 1 (chaperonin)	+1.39	+1.28	+1.33

Numbers represent the ratio of the values of treated compared with untreated MCF-7 M2 spheres obtained by microarray data analysis. Statistical significance was calculated with the Illumina DiffScore, only g enes with a DiffScore ≤−30 and ≥30, corresponding to a *p*-value of 0.001, were considered as statistically significant. ns: non significant.

Leptin increases patient-derived mammosphere formation/self-renewal activity

The role of leptin in the regulation of BCSC activity was then evaluated by using patient-derived breast cancer cells isolated from metastatic ascites or pleural effusions. Tumor histology, grade, hormone receptors and HER2 status of the primary tumors were reported in Table 6.

Table 6. *Summary of metastatic patients-derived cancers.*

SAMPLE ID	AGE	SOURCE	Histology	GRADE	ER	PR	HER2
BB3RC29	70	ASC	UN	UN	POS	POS	NEG
BB3RC46	68	ASC	ILC	2	POS	POS	NEG
BB3RC50	46	ASC	IDC	2	POS	POS	NEG
BB3RC59[1]	69	ASC	ILC	2	POS	POS	NEG
BB3RC60	66	ASC	ILC	2	POS	POS	NEG
BB3RC65[2]	62	ASC	ILC	2	POS	POS	NEG
BB3RC66[1]	69	ASC	ILC	2	POS	POS	NEG
BB3RC70[2]	62	ASC	ILC	2	POS	POS	NEG
BB3RC71	48	PE	UN	3	POS	POS	POS
BB3RC79	UN	PE	IDC	3	NEG	NEG	NEG
BB3RC81	55	ASC	IDC	2	POS	POS	NEG
BB3RC84	UN	PE	UN	3	NEG	NEG	NEG
BB3RC90	66	PE	IDC/ILC	2	POS	POS	NEG
BB3RC92	61	ASC	IDC	1	POS	POS	NEG
BB3RC93	UN	ASC	UN	UN	POS	POS	NEG
BB3RC94	41	ASC	UN	UN	POS	POS	NEG

[1,2] These samples were obtained at different time points from the same patients

Sixteen patient-derived breast cancer samples were used in this study. Tumor histology and grade for metastatic samples (ASC and PE) relates to the primary cancer. Abbreviation: **UN** unknown, **PE** pleural effusion, **ASC** ascites sample, **ILC** invasive lobular carcinoma , **IDC** invasive ductal carcinoma, **POS** positive, **NEG** negative, **ER** Estrogen Receptor, **PR** Progesterone Receptor, **HER2,** epidermal growth factor receptor 2.

Mammosphere cultures treated with leptin resulted in a significant increase in MFE compared to untreated samples (n = 10, Figure 13A). Secondary mammosphere formation was observed only in four samples and treatment with leptin significantly increased self-renewal in three of them (Figure 13B). Besides, four human metastatic samples taken from patients with breast cancer were also treated with peptide LDFI. MFE induced by leptin was significantly decreased with the addition of LDFI (Figure 13C). Interestingly, treatment with peptide LDFI alone reduced the mammosphere formation, underlying how this peptide negatively interferes with leptin autocrine loop (Figure 13C). Then, to investigate the direct involvement of OBR in the regulation of mammosphere formation, OBR gene expression was analyzed in cells from metastatic ascites and pleural effusion fluids using microarray data. There was a significant direct correlation between the expression of OBR RNA in cells from the metastatic fluids and MFE ($r = 0.68$; $p = 0.05$, Figure 13D). In agreement with the microarray data obtained in

MCF-7 mammospheres, a significant correlation between MFE and HSP90 gene expression in the same metastatic patient-derived samples (r = 0.71; p = 0.036) was also observed (Figure 13E). These data suggest that patients with higher levels of OBR and HSP90 mRNAs in cells of metastatic fluids have greater ex vivo CSC activity.

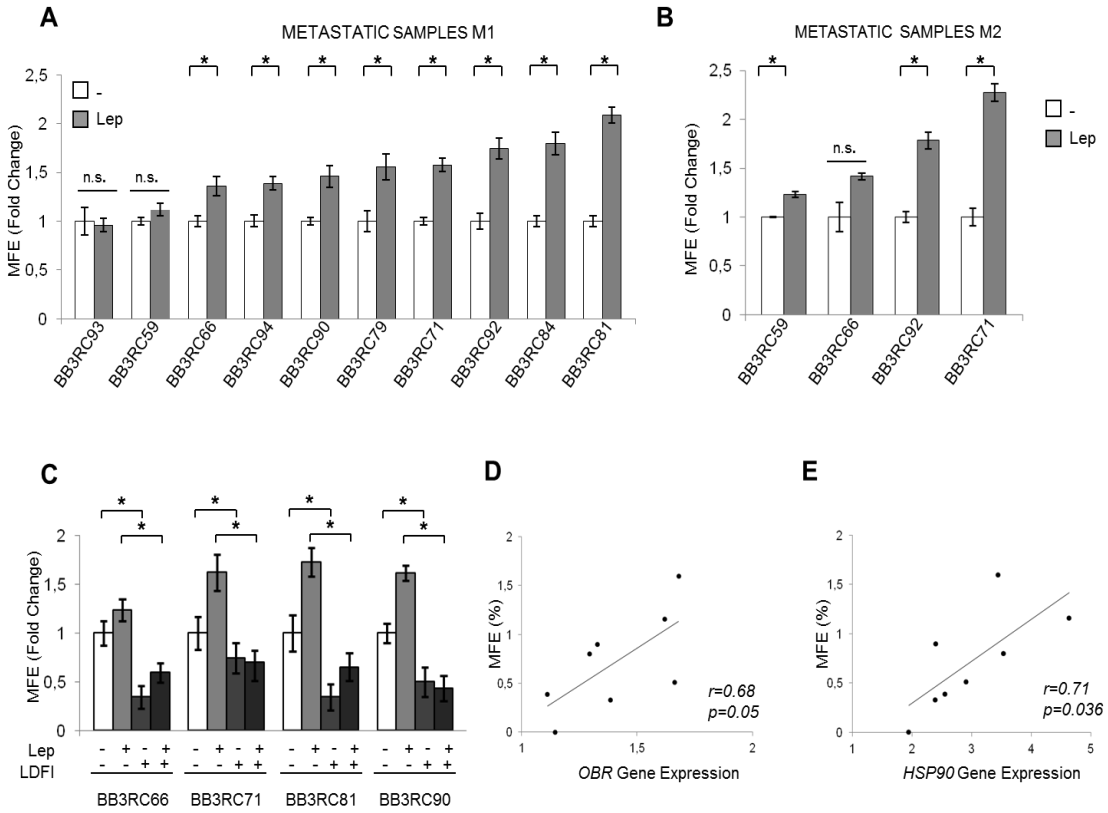

Figure 13: Leptin enhances mammospheres formation/self-renewal activity in patient-derived metastatic cells. 10 metastatic fluid samples obtained from breast cancer patients (BB3RC59/BB3RC66/BB3RC71–94) undergoing palliative drainage of symptomatic ascites or pleural effusions were used (Table 1). MFE in metastatic patient-derived cells grown as primary Metastatic sample M1 (A) or secondary Metastatic sample M2mammospheres (B) in the presence or absence (−) of Lep. C) MFE in 4 Metastatic sample M1 untreated (−) or treated with Lep, peptide LDFI (1 µg/ml), and Lep+LDFI. The values represent the means ± s.d. of three different experiments each performed in triplicate. *p < 0.05. n.s.: non significant. D-E) Correlation between OBR or HSP90 mRNA expression in cells of the metastatic fluids and MFE (8 patients/BB3RC29–70) (Pearson correlation coefficient, r = 0.68, p = 0.05; r = 0.71, p = 0.036, respectively).

OBR expression correlates with reduced overall survival in breast carcinomas

To investigate the clinical significance of OBR gene expression in human breast cancers the relationship between OBR levels and overall survival (OS) of breast cancer patients (n = 781) was estimated by Kaplan–Meier analysis. Survival curves indicated that women with high OBR expression exhibited a lower rate of OS than those with low OBR expression (HR = 1.9, p = 0.022) (Figure 14A). Similarly, breast carcinoma patients with high HSP90 expression had decreased OS compared with those with low HSP90 expression (HR = 2.2, p = 0.00017) (Figure 14B). Basal-like breast cancer is an aggressive tumor subtype, composed by primitive undifferentiated cells Indeed, basal-like breast tumors, which are enriched for CD44+/CD24− cells, exhibit epithelial–mesenchymal transition features and express high levels of stem cellregulatory genes (May CD *et al*., **2011**; Ben-Porath I *et al*., **2008**; Honeth G *et al*., **2008**; Park SY *et al*., **2010**; Sarrió D *et al*., **2008**). In agreement with these observations, the results of the Kaplan-Meier analysis indicated a more relevant discrimination in terms of overall survival between high and low expression of OBR and HSP90 in basal breast cancer patients (n = 143) (HR =4.4, p = 0.011; HR = 5.2, p = 0.013 respectively) (Figure 14C and 14D).

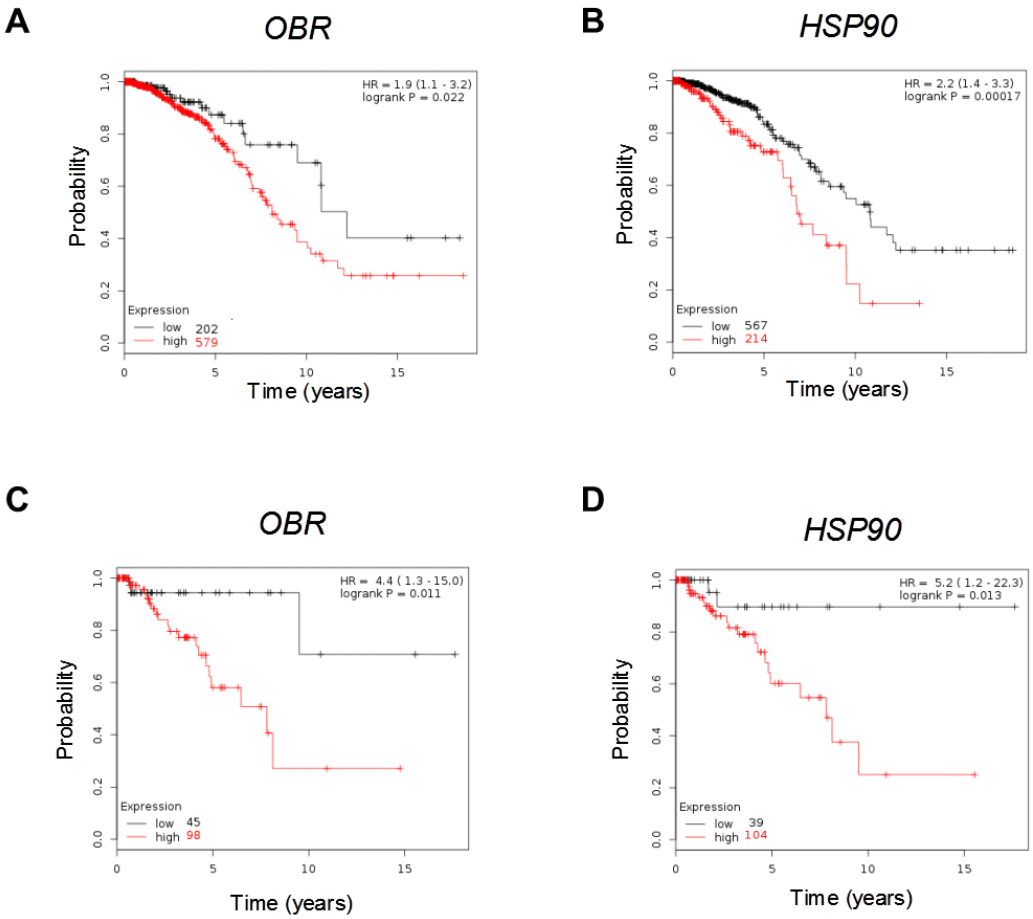

Figure 14: Correlation between OBR and HSP90 mRNA levels and overall survival in breast cancer. Kaplan–Meier survival analysis in breast carcinoma patients (n = 781) with high and low OBR (A) or HSP90 (B). expression analyzed as described in Materials and Methods. Kaplan–Meier survival analysis in basal breast cancer patients (n = 143) with high and low OBR (C) or HSP90 expression (D). Kaplan-Meier survival graph, and hazard ratio (HR) with 95% confidence intervals and logrank Pvalue.

AIM 2

Investigation of the role of NOTCH4 signaling in breast cancer stem cell activity induced by endocrine treatments

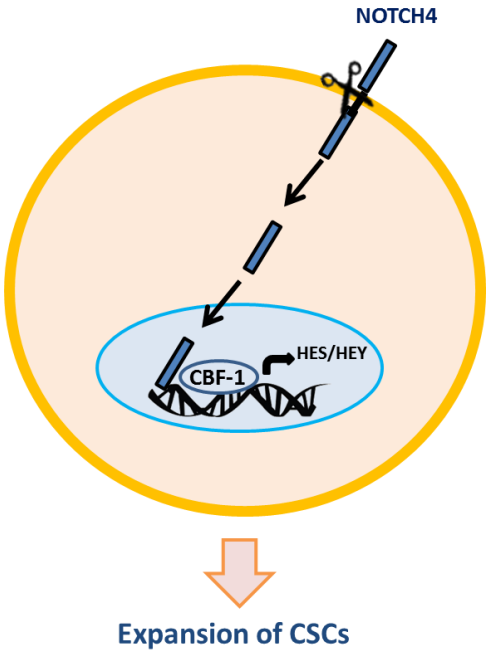

BCSC activity is enriched by Tamoxifen and Fulvestrant

Having shown that among the extrinsic signals, leptin is an important molecule that mediates the interaction between stromal cells and BCSCs, we next investigated the role of Notch4, as an intrinsic signal, on the regulation of BCSC activity, in particular induced by anti-estrogen treatments. First, we tested the effect of Tamoxifen on the mammosphere formation efficiency of patient-derived ER+ tumor cells, whose characteristics are summarized in table 7.

Table 7. Summary of metastatic patients-derived cancers.

SAMPLE ID	TYPE	GRADE	ER	PR	HER2	chemotherapy	Hormonal therapy	Targeted therapy
BB3RC49	IDC	2	+	+	-	FEC Paclitaxel	Letrozole Exemestane Tamoxifen	
BB3RC50	IDC	2	+	+	-	FEC Paclitaxel Capecitabine Vinorelbine	Anastrazole Exemestane Tamoxifen Fulvestrant	
BB3RC59[1] BB3RC61[1] BB3RC66[1]	ILC	2	+	+	-	EOX Capecitabine Paclitaxel	Letrozole Tamoxifen Exemestane Fulvestrant	
BB3RC68	IDC	2	+	ND	-	FEC Capecitabine Paclitaxel	Tamoxifen Fulvestrant	
BB3RC69[2] BB3RC70[2]	ILC	2	+	+	-	ECF	Tamoxifen Letrozole Anastrozole Fulvestrant	
BB3RC71	IDC	3	+	+	+	FEC Capecitabine Vinorelbine Docetaxel Epirubicin	Tamoxifen Anastrozole Fulvestrant Exemestane	Herceptin Lapatinib

[1,2] These samples were obtained at different time points from the same patients

Abbreviations: **IDC**: invasive ductal carcinoma; **ILC**: invasive lobular carcinoma; **FEC**: 5-FU, Epirubicin and Cyclophosphamide; **ECF**: Epirubicin, Cisplatin, 5-FU; **EOX**: Epirubicin, Oxaliplatin, Capecitabine; **ND**: not determined.
NB: ER, PR and HER2 were assessed in the primary breast cancer tissue sample.

Primary mammospheres cultured in the presence of ethanol (Control) or 10^{-6} M 4-hydroxy-tamoxifen (Tamoxifen) were dissociated and re-plated in secondary mammosphere suspension culture for a further 7–9 days to measure self-renewal of mammosphere initiating cells treated in the first generation. We found that Tamoxifen increases mammosphere self-renewal by about 2-fold (Figures 15A). Next, nine patient samples were grown in adherence and treated with Tamoxifen or Fulvestrant for 7-9 days to evaluate the ALDH activity, another functional assay for CSCs (Figure 15B). Our results showed a significant increase in ALDH enzymatic activity after Tamoxifen and

Fulvestrant treatment compared to the control condition (Figures 15C and 15D).These data suggest that endocrine therapies, given for a period of a few days, enrich for stem cell activity.

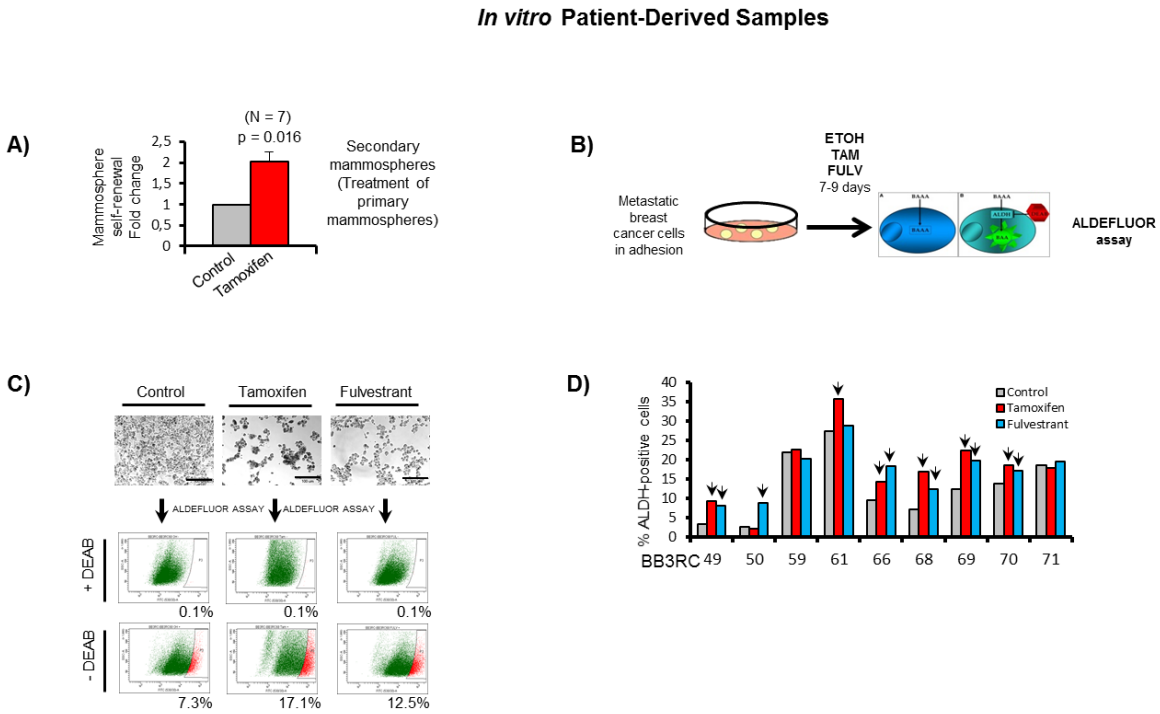

Figure 15: Tamoxifen or Fulvestrant treatment of ER+ patient-derived samples enriches for cells with CSC properties. A) Mammosphere self-renewal of freshly isolated ER+ early and metastatic patient-derived samples. p value was calculated with Wilcoxon signedrank test. B) metastatic BC cells were treated in adherence with Tamoxifene and Fulvestrant and then processed for FACS analysis. C) representative micrographs of metastatic BC cells before fluorescence-activated cell sorting (FACS) analysis of ALDH1 enzymatic activity (ALDEFLUOR assay). ALDH-positive cells were discriminated from ALDH-negative cells using the ALDH inhibitor DEAB. D) Percentage of ALDH-positive cells in nine ER+ metastatic BC patient-derived samples. Arrows indicate fold change greater than 20% compared to control.

Then, we tested the *in vivo* impact of endocrine therapies on stem cell activity in ER+ BC using PDXs grown subcutaneously in mice. We used both an early (HBCx34) and metastatic (BB3RC31) ER+ PDX tumor that both maintain biological characteristics, such as the expression of ER, PR and HER2 (Figure 16A) and estrogen dependence (Figure 16B) of the patient primary tumor from which they were derived. Using a 14-day *in vivo* ‘‘window’’ treatment (Figure 16C), we showed that both Tamoxifen and

Fulvestrant treatment decrease proliferation (Figure 16D). However, there is an increase in MFE and ALDH enzymatic activity (Figures 16E and 16F), suggesting a mechanism for endocrine resistance driven by enrichment for a stem cell phenotype.

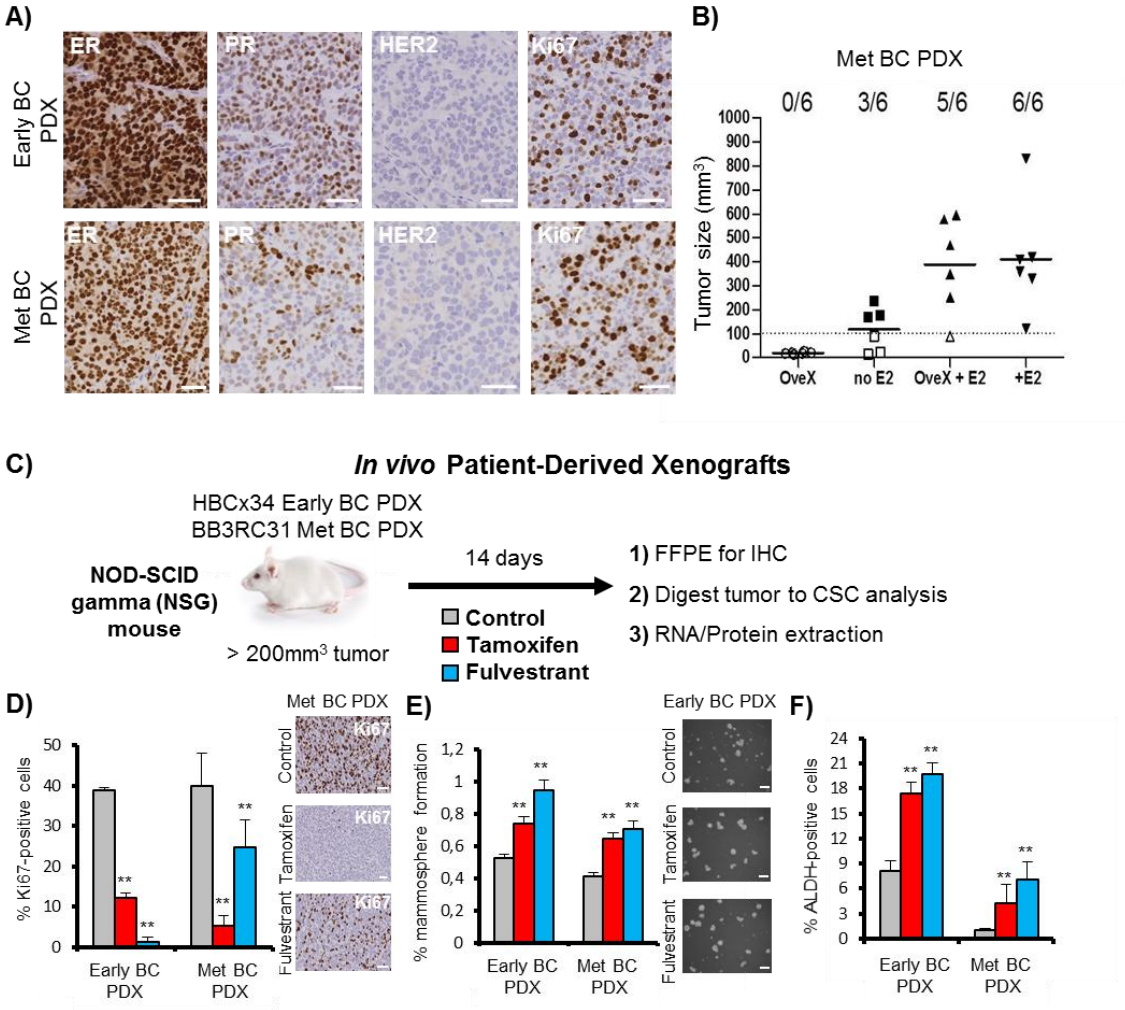

Figure 16: Tamoxifen or Fulvestrant treatment of ER+ patient-derived xenografts enriches for cells with CSC properties. A) Early (HBCx34) and metastatic (BB3RC31) xenograft tumor sections stained for ER, PR, HER2 and Ki67 by immunohistochemistry. Scale bars = 100µm. B) Ovariectomized mice and administration of estrogen in the drinking water (8µg/ml) were used to perform an estrogen dependence test of metastatic BB3RC31 PDX. Graph shows tumor formation and size at 120 days after implantation. Tumor formation was determined by counting tumors greater than 100 mm^3 (tumors bigger than 100 mm^3 are represented by solid forms and tumors smaller than 100 mm^3 are represented by hollow forms). Mean of each group is represented by horizontal bar. OveX- Ovariectomized; E2 – Estrogen. C–F) Early (HBCx34) and metastatic (BB3RC31) BC estrogen-dependent PDX tumors treated for 14 days with Tamoxifen (10 mg/kg/day, oral gavage; red bars) or Fulvestrant (200 mg/ kg/week, subcutaneous injection; blue bars). Gray bars correspond to vehicle control. FFPE, formalin-fixed paraffin-embedded. (D) Representative micrographs and quantification of Ki67 expression determined by immunohistochemistry (IHC). (E) Percentage of MFE. (F) ALDH-positive cells (%) determined using the ALDEFLUOR assay.

Tamoxifen or Fulvestrant treatment upregulates Notch target genes

Recently, the contribution of Notch pathway in endocrine therapy resistance has been reported by several studies (Magnani L *et al*., **2013**; O'Brien CS *et al*., **2011**; Yun J et al., **2013**). In particular, it has been demonstrated that Notch signaling is increased in endocrine therapies resistant cells and their growth can be abrogated by blocking Notch signalling, which is activated in these cells. According with these observations, we found, in ER+ cell lines, MCF-7, T47D, and ZR-75-1, an increased expression of Notch target genes, preferentially HEY1 and HES1, after Tamoxifen or Fulvestrant tratment for 6 days (Figure 17A). Similarly, in tamoxifen-resistant (TAMR) or fulvestrant-resistant (FULVR) MCF-7 models, which have acquired resistance after longterm Tamoxifen or Fulvestrant treatment, we found an upregulation of Notch target genes and increased Notch transcriptional activity (Figure 17B).

In addition, the BC PDX tumors treated *in vivo* with Tamoxifen or Fulvestrant for 2 weeks showed increased HEY1 and HES1 expression (Figure 17C), supporting an increased role for the Notch signaling pathway after endocrine therapies.

Taken together these data, strongly support the hypothesis that Notch signaling is highly activated in endocrine-resistance context.

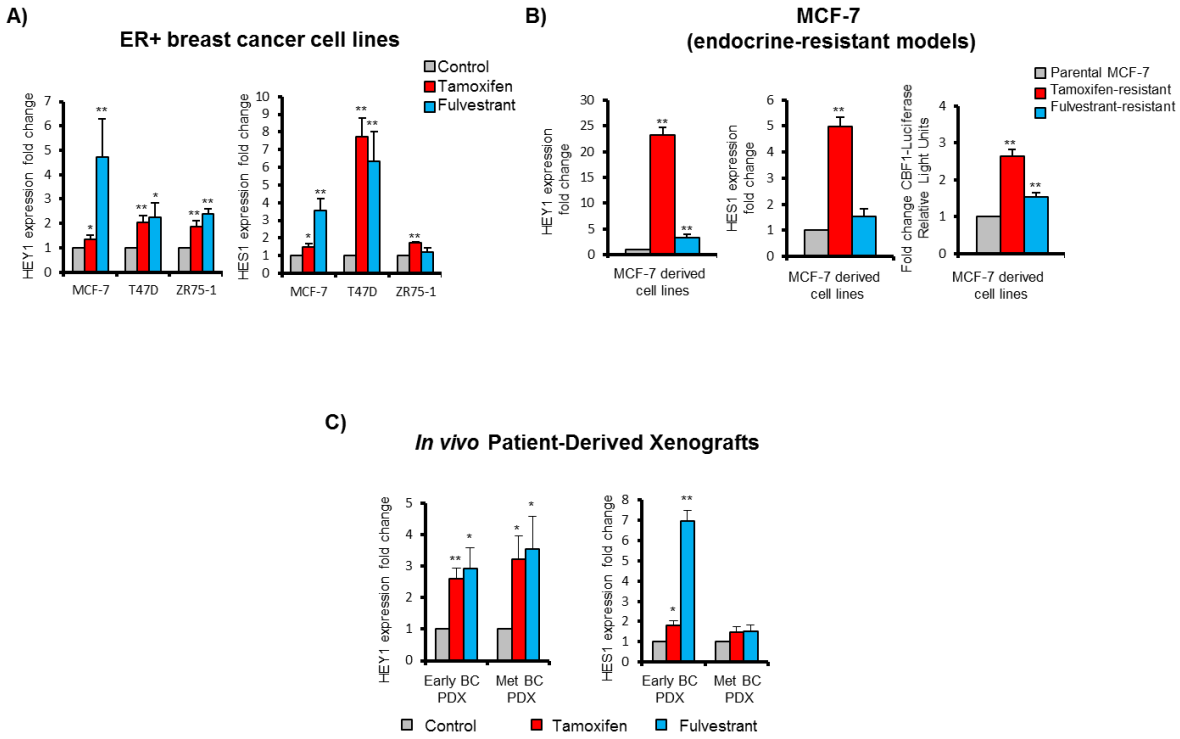

Figure 17: ***Tamoxifen or Fulvestrant treatment increases Notch target genes expression in ER+ cancer cell lines and ER+ patient-derived xenografts.*** A) Expression of Notch target genes HEY1 and HES1 was assessed by quantitative real-time PCR analysis and compared to control to determine fold change. MCF-7, T47D and ZR-75-1 cells were treated with 10^{-6} M tamoxifen (red bar) and 10^{-7} M fulvestrant (blue bar) for six days. B) Expression of HEY1 and HES1 in endocrine-resistant cells compared to the parental MCF-7 cells (two left hand panels). Notch transcriptional activity in endocrine-resistant cells compared to control was determined by relative firefly luciferase activity of 10x CBF1 reporter (right hand panel).C) Early (HBCx34) and metastatic (BB3RC31) BC PDXs: the effect of *in vivo* treatment for 14 days with tamoxifen (10 mg/kg/day, oral gavage) or fulvestrant (200 mg/kg/week, subcutaneous injection) on HEY1 and HES1. Data are represented as mean ± SEM. * $p < 0.05$, ** $p < 0.01$

JAG1 and NOTCH4 receptor signaling drives endocrine resistance

Notch pathway comprises five ligands in the sending cell that bind to any of four receptors present on the signal-receiving cell. In order to understand which Notch receptors and ligands are regulated by anti-estrogen treatments, we assessed their expression in parental, TAMR, and FULVR cell lines. NOTCH4, its intracellular domain (ICD) and HES1 were upregulated (figure 18A *left panel*) while NOTCH1, -2, and -3 were downregulated (Figure 18A *middle panel*) in the resistant versus parental cell lines. Moreover, the Notch ligand JAG1 was found to be highly expressed in both resistant

models, while the expression of ligands DLL1 and DLL4 was unchanged (Figure 18A *right panel*). JAG1 and NOTCH4-ICD were also upregulated after 14-day window treatment of PDXs *in vivo* and short-term treatment with Tamoxifen or Fulvestrant of MCF-7 cells *in vitro*, suggesting that activation of Notch signaling (demonstrated by increased HES1 expression) is an early event in the acquisition of endocrine resistance (Figures 18B and 18C).

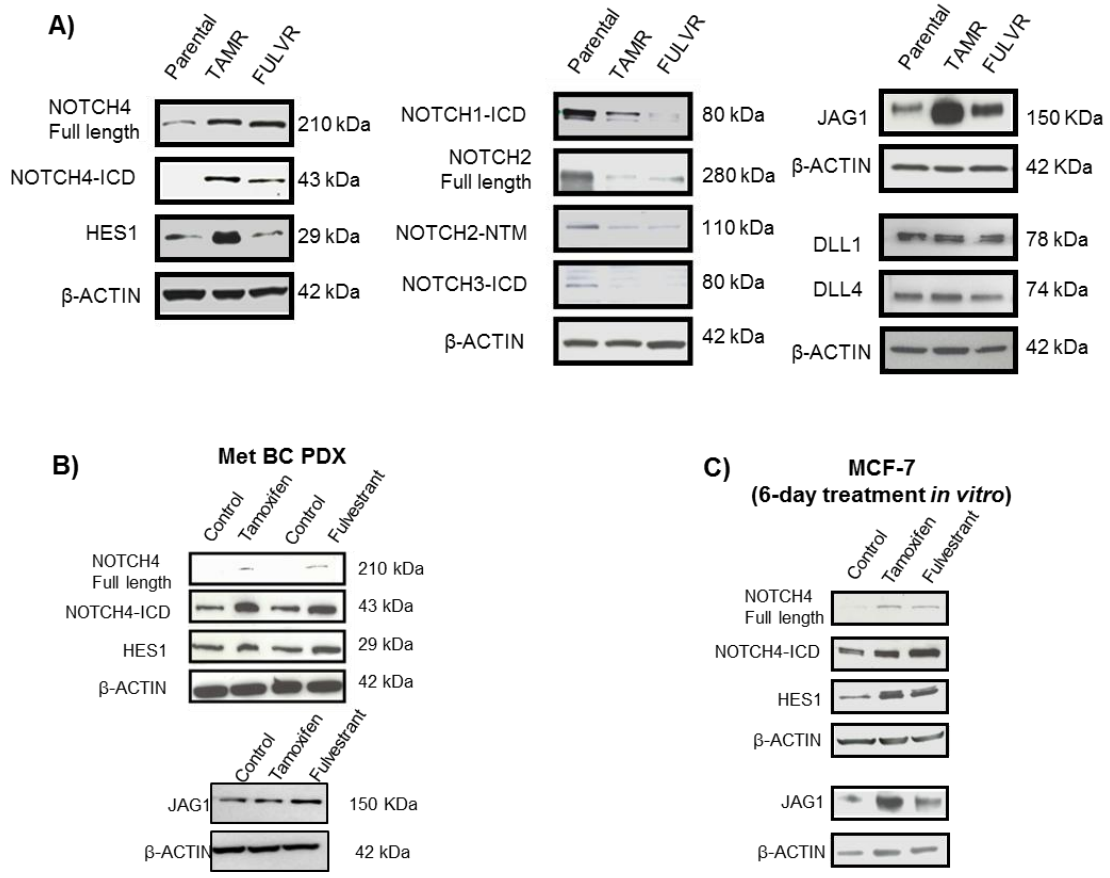

Figure 18: ***Notch receptors and ligands expression in the resistant models used in the study.*** A) Notch receptors and Notch ligands protein expression levels determined by Western Blot in MCF-7 endocrine-resistant cells. B) NOTCH4, HES1, and JAG1 protein expression levels determined by western blot in metastatic (Met) (BB3RC31) BC PDX. (C)NOTCH4, HES1 and JAG1 protein expression levels determined by Western Blot in MCF-7 cells treated with 10^{-6} M Tamoxifen and 10^{-7} M Fulvestrant for 6 days. β-actin was used as a reference for the loading control.

To further confirm the role of NOTCH4 activity in endocrine resistance and the stem cell phenotype, we analyzed loss-of-function phenotypes for NOTCH4-ICD in MCF-7 cells using CRISPR-cas9 approach.

We generated knockout clones of *NOTCH4* gene in MCF7 cells using a D10A mutant version of Cas9 (nickase) with a pair of sgRNAs complementary to opposite strands of the target sites.

First, MCF-7 cells were transfected with sgRNAs targeting the exon 2 of *NOTCH4* and then we isolated clones after 2-3 weeks following single-cell sorting. Genomic alterations were screened using primers flanking the CRISPR target sites and Sanger sequencing was performed to confirm PCR results. The absence of wild-type alleles was assessed either by cloning or by using specific restriction enzymes for target sequences (Figure 19).

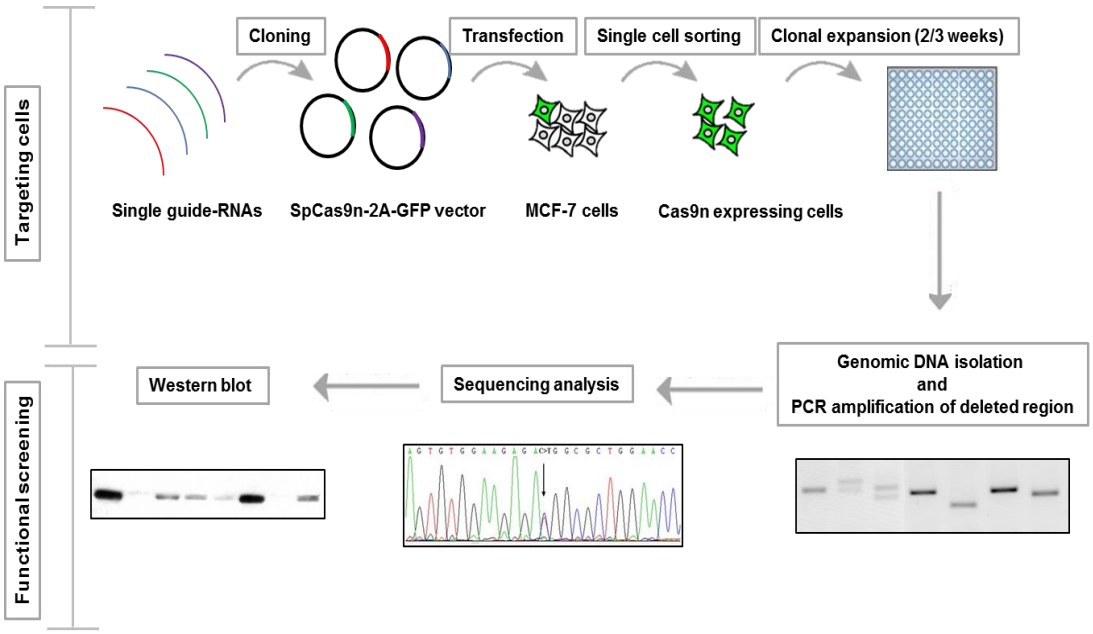

Figure 19. Steps for design, construction, clonal expansion, validation of CRISPR-cas9 technology. sgRNAs were cloned into PX461 vector. After 48h post-trasfection, GFP+ cells were sorted and plated as single cells for clonal expansion. After 14 days, clones were characterized to identify the ones having indel mutations at the target region, by PCR and Sanger Sequencing. Knockout clones were confirmed by Western Blot.

Among several clones, we selected one characterized by a deletion of 19 nucleotides and a deletion of 170 nucleotides, which comprises the entire exon 2 (Figure 20B). A very small amount of NOTCH4-ICD was detected by WB (Figure 20A) even though N4EX2 clone contains a frameshift deletion in both alleles, which we hypothesize to be

due to a small amount of in-frame RNA produced by whole exon 3 skipping, i.e., by splicing of exon 1 donor site to the acceptor sites of exons that are in-frame.

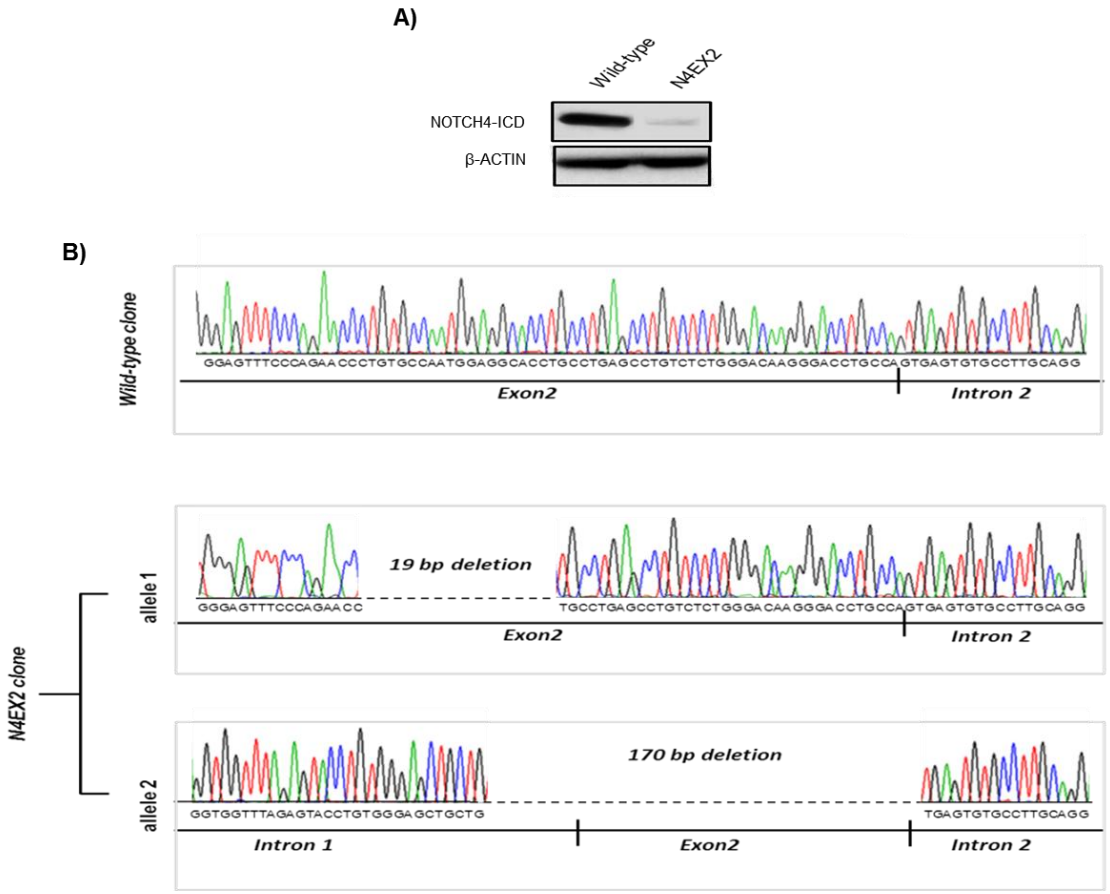

Figure 20. Characterization of N4EX2 clone used in this study. A) NOTCH4 - intracellular domain (ICD) protein levels were determined in wild-type and N4EX2 CRISPR clone by Western Blot. B) Sanger sequencing of wild-type and NOTCH4 CRISPR targeted clone (N4EX2 clone) showing a deletion of 19 nucleotides in the exon 2 and a deletion of 170 nucleotides, which comprises the entire exon 2.

Wild-type MCF-7 cells and the CRISPR clone (N4EX2 cells) were treated in adherence with ethanol, 10^{-6} M Tamoxifen, and 10^{-7} M Fulvestrant for 6 days. N4EX2 clone displayed a significant inhibition of MFE and ALDH-positive cells, especially after Tamoxifen and Fulvestrant treatments, compared to wild-type clone (Figure 21A). In contrast, overexpression of NOTCH4-ICD or JAG1 conferred Tamoxifen and Fulvestrant resistance in parental MCF-7 cells (Figures 21B and 21C). Overall, these results indicate that JAG1 ligand and cleavage of NOTCH4-ICD may be responsible for Notch signaling activation after endocrine treatment, which is in agreement with recent reports that

NOTCH4 expression is increased in TAMR cell lines (Yun *et al*., **2013**; Lombardo *et al*., **2014**).

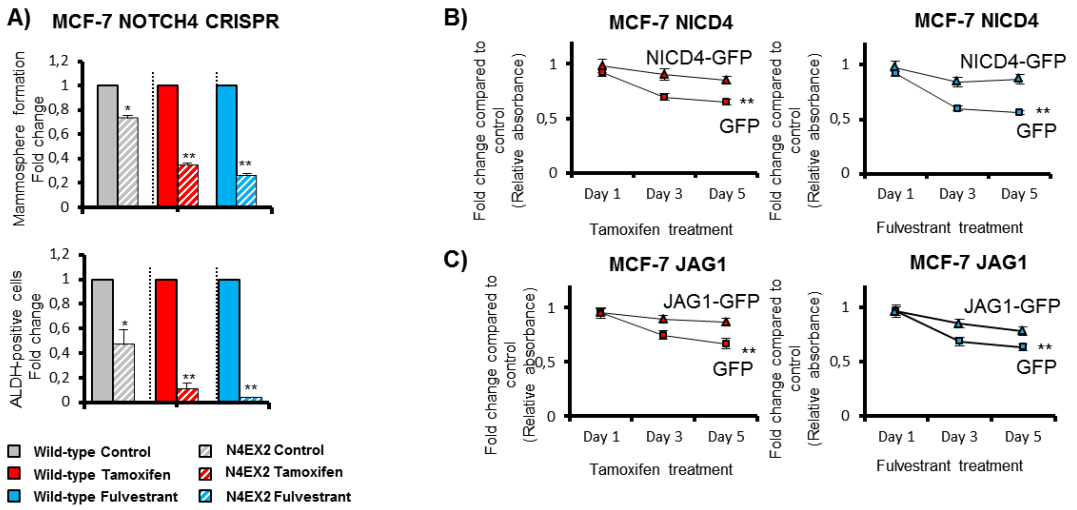

Figure 21. BCSC activity in Notch4 gain or loss of function studies. N4EX2 cells fold change of MFE and ALDH-positive cells after treatments was compared to that of the wild-type cells (A) NICD4 and JAG1 rescue tamoxifen or fulvestrant-inhibited growth: cell number (using sulforhodamine B [SRB] assay, y axis) of MCF-7 overexpressing (B) NICD4-GFP, (C) JAG1-GFP, or GFP control incubated with tamoxifen or fulvestrant for 1, 3, and 5 days (x axis) compared to the respective cell line treated with control ethanol. p values are for the 5-day treatment. Data are represented as mean ± SEM. *p < 0.05; **p < 0.01.

GSI RO4929097 abrogates Tamoxifen and Fulvestrant stimulated CSC activity

In order to confirm the role of NOTCH4 signaling in mediating the effects decribed above, we tested whether the gamma-secretase inhibitor (GSI) RO4929097 would abrogate increases in MFE and ALDH-positive cells induced *in vivo* by anti-estrogens administered in short-term window treatments, ER+ PDX tumors. Tamoxifen and fulvestrant treatments reduced tumor growth (Figure 22A) while increased both MFE and ALDH activity (Figures 22B and 22C). RO4929097 had no impact on tumor growth but significantly inhibited endocrine-stimulated MFE and ALDH activity.

The gold standard for functionally determining tumor-initiating cells is xenograft formation in secondary mouse hosts, which we performed using dissociated cells from PDX tumors treated *in vivo* with anti-estrogens and/or RO4929097. Cells isolated from

tumors treated *in vivo* with RO4929097 had significantly reduced tumor-initiating capacity 90 days post-implantation (Figure 22D). Furthermore, the stimulation of tumorigenicity following *in vivo* tamoxifen and fulvestrant treatment was completely reversed by RO4929097 (Figure 22D). Overall, these data suggest that BCSCs, measured by tumor-initiating activity and enriched by short-term anti-estrogen treatments, are dependent on NOTCH4 signaling that can be blocked by combination treatment with a NOTCH4 inhibitor.

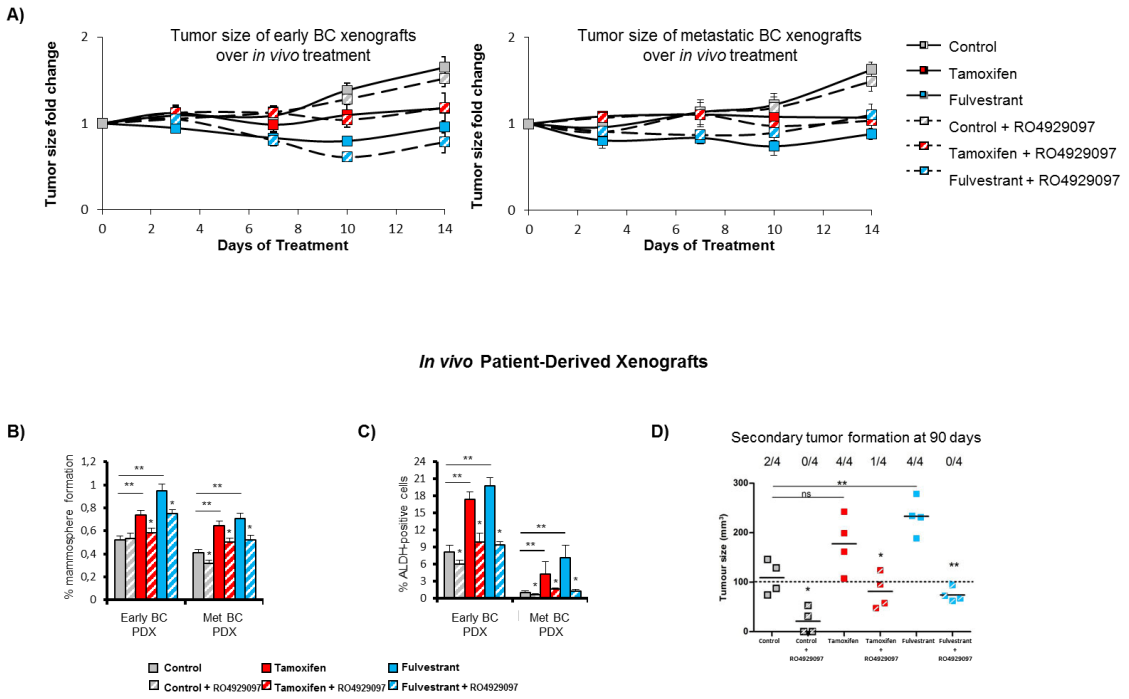

Figure 22. NOTCH4 Inhibition using RO4929097 Abrogates Tamoxifen and Fulvestrant Enrichment of CSC Activities. *A*) Early (HBCx34) and metastatic (BB3RC31) PDXs tumor size variation over 14 days *in vivo* treatments with Tamoxifen (10mg/kg/day, oral gavage) or Fulvestrant (200mg/kg/week, subcutaneous injection) in the presence or absence of the gamma-secretase inhibitor RO4929097 (3mg/kg/day, oral gavage). Tumor size was determined every 3-4 days and fold change was calculated by dividing the tumor size by the size of the respective tumor at day 0. (B) MFE (%). (C) Percentage of ALDH-positive cells. (D) Secondary tumor formation. 100,000 cells of metastatic (BB3RC31) PDX were re-implanted subcutaneously in NSG mice with 90-days low-release estrogen pellets. Tumor growth (>100 mm3) was determined at day 90 after cell injection.

Discussion

Breast cancer is the most common malignancy in women worldwide. Despite advances over the last decades in breast cancer management, this malignancy is still the most common cause of cancer-related mortality among women worldwide.

Breast cancer is considered an heterogeneous disease and it has been classified into different molecular subtypes, defined by gene expression profile, that correlate with clinical behavior and are used to refine therapeutic strategies (Arteaga CL, **2013**, Pinto CA *et al*., **2013**). In the majority of breast cancer cases, treatment failure still occurs, mainly due to metastatic process and resistance to conventional therapy. This might suggest the involvement of a subpopulation of tumor cells able to resist to treatment and to regenerate tumor, also at distant sites. It has been hypothesized that breast cancer stem cells are involved in the process of tumor growth and metastases. Due to their self-renewing and differentiation capabilities, they are now considered the underlying factor in tumor recurrence and the main reason for therapy resistance.

Therefore, the characterization of breast cancer stem cells and a better knowledge about the factors regulating their activity, may contribute to the development of more effective treatment strategies in order to prevent tumor relapse and metastasis.

Our findings contributed to elucidate the role of the extrinsic signals arising from the tumor microenvironment in the regulation of breast cancer stem cell activity. In paricular, we identified, for the first time, leptin as an important paracrine molecule that mediates the interaction between stromal cells and BCSCs, providing novel insights into understanding how CSCs are influenced by the tumor microenvironment (**AIM1**). Next, we focused on the study of intrinsic factors, in particular Notch4 signaling in the regulation of cancer stem cell behaviour. We found that Notch4 plays a crucial role in the enrichment of cancer stem cell population induced by anti-estrogen treatments. Therefore, our investigations provide the rationale for the use of NOTCH4 inhibitors together with anti-estrogen treatments in order to overcome resistance to endocrine therapy and to reduce tumor relapse (**AIM2**).

Leptin as a mediator of tumor stromal interactions mediates BCSC activity

The heterotypic signals arising in the tumor-associated stroma have been shown to be important in inducing and maintaining a stem-like state in the tumor cells through either the secretion of soluble molecules or cell–cell communication (Pattabiraman DR *et al*., **2014**; Beck B *et al*., **2013**). Particularly, in the case of breast carcinoma, it has been reported that various types of stromal cells via growth factors and cytokines may enhance the proliferation and survival of BCSCs, induce angiogenesis, and recruit tumor-associated macrophages and other immune cells, which in turn secrete additional factors promoting tumor cell invasion and metastasis (Korkaya H. *et al*., **2011**). Here we demonstrated, for the first time, that leptin and its receptor play a crucial role in mediating the interaction between stromal cells (CAFs and adipocytes) and BCSCs. The initial conditioned media experiments indicated that the entire complement of secretory proteins released by CAFs and adipocytes significantly increase MFE/self-renewal in breast cancer cells. An important role is played by leptin as fundamental environmental regulator of CSCs in the cancer stem niche. Indeed, either leptin immunodepletion from CAF- and adipocyte-derived CM or inhibition of leptin signaling by using peptide LDFI, a small-molecule that acts as a full leptin receptor antagonist (Catalano S *et al*., **2015**), reduced the effects of CM on mammosphere formation. Gene expression profiling revealed a significant overlap of regulated genes in mammosphere cells following treatment with CAF-, adipocyte-derived CM or leptin. Of particular interest was the observation that genes commonly expressed in all treated-samples include several of those involved in stemness. Among these, the polycomb gene BMI1, which has been reported to play an important role in self-renewal of stem cells and has a positive correlation with clinical grade/stage and poor prognosis (Siddique HR *et al*., **2012**), was one of the most highly induced in all treated cells. One of the features of CSCs is the uncontrolled proliferation, perhaps due to a reduced responsiveness to negative growth regulators or to the loss of contact inhibition and gap junction intercellular communication (Trosko JE *et al*., **2004**). Our results clearly evidenced that a number of genes involved in cell cycle control showed a similar expression profile upon treatment with stromal-CM and leptin. Another

family of genes, crucial in sustaining self-renewal of stem cells (Isolani ME *et al*., **2012**), is the heat shock protein family. We have previously demonstrated that the HSP90, a main functional component of this chaperone complex, is a target of leptin in breast cancer cells (Giordano C *et al*., **2013**). Our microarray data showed that some transcripts of the HSP family were upregulated in stromal-CM and leptin-treated samples. Thus, since the expression pattern of genes regulated by leptin and involved in stem cell biology closely mirrors those modulated by stromal cells, it is reasonable to speculate that leptin may represent a critical paracrine molecule in mediating the microenvironment effects on BCSC activity. It has been reported that leptin is able to regulate and activate several signaling pathways and oncogenes which are critically implicated in BCSCs (Zhou J *et al*., **2007**; Pratt MA *et a*l., **2009**; Guo S *et al*., **2011**; Knight BB *et al*., **2011**; Guo S *et al*., **2012**) and leptin deficiency in MMTV-Wnt-1 transgenic mice results in functional depletion of BCSCs leading to less tumor outgrowth (Zheng Q *et al*., **2011**). Moreover, the expression of the leptin receptor is a characteristic feature of CSCs, which exhibit an increased response to leptin including phosphorylation and activation of STAT3 and induction of stem cell markers, as OCT4 and SOX2 (Feldman DE *et al*., **2012**) . More recently, it has also been demonstrated that OBR is necessary for maintaining a CSC-like state in TNBC cells (Zheng Q *et al*., **2013**) and high OBR expression induced by the adiposity-leptin enriched environment generates a population with enhanced CSC properties and tumorigenic capacity (Chang CC *et al*., **2015**). Our studies extended these previous findings by demonstrating a direct involvement of leptin in sustaining breast cancer cell behavior using both breast cancer cell lines and metastatic breast cancer patient-derived cells. We found that MCF-7 mammospheres exhibited increased OBRmRNA expression, while OBR silencing caused a significant reduction in the sphere-forming efficiency. Treatment with leptin induced an increase in MFE, self-renewal and an enhanced percentage of CD44+/CD24- cell population, through the activation of the classical signaling pathways. Importantly, we also showed that leptin is able to increase the mammosphere formation and self-renewal activity in metastatic breast cancer cells isolated from patients. Moreover, OBRmRNA expression, analyzed in cells from metastatic fluids, directly correlated with mammosphere formation activity *ex vivo*. In agreement with our data of gene expression profile, a significant positive correlation

between MFE and HSP90 mRNA gene expression in the same metastatic patient-derived samples was observed. It has been previously reported that high-grade tumors associated with poor prognosis display an enrichment of BCSCs (Farnie G *et al*., **2007**; Pece S *et al*., **2010**). Here, using Kaplan-Meier analysis we found that OBR expression, which is crucial in maintaining stem cell phenotype, correlated with reduced overall survival in breast carcinomas suggesting its potential role as a prognostic factor. Interestingly, in TNBC patients, a more relevant discrimination in terms of overall survival between high and low expression of OBR could be observed. Finally, we demonstrated that blocking leptin signaling by using the peptide LDFI significantly reduced mammosphere formation in metastatic breast cancer patient-derived cells, suggesting that strategies aimed at inhibiting leptin signaling represent a rationale therapeutic approach to target cancer stem cells. In conclusion, our findings identify, for the first time, leptin as an important paracrine molecule that mediates the interaction between stromal cells and BCSCs, providing novel insights into understanding how CSCs are influenced by the tumor microenvironment. As clinical implications, these data suggest that targeting leptin/leptin receptor signaling generated in the microenvironment may be useful for BCSC eradication and eventually to prevent recurrence and metastasis in patients with breast carcinoma (Figure 23).

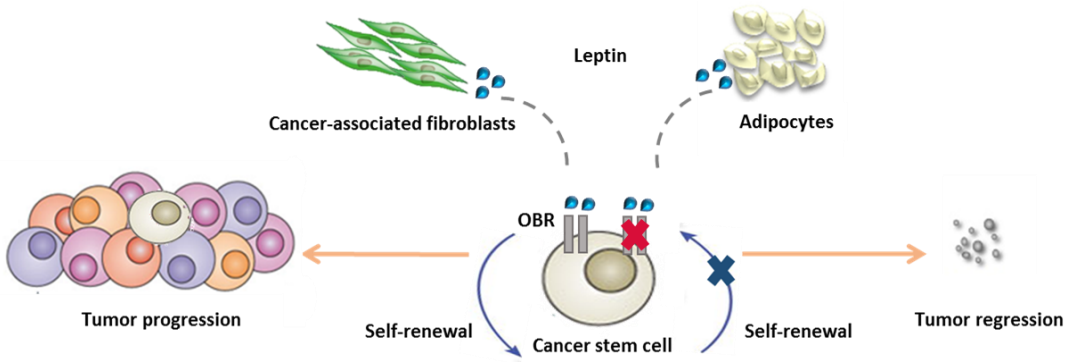

Figure 23. *Schematic representation suggesting that Leptin secreted by stromal cells, CAFs and adopocytes, regulates BCSC activity and it might be responsible of tumor progression (left hand figure). Targeting leptin/leptin receptor signaling generated in the microenvironment may represent an useful strategy for BCSCs eradication and tumor regression (right hand figure).*

Role of NOTCH4 signaling in breast cancer stem cell activity induced by endocrine treatments

Around 75% of breast cancers express estrogen receptor (ER) and are treated with anti-estrogen adjuvant therapies to suppress ER mediated estrogen signaling. (Ali S & Coombes RC **2002**). However, resistance to endocrine therapy frequently occurs in ER+ breast cancer cases and it remains a major challenge in providing effective treatments for these patients. In order to overcome endocrine resistance, intensive research has been conducted to understand the underlying mechanisms and a large body of evidence suggest that cancer stem cells (CSCs) are key in driving cancer metastasis and therapy resistance.

Here, we report that BCSC activity is increased in response to the common endocrine therapies Tamoxifen and Fulvestrant in ER+ patient samples. In addition, using a 14-day *in vivo* ‘‘window’’ treatment, we showed that both Tamoxifen and Fulvestrant treatment are able to decrease proliferation of early and metastatic PDx, while there is an increase in MFE and ALDH enzymatic activity. Our findings suggest that endocrine therapies do not target BCSCs, and this may explain how residual drug-resistant cells are responsible for the relapse of ER+ tumors following hormonal therapy. Although we observe increased BCSC frequency after endocrine treatments, we do not know whether absolute BCSC numbers remain the same and are selected for or whether they can be induced by anti-estrogen treatment.

On the basis of recent observations suggesting a crucial role of Notch pathway in endocrine therapy resistance (Lombardo Y *et al*., **2014**), we investigated its possible involvement in the enrichment of BCSCs after anti-estrogen exposure. We found, in ER+ cell lines and BC PDX tumors, an increased expression of Notch target genes, preferentially HEY1 and HES1, after short-term tamoxifen or fulvestrant treatment. Similarly, in tamoxifen-resistant (TAMR) or fulvestrant-resistant (FULVR) MCF-7 models, Notch target genes expression and its transcriptional activity were significantly up-regulated. Thus our findings, strongly underline the important role of Notch signaling in endocrine-resistance context.

Moreover, according to Harrison et al. work that identifies NOTCH4 receptor as a crucial player in BCSC activity (Harrison H *et al*., **2010**), we found this receptor and its ligand significantly upregulated in the resistant cell lines, as well as in anti-estrogen treated PDXs *in vivo*.

The best described strategy for inhibition of Notch signaling is the use of small-molecule GSIs, which prevent the release of Notch ICD (NICD). In our study, the GSI RO4929097 specifically targets NOTCH4 cleavage in anti-estrogen-treated cells and, thus, decreases BCSC activity *in vitro* (MFE and ALDH activity) and tumor initiation *in vivo*. Our investigations in ER+ PDX tumors provide the rationale for the use of NOTCH4 inhibitors together with endocrine therapies in the adjuvant or advanced settings (Figure 24). In conclusion, our data establish that tamoxifen and fulvestrant select for stem cell activity in short- and long-term treated BC cells, as well as in early and metastatic-endocrine-treated patient-derived samples and PDXs. Overall, these results suggest that ER+ BC recurrence after endocrine therapies, which target the majority of cells, will be reduced by targeting the JAG1+/NOTCH4+ BCSC population.

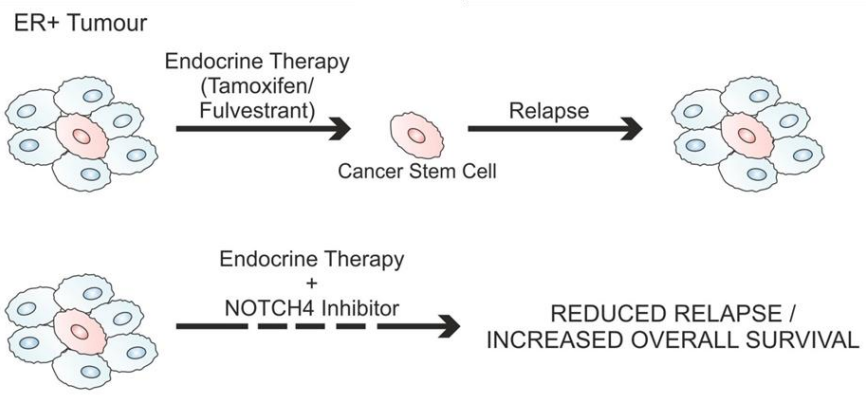

Figure 24. *Diagram suggesting that endocrine therapies do not target BCSCs and emphasizing the need of targeting residual drug-resistant cells to eliminate all cancer cells and prevent long-term recurrences of ER+ BC.*

Conclusions

Our study highlitghs the important role of both intrinsic and extrinsic factors in the regulation of BCSC activity and provides new possible strategies for BCSCs eradication to improve the clinical outcome of breast cancer patients. In particular, assessed the role of leptin as an important paracrine molecule that mediates the interaction between stromal cells and BCSCs, we can conclude that blocking leptin/leptin receptor signaling may represent a potential therapeutic target to reduce disease progression. Moreover, among the intrinsic signals, we identified Notch4 as a crucial player in driving endocrine resistance depending on BCSC activity, and we can speculate that the use of NOTCH4 inhibitors together with anti-estrogen treatments may be useful to overcome resistance to endocrine therapy and to reduce tumor relapse.

References

Al-Hajj M, Wicha MS, Benito-Hernandez A, Morrison SJ, Clarke MF. Prospective identification of tumorigenic breast cancer cells. Proceedings of the National Academy of Sciences of the United States of America. (2003) 100 (7):3983–3988.

Ali S, Coombes RC. Endocrine-responsive breast cancer and strategies for combating resistance. Nat Rev Cancer. (2002) Feb; 2(2):101-12.

Andò S, Barone I, Giordano C, Bonofiglio D, Catalano S. The Multifaceted Mechanism of Leptin Signaling within Tumor Microenvironment in Driving Breast Cancer Growth and Progression. Front Oncol. (2014) Nov 26; 4:340.

Arteaga CL. Progress in breast cancer: overview. Clin Cancer Res. (2013) Dec 1; 19(23):6353-9.

Barone I, Catalano S, Gelsomino L, Marsico S, Giordano C, Panza S, Bonofiglio D, Bossi G, Covington KR, Fuqua SA, Andò S. Leptin mediates tumor-stromal interactions that promote the invasive growth of breast cancer cells. Cancer Res. (2012) Mar 15; 72(6):1416-27.

Beck B, Blanpain C. Unravelling cancer stem cell potential. Nat Rev Cancer. (2013) Oct; 13(10):727-38.

Ben-Porath I, Thomson MW, Carey VJ, Ge R, Bell GW, Regev A, Weinberg RA. An embryonic stem cell-like gene expression signature in poorly differentiated aggressive human tumors. Nat Genet. (2008) May; 40(5):499-507.

Catalano S, Leggio A, Barone I, De Marco R, Gelsomino L, Campana A, Malivindi R, Panza S, Giordano C, Liguori A, Bonofiglio D, Liguori A, Andò S. A novel leptin antagonist peptide inhibits breast cancer growth in vitro and in vivo. J Cell Mol Med. (2015) May; 19(5):1122-32.

Chang CC, Wu MJ, Yang JY, Camarillo IG, Chang CJ. Leptin-STAT3-G9a Signaling Promotes Obesity-Mediated Breast Cancer Progression. Cancer Res. (2015) Jun 1; 75(11):2375-86.

Cirillo D, Rachiglio AM, la Montagna R, Giordano A, Normanno N. Leptin signaling in breast cancer: an overview. J Cell Biochem. (2008) Nov 1; 105(4):956-64.

Davies C, Godwin J, Gray R, Clarke M, Cutter D, Darby S, McGale P, Pan HC, Taylor C, Wang YC, Dowsett M, Ingle J, Peto R. Relevance of breast cancer hormone receptors and other factors to the efficacy of adjuvant tamoxifen: patient-level meta-analysis of randomised trials. Lancet. (2011) Aug 27; 378(9793):771-84.

Dontu G, Abdallah WM, Foley JM, Jackson KW, Clarke MF, Kawamura MJ, Wicha MS. In vitro propagation and transcriptional profiling of human mammary stem/progenitor cells. Genes Dev. (2003) May 15; 17(10):1253-70.

Farnie G, Clarke RB, Spence K, Pinnock N, Brennan K, Anderson NG, Bundred NJ. Novel cell culture technique for primary ductal carcinoma in situ: role of Notch and epidermal growth factor receptor signaling pathways. J Natl Cancer Inst. (2007) Apr 18;99(8):616-27.

Feldman DE, Chen C, Punj V, Tsukamoto H, Machida K. Pluripotency factor-mediated expression of the leptin receptor (OB-R) links obesity to oncogenesis through tumor-initiating stem cells. Proc Natl Acad Sci U S A. (2012) Jan 17; 109(3):829-34.

Giordano C, Vizza D, Panza S, Barone I, Bonofiglio D, Lanzino M, Sisci D, De Amicis F, Fuqua SA, Catalano S, Andò S. Leptin increases HER2 protein levels through a STAT3-mediated up-regulation of Hsp90 in breast cancer cells. Mol Oncol. (2013) Jun; 7(3):379-91.

Gyorffy B, Lanczky A, Eklund AC, Denkert C, Budczies J, Li Q, Szallasi Z. An online survival analysis tool to rapidly assess the effect of 22,277 genes on breast cancer prognosis using microarray data of 1,809 patients. Breast Cancer Res Treat. (2010); 123:725–731.

Guo S, Gonzalez-Perez RR. Notch, IL-1 and leptin crosstalk outcome (NILCO) is critical for leptin-induced proliferation, migration and VEGF/VEGFR-2 expression in breast cancer. PLoS One (2011) 6:e21467.

Guo S, Liu M, Wang G, Torroella-Kouri M, Gonzalez-Perez RR. Oncogenic role and therapeutic target of leptin signaling in breast cancer and cancer stem cells. Biochim Biophys Acta (2012); 1825:207–22.

Harrison H, Farnie G, Howell SJ, Rock RE, Stylianou S, Brennan KR, Bundred NJ, Clarke RB. Regulation of breast cancer stem cell activity by signaling through the Notch4 receptor. Cancer Res. (2010) Jan 15;70(2):709-18.

Honeth G, Bendahl PO, Ringnér M, Saal LH, Gruvberger-Saal SK, Lövgren K, Grabau D, Fernö M, Borg A, Hegardt C. The CD44+/CD24- phenotype is enriched in basal-like breast tumors. Breast Cancer Res. (2008); 10(3):R53.

Ishikawa M, Kitayama J, Nagawa H. Enhanced expression of leptin and leptin receptor (OB-R) in human breast cancer. Clin Cancer Res. (2004) Jul 1; 10(13):4325-31.

Isolani ME, Conte M, Deri P, Batistoni R. Stem cell protection mechanisms in planarians: the role of some heat shock genes. Int J Dev Biol. (2012); 56(1-3):127-33.

Jemal A, Siegel R, Xu J, Ward E. Cancer statistics, 2010. CA Cancer J Clin. (2010) Sep-Oct; 60(5):277-300.

Kakarala M, Wicha MS. Implications of the cancer stem-cell hypothesis for breast cancer prevention and therapy. J Clin Oncol. (2008) Jun 10; 26(17):2813-20.

Knight BB, Oprea-Ilies GM, Nagalingam A, Yang L, Cohen C, Saxena NK. Survivin upregulation, dependent on leptin-EGFR-Notch1 axis, is essential for leptin-induced migration of breast carcinoma cells. Endocr Relat Cancer (2011); 18:413–28.

Korkaya H, Liu S, Wicha MS. Breast cancer stem cells, cytokine networks, and the tumor microenvironment. J Clin Invest. (2011) Oct; 121(10):3804-9.

Li X, Lewis MT, Huang J, Gutierrez C, Osborne CK, Wu MF, Hilsenbeck SG, Pavlick A, Zhang X, Chamness GC, Wong H, Rosen J, Chang JC. Intrinsic resistance of tumorigenic breast cancer cells to chemotherapy. J Natl Cancer Inst. (2008) May 7; 100(9):672-9.

Liu S, Dontu G, Wicha MS. Mammary stem cells, self-renewal pathways, and carcinogenesis. Breast Cancer Res. (2005); 7(3):86-95.

Lombardo Y, Filipović A, Molyneux G, Periyasamy M, Giamas G, Hu Y, Trivedi PS, Wang J, Yagüe E, Michel L, Coombes RC. Nicastrin regulates breast cancer stem cell properties and tumor growth in vitro and in vivo. Proc Natl Acad Sci U S A. (2012) Oct 9; 109(41):16558-63.

Magnani L, Stoeck A, Zhang X, Lanczky A, Mirabella AC, Wang TL, Gyorffy B, Lupien M: Genome-wide reprogramming of the chromatin landscape underlies endocrine therapy resistance in breast cancer. Proc Natl Acad Sci U S A (2013) Apr 16; 110:E1490–E1499.

May CD, Sphyris N, Evans KW, Werden SJ, Guo W, Mani SA. Epithelial-mesenchymal transition and cancer stem cells: a dangerously dynamic duo in breast cancer progression. Breast Cancer Res. (2011) Feb 8; 13(1):202.

Miyoshi Y, Funahashi T, Tanaka S, Taguchi T, Tamaki Y, Shimomura I, and Noguchi S. High expression of leptin receptor mRNA in breast cancer tissue predicts poor prognosis for patients with high, but not low, serum leptin levels. Int J Cancer. (2006) 118: 1414-1419.

Nassa G, Tarallo R, Giurato G, De Filippo MR, Ravo M, Rizzo F, Stellato C, Ambrosino C, Baumann M, Lietzen N, Nyman TA, Weisz A. Post-transcriptional regulation of human breast cancer cell proteome by unliganded estrogen receptor beta via microRNAs. Mol Cell Proteomics. (2014); 13:1076–1090.

Newman G, Gonzalez-Perez RR. Leptin-cytokine crosstalk in breast cancer. Mol Cell Endocrinol. (2014) Jan 25; 382(1):570-82.

O'Brien CS, Farnie G, Howell SJ, Clarke RB: Breast cancer stem cells and their role in resistance to endocrine therapy. Hormones Cancer (2011) Apr, 2:91–103.

Palmieri C, Patten DK, Januszewski A, Zucchini G, Howell SJ. Breast cancer: current and future endocrine therapies. Mol Cell Endocrinol. (2014) Jan 25; 382(1):695-723.

Park SY, Lee HE, Li H, Shipitsin M, Gelman R, Polyak K. Heterogeneity for stem cell-related markers according to tumor subtype and histologic stage in breast cancer. Clin Cancer Res. (2010) Feb 1; 16(3):876-87.

Pattabiraman DR, Weinberg RA. Tackling the cancer stem cells - what challenges do they pose? Nat Rev Drug Discov. (2014) Jul; 13(7):497-512.

Pece S, Tosoni D, Confalonieri S, Mazzarol G, Vecchi M, Ronzoni S, Bernard L, Viale G, Pelicci PG, Di Fiore PP. Biological and molecular heterogeneity of breast cancers correlates with their cancer stem cell content. Cell. (2010) Jan 8; 140(1):62-73.

Phillips TM, McBride WH, Pajonk F. The response of CD24 (-/low)/CD44+ breast cancer-initiating cells to radiation. J Natl Cancer Inst. (2006) Dec 20; 98(24):1777-85.

Pinto CA, Widodo E, Waltham M, Thompson EW. Breast cancer stem cells and epithelial mesenchymal plasticity – implications for chemoresistance. Cancer Lett (2013); 341:56–62.

Pratt MA, Tibbo E, Robertson SJ, Jansson D, Hurst K, Perez-Iratxeta C, Lau R, Niu MY. The canonical NF-kappaB pathway is required for formation of luminal mammary neoplasias and is activated in the mammary progenitor population. Oncogene. (2009) Jul 30; 28(30):2710-22.

Sarrió D, Rodriguez-Pinilla SM, Hardisson D, Cano A, Moreno-Bueno G, Palacios J. Epithelial-mesenchymal transition in breast cancer relates to the basal-like phenotype. Cancer Res. (2008) Feb 15; 68(4):989-97.

Saxena NK, Sharma D. Multifaceted leptin network: the molecular connection between obesity and breast cancer. J Mammary Gland Biol Neoplasia. (2013) Dec; 18(3-4):309-20.

Siddique HR, Saleem M. Role of BMI1, a stem cell factor, in cancer recurrence and chemoresistance: preclinical and clinical evidences. Stem Cells. (2012) Mar; 30(3):372-

Stylianou S, Clarke RB, Brennan K. Aberrant activation of notch signaling in human breast cancer. Cancer Res. 2006 Feb 1;66(3):1517-25.

Trosko JE, Chang CC, Upham BL, Tai MH. Ignored hallmarks of carcinogenesis: stem cells and cell-cell communication. Ann N Y Acad Sci. (2004) Dec; 1028:192-201.

Visvader JE, Lindeman GJ. Cancer stem cells in solid tumours: accumulating evidence and unresolved questions. Nat Rev Cancer. (2008) Oct; 8(10):755-68.

Wickham. The Split-Apply-Combine Strategy for DataAnalysis. J Stat Softw. (2011); 40:1–29.

Yun J, Pannuti A, Espinoza I, Zhu H, Hicks C, Zhu X, Caskey M, Rizzo P, D'Souza G, Backus K, Denning MF, Coon J, Sun M, Bresnick EH, Osipo C, WuJ, Strack PR, Tonetti DA, Miele L: Crosstalk between PKCalpha and Notch-4 in endocrine-resistant breast cancer cells. Oncogenesis (2013) Aug 5; 2:e6.

Zheng Q, Dunlap SM, Zhu J, Downs-Kelly E, Rich J, Hursting SD, Berger NA, Reizes O. Leptin deficiency suppresses MMTV-Wnt-1 mammary tumor growth in obese mice and abrogates tumor initiating cell survival. Endocr Relat Cancer. (2011) Jul 11;18(4):491-503.

Zheng Q, Banaszak L, Fracci S, Basali D, Dunlap SM, Hursting SD, Rich JN, Hjlemeland AB, Vasanji A, Berger NA, Lathia JD, Reizes O. Leptin receptor maintains cancer stem-like properties in triple negative breast cancer cells. Endocr Relat Cancer. (2013) Oct 14; 20(6):797-808.

Zhou J, Wulfkuhle J, Zhang H, Gu P, Yang Y, Deng J, Margolick JB, Liotta LA, Petricoin E 3rd, Zhang Y. Activation of the PTEN/mTOR/STAT3 pathway in breast cancer stem-like cells is required for viability and maintenance. Proc Natl Acad Sci U S A. (2007) Oct 9; 104(41):16158-63.

AUTHOR OF FIVE FULL PAPER

1. Barone I, Giordano C, Panza S, **Chemi F**, Bonofiglio D, Lanzino M, Rizza P, Romeo F, Fuqua S, Maggiolini M, Catalano S, Andò S. Tamoxifen through GPER Upregulates Aromatase Expression: a Novel Mechanism Sustaining Tamoxifen-Resistant Breast Cancer Cell Growth. *Breast Cancer Research and Treatment* 2014 Jul; 146(2):273-85.
2. Simões BM, O'Brien CS, Eyre R, Silva A, Yu L, Sarmiento-Castro A, Alférez DG, Spence K, Santiago-Gómez A, **Chemi F**, Acar A, Gandhi A, Howell A, Brennan K, RydénL, Catalano S, Andó S, Gee J, Ucar A, Sims AH, Marangoni E, Farnie G, Landberg G, Howell SJ, Clarke RB. Anti-estrogen Resistance in Human Breast Tumors Is Driven by JAG1-NOTCH4-Dependent Cancer Stem Cell Activity. *Cell Report*. 2015 Sep 29;12(12):1968-77.
3. Giordano C, **Chemi F**, Panza S, Barone I, Bonofiglio D, Lanzino M, Cordella A, Campana A, Hashim A, Rizza P, Leggio A, Győrffy B, Simões B, Clarke R, Weisz A, Catalano S, Andò S. Leptin as a Mediator of Tumor-Stromal Interactions Promotes Breast Cancer Stem Cell Activity. *Oncotarget* 2015 Oct 27.
4. Fedora G, Barone I, Aiello F, Brancale A, Cancellieri M, Badolato M, **Chemi F**, Giordano C, Vircillo V, Bonofiglio D, Garofalo A, Andò S, Catalano S. Identification of Novel 2-(1H-Indol-1-yl)benzohydrazides CXCR4 Ligands Impairing Breast Cancer Growth and Motility. *Future Medicinal Chemistry*, in press (2015).
5. Panza S, Malivindi R, **Chemi F**, Rago V, Giordano C, Barone I, Bonofiglio D, Gelsomino L, Andò S, Catalano S. Glucocorticoid receptor as a potential target to decrease aromatase expression and inhibit Leydig tumor growth. *The American Journal of Pathology*, under revision (2015).

AUTHOR OF 11 ABSTRACT

6. **Chemi F**, Giordano C, Vizza D, Panza S, Barone I, Bonofiglio D, Lanzino M, Catalano S, Andò S. Leptin Increases HER2 Levels through a STAT3-mediated Up-regulation of Hsp90 in Breast Cancer cells Convegno Fondazione Lilly Funaro, Cosenza, Italy, March 1-2, 2013, (oral communication).
7. Malivindi R, Panza S, Pellicanò MA, **Chemi F**, Rizza P, Catalano S, Andò S.Glucocorticoid receptor (GR) inhibits aromatase expression in tumor Leydig cells.Farmaci e Prodotti per la Salute: Nuove Prospettive nella Ricerca Traslazionale. Conference proceedings. Università della Calabria, 8th April 2013.
8. Barone I, Campana A, Gelsomino L, **Chemi F**, Panza S, Giordano C, Marsico S, Lanzino M, Bonofiglio D, Fuqua S, Catalano S, Andò S. Aromatase Inhibitor Resistance in Breast Cancer: a Potential Role for Inflammation. SIPMET/ASIP Young Scientist Meeting, Rome, Italy, October 23-24, 2013.

9. **Chemi F** , Catalano S, Giordano C, Panza S, Bonofiglio D, Lanzino M, Rizza P, Romeo F, Fuqua S, Maggiolini M, Andò S, Barone I. Tamoxifen through GPER Upregulates Aromatase Expression: a Novel Mechanism Sustaining Tamoxifen Resistant Breast Cancer Cell Growth. Convegno Fondazione Lilly Funaro, Cosenza, Italy, March 21-22, 2014, (oral communication).
10. Giordano C, Mancuso R, **Chemi F**, Catalano S, Andò S, Gabriele B. Biological Evaluation of Benzofuran-2-acetic Esters as antiploriferative Agents in Breast Cancer Cells. XV Congresso Nazionale della Società Chimica Italiana, Arcavacata di Rende (Cosenza); 7-12 settembre 2014.
11. Malivindi R, Panza S, Perri A, **Chemi F,** Catalano S, Andò. Activated Glucocorticoid Receptor (GR) Inhibits Aromatase Expression in Tumor Leydig Cells. XI Congresso Nazionale SIAMS, Cagliari, Italy, November 13-15, 2014.
12. Simões B, Alferez D , Eyre R , Spence K, Santiago-Gomez A , Tanaka I , **Chemi F** , Kohler B , Sims A, Marangoni E , Gee J, Howat D, Howell S, Clarke R. Sulforadex targets breast cancer stem-like cells in patient-derived cells and xenograft tumours. AACR annual meeting, Philadelphia, USA, April 18-22, 2015.
13. **Chemi F**, Simões B, Ucar A, Santiago-Gómez A, Tanaka I, Catalano S, Andó S and Clarke R. Knockout of NOTCH4 and JAG1 in MCF7 cells using CRISPR-Cas9 targeting of 2 independent exons. ENBDC Annual Meeting, Weggis, Switzerland, April 23-25, 2015.
14. Catalano S, Giordano C, Panza S, **Chemi F**, Barone I, Bonofiglio D, Cordella A, Hashim A, Simões B, Clarke R, Weisz A, Andò S. Leptin as a Mediator of Tumor-Stromal Interactions Promotes Breast Cancer Stem Cell Activity. ASIP Boston, USA, March 28-April 1, 2015 Supplement to The Faseb Journal 2015, vol 29.
15. **Chemi F,** Giordano C, Panza S, Barone I, Bonofiglio D, Cordella A, Hashim A, Simões B, Clarke R, Weisz A, Catalano S and Andò S. Leptin as a Mediator of Tumor-Stromal Interactions Promotes Breast Cancer Stem Cell Activity. SIPMET Young Scientist Meeting, Alba, Italy, September 11-13, 2015, (oral communication).
16. Giordano C, Panza S, **Chemi F**, Barone I, Bonofiglio D, Cordella A, Hashim A, Győrffy B, Simões B, Clarke R, Weisz A, Catalano S and Andò S. Leptin as a Mediator of Tumor-Stromal Interactions Promotes Breast Cancer Stem Cell Activity. SABCS, San Antonio, USA, December 8-12, 2015.

Breast Cancer Res Treat (2014) 146:273–285
DOI 10.1007/s10549-014-3017-4

PRECLINICAL STUDY

Tamoxifen through GPER upregulates aromatase expression: a novel mechanism sustaining tamoxifen-resistant breast cancer cell growth

Stefania Catalano · Cinzia Giordano · Salvatore Panza · Francesca Chemi · Daniela Bonofiglio · Marilena Lanzino · Pietro Rizza · Francesco Romeo · Suzanne A. W. Fuqua · Marcello Maggiolini · Sebastiano Andò · Ines Barone

Received: 10 February 2014 / Accepted: 28 May 2014 / Published online: 14 June 2014

Abstract Tamoxifen resistance is a major clinical challenge in breast cancer treatment. Aromatase inhibitors are effective in women who progressed or recurred on tamoxifen, suggesting a role of local estrogen production by aromatase in driving tamoxifen-resistant phenotype. However, the link between aromatase activity and tamoxifen resistance has not yet been reported. We investigated whether long-term tamoxifen exposure may affect aromatase activity and/or expression, which may then sustain tamoxifen-resistant breast cancer cell growth. We employed MCF-7 breast cancer cells, tamoxifen-resistant MCF-7 cells (MCF-7 TR1 and TR2), SKBR-3 breast cancer cells, cancer-associated fibroblasts (CAFs1 and CAFs2). We used tritiated-water release assay, realtime-RT-PCR, and immunoblotting analysis for evaluating aromatase activity and expression; anchorage-independent assays for growth; reporter-gene, electrophoretic-mobility-shift, and chromatin-immunoprecipitation assays for promoter activity studies. We demonstrated an increased aromatase activity and expression, which supports proliferation in tamoxifen-resistant breast cancer cells. This is mediated by the G-protein-coupled receptor GPR30/GPER, since knocking-down GPER expression or treatment with a GPER antagonist reversed the enhanced aromatase levels induced by long-term tamoxifen exposure. The molecular mechanism was investigated in ER-negative, GPER/aromatase-positive SKBR3 cells, in which tamoxifen acts as a GPER agonist. Tamoxifen treatment increased aromatase promoter activity through an enhanced recruitment of c-fos/c-jun complex to AP-1 responsive elements located within the promoter region. As tamoxifen via GPER induced aromatase expression also in CAFs, this pathway may be involved in promoting aggressive behavior of breast tumors in response to tamoxifen treatment. Blocking estrogen production and/or GPER signaling activation may represent a valid option to overcome tamoxifen-resistance in breast cancers.

Keywords Aromatase · GPER · Tamoxifen resistance · Breast cancer

Stefania Catalano and Cinzia Giordano are joint first authors. Sebastiano Andò and Ines Barone joint senior authors.

Electronic supplementary material The online version of this article (doi:10.1007/s10549-014-3017-4) contains supplementary material, which is available to authorized users.

S. Catalano · S. Panza · F. Chemi · D. Bonofiglio · M. Lanzino · P. Rizza · M. Maggiolini · S. Andò (✉) · I. Barone (✉)
Department of Pharmacy, Health and Nutritional Sciences, University of Calabria, 87036 Arcavacata di Rende, CS, Italy
e-mail: sebastiano.ando@unical.it

I. Barone
e-mail: inesbarone@virgilio.it

C. Giordano
Centro Sanitario, University of Calabria, Arcavacata di Rende, CS, Italy

F. Romeo
Division of Anatomo-Pathology, Annunziata Hospital, Cosenza, Italy

S. A. W. Fuqua
Breast Center, Baylor College of Medicine, Houston, TX, USA

Introduction

Breast cancer is a hormone-dependent disease that relies on the mitogenic effects of estrogens to drive carcinogenesis. Estrogens are synthesized from androgens by aromatase cytochrome P450, an enzyme expressed at higher levels in

cancer than in normal breast [1–4]. The control mechanism of aromatase expression occurs transcriptionally through the alternative use of tissue-specific promoters, for instance, the promoter II/1.3 in breast cancer [5, 6]. In addition, we have previously proposed phosphorylation/dephosphorylation of aromatase as a switch to rapidly modulate aromatase enzymatic activity in breast cancer cells [7, 8]. Aromatase-transfected breast cancer cells as well as transgenic mouse models have revealed that "in situ" produced estrogens play a more important role than circulating estrogens in breast tumor promotion [9–12].

The classic effects of estrogens on breast cancer progression are mediated through the transcriptional program of estrogen receptor (ER)-α and its target genes. In addition, estrogen-dependent signaling pathways involving a G-protein-coupled receptor, named as GPER/GPR30, was also reported [13]. Indeed, ER-positive and ER-negative breast cancer cells express GPER [14, 15]. In some situations, GPER and ERs are both required, whereas in other GPER can act in the absence of ERs to mediate some rapid signaling events and activate transcription of several genes, following estrogen exposure [13]. Similar to ER, GPER is not only activated by estrogenic compounds, but also by partially antagonist such as tamoxifen, thereby stimulating cell proliferation in different cell lines [16–21].

The selective ER modulator tamoxifen is the first-line endocrine therapy for hormone-responsive breast cancers. However, de novo and acquired resistance frequently occurs. Several mechanisms for the development of resistance have been proposed, including the loss of ERα expression or function [22], the presence of ER mutants [23–26], alterations in the balance of co-regulators, changes in tamoxifen uptake or metabolism, increased oncogenic kinase signaling [27–31], and deregulated cell proliferation [32]. In this regard, recent studies have suggested that GPER receptor activation may represent an additional mechanism involved in the development of tamoxifen resistance [33–35]. Indeed, GPER overexpression was associated with tumor progression and a higher risk of developing metastatic disease in patients with breast cancer, as revealed by a National-Cancer-Institute-sponsored survey of breast carcinomas [15]. Of note, a novel tamoxifen analogue, STX, was demonstrated to enhance aromatase gene expression in a GPER-dependent manner and promote endometrial cell proliferation, implying that this receptor is likely to play a positive role in estrogen production and in promoting endometriosis and endometrial cancers [36].

Here, we demonstrate that tamoxifen-resistant MCF-7 breast cancer cells exhibit an enhanced aromatase enzymatic activity and expression, that is dependent on the GPER receptor. Our results have provided a novel cellular signaling paradigm, which is initiated by tamoxifen activation of GPER and converges on an AP-1 complex to up-regulate aromatase gene transcription. Thus, we can speculate that such a pathway might contribute to increase local estrogen levels and promote cell proliferation in endocrine-resistant breast cancers.

Materials and methods

Cell cultures

Human MCF-7 and SKBR3 breast cancer cells were cultured according to supplier's instruction. Tamoxifen-resistant MCF-7 cells were generated as previously described [37]. Briefly, we cultured parental MCF-7 cells in phenol red-containing MEM medium supplemented with 5 % FBS, and 10^{-6} M 4-hydroxy-tamoxifen (TR1 cells) or in phenol red-free MEM medium supplemented with 5 % charcoal-stripped FBS, and 10^{-7} M 4-hydroxy-tamoxifen (TR2 cells) for longer than 1 year. Cancer-associated fibroblasts (CAFs) were obtained as described [38].

Plasmids and reagents

PII/1.3-Luc plasmid containing human aromatase promoters II/I.3 ligated to a luciferase reporter gene was from Dr Simpson, Dr Clyne (Prince Henry's Institute of Medical Research/Australia). Deletions of AP-1 sequences in PII/1.3-Luc were previously described [39]. Human ERα expression vector (HEGO) was from Dr Picard (University of Geneve/Switzerland). Short-hairpin construct against human GPER (shGPER) was previously described [40]. His_6-arom plasmid construct was generated as described [8]. The GPER antagonist G15 was from Tocris and the GPER agonist G1 from Biomol Research Laboratories Inc.

Aromatase activity assay

The aromatase activity was measured by the tritiated water release assay as described [39]. Briefly, cells were incubated with 0.5 μM [1β-^{3}H]androst-4-ene-3,17-dione as substrate at 37 °C for 5 h under an air-CO_2 (5 %) atmosphere.

Real-time RT-PCR assays

Analysis of aromatase gene expression was performed by real-time reverse transcription-PCR as described [41]. Primers included: forward 5′-ACCCTTCTGCGTCGTGTGA-3′ and reverse 5′-TCTGTGGAAATCCTGCGTCTT-3′ (P450arom); forward 5′-CCCACTCCTCCACCTTTGAC-3′ and reverse 5′-TGTTGCTGTAGCCAAATTCGTT-3′ (GAPDH, housekeeping gene).

Immunoblotting analysis

Protein extracts were subjected to SDS-PAGE, as described [42]. Primary antibodies: anti-aromatase (1:250, Serotec), anti-GPER (1:1,000)/-ERα (1:1,000)/-β-Actin (1:10,000) (Santa Cruz Biotechnology). Secondary antibodies: goat anti-mouse (1:2,000) or anti-rabbit (1:7,000), Santa Cruz Biotechnology.

Detection of His_6-tagged aromatase protein by immunoblotting analysis

Detection of His_6-tagged aromatase protein was described [8]. Antibodies: anti-aromatase, -phosphotyrosine-containing proteins (Santa Cruz Biotechnology).

Transient transfection

For evaluation of aromatase expression, cells were transiently transfected with HEGO or empty vectors (3 μg/well) using FuGENE6 (Promega) according to the manufacturer. For luciferase gene assays, cells were transfected with different PII/1.3-Luc constructs (1 μg/well). 24 h after transfection, cells were treated as indicated. Luciferase activity was assayed as described [43].

GPER knock-down

Cells were transiently transfected with short hairpin (sh) or shGPER vectors (1 μg/well) using FuGENE6 as described [40]. Forty hours after transfection, cells were harvested and used for different experimental procedures. The shRNA construct used showed 83 % knockdown efficiency.

Electrophoretic mobility shift assays-EMSA

Nuclear extracts were prepared as described [44]. DNA sequences used as probe or cold competitors are the following (nucleotide motifs of interest are underlined and mutations are shown as lowercase letters): AP-1, 5′-ATGGCCTGAGTGAGTCACTTTGAATTC-3′; mutated AP-1, 5′-ATGGCCTGAGTtcaTCACTTTGAATTC-3′. Probe generation, protein-binding reactions and incubations with anti-c-fos/-c-jun antibodies (Santa Cruz Biotechnology) were previously described [41].

Chromatin immunoprecipitation-ChIP assays

DNA/protein complexes were extracted as described [45]. The precleared chromatin was immunoprecipitated with anti-c-fos/-c-jun/-Polymerase II antibodies. Samples and input were used for PCR using the primers flanking AP-1 sequence in PII/1.3 promoter region: 5′-GGCCCATGGTCCAAGAGATT-3′ and 5′-TTGAGGTCTTCTCAGAGCCT-3′.

Soft agar assays

Cells (10^4/well) were plated in 4 ml of 0.35 % agarose with 5 % charcoal-stripped FBS in phenol red-free media in six-well plates. After two days, media containing vehicle or treatments were added to the top layer and replaced every 2 days. Anchorage-independent growth was assessed as described [45].

Statistical analysis

Data were analyzed for statistical significance with two-tailed Student's test using GraphPadPrism4. Standard deviations/SD are shown.

Results

Tamoxifen-resistant MCF-7 breast cancer cells exhibit enhanced aromatase activity and expression

We initially examined the effects of tamoxifen on aromatase activity in parental MCF-7 and tamoxifen-resistant breast cancer cells (MCF-7 TR1), previously generated in our laboratory as a suitable model system to study acquired resistance to endocrine therapy [37, 46]. We found that tamoxifen treatment was not able to affect aromatase activity values in parental tamoxifen-sensitive cells after 24 and 48 h of treatment (data not shown), whereas long-term treatment with tamoxifen resulted in ~3fold higher aromatase enzymatic activity values (Fig. 1a). Accordingly, realtime RT-PCR and immunoblotting analysis revealed an increased mRNA and protein expression in MCF-7 TR1 cells compared to parental cells (Fig. 1b, c).

As a biological consequence of an enhanced aromatase expression, we evaluated the effects of the aromatizable androgen, androsten-4-ene-3,17-dione (AD), on anchorage-independent proliferation (Fig. 1d). As expected, control basal growth of MCF-7 TR1 cells was significantly elevated compared with parental cells. In line with other studies [47, 48], androgen exposure reduced cell growth in parental MCF-7 cells. In contrast, AD treatment resulted in an increased colony number in MCF-7 TR1 cells, consistently with its metabolic transformation into estrogens by cells, which displayed high aromatase levels. Concomitantly, exposure of MCF-7 TR1 cells to the non-steroidal aromatase inhibitor anastrozole completely reversed the stimulatory effects induced by AD on growth (Fig. 1e).

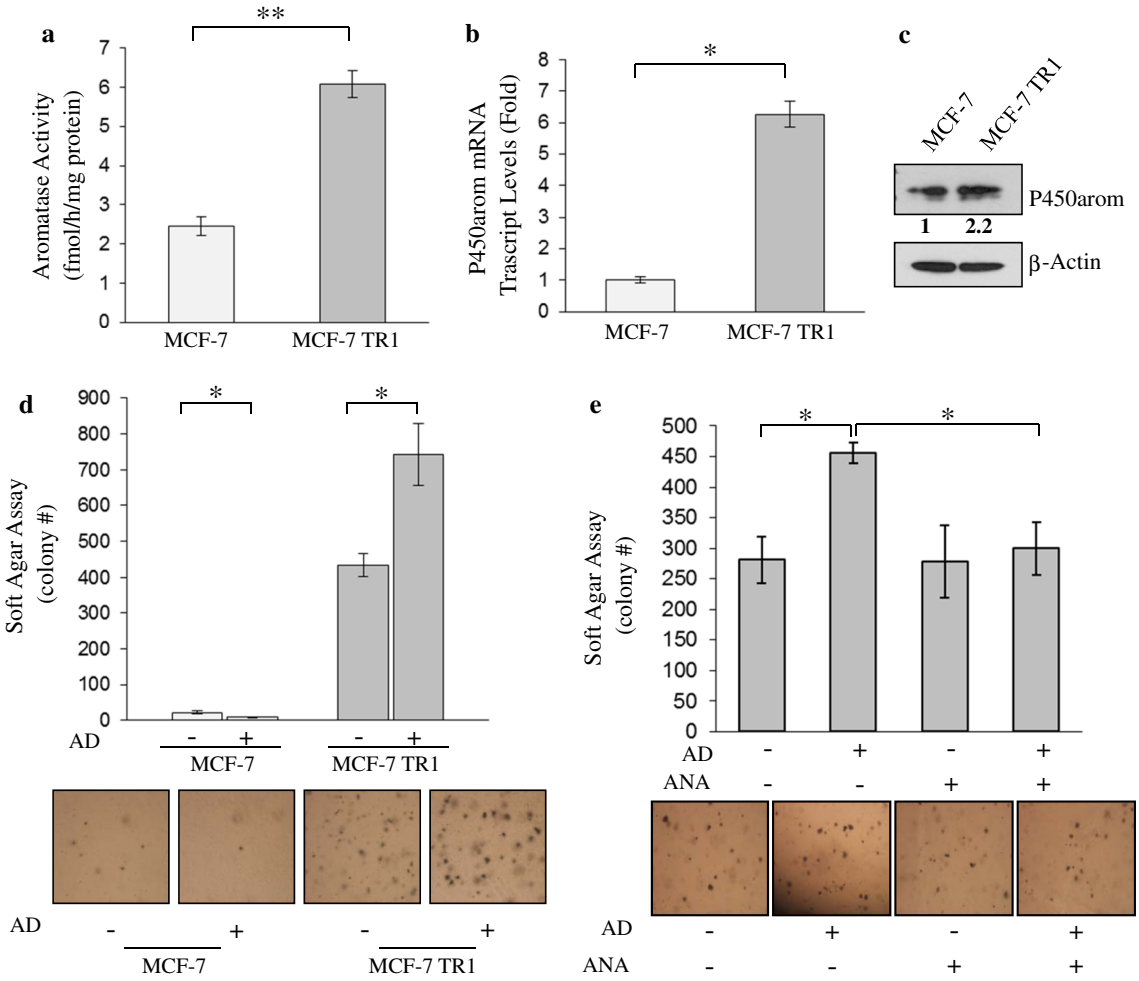

Fig. 1 Aromatase activity and expression in tamoxifen-resistant MCF-7 breast cancer cells. **a** Aromatase activity in MCF-7 and MCF-7 TR1 cells. The results obtained were expressed as fentomoles per hour and normalized to milligrams of protein (fmol/h/mg of protein). **b** Aromatase (P450arom) mRNA content, evaluated by real-time RT–PCR, in MCF-7 and MCF-7 TR1 cells. Each sample was normalized to its GAPDH mRNA content. The values represent the mean ± SD of three different experiments, each performed with triplicate samples. **c** Immunoblotting analysis of aromatase protein levels (P450arom) in total protein extracts from MCF-7 and MCF-7 TR1 cells. β-Actin was used as loading control. *Numbers* represent the average fold change versus parental MCF-7 cells normalized for β-Actin. *Blots* are representative of at least three independent experiments. **d** *Upper panel* soft-agar growth assay in MCF-7 and MCF-7 TR1 cells treated with vehicle (−) or the aromatizable androst-4-ene-3,17-dione (AD, 10 nM). *Lower panel* a typical well for each condition is shown. **e** *Upper panel* soft-agar growth assay in MCF-7 TR1 cells treated with vehicle (−) or AD 10 nM with or without the aromatase inhibitor anastrozole (ANA, 1 μM). *Lower panel,* a typical well for each condition is shown. After 14 days of growth, colonies >50 μm diameter were counted. Data are the mean colony number ± SD of three plates of three independent experiments. *$p < 0.05$, **$p < 0.001$

Increased aromatase expression via GPER in tamoxifen-resistant breast cancer cells

Since tamoxifen acts as an agonist for the newly discovered G-protein coupled receptor (GPER) [16–21] and this receptor plays an important role in the development of tamoxifen-resistance in breast cancer [33, 34], we then evaluated whether GPER may be involved in the increased aromatase expression and activity detected in our model system. To this aim, we knocked-down GPER expression by shRNA technologies (Fig. 2a) and used a selective GPER antagonist G15. In both experimental conditions aromatase mRNA levels and activity were significantly reduced in MCF-7 TR1 cells (Fig. 2b, c). Similar results were obtained in an additional tamoxifen-resistant model MCF-7 TR2 (Supplementary Fig. 1a, b), indicating that GPER may contribute to enhance aromatase expression in tamoxifen-resistant breast cancer cells. In addition, consistently with the high levels of aromatase found in MCF-7 TR2, the aromatase substrate AD increased anchorage-independent growth, which was abrogated in the presence of anastrazole (Supplementary Fig. 1c).

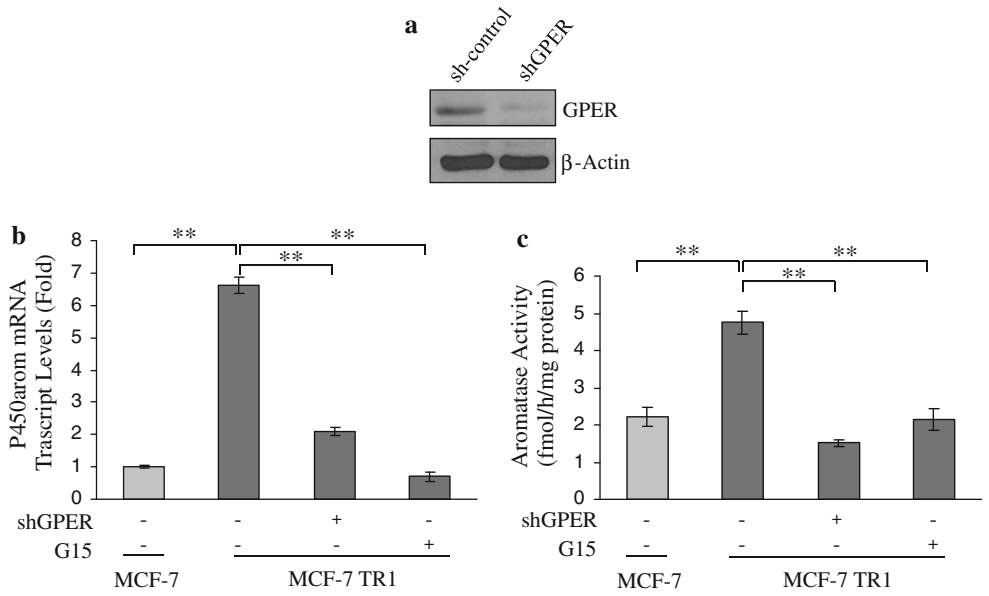

Fig. 2 GPER mediates aromatase induction in tamoxifen-resistant MCF-7 breast cancer cells. **a** Immunoblotting analysis for GPER expression in cells transfected with control shRNA (sh-control) or GPER shRNA (shGPER). β-Actin was used as loading control. **b** P450arom mRNA content and **c** aromatase activity in MCF-7 and MCF-7 TR1 cells transfected with shGPER or treated for 24 h with the GPER antagonist G15 (1 μM). The values represent the mean ± SD of three different experiments, each performed with triplicate samples. $^{**}p < 0.001$

Tamoxifen stimulates aromatase expression in SKBR3 breast cancer cells

To better understand the molecular mechanisms underlying the involvement of GPER in mediating tamoxifen-associated aromatase expression, we used as an experimental model ER-negative, GPER/aromatase-positive SKBR3 cells, in which tamoxifen acts as a GPER agonist [49, 50]. We found that aromatase mRNA and protein levels were increased in a time-dependent manner after tamoxifen treatment (Fig. 3a, b). GPER gene silencing blocked the induction of aromatase expression mediated by tamoxifen (Fig. 3c, d). Of note, the induction of aromatase expression with tamoxifen treatment was further potentiated in SKBR3 cells transiently transfected with an ERα expression vector (Supplementary Fig. 2a, b). This is consistent with other reports of the existence of functional crosstalk between ERα and GPER in cell contexts expressing both receptors [35].

Tamoxifen up-regulates aromatase promoter activity through AP-1 in SKBR3 breast cancer cells

We then investigated if the up-regulatory effects of tamoxifen on aromatase expression were due to its ability to influence aromatase gene transcriptional activity. Thus, SKBR3 breast cancer cells were transfected with a luciferase reporter construct containing the human aromatase promoter II/1.3 (PII/1.3-Luc) and then treated with increasing concentrations of tamoxifen (Fig. 4a). We found a significant dose-dependent activation of PII/1.3 promoter upon tamoxifen exposure. As expected, treatment with G1, a selective GPER agonist, resulted in a strong increase in aromatase promoter activity. Concomitantly, transfection with shGPER abolished the ability of tamoxifen to induce aromatase gene transcription (Fig. 4b). Because GPER signaling is able to activate the transcription of several genes via AP-1 complex [49, 51, 52], we focused our attention on the AP-1 motifs present in the aromatase promoter as possible effectors of tamoxifen action [39]. Therefore, we performed functional assays using PII/1.3-Luc constructs with AP-1 deleted sites at position −498 (AP-1 −498), −935 (AP-1 −935), and at both sites (AP-1 −498/−935) (Fig. 4c). The responsiveness to tamoxifen and G1 was no longer observed in cells transfected with all the AP-1 deleted constructs, underlining how AP-1 motifs may be crucial in mediating aromatase promoter activation upon the antiestrogen treatment.

c-fos/c-jun complex is recruited at AP-1 sites of aromatase promoter region in SKBR3 cells

The specific role of AP-1 motifs in mediating the stimulatory effects of tamoxifen on aromatase gene expression was explored using EMSA and ChIP assays. Using synthetic radiolabeled oligonucleotides bearing the AP-1 site present in the aromatase promoter region (Fig. 5a, lane 1), we observed the formation of a protein complex in nuclear

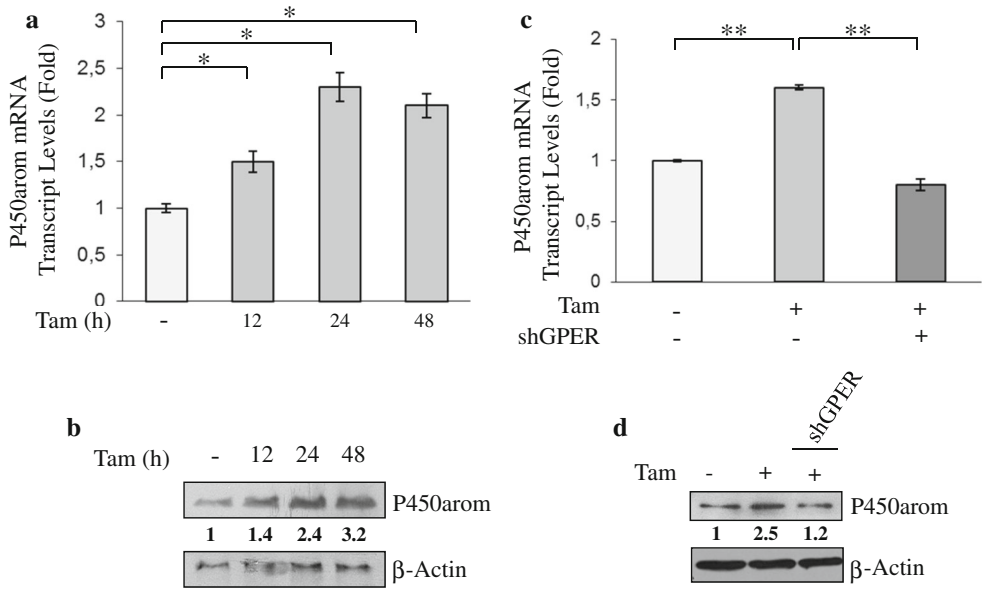

Fig. 3 Tamoxifen effects on aromatase expression in SKBR3 breast cancer cells. **a** P450arom mRNA content, evaluated by real-time RT–PCR, in SKBR3 cells treated for 12, 24 and 48 h with vehicle (−) or tamoxifen (Tam, 1 μM). The values represent the mean ± SD of three different experiments, each performed with triplicate samples. *$p < 0.05$. **b** Immunoblotting analysis of P450arom protein levels in cells treated with Tam 1 μM as indicated. β-Actin was used as loading control. *Numbers* represent the average fold change versus vehicle-treated cells normalized for β-Actin. **c** P450arom mRNA content, evaluated by real-time RT-PCR, in SKBR3 cells transfected with GPER shRNA (shGPER) and then treated for 24 h with vehicle (−) or Tam 1 μM. The values represent the mean ± SD of three different experiments, each performed with triplicate samples. **$p < 0.001$. **d** Immunoblotting analysis of P450arom protein levels in total protein extracts from SKBR3 cells transfected with shGPER and then treated for 24 h with vehicle (−) or Tam 1 μM. β-Actin was used as loading control. *Numbers* represent the average fold change versus vehicle-treated cells normalized for β-Actin. *Blots* are representative of at least three independent experiments

extracts from SKBR3 cells, which was specifically abrogated by incubation with 100-fold excess of unlabeled probe (Fig. 5a, lane 2). This inhibition was no longer observed when mutated oligodeoxyribonucleotide probe was used as a competitor (Fig. 5a, lane 3). Interestingly, treatment with tamoxifen strongly increased the DNA-binding protein complex compared with control samples in a time-dependent manner (Fig. 5a, lanes 4–6). The inclusion of anti-c-fos and anti-c-jun antibodies in the reaction attenuated the enhanced complex formation induced by tamoxifen, suggesting the presence of both proteins in the complex (Fig. 5b, lanes 4–5). Non specific control IgG did not reduce intensity of tamoxifen-associated specific band (Fig. 5b, lane 3).

Moreover, ChIP assays were performed. Protein-chromatin complexes were immunoprecipitated from SKBR3 cells treated or not with tamoxifen using antibodies against c-fos, c-jun or RNA-polymerase II (Fig. 5c). The precipitated DNA was quantified using PCR with primers spanning the AP-1 element in the aromatase promoter. We demonstrated, after tamoxifen treatment, an enhanced recruitment of the AP-1 complex, concomitantly with an increased association of RNA-polymerase II to the aromatase regulatory region, indicating that the chromatin in this region is probably in a better permissive environment for gene transcription.

Taken together, these results dissect a novel molecular mechanism by which tamoxifen via GPER/AP-1 up-regulates transcriptionally aromatase expression.

Rapid increase of aromatase activity induced by tamoxifen treatment in Tam^R MCF-7 breast cancer cells

We have previously shown that 17β-estradiol (E_2) rapidly enhanced phosphorylation of the 361 tyrosine residue of aromatase protein and consequentially its enzymatic activity in breast cancer cells [8]. Therefore, we asked whether tamoxifen was able to increase aromatase activity also through post-transcriptional mechanisms in tamoxifen-resistant cells. As expected, short-time exposure with E_2 significantly enhanced aromatase activity in both parental and MCF-7 TR1 cells (Fig. 6a). Treatment with tamoxifen for 10 min did not result in any changes in parental cells, while it induced a significant increase in resistant cells (Fig. 6a). This was concomitant with an enhancement of phosphotyrosine levels of the His_6-tagged purified aromatase protein in both basal and tamoxifen-treated MCF-7 TR1 cells (Fig. 6b).

Hence, we suggest that tamoxifen-induced activation of aromatase in endocrine-resistant breast cancer cells is

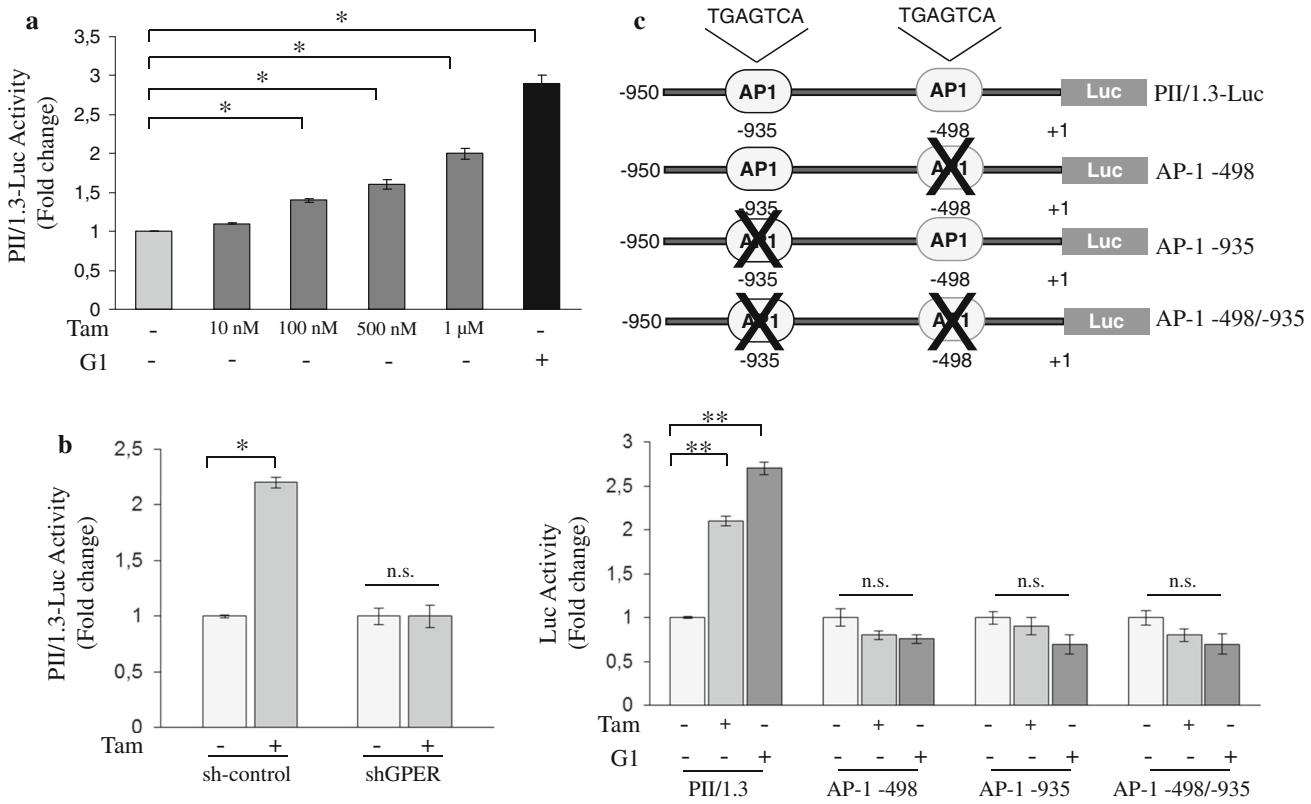

Fig. 4 Tamoxifen induces human aromatase PII/1.3 promoter activity. **a** SKBR3 cells transiently transfected with a PII/1.3-Luc reporter gene, containing the human aromatase promoter II and I.3 sequence, were treated with vehicle (−), Tam (10, 100, 500 nM, 1 μM) or the selective GPER agonist G1 (1 μM) for 24 h and then luciferase activity was measured. **b** SKBR3 cells were transiently co-transfected with a PII/1.3-Luc reporter gene and with either sh-control or shGPER plasmid. After transfection cells were treated with vehicle (−) or with Tam 1 μM for 24 h, and then luciferase activity was measured. **c** *Upper panel* schematic representation of PII/1.3-Luc constructs used in this study and described in "Materials and methods". *Lower panel* aromatase transcriptional activity in SKBR3 cells transfected with different promoter constructs is shown. After transfection with the indicated constructs, cells were treated with vehicle (−), Tam 1 μM or G1 1 μM for 24 h. The values represent the mean ± SD of three different experiments each performed in triplicate. n*s* nonsignificant, $*p < 0.05$, $**p < 0.001$

mediated at least in part by phosphorylation-dependent events coupled with transcriptional activation.

Aromatase expression is up-regulated by tamoxifen through GPER in breast CAFs

Given the relevant contribution of the microenvironment to cancer cell growth and progression [53], we finally examined the potential role of tamoxifen and GPER on aromatase regulation in fibroblasts isolated from biopsies of primary breast tumors (CAFs1 and CAFs2). Immunoblotting analysis revealed that CAFs expressed GPER and aromatase, but not ERα (Fig. 7a). CAFs were treated with tamoxifen with/without the GPER antagonist G15 and aromatase mRNA and protein levels were assessed (Fig. 7b, c). Treatment with tamoxifen resulted in a significant increase of aromatase expression that was no longer evident in cells treated with G15, supporting a functional role for GPER also in the induction of aromatase in CAFs.

Discussion

Despite significant advances in the treatment options of breast cancer following the introduction of tamoxifen, de novo and acquired resistance remains a major clinical concern. Aromatase inhibitors have been shown to be effective in women who have progressed or recurred on tamoxifen, suggesting a role of local estrogen production by aromatase in driving tamoxifen-resistant phenotype. However, the effects of long-term tamoxifen exposure on aromatase activity and/or expression have not yet been reported. Here, we show an increased expression and activity of aromatase, which may contribute to sustained growth and progression of tamoxifen-resistant breast cancer cells, as compared to parental-sensitive cells. Indeed, tamoxifen through GPER activation is able to enhance the recruitment of the c-fos/c-jun complex to the AP-1 motifs within the human aromatase promoter gene.

As time progresses, cellular and physiological roles of GPER are becoming better defined. Indeed, estrogenic

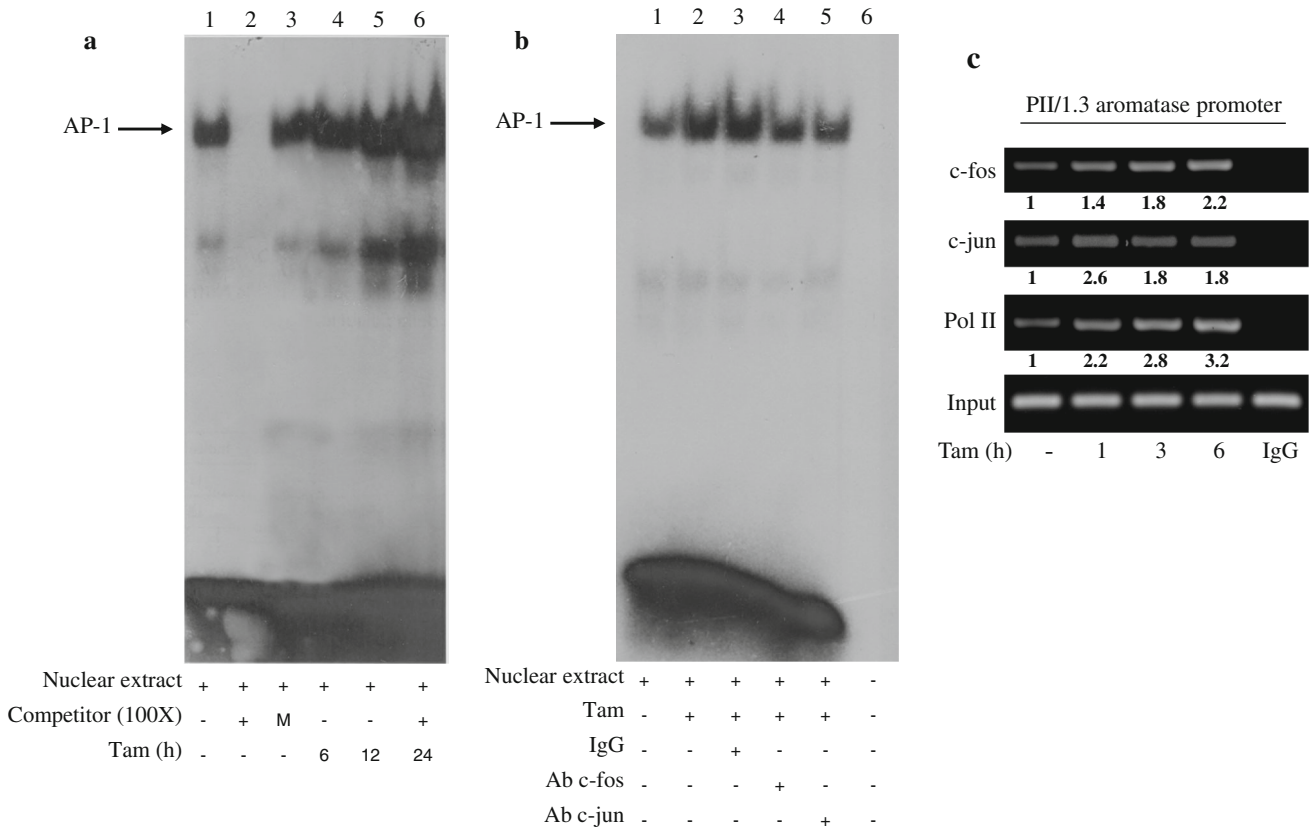

Fig. 5 Tamoxifen regulates aromatase promoter activity through AP-1 binding sites. **a** Nuclear extracts from SKBR3 cells were incubated with a double-stranded AP-1 specific sequence probe labeled with [γ^{32}P]ATP and subjected to electrophoresis in a 6 % polyacrylamide gel (*lane 1*). Competition experiments were performed adding as competitor a 100-fold molar excess of unlabeled probe (*lane 2*) or a 100-fold molar excess of unlabeled oligonucleotide containing a mutated AP-1 sequence (M, *lane 3*). *Lanes 4*, *5* and *6* nuclear extracts from SKBR3 cells treated with Tam 1 μM for 6, 12 and 24 h, respectively. **b** Nuclear extracts from SKBR3 cells incubated with a double-stranded AP-1 specific sequence probe labeled with [γ^{32}P] ATP (*lane 1*). *Lane 2* nuclear extracts from SKBR3 cells treated with Tam 1 μM for 24 h. *Lanes 3*, *4*, and *5* Tam-treated nuclear extracts incubated with anti-IgG (negative control), anti-c-fos, and anti-c-jun antibodies, respectively. *Lane 6* probe alone. **c** SKBR3 cells were treated with vehicle (−) or with Tam for 1, 3 and 6 h, cross-linked with formaldehyde and lysed. The precleared chromatin was immunoprecipitated with anti-c-fos, anti-c-jun, anti-RNA polymerase II (Pol II) antibodies. IgG, negative control. A 5 μl volume of each sample and input was analyzed by PCR using specific primers to amplify aromatase PII/1.3 promoter sequence, including the AP-1 site. Similar results were obtained in multiple independent experiments. *Numbers* represent the average fold change versus vehicle-treated cells normalized for input samples

GPER signaling was found to mediate the proliferation and migration of breast and other carcinoma cell lines [20, 21, 40, 52, 54–56]. GPER expression was also associated with biologic measures of poor outcomes, including elevated HER2 protein, larger tumor size, and distant metastasis, in a survey of 321 primary breast tumors [55], although any correlation was evident in an Asian population-based cohort of 118 women with breast infiltrating carcinoma [57]. Recently, an elegant study of Ignatov et al. [34] demonstrates that GPER expression independently predicts a poor relapse-free survival in breast cancer patients treated with tamoxifen as compared with patients treated with aromatase inhibitors or tamoxifen followed by aromatase inhibitors. This suggests that GPER positivity might identify a subgroup of patients who would benefit from estrogen deprivation, produced by aromatase inhibitors as adjuvant therapeutic strategy. However, more definitive evidence is needed. Here, we have shown in tamoxifen-resistant MCF-7 breast cancer cells that long-term exposure to tamoxifen resulted in an increased aromatase expression in terms of mRNA and protein levels along with an enhancement of its enzymatic activity. These effects are completely reversed by knocking-down GPER expression as well as by the synthetic GPER selective antagonist G15, demonstrating the involvement of GPER in aromatase up-regulation. We have also reproduced similar results in ERα-negative and GPER-positive SKBR3 breast cancer cells, indicating how GPER-mediated aromatase induction may represent a general mechanism in cellular contexts in which tamoxifen may lose its estrogen antagonistic activity.

In humans, distinctive tissue-specific promoters are employed to direct aromatase mRNA expression from a

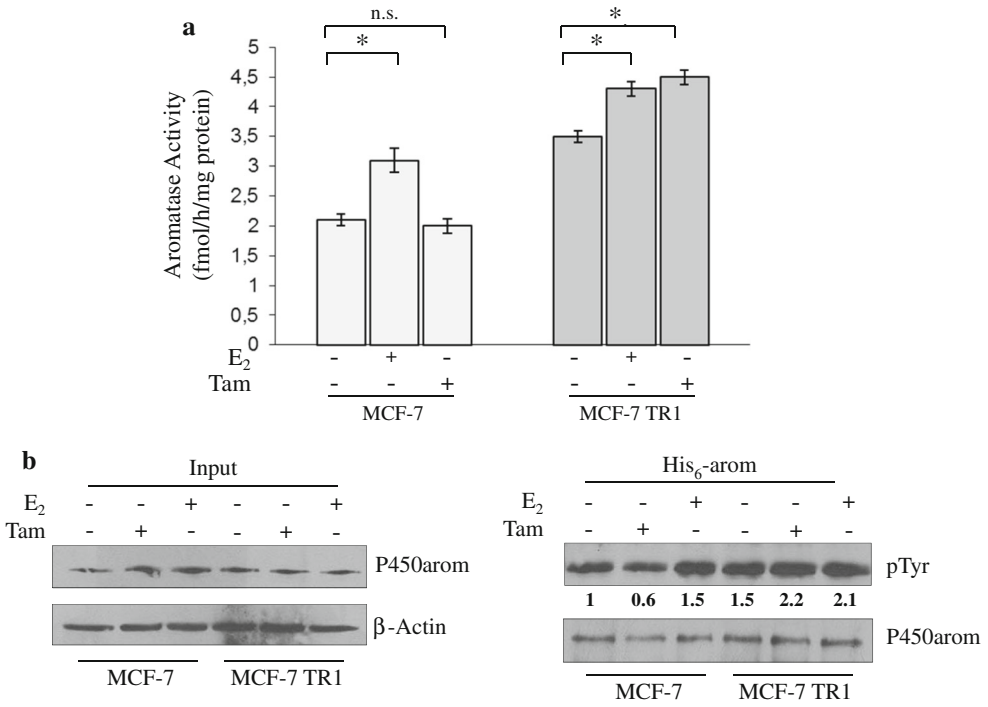

Fig. 6 Rapid effects of tamoxifen on aromatase activity in tamoxifen-resistant MCF-7 breast cancer cells. **a** MCF-7 and MCF-7 TR1 cells were treated with vehicle (−), 17β-estradiol (E_2) 10 nM or Tam 1 μM for 10 min and then aromatase activity was performed. The results obtained were expressed as fentomoles per hour and normalized to milligrams of protein (fmol/h/mg of protein). *ns* nonsignificant; $*p < 0.05$. **b** MCF-7 and MCF-7 TR1 cells transiently transfected with His_6-arom plasmid were treated with vehicle (−), E_2 10 nM or Tam 1 μM for 10 min. Aromatase was purified using Ni–NTA agarose beads after which the complexes were resolved in SDS-PAGE. Immunoblotting was performed using the anti-phosphotyrosine (pTyr) and anti-aromatase (P450arom) antibodies (*right panel*). *Numbers* represent the average fold change versus vehicle-treated MCF-7 cells normalized for P450arom. Whole-cell lysates were used as input controls and β-Actin was used as loading control (*left panel*). *Blots* are representative of at least three independent experiments

single gene, with exons 1.3 and PII representing the two major exons present in aromatase mRNAs isolated from breast tumors. Different functional motifs were identified in the PII/1.3 aromatase promoter: c-AMP responsive elements, a CRE-like sequence, an Ad4BP/SF-1 (steroidogenic factor-1) binding site and AP-1 (activating protein-1) motifs [5, 6]. We demonstrated by functional studies, using a construct containing human PII/1.3 aromatase promoter region, that tamoxifen treatment induced a dose-dependent increase in transcriptional activity, that was abrogated in cells transfected with a short hairpin RNA construct against GPER. The observed up-regulatory effects of tamoxifen were no longer evident when promoter fusion constructs containing AP-1 deleted elements were employed. These results suggest that the integrity of the AP-1 sequences is a prerequisite for the induction mediated by tamoxifen on aromatase promoter activity.

The AP-1 family of transcription factors consists of multiple Jun (c-Jun/JunB/JunD) and Fos (c-Fos/FosB/Fra-1/Fra-2) members [58]. The AP-1 complex represents a critical connecting node for many signal transduction pathways involved in malignant transformation and progression. Interestingly, GPER-mediated up-regulation of c-fos by 17β-estradiol, estrogen-like compounds and tamoxifen represents an early molecular event associated with growth stimulation in several cancer cells, as breast cancer cells [20, 35, 49, 52]. In line with these findings, EMSA experiments revealed that nuclear extracts from tamoxifen-treated cells exhibited an increase in AP-1 DNA-binding complex that was immunodepleted by both anti-c-fos and anti-c-jun antibodies. Furthermore, ChIP analysis showed an enhanced recruitment of c-fos/c-jun complex to the AP-1 site within the aromatase gene promoter, which was concomitant with an increased RNA polymerase II occupancy. Collectively, these data support the positive role for tamoxifen through AP-1 complex in inducing aromatase gene transcriptional machinery.

GPER was traditionally recognized to mediate rapid signaling by modulating second messengers and kinase pathways [50]. We previously demonstrated, in human breast cancer cells, that the regulation of aromatase also occurs through post-transcriptional mechanisms, involving enhanced tyrosine phosphorylation levels of the enzyme through c-Src [7, 8], whose intracellular tyrosine kinase

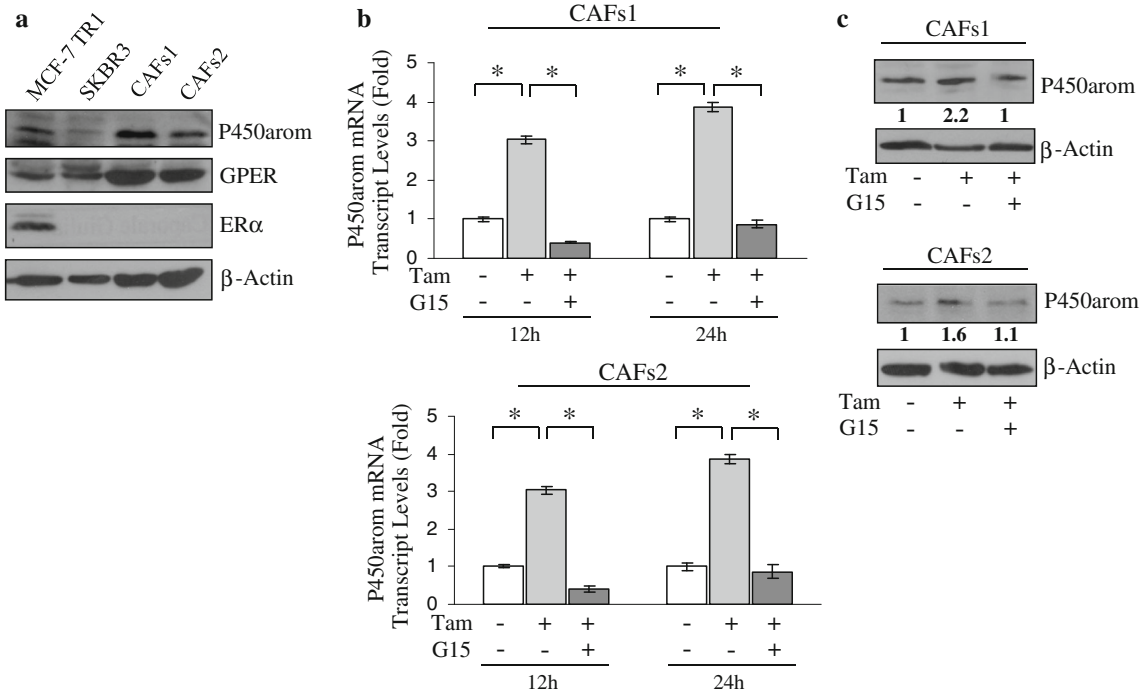

Fig. 7 Tamoxifen modulates aromatase expression in breast cancer-associated fibroblasts (CAFs). **a** Immunoblotting analysis of P450arom, GPER, and ERα in total protein extracts from MCF-7 TR1, SKBR3, CAFs1 and CAFs2 cells. β-Actin was used as loading control. **b** P450arom mRNA levels, evaluated by real-time RT-PCR, in CAFs1 and CAFs2 treated for 12 and 24 h with vehicle (−) or Tam 1 μM in the presence or not of the specific GPER antagonist G15 (1 μM). Each sample was normalized to its GAPDH mRNA content. The values represent the mean ± SD of three different experiments, each performed with triplicate samples. *$p < 0.05$. **c** Immunoblotting analysis of P450arom protein levels in total protein extracts from CAFs1 and CAFs2 treated as indicated for 24 h. β-Actin was used as loading control. *Numbers* represent the average fold change versus vehicle (−)-treated cells normalized for β-Actin. *Blots* are representative of three independent experiments

activity increased during development of tamoxifen resistance [59, 60]. Surprisingly, we found that short-term exposure to tamoxifen induced an increase in aromatase activity along with an enhancement of phosphotyrosine levels of the purified aromatase protein in resistant cells. As expected, we did not observe any effects in endocrine-sensitive breast cancer cells, accordingly with the lack of any tamoxifen effects on aromatase activity after 24 and 48 h of treatment. This could be explained by several evidences showing a predominant role for ERα and only a secondary one for GPER in transmitting any estrogen/tamoxifen actions in parental MCF-7 cells [33, 35]. Therefore, our results suggest that in addition to a transcriptional control of aromatase expression, tamoxifen also induced activation of aromatase via non genomic events in endocrine-resistant breast cancer cells.

The biological significance of the enhanced aromatization induced by tamoxifen is underlined by growth studies, in which treatment with the aromatase substrate androstenedione, through its conversion into estradiol, significantly enhanced anchorage-independent proliferation in tamoxifen-resistant breast cancer cells. As expected, these stimulatory effects were reversed by inhibition of aromatase enzymatic activity by anastrozole. In contrast, androstenedione exposure reduced cell growth in parental MCF-7 cells, as revealed in our and other studies [47, 48].

The phenotype behavior of malignant cells appears to be regulated not only by cell autonomous signals, but it is also dependent on heterotypic signals coming from surrounding stromal cells, able to create a specific and local microenvironment to tightly control breast cancer proliferation and differentiation. Among the stromal cells, cancer-associated fibroblasts (CAFs) play an active role in determining tumor progression [38, 61, 62]. Indeed, CAFs up-regulate aromatase expression and increase local estrogen production within the tumor microenvironment and may contribute to endocrine resistance [63]. On the other hand, GPER signaling activation is a functionally important signaling component in CAFs [18, 51, 64]. According to these findings, we found that GPER was able to modulate the induction of aromatase expression also in CAFs treated with tamoxifen, further supporting the potential role exerted by the GPER-dependent aromatase up-regulation in tumor progression.

Estrogens induce genomic-nuclear ER activity, which can be antagonized by tamoxifen. However, both estrogens and tamoxifen can turn on nongenomic membrane and/or

cytoplasmic ER which, in turn, activate various components of growth factor tyrosine kinase receptors and cellular kinase cascades. Subsequent phosphorylation of ER and its coregulators potentiates the genomic-nuclear activity of ER even when bound to tamoxifen, resulting in endocrine resistance [29, 65]. In addition, in tamoxifen-resistant cells the ability of GPER to mediate estrogen or tamoxifen action may be strengthened because of its translocation to cell surface [66]. In the present study, we demonstrate that long-term exposure to tamoxifen enhanced aromatase expression via GPER in breast cancer cells as well as in breast CAFs, providing evidences for a novel mechanism of autocrine and paracrine growth stimulation by estrogens in hormone-resistant breast cancers. Interestingly, the effects of tamoxifen via GPER in inducing local estrogen production and in promoting cell proliferation may occur in cancer cells where tamoxifen loses its antiestrogenic activity, such as endometrial [36] and tamoxifen-resistant breast cancer cells. In conclusion, we speculate that blocking estrogen production and/or GPER signaling activation might offer alternative therapeutic strategies in treating hormone-resistant breast cancers, lowering likely the risk of endometrial hyperplasia and cancers in women with chronic tamoxifen treatment.

Acknowledgments This work was supported by Associazione Italiana Ricerca sul Cancro (AIRC) grant IG11595. Futuro in Ricerca 2012 RBFR12FI27 to IB. European Commission/FSE/Regione Calabria to FC and SP. MM was supported by Associazione Italiana per la Ricerca sul Cancro (project no. 12849/2012), AIRC project Calabria 2011 (http://www.airc.it/) and Fondazione Cassa di Risparmio di Calabria e Lucania.

Conflict of interest The authors declared no conflict of interest and no financial relationship with the organization that sponsored the research.

References

1. Harada N (1997) Aberrant expression of aromatase in breast cancer tissues. J Steroid Biochem Mol Biol 61:175–184
2. James VH, McNeill JM, Lai LC et al (1987) Aromatase activity in normal breast and breast tumor tissues: in vivo and in vitro studies. Steroids 50:269–279
3. Esteban JM, Warsi Z, Haniu M et al (1992) Detection of intratumoral aromatase in breast carcinomas. An immunohistochemical study with clinicopathologic correlation. Am J Pathol 140:337–343
4. Chen S, Masri S, Wang X et al (2006) What do we know about the mechanisms of aromatase inhibitor resistance? J Steroid Biochem Mol Biol 102:232–240
5. Simpson ER, Michael MD, Agarwal VR et al (1997) Cytochromes P450 11: expression of the CYP19 (aromatase) gene: an unusual case of alternative promoter usage. FASEB J 11:29–36
6. Bulun SE, Sebastian S, Takayama K et al (2003) The human CYP19 (aromatase P450) gene: update on physiologic roles and genomic organization of promoters. J Steroid Biochem Mol Biol 86:219–224
7. Barone I, Giordano C, Malivindi R et al (2012) Estrogens and PTP1B function in a novel pathway to regulate aromatase enzymatic activity in breast cancer cells. Endocrinology 153:5157–5166
8. Catalano S, Barone I, Giordano C et al (2009) Rapid estradiol/ERalpha signaling enhances aromatase enzymatic activity in breast cancer cells. Mol Endocrinol 23:1634–1645
9. Maggiolini M, Carpino A, Bonofiglio D et al (2001) The direct proliferative stimulus of dehydroepiandrosterone on MCF7 breast cancer cells is potentiated by overexpression of aromatase. Mol Cell Endocrinol 184:163–171
10. Sun XZ, Zhou D, Chen S (1997) Autocrine and paracrine actions of breast tumor aromatase. A three-dimensional cell culture study involving aromatase transfected MCF-7 and T-47D cells. J Steroid Biochem Mol Biol 63:29–36
11. Yue W, Zhou D, Chen S et al (1994) A new nude mouse model for postmenopausal breast cancer using MCF-7 cells transfected with the human aromatase gene. Cancer Res 54:5092–5095
12. Tekmal RR, Ramachandra N, Gubba S et al (1996) Overexpression of int-5/aromatase in mammary glands of transgenic mice results in the induction of hyperplasia and nuclear abnormalities. Cancer Res 56:3180–3185
13. Prossnitz ER, Maggiolini M (2009) Mechanisms of estrogen signaling and gene expression via GPR30. Mol Cell Endocrinol 308:32–38
14. Revankar CM, Cimino DF, Sklar LA et al (2005) A transmembrane intracellular estrogen receptor mediates rapid cell signaling. Science 307:1625–1630
15. Filardo EJ (2002) Epidermal growth factor receptor (EGFR) transactivation by estrogen via the G-protein-coupled receptor, GPR30: a novel signaling pathway with potential significance for breast cancer. J Steroid Biochem Mol Biol 80:231–238
16. Prossnitz ER, Oprea TI, Sklar LA et al (2008) The ins and outs of GPR30: a transmembrane estrogen receptor. J Steroid Biochem Mol Biol 109:350–353
17. Filardo EJ, Quinn JA, Bland KI et al (2000) Estrogen-induced activation of Erk-1 and Erk-2 requires the G protein-coupled receptor homolog, GPR30, and occurs via trans-activation of the epidermal growth factor receptor through release of HB-EGF. Mol Endocrinol 14:1649–1660
18. Pandey DP, Lappano R, Albanito L et al (2009) Estrogenic GPR30 signalling induces proliferation and migration of breast cancer cells through CTGF. EMBO J 28:523–532
19. Thomas P, Pang Y, Filardo EJ et al (2005) Identity of an estrogen membrane receptor coupled to a G protein in human breast cancer cells. Endocrinology 146:624–632
20. Vivacqua A, Bonofiglio D, Recchia AG et al (2006) The G protein-coupled receptor GPR30 mediates the proliferative effects induced by 17beta-estradiol and hydroxytamoxifen in endometrial cancer cells. Mol Endocrinol 20:631–646
21. Vivacqua A, Bonofiglio D, Albanito L et al (2006) 17beta-estradiol, genistein, and 4-hydroxytamoxifen induce the proliferation of thyroid cancer cells through the g protein-coupled receptor GPR30. Mol Pharmacol 70:1414–1423
22. Encarnacion CA, Ciocca DR, McGuire WL et al (1993) Measurement of steroid hormone receptors in breast cancer patients on tamoxifen. Breast Cancer Res Treat 26:237–246
23. Giordano C, Cui Y, Barone I et al (2009) Growth factor-induced resistance to tamoxifen is associated with a mutation of estrogen receptor alpha and its phosphorylation at serine 305. Breast Cancer Res Treat 119:71–85

24. Barone I, Brusco L, Fuqua SA (2010) Estrogen receptor mutations and changes in downstream gene expression and signaling. Clin Cancer Res 16:2702–2708
25. Barone I, Iacopetta D, Covington KR et al (2010) Phosphorylation of the mutant K303R estrogen receptor alpha at serine 305 affects aromatase inhibitor sensitivity. Oncogene 29:2404–2414
26. Barone I, Cui Y, Herynk MH et al (2009) Expression of the K303R estrogen receptor-alpha breast cancer mutation induces resistance to an aromatase inhibitor via addiction to the PI3K/Akt kinase pathway. Cancer Res 69:4724–4732
27. Blume-Jensen P, Hunter T (2001) Oncogenic kinase signalling. Nature 411:355–365
28. Martin LA, Farmer I, Johnston SR et al (2003) Enhanced estrogen receptor (ER) alpha, ERBB2, and MAPK signal transduction pathways operate during the adaptation of MCF-7 cells to long term estrogen deprivation. J Biol Chem 278:30458–30468
29. Schiff R, Massarweh SA, Shou J et al (2004) Cross-talk between estrogen receptor and growth factor pathways as a molecular target for overcoming endocrine resistance. Clin Cancer Res 10:331S–336S
30. Sabnis GJ, Jelovac D, Long B et al (2005) The role of growth factor receptor pathways in human breast cancer cells adapted to long-term estrogen deprivation. Cancer Res 65:3903–3910
31. Staka CM, Nicholson RI, Gee JM (2005) Acquired resistance to oestrogen deprivation: role for growth factor signalling kinases/oestrogen receptor cross-talk revealed in new MCF-7X model. Endocr Relat Cancer 12(Suppl 1):S85–S97
32. Evan GI, Brown L, Whyte M et al (1995) Apoptosis and the cell cycle. Curr Opin Cell Biol 7:825–834
33. Ignatov A, Ignatov T, Roessner A et al (2010) Role of GPR30 in the mechanisms of tamoxifen resistance in breast cancer MCF-7 cells. Breast Cancer Res Treat 123:87–96
34. Ignatov A, Ignatov T, Weissenborn C et al (2011) G-protein-coupled estrogen receptor GPR30 and tamoxifen resistance in breast cancer. Breast Cancer Res Treat 128:457–466
35. Vivacqua A, Lappano R, De Marco P et al (2009) G protein-coupled receptor 30 expression is up-regulated by EGF and TGF alpha in estrogen receptor alpha-positive cancer cells. Mol Endocrinol 23:1815–1826
36. Lin BC, Suzawa M, Blind RD et al (2009) Stimulating the GPR30 estrogen receptor with a novel tamoxifen analogue activates SF-1 and promotes endometrial cell proliferation. Cancer Res 69:5415–5423
37. Barone I, Brusco L, Gu G et al (2011) Loss of Rho GDIalpha and resistance to tamoxifen via effects on estrogen receptor alpha. J Natl Cancer Inst 103:538–552
38. Barone I, Catalano S, Gelsomino L et al (2012) Leptin mediates tumor-stromal interactions that promote the invasive growth of breast cancer cells. Cancer Res 72:1416–1427
39. Catalano S, Marsico S, Giordano C et al (2003) Leptin enhances, via AP-1, expression of aromatase in the MCF-7 cell line. J Biol Chem 278:28668–28676
40. Albanito L, Sisci D, Aquila S et al (2008) Epidermal growth factor induces G protein-coupled receptor 30 expression in estrogen receptor-negative breast cancer cells. Endocrinology 149:3799–3808
41. Catalano S, Malivindi R, Giordano C et al (2010) Farnesoid X receptor, through the binding with steroidogenic factor 1-responsive element, inhibits aromatase expression in tumor Leydig cells. J Biol Chem 285:5581–5593
42. Plastina P, Bonofiglio D, Vizza D et al (2012) Identification of bioactive constituents of Ziziphus jujube fruit extracts exerting antiproliferative and apoptotic effects in human breast cancer cells. J Ethnopharmacol 140:325–332
43. Catalano S, Panza S, Malivindi R et al (2013) Inhibition of Leydig tumor growth by farnesoid X receptor activation: the in vitro and in vivo basis for a novel therapeutic strategy. Int J Cancer 132:2237–2247
44. Andrews NC, Faller DV (1991) A rapid micropreparation technique for extraction of DNA-binding proteins from limiting numbers of mammalian cells. Nucleic Acids Res 19:2499
45. Gu G, Barone I, Gelsomino L et al (2012) Oldenlandia diffusa extracts exert antiproliferative and apoptotic effects on human breast cancer cells through ERalpha/Sp1-mediated p53 activation. J Cell Physiol 227:3363–3372
46. Giordano C, Catalano S, Panza S et al (2011) Farnesoid X receptor inhibits tamoxifen-resistant MCF-7 breast cancer cell growth through downregulation of HER2 expression. Oncogene 30:4129–4140
47. Macedo LF, Guo Z, Tilghman SL et al (2006) Role of androgens on MCF-7 breast cancer cell growth and on the inhibitory effect of letrozole. Cancer Res 66:7775–7782
48. Lanzino M, Maris P, Sirianni R et al (2013) DAX-1, as an androgen-target gene, inhibits aromatase expression: a novel mechanism blocking estrogen-dependent breast cancer cell proliferation. Cell Death Dis 4:e724
49. Maggiolini M, Vivacqua A, Fasanella G et al (2004) The G protein-coupled receptor GPR30 mediates c-fos up-regulation by 17beta-estradiol and phytoestrogens in breast cancer cells. J Biol Chem 279:27008–27016
50. Carmeci C, Thompson DA, Ring HZ et al (1997) Identification of a gene (GPR30) with homology to the G-protein-coupled receptor superfamily associated with estrogen receptor expression in breast cancer. Genomics 45:607–617
51. Vivacqua A, Romeo E, De Marco P et al (2012) GPER mediates the Egr-1 expression induced by 17beta-estradiol and 4-hydroxitamoxifen in breast and endometrial cancer cells. Breast Cancer Res Treat 133:1025–1035
52. Albanito L, Madeo A, Lappano R et al (2007) G protein-coupled receptor 30 (GPR30) mediates gene expression changes and growth response to 17beta-estradiol and selective GPR30 ligand G-1 in ovarian cancer cells. Cancer Res 67:1859–1866
53. Hanahan D, Weinberg RA (2000) The hallmarks of cancer. Cell 100:57–70
54. Albanito L, Lappano R, Madeo A et al (2008) G-protein-coupled receptor 30 and estrogen receptor-alpha are involved in the proliferative effects induced by atrazine in ovarian cancer cells. Environ Health Perspect 116:1648–1655
55. Filardo EJ, Graeber CT, Quinn JA et al (2006) Distribution of GPR30, a seven membrane-spanning estrogen receptor, in primary breast cancer and its association with clinicopathologic determinants of tumor progression. Clin Cancer Res 12:6359–6366
56. Sirianni R, Chimento A, Ruggiero C et al (2008) The novel estrogen receptor, G protein-coupled receptor 30, mediates the proliferative effects induced by 17beta-estradiol on mouse spermatogonial GC-1 cell line. Endocrinology 149:5043–5051
57. Kuo WH, Chang LY, Liu DL et al (2007) The interactions between GPR30 and the major biomarkers in infiltrating ductal carcinoma of the breast in an Asian population. Taiwan J Obstet Gynecol 46:135–145
58. Angel P, Karin M (1991) The role of Jun, Fos and the AP-1 complex in cell-proliferation and transformation. Biochim Biophys Acta 1072:129–157
59. Morgan L, Gee J, Pumford S et al (2009) Elevated Src kinase activity attenuates tamoxifen response in vitro and is associated with poor prognosis clinically. Cancer Biol Ther 8:1550–1558
60. Fan P, Wang J, Santen RJ et al (2007) Long-term treatment with tamoxifen facilitates translocation of estrogen receptor alpha out of the nucleus and enhances its interaction with EGFR in MCF-7 breast cancer cells. Cancer Res 67:1352–1360
61. Fidler IJ (2003) The pathogenesis of cancer metastasis: the 'seed and soil' hypothesis revisited. Nat Rev Cancer 3:453–458

62. Witz IP (2008) Yin-Yang activities and vicious cycles in the tumor microenvironment. Cancer Res 68:9–13
63. Martinez-Outschoorn UE, Goldberg A, Lin Z et al (2011) Anti-estrogen resistance in breast cancer is induced by the tumor microenvironment and can be overcome by inhibiting mitochondrial function in epithelial cancer cells. Cancer Biol Ther 12:924–938
64. Madeo A, Maggiolini M (2010) Nuclear alternate estrogen receptor GPR30 mediates 17beta-estradiol-induced gene expression and migration in breast cancer-associated fibroblasts. Cancer Res 70:6036–6046
65. Normanno N, Di Maio M, De Maio E et al (2005) Mechanisms of endocrine resistance and novel therapeutic strategies in breast cancer. Endocr Relat Cancer 12:721–747
66. Mo Z, Liu M, Yang F et al (2013) GPR30 as an initiator of tamoxifen resistance in hormone-dependent breast cancer. Breast Cancer Res 15:R114

Cell Reports

Anti-estrogen Resistance in Human Breast Tumors Is Driven by JAG1-NOTCH4-Dependent Cancer Stem Cell Activity

Graphical Abstract

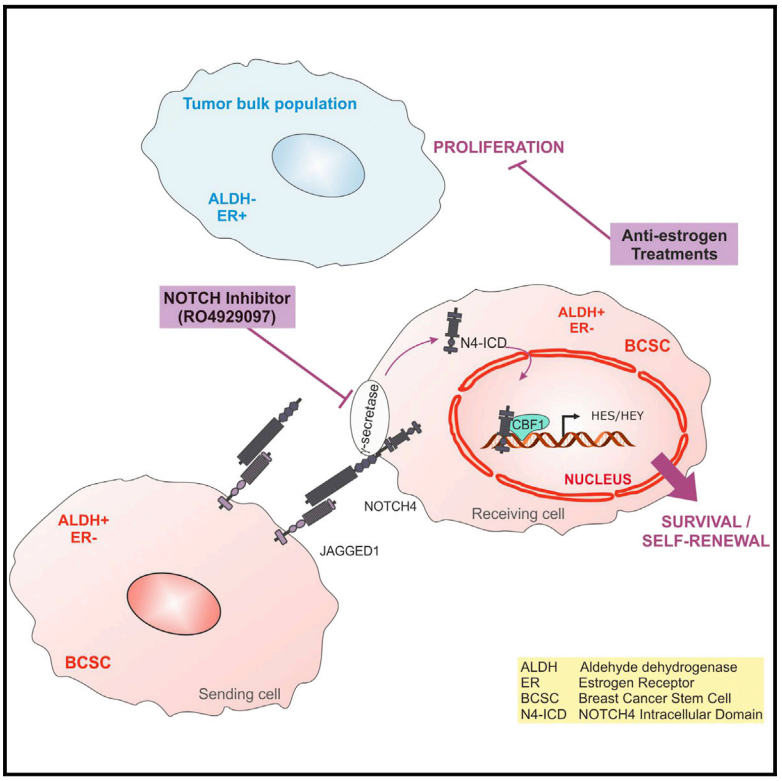

Highlights

- Anti-estrogen therapies selectively enrich for BCSCs and activate Notch signaling
- Notch pathway activation and ALDH1 predict for anti-estrogen treatment failure
- Targeting of Notch4 reduces the population of BCSCs
- Notch inhibitors might prevent relapse or overcome resistance in ER+ tumors

Authors

Bruno M. Simões, Ciara S. O'Brien, Rachel Eyre, ..., Göran Landberg, Sacha J. Howell, Robert B. Clarke

Correspondence

sacha.howell@christie.nhs.uk (S.J.H.), robert.clarke@manchester.ac.uk (R.B.C.)

In Brief

Breast cancers frequently develop resistance to anti-estrogen treatment, which makes it imperative to understanding how therapy resistance develops. Here, Simões et al. show that combining standard anti-estrogen therapies with anti-Notch4 drugs targeting breast cancer stem cells should improve treatment of ER+ breast cancer patients by preventing relapse due to therapy resistance.

Simões et al., 2015, Cell Reports *12*, 1968–1977
September 29, 2015
http://dx.doi.org/10.1016/j.celrep.2015.08.050

OPEN ACCESS
CellPress

Cell Reports
Report

Anti-estrogen Resistance in Human Breast Tumors Is Driven by JAG1-NOTCH4-Dependent Cancer Stem Cell Activity

Bruno M. Simões,[1,9] Ciara S. O'Brien,[1,9] Rachel Eyre,[1] Andreia Silva,[1] Ling Yu,[1] Aida Sarmiento-Castro,[1] Denis G. Alférez,[1] Kath Spence,[1] Angélica Santiago-Gómez,[1] Francesca Chemi,[1,2] Ahmet Acar,[3] Ashu Gandhi,[4] Anthony Howell,[1] Keith Brennan,[3] Lisa Rydén,[5] Stefania Catalano,[2] Sebastiano Andó,[2] Julia Gee,[6] Ahmet Ucar,[1,3] Andrew H. Sims,[7] Elisabetta Marangoni,[8] Gillian Farnie,[1] Göran Landberg,[1] Sacha J. Howell,[1,*] and Robert B. Clarke[1,*]

[1]Breast Cancer Now Research Unit, Institute of Cancer Sciences, University of Manchester, Wilmslow Road, Manchester M20 4BX, UK
[2]Department of Pharmacy, Health and Nutritional Sciences, University of Calabria, 87036 Arcavacata di Rende, Cosenza, Italy
[3]Faculty of Life Sciences, University of Manchester, Oxford Road, Manchester M13 9PT, UK
[4]Manchester Academic Health Science Centre, University Hospital of South Manchester NHS Foundation Trust, Southmoor Road, Manchester M23 9LT, UK
[5]Department of Surgery, Clinical Sciences, Lund University, Skåne University Hospital, 21428 Malmö, Sweden
[6]Cardiff School of Pharmacy and Pharmaceutical Sciences, University of Cardiff, Cardiff, Wales CF10 3NB, UK
[7]Applied Bioinformatics of Cancer Group, Systems Medicine Building, Western General Hospital, University of Edinburgh, Edinburgh EH4 2XU, UK
[8]Laboratoire d'Investigation Préclinique, Institut Curie, 26 rue d'Ulm 75248 Paris Cedex 05, France
[9]Co-first author
*Correspondence: sacha.howell@christie.nhs.uk (S.J.H.), robert.clarke@manchester.ac.uk (R.B.C.)
http://dx.doi.org/10.1016/j.celrep.2015.08.050

SUMMARY

Breast cancers (BCs) typically express estrogen receptors (ERs) but frequently exhibit de novo or acquired resistance to hormonal therapies. Here, we show that short-term treatment with the anti-estrogens tamoxifen or fulvestrant decrease cell proliferation but increase BC stem cell (BCSC) activity through JAG1-NOTCH4 receptor activation both in patient-derived samples and xenograft (PDX) tumors. In support of this mechanism, we demonstrate that high ALDH1 predicts resistance in women treated with tamoxifen and that a NOTCH4/HES/HEY gene signature predicts for a poor response/prognosis in 2 ER+ patient cohorts. Targeting of NOTCH4 reverses the increase in Notch and BCSC activity induced by anti-estrogens. Importantly, in PDX tumors with acquired tamoxifen resistance, NOTCH4 inhibition reduced BCSC activity. Thus, we establish that BCSC and NOTCH4 activities predict both de novo and acquired tamoxifen resistance and that combining endocrine therapy with targeting JAG1-NOTCH4 overcomes resistance in human breast cancers.

INTRODUCTION

Resistance to endocrine therapies such as selective estrogen receptor (ER) modulators (SERMs; e.g., tamoxifen), selective ER downregulators (SERDs; e.g., fulvestrant), and the aromatase inhibitors is seen in 50%–60% of early breast cancer (BC) cases and develops in almost all patients with advanced disease (Davies et al., 2011; Palmieri et al., 2014).

Evidence suggests that tumor-initiating or cancer stem-like cells (CSCs) are responsible for tumor recurrence after chemo- and endocrine therapy (Li et al., 2008; Creighton et al., 2009). Al-Hajj et al. (2003) were the first to show that tumor-initiating cells were capable of recapitulating the original tumor phenotype when transplanted into immunodeficient mice. In vitro functional assays for BC stem cell (BCSC) activity include aldehyde dehydrogenase 1 (ALDH1) enzyme activity and the capacity to form clonogenic mammospheres in suspension culture (Ginestier et al., 2007). It has been demonstrated that the BCSC population is ER negative/low and resistant to the direct effects of endocrine therapy (Simões et al., 2011; Harrison et al., 2013; Piva et al., 2014).

We have shown that aberrant Notch activation transforms normal breast cells, is found in pre-invasive and invasive human BCs, and correlates with early recurrence (Stylianou et al., 2006; Farnie et al., 2007). Moreover, we reported that inhibition of Notch signaling, particularly NOTCH4 receptor, reduced BCSC activity (Harrison et al., 2010).

Here, using patient-derived ER+ BC samples and patient-derived xenografts (PDXs), we report that short-term treatment with endocrine therapies enriches for JAG1-NOTCH4-regulated BCSCs, suggesting that these effects are not through genetic selection. Furthermore, we show that ALDH1 expression and NOTCH4 activation in human primary tumors are predictive of resistance to endocrine treatments. Finally, we demonstrate that NOTCH inhibition in vivo reduces BCSC activity in long-term acquired resistant PDX tumors. Thus, we propose that inhibiting Notch signaling will help overcome endocrine therapy resistance and recurrence in ER+ BC.

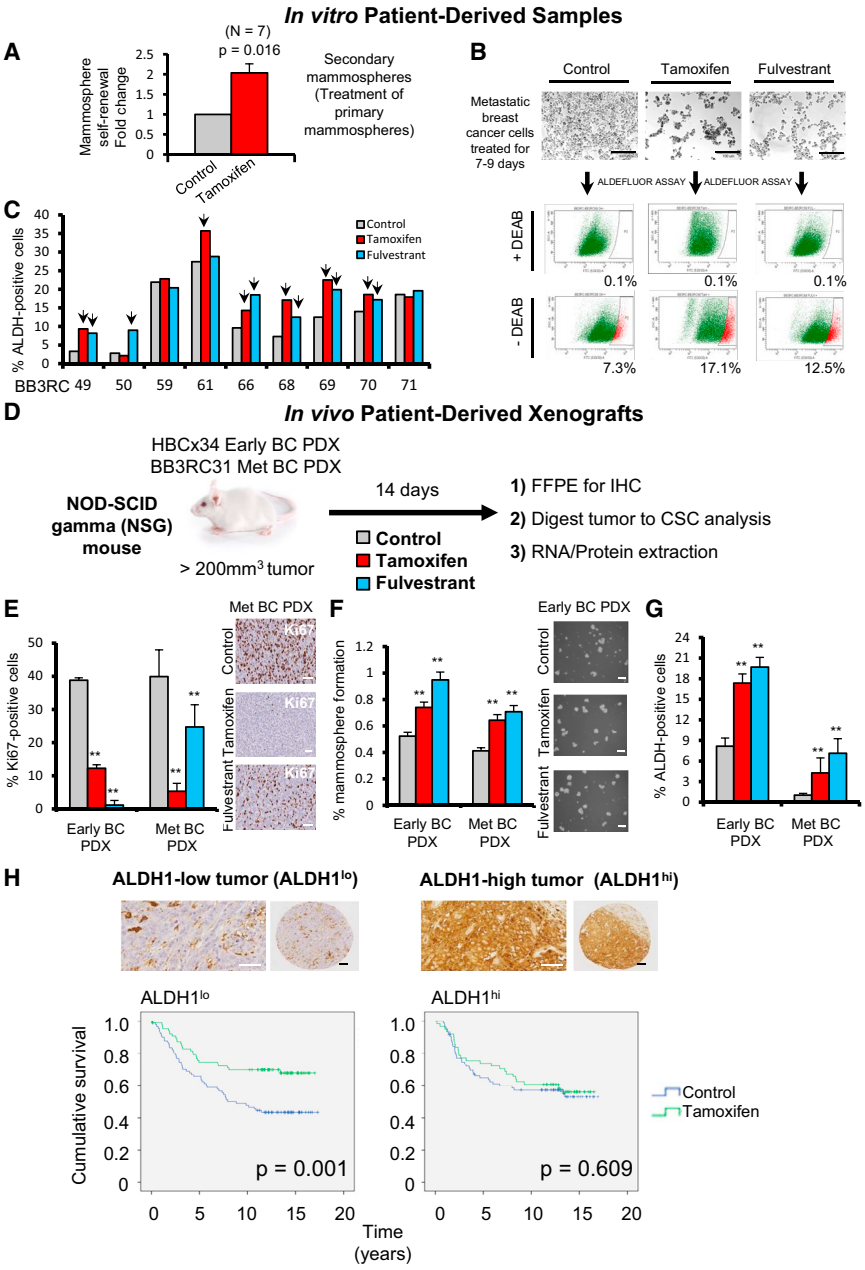

Figure 1. Tamoxifen or Fulvestrant Treatment of ER+ Patient-Derived Samples and PDXs Selectively Enriches for Cells with CSC Properties

High BCSC frequency is associated with worse outcomes for tamoxifen-treated BC patients.

(A) Mammosphere self-renewal of freshly isolated ER+ early and metastatic patient-derived samples. Primary mammospheres cultured in the presence of ethanol (Control) or 10^{-6} M 4-hydroxy-tamoxifen (Tamoxifen) were dissociated and re-plated in secondary mammosphere suspension culture for a further 7–9 days to measure self-renewal of mammosphere-initiating cells treated in the first generation. p value was calculated with Wilcoxon signed-rank test.

(B) Representative micrographs of metastatic BC cells before fluorescence-activated cell sorting (FACS) analysis of ALDH1 enzymatic activity (ALDEFLUOR assay). ALDH-positive cells were discriminated from ALDH-negative cells using the ALDH inhibitor DEAB.

(C) Percentage of ALDH-positive cells in nine ER+ metastatic BC patient-derived samples. Cells were grown in adherence with ethanol (Control), tamoxifen (10^{-6} M), or fulvestrant (10^{-7} M) for 7–9 days. Arrows indicate fold change greater than 20% compared to control.

(D–G) Early (HBCx34) and metastatic (BB3RC31) BC estrogen-dependent PDX tumors treated in vivo for 14 days with tamoxifen (10 mg/kg/day, oral gavage; red bars) or fulvestrant (200 mg/kg/week, subcutaneous injection; blue bars). Gray bars correspond to vehicle control. FFPE, formalin-fixed paraffin-embedded. (E) Representative micrographs and quantification of Ki67 expression determined by immunohistochemistry (IHC). (F) Percentage of MFE. (G) ALDH-positive cells (%) determined using the ALDEFLUOR assay.

(H) ALDH1 expression was assessed by immunohistochemistry in breast tumor epithelial cells, and the percentage of positive cells was scored. Representative micrographs of ALDH-high ($ALDH^{hi}$) and -low ($ALDH^{lo}$) epithelial expression are shown. Kaplan-Meier curves represent cumulative survival for the $ALDH^{lo}$ population and $ALDH^{hi}$ population of a cohort of 322 pre-menopausal ER+ BC patients who participated in a randomized trial of 2 years of adjuvant tamoxifen treatment versus no systemic treatment (control). Vertical bars on survival curves indicate censored cases. p values are based on a log-rank (Mantel-Cox) test of equality of survival distributions.

Scale bars, 100 μm. Data are represented as mean ± SEM. *p < 0.05; **p < 0.01.

See also Figure S1.

RESULTS

BCSC Activity Is Enriched by Tamoxifen and Fulvestrant

We tested the effect of the anti-estrogen tamoxifen on the mammosphere-forming efficiency (MFE) of patient-derived ER+ tumor cells and found that tamoxifen increases mammosphere self-renewal by about 2-fold (Figures 1A, S1A, and S1B). Next, we investigated ALDH activity, another functional assay for CSCs, in nine patient samples treated with tamoxifen or fulvestrant and showed significant increases in ALDH enzymatic activity in seven patients (Figures 1B and 1C). These data suggest that endocrine therapies, given for a period of a few days, enrich for stem cell activity.

Then, we tested the in vivo impact of endocrine therapies on stem cell activity in ER+ BC using PDXs grown subcutaneously in mice. We used both an early (treatment-naive; early BC) and a metastatic ER+ PDX tumor that both maintain biological characteristics (such as the expression of ER and estrogen

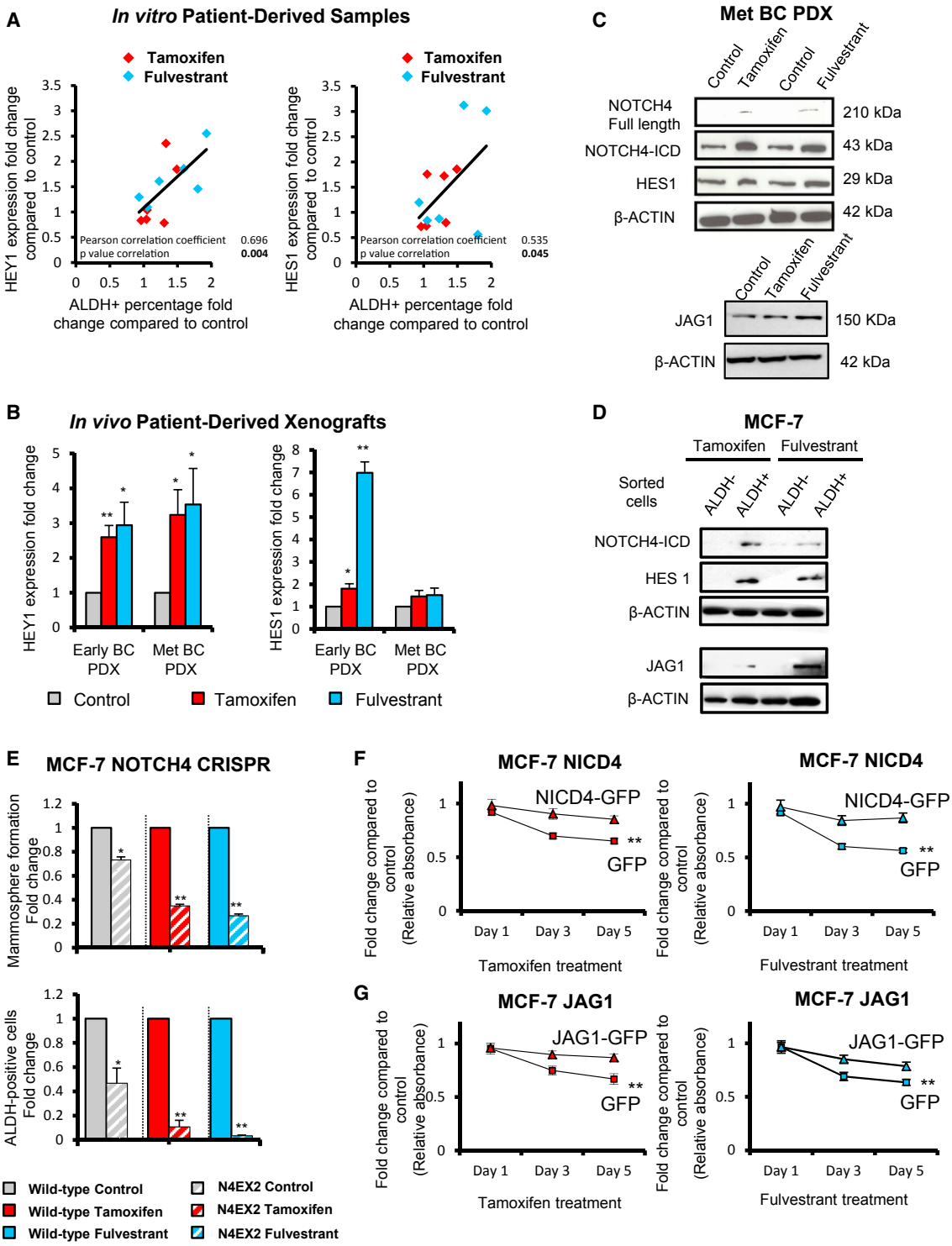

Figure 2. Tamoxifen or Fulvestrant Treatment Upregulates Notch Target Genes in Patient-Derived Samples and PDXs

JAG1-NOTCH4 receptor signaling in ALDH-positive cells drives Notch activity in endocrine-resistant BC.

(A and B) Expression of Notch target genes *HEY1* and *HES1* was assessed by real-time qPCR analysis and compared to control to determine fold change. (A) Metastatic BC patient-derived cells were treated for 7–9 days with ethanol (control), tamoxifen (10^{-6} M), or fulvestrant (10^{-7} M) and a correlation between fold change of expression of HEY1 and HES1 and fold change of percentage of ALDH-positive cells is shown. (B) Early (HBCx34) and metastatic (BB3RC31) BC PDXs: the effect of in vivo treatment for 14 days with tamoxifen (10 mg/kg/day, oral gavage) or fulvestrant (200 mg/kg/week, subcutaneous injection) on *HEY1* and *HES1*.

(legend continued on next page)

dependence) of the patient primary tumor from which they were derived (Figures S1D and S1E). The estrogen dependence of the HBCx34 PDX model (early BC) has been previously reported (Cottu et al., 2012). Using a 14-day in vivo "window" treatment (Figure 1D), we showed that both tamoxifen and fulvestrant treatment decrease proliferation (Figure 1E). However, there is an increase in MFE and ALDH enzymatic activity (Figures 1F and 1G), suggesting a mechanism for endocrine resistance driven by enrichment for a stem cell phenotype.

The mechanism for this enrichment by anti-estrogens may be partly explained by more than 90% of sorted ALDH-positive cells being ER negative (Figure S1C). Thus, we hypothesized that frequency of ALDH-positive cells would predict for response to tamoxifen treatment, and we analyzed ALDH1 in 322 ER+ BC samples taken prior to a randomized trial of tamoxifen versus no systemic treatment. ALDH1 percentage dichotomized at the median value predicted benefit from tamoxifen so that improvement in survival (i.e., a response to treatment) was only seen in women with low epithelial ALDH1 expression (Figure 1H; Table S3). We saw no significant difference in recurrence between control treated patients with high versus low ALDH1 expression ($p = 0.59$). These data, from a prospective randomized trial, establish for the first time that ALDH-positive cell frequency predicts response to tamoxifen treatment, suggesting that stem cell numbers may be responsible for de novo endocrine resistance.

Tamoxifen or Fulvestrant Treatment Upregulates Notch Target Genes

We analyzed the patient-derived BC cells that were treated with tamoxifen and fulvestrant in Figures 1B and 1C and found that increased numbers of ALDH-positive cells were strongly correlated to increased expression of Notch target genes (*HEY1* and *HES1*) (Figure 2A). In addition, the BC PDX tumors treated in vivo with tamoxifen or fulvestrant (Figure 1D) for 2 weeks showed increased *HEY1* and *HES1* expression (Figure 2B), supporting an increased role for the Notch signaling pathway after endocrine therapies.

In ER+ cell lines (MCF-7, T47D, and ZR-75-1) in vitro, treatment with tamoxifen or fulvestrant for 6 days preferentially increased expression of *HEY1* and *HES1* (Figure S2A). Similarly, in tamoxifen-resistant (TAMR) or fulvestrant-resistant (FULVR) MCF-7 models, which have acquired resistance after long-term tamoxifen or fulvestrant treatment, we found upregulation of Notch target genes and increased Notch transcriptional activity (Figure S4A).

JAG1 and NOTCH4 Receptor Signaling Drives Endocrine Resistance

Next, we assessed the expression of Notch receptors and ligands in parental, TAMR, and FULVR cell lines. NOTCH4 and its intracellular domain (ICD) were upregulated while NOTCH1, -2, and -3 were downregulated (Figure S4B) in the resistant versus parental cell lines. We found the Notch ligand JAG1 to be highly expressed in both resistant models (Figure S4B), while expression of the other four ligands was either unchanged (DLL1 and DLL4; Figure S4B) or absent (JAG2 and DLL3; data not shown). JAG1 and NOTCH4-ICD were also upregulated after a 14-day window treatment of PDXs in vivo, and after short-term treatment with tamoxifen or fulvestrant of MCF-7 cells in vitro, suggesting that activation of Notch signaling (demonstrated by increased HES1 expression) is an early event in the acquisition of endocrine resistance (Figures 2C and S2B). Importantly, JAG1, NOTCH4-ICD, and HES1 are expressed at higher levels in ALDH-positive cells, which suggests JAG1-NOTCH4 signaling between ALDH-positive cells (Figure 2D).

To further confirm the role of NOTCH4 activity in endocrine resistance and the stem cell phenotype, we analyzed loss-of- and gain-of-function phenotypes for NOTCH4-ICD in MCF-7 cells. Genomic disruption of exon 2 of *NOTCH4* by using a CRISPR approach led to loss of protein expression (Figures S2C–S2E) and a significant inhibition of MFE and ALDH-positive cells, especially after tamoxifen and fulvestrant treatments (Figure 2E). In contrast, overexpression of NOTCH4-ICD or JAG1 conferred tamoxifen and fulvestrant resistance in parental MCF-7 cells (Figures 2F and 2G).

Overall, these results indicate that JAG1 ligand and cleavage of NOTCH4-ICD may be responsible for Notch signaling activation after endocrine treatment, which is in agreement with recent reports that NOTCH4 expression is increased in TAMR cell lines (Yun et al., 2013; Lombardo et al., 2014).

GSI RO4929097 Abrogates Tamoxifen- and Fulvestrant-Stimulated CSC Activity

In order to inhibit NOTCH4 signaling, we used the gamma-secretase inhibitor (GSI) RO4929097, which we found to be effective in reducing levels of the active NOTCH4 ICD in endocrine-resistant models (Figure S4C). RO4929097 inhibited *HEY1* and *HES1* expression, as well as CBF1-Notch transcriptional activity in TAMR and FULVR cell lines, but not in parental MCF-7 cells (Figure S4D). Therefore, we tested whether RO4929097 would abrogate increases in MFE and ALDH-positive cells induced in vivo by anti-estrogens administered in short-term window

(C) NOTCH4, HES1, and JAG1 protein expression levels determined by western blot in metastatic (Met) (BB3RC31) BC PDX. β-actin was used as a reference for the loading control.
(D) NOTCH4, HES1, and JAG1 protein expression levels were determined by western blot in MCF-7 ALDH-negative and ALDH-positive sorted cells. MCF-7 cells were treated with tamoxifen or fulvestrant for 6 days before ALDH sorting.
(E) Wild-type MCF-7 cells (filled bars) and a CRISPR clone containing a disruption of *NOTCH4* exon 2 (N4EX2 cells, hatched bars) treated in adherence with ethanol (Control, gray bars), 10^{-6} M tamoxifen (red bars), and 10^{-7} M fulvestrant (blue bars) for 6 days. N4EX2 cells' fold change of MFE and ALDH-positive cells after treatments was compared to that of the wild-type cells.
(F and G) NICD4 and JAG1 rescue tamoxifen- or fulvestrant-inhibited growth: cell number (using sulforhodamine B [SRB] assay, y axis) of MCF-7 overexpressing (F) NICD4-GFP, (G) JAG1-GFP, or GFP control incubated with tamoxifen or fulvestrant for 1, 3, and 5 days (x axis) compared to the respective cell line treated with control ethanol. p values are for the 5-day treatment.
Data are represented as mean ± SEM. *$p < 0.05$; **$p < 0.01$.
See also Figures S2 and S4.

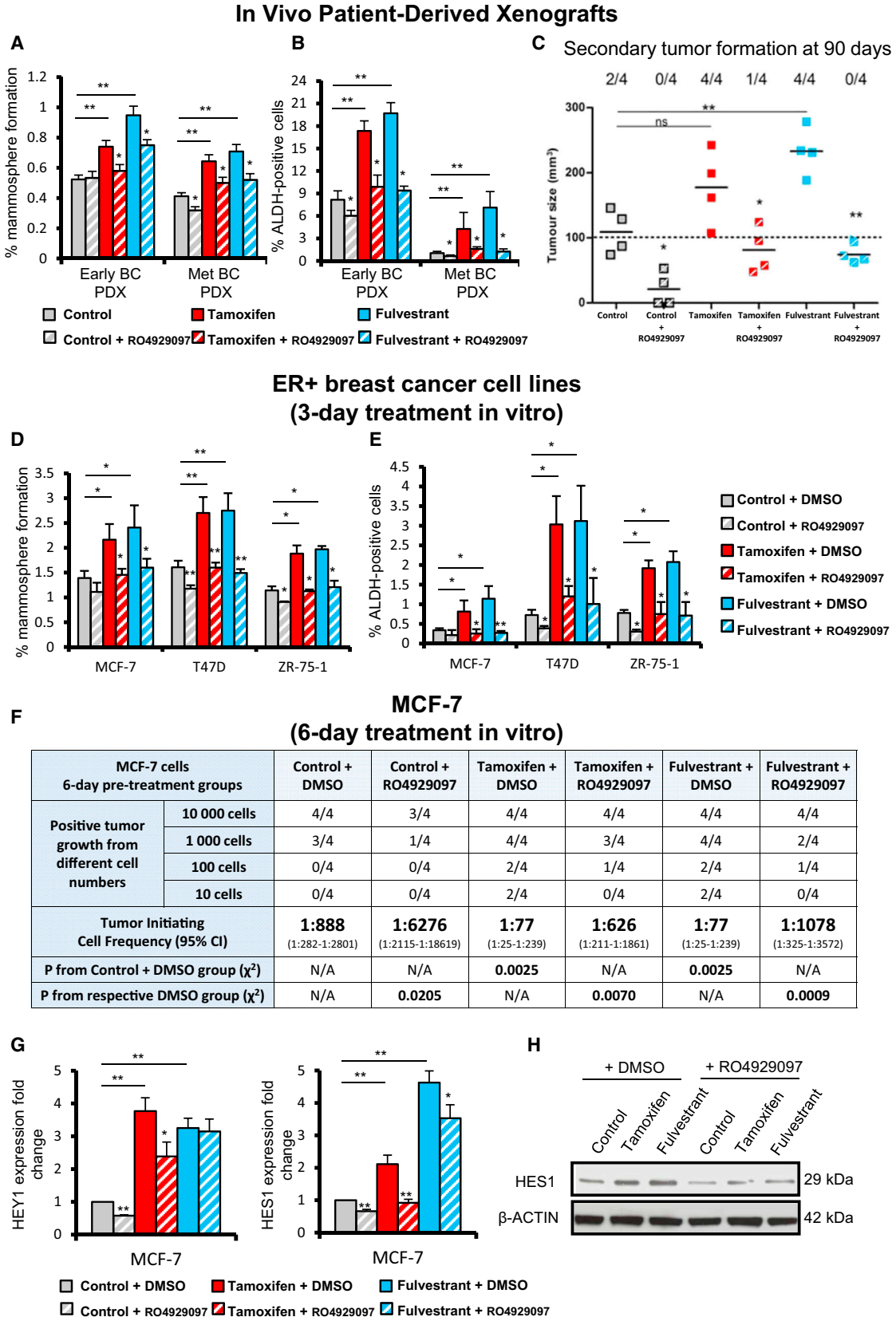

F

MCF-7
(6-day treatment in vitro)

MCF-7 cells 6-day pre-treatment groups		Control + DMSO	Control + RO4929097	Tamoxifen + DMSO	Tamoxifen + RO4929097	Fulvestrant + DMSO	Fulvestrant + RO4929097
Positive tumor growth from different cell numbers	10 000 cells	4/4	3/4	4/4	4/4	4/4	4/4
	1 000 cells	3/4	1/4	4/4	3/4	4/4	2/4
	100 cells	0/4	0/4	2/4	1/4	2/4	1/4
	10 cells	0/4	0/4	2/4	0/4	2/4	0/4
Tumor Initiating Cell Frequency (95% CI)		**1:888** (1:282-1:2801)	**1:6276** (1:2115-1:18619)	**1:77** (1:25-1:239)	**1:626** (1:211-1:1861)	**1:77** (1:25-1:239)	**1:1078** (1:325-1:3572)
P from Control + DMSO group (χ^2)		N/A	N/A	**0.0025**	N/A	**0.0025**	N/A
P from respective DMSO group (χ^2)		N/A	**0.0205**	N/A	**0.0070**	N/A	**0.0009**

(legend on next page)

treatments, using the same estrogen-dependent ER+ PDX tumors as in Figures 1D–1G. Tamoxifen and fulvestrant treatments reduced tumor growth and proliferation (Figures S3A and S3B) while increasing both MFE and ALDH activity (Figures 3A and 3B). RO4929097 had no impact on growth or proliferation (% Ki67; Figure S3B) but significantly inhibited endocrine-stimulated MFE and ALDH activity (Figures 3A and 3B). The gold standard for functionally determining tumor-initiating cells is xenograft formation in secondary mouse hosts, which we performed using dissociated cells from PDX tumors treated in vivo with anti-estrogens and/or RO4929097. Cells isolated from tumors treated in vivo with RO4929097 had significantly reduced tumor-initiating capacity 90 days post-implantation (Figure 3C). Furthermore, the stimulation of tumorigenicity following in vivo tamoxifen and fulvestrant treatment was completely reversed by RO4929097 (Figure 3C). Overall, these data suggest that BCSCs, measured by tumor-initiating activity and enriched by short-term anti-estrogen treatments, are dependent on NOTCH4 signaling that can be blocked by combination treatment with a NOTCH4 inhibitor.

To further substantiate this finding, we analyzed MFE and ALDH activity of MCF-7, T47D, and ZR-75-1 cells treated for 3 days with tamoxifen or fulvestrant in combination with RO4929097. In all cases, RO4929097 reduced MFE and ALDH-positive cells (Figures 3D and 3E). To confirm that RO4929097 reduced the tumor-initiating capacity, we conducted in vivo limiting dilution transplantation of MCF-7 cells. Extreme limiting dilution analysis (ELDA) revealed an 11-fold enrichment in tumor-initiating cell frequency following tamoxifen or fulvestrant pre-treatment, which was reversed by co-treatment with RO4929097 (Figure 3F). Inhibition of NOTCH4 cleavage/activation by RO4929097 was evidenced by decreased HEY1 and HES1 mRNA and protein levels (Figures 3G and 3H). Thus, we established, using PDX models and cell lines in tumor-initiating cell assays, that NOTCH4 inhibition reduces BCSC activity induced by anti-estrogen treatment.

NOTCH4 Inhibition Targets CSCs in TAMR PDX Models

The next question we asked was whether inhibiting NOTCH4 signaling to target BCSCs will overcome long-term acquired anti-estrogen resistance in ER+ BC patients. We investigated RO4929097 treatment in two established PDXs (HBCx22 and HBCx34) that have long-term acquired resistance to tamoxifen in vivo. Analysis of HES1 expression by immunohistochemistry revealed that these two TAMR PDXs displayed increased Notch signaling activation compared to the parental control (Figure 4A). Notably, the TAMR HBCx34 PDX model has a higher percentage of MFE and ALDH activity than the endocrine-sensitive HBCx34 PDX model (compare Figures 1F and 1G with Figures 4B and 4C). These data suggest that acquired tamoxifen resistance in PDX models involves enrichment for BCSC activity through Notch signaling. Treatment with RO4929097 for 14 days demonstrates that MFE and ALDH activity can be significantly reduced in TAMR PDX tumors in vivo (Figures 4B–4D).

NOTCH4/HES/HEY Gene Signature Predicts for Resistance to Tamoxifen Treatment and Prognosis in ER+ Tumors

Based on the aforementioned observations, we hypothesized that NOTCH4 activity, comprising a NOTCH4/HES/HEY gene signature, would predict for response to tamoxifen treatment. In gene expression data from 669 pre-treatment tumors from four published Affymetrix microarray datasets of ER+ patients who subsequently received adjuvant tamoxifen therapy, we found *NOTCH4*, *HES1*, *HEY1*, and *HEY2* to be co-expressed in some tumors, as demonstrated in the heatmap ordered from left to right by the sum of the four genes (Figure 5A). Importantly, elevated expression of these Notch genes before treatment was significantly associated with distant metastasis (Figure 5A) and with reduced overall survival in an independent cohort of 343 untreated ER+ patients (Figure 5B). Thus, *NOTCH4* gene expression and activity in tumors before treatment with endocrine therapy predicts sensitivity to treatment, indicating that this signaling pathway predicts de novo as well as acquired endocrine resistance. These data strengthen the case for therapies against NOTCH4 to target the endocrine-resistant ALDH-positive cells responsible for relapse of ER+ tumors following hormonal therapy (Figure 5C).

DISCUSSION

Here, we report that BCSC activity and frequency are increased in response to the common endocrine therapies tamoxifen and fulvestrant in ER+ patient samples and in early and metastatic PDXs. Our findings suggest that endocrine therapies do not target BCSCs, and this may explain how residual drug-resistant cells are responsible for the relapse of ER+ tumors following hormonal therapy. Although we observe increased BCSC frequency after endocrine treatments, we do not know whether absolute BCSC numbers remain the same and are selected for or whether

Figure 3. NOTCH4 Inhibition using RO4929097 Abrogates Tamoxifen and Fulvestrant Enrichment of CSC Activities

(A–C) Early (HBCx34) and metastatic (Met) (BB3RC31) PDX tumors treated in vivo for 14 days with tamoxifen (10 mg/kg/day, oral gavage) or fulvestrant (200 mg/kg/week, subcutaneous injection) in the presence or absence of the NOTCH4 inhibitor RO4929097 (3 mg/kg/day, oral gavage). (A) MFE (%). (B) Percentage of ALDH-positive cells. (C) Secondary tumor formation. 100,000 cells of metastatic (BB3RC31) PDX were re-implanted subcutaneously in NSG mice with 90-day slow-release estrogen pellets. Tumor growth (>100 mm^3) was determined at day 90 after cell injection.

(D and E) MCF-7, T47D, and ZR-75-1 cells were pre-treated in adherence with 10^{-6} M tamoxifen (red bars) and 10^{-7} M fulvestrant (blue bars) with RO4929097 (10 μM; hatched bars) or DMSO (filled bars) for 72 hr. (D) MFE and (E) percentage of ALDH-positive cells were assessed after pre-treatments.

(F–H) MCF-7 cells were pre-treated in adherence for 6 days in the presence of RO4929097 (10 μM; hatched bars) or DMSO (filled bars). (F) In vivo experiments were carried out in NSG mice with 90-day slow-release estrogen pellets. Tumor growth (>100 mm^3) was assessed at day 60 and is represented as mice positive for growth/mice tested for each cell number tested. ELDA of tumor-initiating cell frequency is shown. (G) Expression of *HEY1* and *HES1* by real-time PCR was compared to the control. (H) HES1 protein expression levels determined by western blot.

Data are represented as mean ± SEM. p values refer to hatched bars compared to filled control bars. *$p < 0.05$; **$p < 0.01$.

See also Figures S3 and S4.

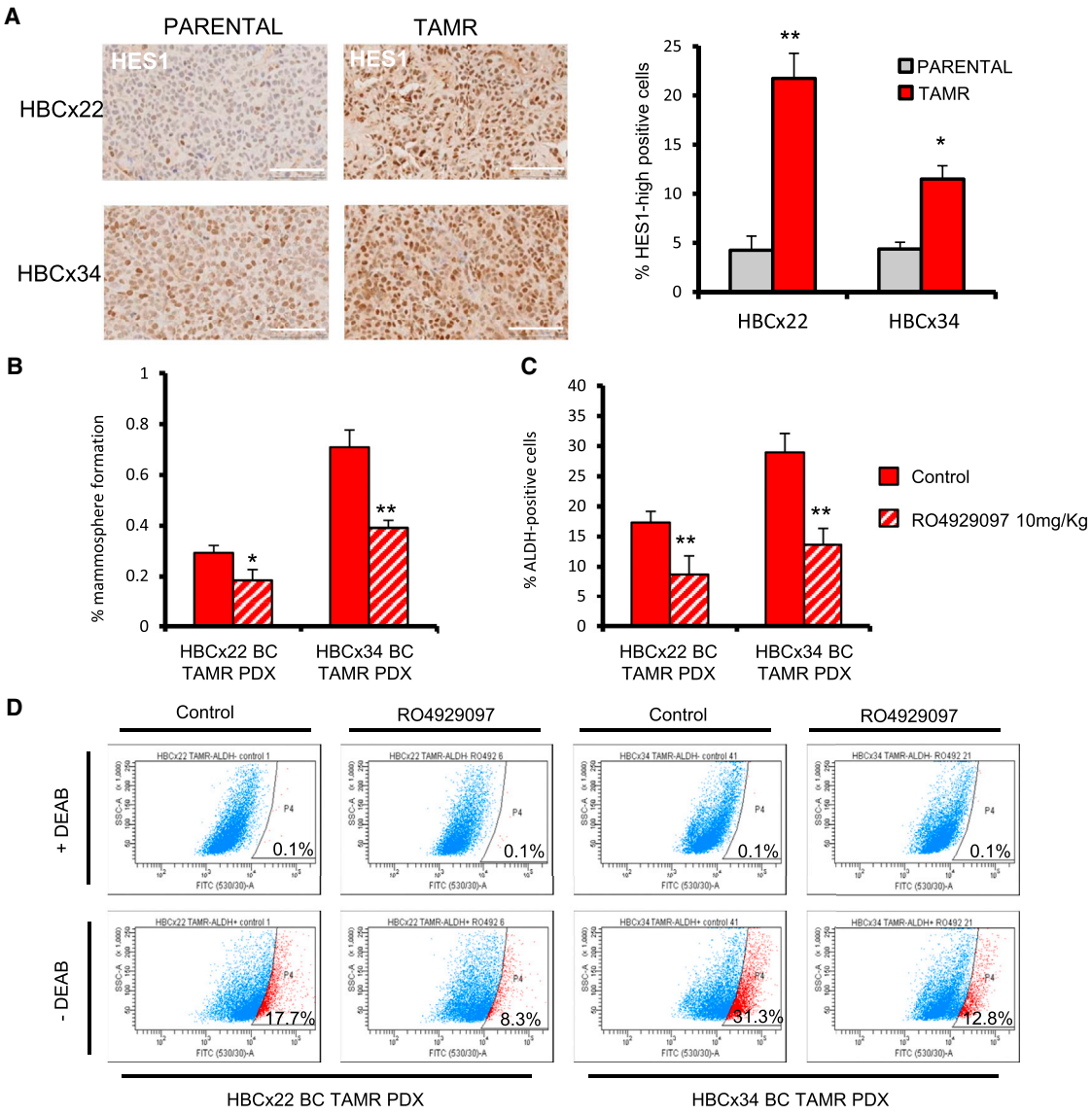

Figure 4. HBCx22 and HBCx34 TAMR PDXs Express High Levels of HES1

NOTCH4 inhibitor RO4929097 targets CSCs in tamoxifen-resistant (TAMR) PDXs.

(A) Representative micrographs and quantification of HES1 expression determined by immunohistochemistry. Scale bars, 100 μm.

(B–D) HBCx22 and HBCx34 TAMR PDXs treated in vivo for 14 days in the presence or absence of the GSI RO4929097 (10 mg/kg/day, oral gavage). (B) MFE (%). (C) Percentage of ALDH-positive cells. (D) Representative FACS plots of ALDEFLUOR assay. ALDH-positive cells were discriminated from ALDH-negative cells using the ALDH inhibitor DEAB.

Data are represented as mean ± SEM. *$p < 0.05$; **$p < 0.01$.

See also Figure S4.

they can be induced by anti-estrogen treatment. Tamoxifen and fulvestrant are clearly successful in reducing BC recurrence in some patients. In other patients with poorer outcome after endocrine therapies, we demonstrate that tumors have high pre-treatment levels of ALDH1 expression and NOTCH4 activation. Moreover, we found that treating ER+ BC cells with endocrine therapies specifically increases JAG1-NOTCH4 signaling and that combining endocrine therapies with a Notch pathway inhibitor can prevent BCSC enrichment induced by endocrine therapies. Thus, our findings in patient-derived BCSCs establish that JAG1 ligand signaling through the NOTCH4 receptor in ALDH-positive cell populations is a determining factor in the acquisition of endocrine resistance.

The best described strategy for inhibition of Notch signaling is the use of small-molecule GSIs, which prevent the release of Notch ICD (NICD). In our study, the GSI RO4929097 specifically targets NOTCH4 cleavage in anti-estrogen-treated cells and, thus, decreases BCSC activity in vitro (MFE and ALDH activity)

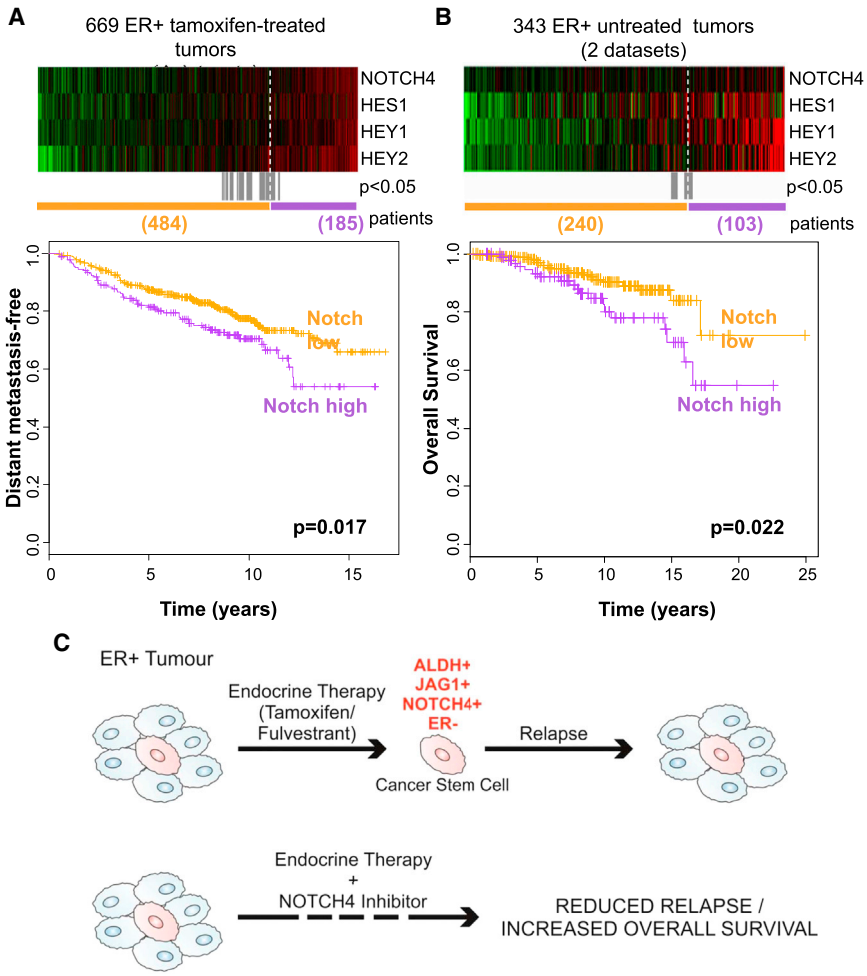

Figure 5. NOTCH4 Receptor Activity Predicts for Resistance to Tamoxifen Treatment and Prognosis in ER+ Tumors

(A and B) *NOTCH4*, *HES1*, *HEY1*, and *HEY2* genes in ER+ primary tumors from (A) tamoxifen-treated or (B) untreated patients are co-expressed in the heatmap ranked from left to right using the four-gene signature. Colors are $\log_2$ mean-centered values; red indicates high, and green indicates low. All significant cut-points ($p < 0.05$) are shown in gray. Kaplan-Meier analysis using the optimum cut-point (dashed white line) demonstrates that elevated expression of the Notch genes is significantly associated with an increased rate of (A) distant metastasis and (B) decreased overall survival. Vertical bars on survival curves indicate censored cases. p values are based on a log-rank (Mantel-Cox) test.

(C) Diagram suggesting that endocrine therapies do not target BCSCs and emphasizing the need of targeting residual drug-resistant cells to eliminate all cancer cells and prevent long-term recurrences of ER+ BC.

and tumor initiation in vivo. Our investigations in ER+ PDX tumors provide the rationale for the use of NOTCH4 inhibitors together with endocrine therapies in the adjuvant or advanced settings (Figure 5C). Significantly, we demonstrated the utility of RO4929097 to target BCSCs in pre-clinical models of TAMR patient tumors.

In conclusion, our data establish that tamoxifen and fulvestrant select for stem cell activity in short- and long-term-treated BC cells, as well as in early endocrine therapy naive and metastatic-endocrine-treated patient-derived samples and PDXs. Importantly, we report that low numbers of stem cells and low Notch signaling activation in patient tumors predict response to tamoxifen therapy and better survival. Overall, these results suggest that ER+ BC recurrence after endocrine therapies, which target the majority of cells (ER+ cells), will be reduced by targeting the JAG1+/NOTCH4+/ALDH1+/ER− BCSC population.

EXPERIMENTAL PROCEDURES

Patient-Derived Samples

Early BC samples were collected in RPMI (GIBCO), dissected into 1- to 2-mm^3 cubes and digested with the Human Tumor Dissociation Kit (Miltenyi Biotec) for 2 hr at 37°C. Digested tissue was filtered sequentially through 100- and 40-μm cell strainers, then centrifuged at 300 × g for 5 min and washed in PBS.

Metastatic samples (ascites or pleural effusions) were centrifuged at 1,000 × g for 10 min at 4°C. The cell pellets were diluted in PBS. Erythrocytes and leucocytes were removed using Lymphoprep (Axis-Shield) and CD45-negative magnetic sorting (Miltenyi Biotec), respectively. Cells were cultured in adherence for 7–9 days in DMEM/F-12 medium, GlutaMAX (GIBCO) with 10% fetal bovine serum (FBS; GIBCO), 10 μg/ml insulin (Sigma-Aldrich), 10 μg/ml hydrocortisone (Sigma-Aldrich), and 5 ng/ml epidermal growth factor (EGF; Sigma-Aldrich), in 10^{-6} M 4-OH tamoxifen (Sigma-Aldrich, H7904), 10^{-7} M fulvestrant (ICI 182,780, Tocris, 1047), or ethanol (control).

Clinico-pathological details of the samples are summarized in Tables S1 (primary BC) and S2 (metastatic BC).

Please refer to the Supplemental Experimental Procedures for further details.

PDXs and In Vivo Experiments

Mouse studies commenced in 8- to 12-week-old female mice and were conducted in accordance with the UK Home Office Animals (Scientific Procedures) Act 1986, using NSG (NOD.Cg-*Prkdc*^{scid} *Il2rg*^{tm1Wjl}/SzJ) mice. All in vivo work was performed with a minimum of n = 4 mice per condition.

Serial passaging of the PDX was carried out by implanting small fragments of the tumor subcutaneously into dorsal flanks of NSG mice. Early (HBCx34) and metastatic (BB3RC31) BC estrogen-dependent PDXs were administered with 8 μg/ml of 17-beta estradiol in drinking water at all times and were treated with drugs when tumors reached 200–300 mm^3. Experiments were performed using PDX tumors between passages 5 and 8. Animal weight and tumor size was measured bi-dimensionally using callipers twice a week.

Tamoxifen citrate (Sigma, T9262, 10 mg/kg/day) and RO4929097 (Cellagen Technology, 3 mg/kg/day) were administered by oral gavage (0.1 ml per dose) on a basis of 5 days out of 7 (weekends excluded) for 14 days. Tamoxifen citrate and RO4929097 were prepared in 1% carboxymethylcellulose (Sigma, C9481) dissolved in distilled water. Fulvestrant (kindly provided by AstraZeneca, 200 mg/kg/week) was administered by subcutaneous injection

(0.1 ml per dose) on a weekly basis for 14 days. The HBCx22 and HBCx34 TAMR PDXs were treated for 14 days in the presence or absence of the GSI RO4929097 (10 mg/kg/day, oral gavage). Xenografts were collected in ice-cold DMEM for live-cell assays, histological analysis, and RNA and protein extraction. PDX single-cell suspension was obtained using a collagenase-hyaluronidase mixture for digestion (Stem Cell Technologies).

Please refer to the Supplemental Experimental Procedures for further details.

Mammosphere Colony Assay

MFE was calculated by dividing the number of mammospheres formed ($\geq$50 μm) by the original number of single cells seeded (500 cells per square centimeter for primary cells) and is expressed as fold change normalized to control or as the mean percentage of MFE (Shaw et al., 2012).

Please refer to the Supplemental Experimental Procedures for further details.

Tamoxifen Trial Study

Premenopausal BC patients with invasive stage II disease were enrolled in SBII:2a, a Swedish clinical trial in which patients were randomly assigned to receive 2 years of adjuvant tamoxifen or no treatment (control) and followed up for recurrence-free and overall survival (Rydén et al., 2005). Our data represent cumulative survival for a cohort of 322 premenopausal ER+ BC patients stratified by ALDH-low (below median) and ALDH-high (above median) expression over time.

Notch Gene Expression Signature

The gene expression data on 669 ER+ tamoxifen-treated tumors (GSE6532, GSE9195, GSE17705, and GSE12093) and 343 ER+ untreated tumors (GSE2034 and GSE7390) are from published Affymetrix microarray datasets.

Please refer to the Supplemental Experimental Procedures for additional details.

Statistical Analysis

If not stated otherwise, a two-tailed Student's t test was performed for statistical analysis. A value of $p < 0.05$ was considered to be statistically significant. Error bars represent the SEM of at least three independent experiments. Data are shown as mean ± SEM.

SUPPLEMENTAL INFORMATION

Supplemental Information for this article includes Supplemental Experimental Procedures, four figures, and three tables and can be found with this article online at http://dx.doi.org/10.1016/j.celrep.2015.08.050.

AUTHOR CONTRIBUTIONS

B.M.S. and C.S.O.: conception and design, collection and/or assembly of data, data analysis and interpretation, and manuscript writing. R.E., A.S., L.Y., A.S.-C., D.G.A., K.S., A.S.-G., F.C., A.A., S.C., S.A., A.U., and G.F.: collection and/or assembly of data, data analysis and interpretation, and manuscript critique. A.G.: study recruitment, collection of BC tissue, and manuscript critique. A.H. and K.B.: conception, design, and manuscript critique. J.G.: generation of resistant cell lines and manuscript critique. L.R. and G.L.: Tamoxifen trial study and BC clinical pathology expertise and manuscript critique. A.H.S.: gene expression analysis and manuscript critique. E.M.: generation of PDX and manuscript critique. S.J.H. and R.B.C.: conception and design, data analysis and interpretation, manuscript writing, and final approval of manuscript.

ACKNOWLEDGMENTS

We are a Breast Cancer Now-funded research group (Institute of Cancer Sciences, University of Manchester). We are grateful for funding from the Cancer Research UK (C.S.O.), Medical Research Council (A.S.-C.), Fundación Alfonso Martín Escudero (A.S.-G.), and MultiFun EU FP7 grant #262943 (B.M.S. and K.S.). We thank Allan Jordan and Rebecca Newton (Drug Discovery Unit, Cancer Research UK Manchester Institute) for advice regarding small-molecule Notch inhibitors and Anne Lykkesfeldt for advice on the use of TAMR MCF-7 cells (Danish Cancer Society Research Center). We acknowledge the South-East Swedish Breast Cancer Group for providing access to clinical data and tumor tissue.

Received: March 17, 2015
Revised: July 15, 2015
Accepted: August 17, 2015
Published: September 17, 2015

REFERENCES

Al-Hajj, M., Wicha, M.S., Benito-Hernandez, A., Morrison, S.J., and Clarke, M.F. (2003). Prospective identification of tumorigenic breast cancer cells. Proc. Natl. Acad. Sci. USA *100*, 3983–3988.

Cottu, P., Marangoni, E., Assayag, F., de Cremoux, P., Vincent-Salomon, A., Guyader, Ch., de Plater, L., Elbaz, C., Karboul, N., Fontaine, J.J., et al. (2012). Modeling of response to endocrine therapy in a panel of human luminal breast cancer xenografts. Breast Cancer Res. Treat. *133*, 595–606.

Creighton, C.J., Li, X., Landis, M., Dixon, J.M., Neumeister, V.M., Sjolund, A., Rimm, D.L., Wong, H., Rodriguez, A., Herschkowitz, J.I., et al. (2009). Residual breast cancers after conventional therapy display mesenchymal as well as tumor-initiating features. Proc. Natl. Acad. Sci. USA *106*, 13820–13825.

Davies, C., Godwin, J., Gray, R., Clarke, M., Cutter, D., Darby, S., McGale, P., Pan, H.C., Taylor, C., Wang, Y.C., et al.; Early Breast Cancer Trialists' Collaborative Group (EBCTCG) (2011). Relevance of breast cancer hormone receptors and other factors to the efficacy of adjuvant tamoxifen: patient-level meta-analysis of randomised trials. Lancet *378*, 771–784.

Farnie, G., Clarke, R.B., Spence, K., Pinnock, N., Brennan, K., Anderson, N.G., and Bundred, N.J. (2007). Novel cell culture technique for primary ductal carcinoma in situ: role of Notch and epidermal growth factor receptor signaling pathways. J. Natl. Cancer Inst. *99*, 616–627.

Ginestier, C., Hur, M.H., Charafe-Jauffret, E., Monville, F., Dutcher, J., Brown, M., Jacquemier, J., Viens, P., Kleer, C.G., Liu, S., et al. (2007). ALDH1 is a marker of normal and malignant human mammary stem cells and a predictor of poor clinical outcome. Cell Stem Cell *1*, 555–567.

Harrison, H., Farnie, G., Howell, S.J., Rock, R.E., Stylianou, S., Brennan, K.R., Bundred, N.J., and Clarke, R.B. (2010). Regulation of breast cancer stem cell activity by signaling through the Notch4 receptor. Cancer Res. *70*, 709–718.

Harrison, H., Simoes, B.M., Rogerson, L., Howell, S.J., Landberg, G., and Clarke, R.B. (2013). Oestrogen increases the activity of oestrogen receptor negative breast cancer stem cells through paracrine EGFR and Notch signalling. Breast Cancer Res. *15*, R21.

Li, X., Lewis, M.T., Huang, J., Gutierrez, C., Osborne, C.K., Wu, M.F., Hilsenbeck, S.G., Pavlick, A., Zhang, X., Chamness, G.C., et al. (2008). Intrinsic resistance of tumorigenic breast cancer cells to chemotherapy. J. Natl. Cancer Inst. *100*, 672–679.

Lombardo, Y., Faronato, M., Filipovic, A., Vircillo, V., Magnani, L., and Coombes, R.C. (2014). Nicastrin and Notch4 drive endocrine therapy resistance and epithelial to mesenchymal transition in MCF7 breast cancer cells. Breast Cancer Res. *16*, R62.

Palmieri, C., Patten, D.K., Januszewski, A., Zucchini, G., and Howell, S.J. (2014). Breast cancer: current and future endocrine therapies. Mol. Cell. Endocrinol. *382*, 695–723.

Piva, M., Domenici, G., Iriondo, O., Rábano, M., Simões, B.M., Comaills, V., Barredo, I., López-Ruiz, J.A., Zabalza, I., Kypta, R., and Vivanco, Md. (2014). Sox2 promotes tamoxifen resistance in breast cancer cells. EMBO Mol. Med. *6*, 66–79.

Rydén, L., Jönsson, P.E., Chebil, G., Dufmats, M., Fernö, M., Jirström, K., Källström, A.C., Landberg, G., Stål, O., Thorstenson, S., et al. (2005). Two years of adjuvant tamoxifen in premenopausal patients with breast cancer: a randomised, controlled trial with long-term follow-up. Eur. J. Cancer *41*, 256–264.

Shaw, F.L., Harrison, H., Spence, K., Ablett, M.P., Simões, B.M., Farnie, G., and Clarke, R.B. (2012). A detailed mammosphere assay protocol for the quantification of breast stem cell activity. J. Mammary Gland Biol. Neoplasia *17*, 111–117.

Simões, B.M., Piva, M., Iriondo, O., Comaills, V., López-Ruiz, J.A., Zabalza, I., Mieza, J.A., Acinas, O., and Vivanco, M.D. (2011). Effects of estrogen on the proportion of stem cells in the breast. Breast Cancer Res. Treat. *129*, 23–35.

Stylianou, S., Clarke, R.B., and Brennan, K. (2006). Aberrant activation of notch signaling in human breast cancer. Cancer Res. *66*, 1517–1525.

Yun, J., Pannuti, A., Espinoza, I., Zhu, H., Hicks, C., Zhu, X., Caskey, M., Rizzo, P., D'Souza, G., Backus, K., et al. (2013). Crosstalk between PKCα and Notch-4 in endocrine-resistant breast cancer cells. Oncogenesis *2*, e60.

Leptin as a mediator of tumor-stromal interactions promotes breast cancer stem cell activity

Cinzia Giordano[1,*], Francesca Chemi[2,*], Salvatore Panza[2,*], Ines Barone[2], Daniela Bonofiglio[2], Marilena Lanzino[2], Angela Cordella[3], Antonella Campana[2], Adnan Hashim[4,5], Pietro Rizza[2], Antonella Leggio[2], Balázs Győrffy[7,8,9], Bruno M. Simões[6], Robert B. Clarke[6], Alessandro Weisz[4], Stefania Catalano[2,], Sebastiano Andò[1,2,**]**

[1]Centro Sanitario, University of Calabria, Arcavacata di Rende, CS, Italy

[2]Department of Pharmacy, Health and Nutritional Sciences, University of Calabria, Arcavacata di Rende, CS, Italy

[3]IRCCS SDN (Istituto di Ricerca Diagnostica e Nucleare), Napoli, Italy

[4]Laboratory of Molecular Medicine and Genomics, Department of Medicine and Surgery, University of Salerno, Baronissi (SA), Italy

[5]Norwegian Centre for Molecular Medicine (NCMM), University of Oslo, Norway

[6]Breast Cancer Now Research Unit, Institute of Cancer Sciences, University Manchester, UK

[7]MTA TTK Lendület Cancer Biomarker Research Group, Budapest, Hungary

[8]2nd Dept. of Pediatrics, Semmelweis University, Budapest, Hungary

[9]MTA-SE Pediatrics and Nephrology Research Group, Budapest, Hungary

[*]These authors have equally contributed to this work

[**]Joint senior authors

Correspondence to:
Sebastiano Andò, **e-mail:** sebastiano.ando@unical.it
Stefania Catalano, **e-mail:** stefcatalano@libero.it

Keywords: *breast cancer, leptin, microenvironment, CAFs, breast cancer stem cells*

Received: *July 08, 2015* ***Accepted:*** *October 15, 2015* ***Published:*** *October 27, 2015*

ABSTRACT

Breast cancer stem cells (BCSCs) play crucial roles in tumor initiation, metastasis and therapeutic resistance. A strict dependency between BCSCs and stromal cell components of tumor microenvironment exists. Thus, novel therapeutic strategies aimed to target the crosstalk between activated microenvironment and BCSCs have the potential to improve clinical outcome. Here, we investigated how leptin, as a mediator of tumor-stromal interactions, may affect BCSC activity using patient-derived samples (*n* = 16) and breast cancer cell lines, and determined the potential benefit of targeting leptin signaling in these model systems. Conditioned media (CM) from cancer-associated fibroblasts and breast adipocytes significantly increased mammosphere formation in breast cancer cells and depletion of leptin from CM completely abrogated this effect. Mammosphere cultures exhibited increased leptin receptor (*OBR*) expression and leptin exposure enhanced mammosphere formation. Microarray analyses revealed a similar expression profile of genes involved in stem cell biology among mammospheres treated with CM and leptin. Interestingly, leptin increased mammosphere formation in metastatic breast cancers and expression of *OBR* as well as *HSP90*, a target of leptin signaling, were directly correlated with mammosphere formation in metastatic samples (*r* = 0.68/*p* = 0.05; *r* = 0.71/*p* = 0.036, respectively). Kaplan–Meier survival curves indicated that *OBR* and *HSP90* expression were associated with reduced overall survival in breast cancer patients (HR = 1.9/*p* = 0.022; HR = 2.2/*p* = 0.00017, respectively). Furthermore, blocking leptin signaling by using a full leptin receptor antagonist significantly reduced

mammosphere formation in breast cancer cell lines and patient-derived samples. Our results suggest that leptin/leptin receptor signaling may represent a potential therapeutic target that can block the stromal-tumor interactions driving BCSC-mediated disease progression.

INTRODUCTION

Carcinoma of the breast is the most common malignancy and the leading cause of cancer-related death in women worldwide [1]. Despite improvements in diagnosis and treatment, metastatic or recurrent disease and resistance to therapy remain the principal causes of death for breast cancer patients.

In the last years, multiple reports have shown that a subpopulation of cancer cells displaying stem cell properties and named as cancer stem cells (CSCs) plays a crucial role in sustaining tumor growth and progression. These cells are characterized by their ability to undergo self-renewal, a process that drives tumorigenesis, and to differentiate into the non-self-renewing cells forming the tumor bulk [2, 3]. From a clinical point of view, the main concern with CSCs is related to their resistance to conventional treatments (e.g. endocrine-, chemo- and radio-therapy), a feature that might be the underlying cause of tumor recurrence and metastases [4–6]. Similar to embryonic and somatic stem cells, the self-renewal and differentiation of CSCs are regulated by both intrinsic and extrinsic pathways whose dysregulation may be a key event initiating carcinogenesis. Among the intrinsic pathways, an important role is displayed by developmental signals such as Wnt, Hedgehog, Janus kinase 2-signal transducer and activator of transcription 3 (JAK2-STAT3) and Notch pathways that are frequently deranged in cancers [7]. Extrinsic signals that regulate stem cell behaviour originate in the surrounding stem cell microenvironment, termed as cancer stem niche. This niche contains a number of cell types, including mesenchymal stem cells (MSCs), cancer-associated fibroblasts (CAFs), adipocytes, endothelial and immune cells, all of which, through networks of cytokines and growth factors, have been shown to influence tumor growth and metastasis [8]. Thus, strategies aimed to specifically target the interaction between CSCs and their microenvironment may represent an important approach to improve patient outcome.

Adipocytes and CAFs are the major components in breast cancer microenvironment, and along with their secreted factors represent key players in stroma-epithelial cell interactions. As an important paracrine mediator, the adipocyte-derived cytokine leptin, that we have recently demonstrated to be also secreted by CAFs [9], has been correlated with breast cancer occurrence. Leptin exerts its biologic function through binding to its receptor (OBR) which activates multiple downstream signaling pathways such as those involving JAK2-STAT3, mitogen-activated protein kinase (MAPK), and phosphatidylinositol 3-kinase/protein kinase B (PI3K/AKT) [10]. Leptin and both short and long OBR isoforms are overexpressed in breast cancer, especially in higher grade tumors and are associated with distant metastases [11, 12]. It has been extensively demonstrated that this cytokine, acting in an autocrine, endocrine and paracrine manner, may modulate many aspects of breast tumorigenesis from initiation and primary tumor growth to metastatic progression [13–15]. Besides, crosstalk with other different signaling molecules such as estrogens, growth factors and inflammatory cytokines further increases leptin impact on breast tumor progression [16–21]. Moreover, leptin is able to shape the tumor microenvironment within the mammary gland by inducing multiple concurrent events such as migration of endothelial cells, angiogenesis and recruitment of macrophages and monocytes [13–15, 22]. Interestingly, recent studies have also reported that leptin signaling may be involved in the promotion of CSC phenotype [23–25] and that inhibition of STAT3 suppresses leptin-induced CSC activity and cancer progression in diet-induced obese rats [26].

The aim of the current study was to evaluate the role of leptin, as a mediator of the tumor-stroma interaction, in regulating breast CSC activity using breast cancer cell lines and patient-derived breast cancer cells isolated from metastatic ascites and pleural effusions. Particularly, we investigated: *i*) the impact of CAFs and adipocytes isolated from stromal breast tissues on mammosphere formation and self-renewal in breast cancer cells; *ii*) the specific role of leptin and its receptor in influencing breast CSC phenotype in the context of the tumor microenvironment; *iii*) the effect of inhibiting leptin signaling as potential therapeutic target to reduce breast CSC activity in *in vitro* and *ex vivo* models.

RESULTS

CAFs and adipocytes induce mammosphere formation in breast cancer cells through leptin secretion

To assess the ability of stromal cells to affect CSC activity in breast cancer cells we performed co-culture experiments. As experimental models for breast CSCs (BCSCs), we used estrogen receptor (ER)-α-positive MCF-7 cells grown as mammospheres. This culture system has been used to characterize, enrich and propagate breast cancer cells with stem-like phenotype, relying on the feature of stem cells to escape anoikis and grow as spheroids in anchorage-independent conditions [27]. MCF-7 mammosphere cells were characterized by flow

cytometric analysis that revealed an enrichment of $CD44^+/CD24^-$ subpopulation compared to MCF-7 monolayer cells (Supplementary Figure S1A). In addition, real-time PCR further revealed that genes associated with stem cell phenotype, including *OCT4, N-CAD, BMI1, SOX4*, were expressed in mammosphere cells at higher levels than in monolayer cells (Supplementary Figure S1B). Moreover, MCF-7 mammosphere cells were also analyzed for the expression of ERα (Supplementary Figure S1C and 1D). As stromal cells, we used either CAFs isolated from biopsies of primary breast tumors or human breast adipocytes obtained after preadipocyte differentiation. CAFs possessed the basic fibroblast characteristics with long and spindle-shaped morphology and highly expressed alpha-smooth muscle actin (α-SMA), vimentin, and fibroblast activation protein (*FAP*) (Supplementary Figure 2A and 2B). Adipocytes displayed a classical morphological phenotype characterized by accumulation of lipid droplets associated with the expression of specific markers as PPARγ and leptin (*OB*) (Supplementary Figure S2C). Using co-culture experiments, we examined mammosphere formation from MCF-7 cells in the presence or absence of conditioned media (CM) harvested from CAFs and adipocytes. Compared to the cells cultured alone, MCF-7 cells co-cultured with CAF- or adipocyte-derived CM showed a significant enhancement in mammosphere forming efficiency (MFE) (Figure 1A). Stem cells are maintained in the primary mammospheres through self-renewal, and are able to give rise to secondary mammospheres when cells from the primary spheres are dissociated and allowed to grow in anchorage-independent conditions. Therefore, we carried out secondary mammosphere cultures to examine the effects of CM on BCSC self-renewal. Our experiments demonstrated an increased self-renewal in MCF-7 cells treated with CAF- and adipocyte-derived CM in the first generation compared with the untreated spheres (Figure 1B and 1C). These data suggest that BCSC activity is influenced by

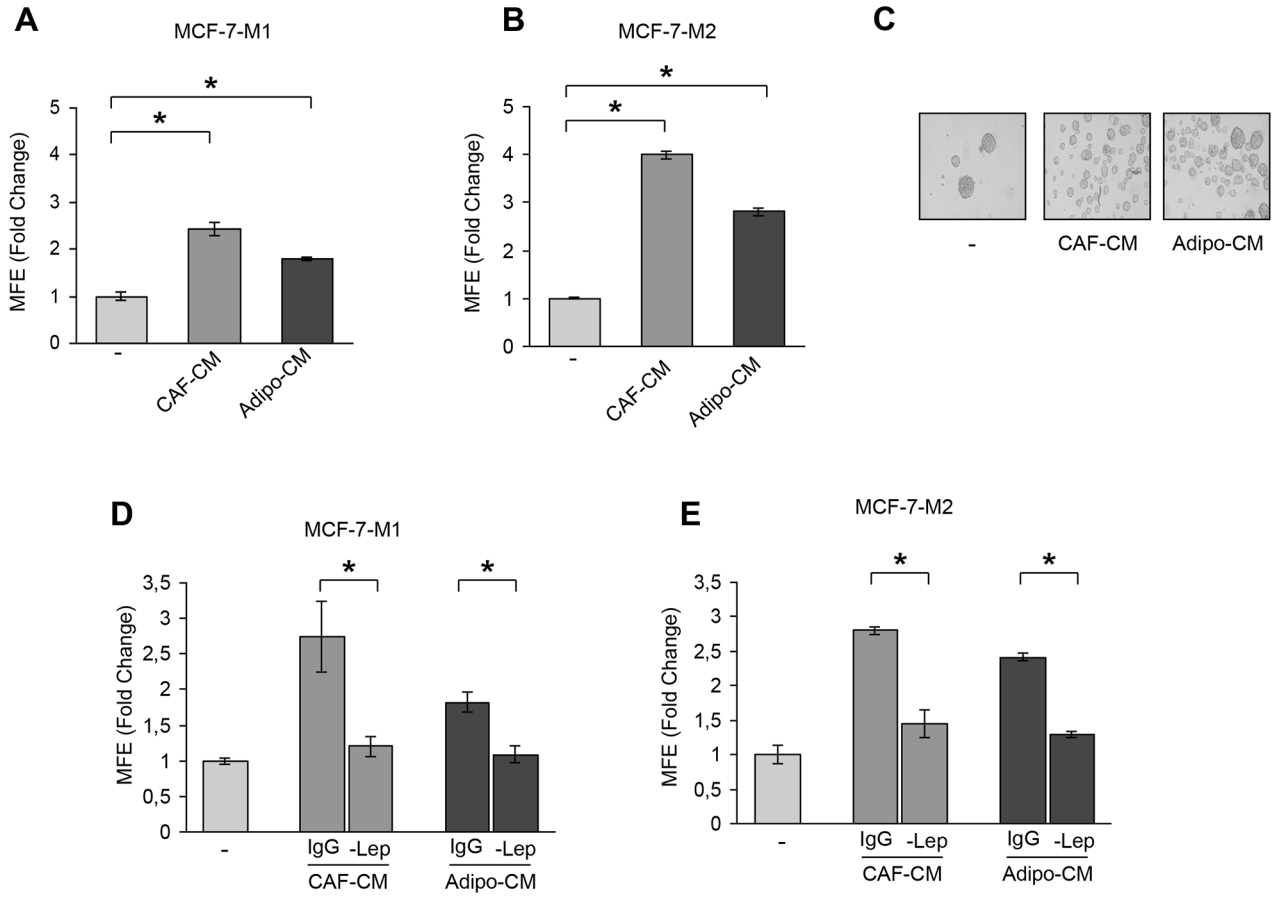

Figure 1: Leptin mediates the effects of stromal cell-CM on breast cancer cell mammosphere formation. Mammosphere Forming Efficiency (MFE) evaluated in MCF-7-M1 (**A**) and MCF-7-M2 (**B**) in the presence or absence (−) of CAF- and Adipocyte-derived Conditioned Media (CAF-CM and Adipo-CM, respectively). MFE was calculated by dividing the number of mammospheres (colonies > 50 μm) formed by the number of the cells plated and expressed as fold change compared to untreated cells (−). (**C**) Representative phase-contrast images of mammospheres treated as in panel (B) are shown. MFE evaluated in MCF-7-M1 (**D**) and MCF-7-M2 (**E**) in the presence or absence (−) of leptin-immunodepleted CAF-CM and Adipo-CM (-Lep). IgG: CM immunodepleted with nonspecific antibody. The values represent the means ± s.d. of three different experiments each performed in triplicate. $*p < 0.05$.

soluble factors secreted from stromal cells. Thus, given the role of leptin as an important cytokine secreted by both CAFs and adipocytes, we assessed the impact of leptin in the context of the heterotypic signaling working in BCSC–stromal interactions. First, ELISA measurement in CM from stromal cells showed that leptin levels were 2,4 ± 0,12 ng/mg protein and 20,32 ± 2 ng/mg protein in CAF- and adipocyte-derived CM, respectively. Leptin was then immunodepleted from CAF- and adipocyte-derived CM using a specific leptin antibody, and resulting media were tested for the ability to induce mammosphere formation in breast cancer cells. AS shown in Figure 1D and 1E, leptin depletion significantly decreased the MFE/self-renewal promoted by stromal cell-derived CM.

Targeting leptin signaling reduces stem cell activity mediated by stromal cells

Our previous experiments indicate that leptin may represent an important paracrine molecule that mediates the interaction between stromal cells and BCSCs. To support this observation, we tested the effect of a full leptin receptor antagonist, peptide LDFI, on BCSC activity. We have previously shown that this peptide inhibits leptin-induced breast cancer growth *in vitro* and exhibits anti-neoplastic activities *in vivo* [28]. Our data demonstrated that treatment with peptide LDFI significantly reduced MFE/self-renewal promoted by stromal cell-derived CM in MCF-7 cells (Figure 2A). To extend the results obtained, we have grown the ERα-negative MDA-MB-231 breast cancer cells as mammospheres and evaluated the effects of CAF- or adipocyte-CM in the presence or absence of peptide LDFI. Treatment of MDA-MB-231 mammosphere cultures with CAF- or adipocyte-derived CM significantly increased MFE/self-renewal and the addition of the OBR antagonist LDFI strongly reduced these effects (Figure 2B), confirming that leptin/leptin receptor may play a crucial role in maintaining the BCSC traits mediated by stromal cells in different cellular backgrounds.

Leptin signaling regulates mammosphere formation/self-renewal activity of breast cancer cells

Having shown that stromal cells regulate BCSC activity through secretion of leptin, we next investigated

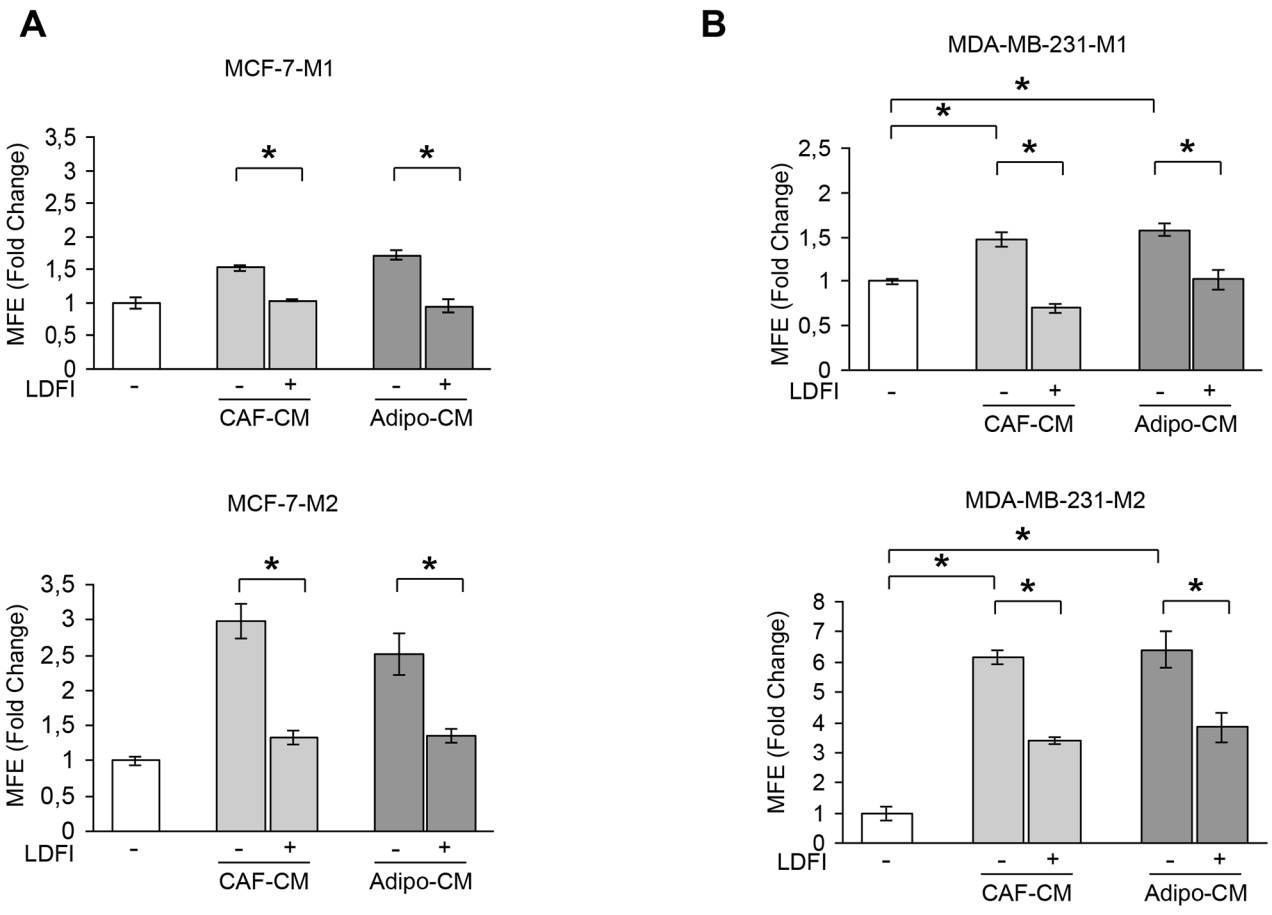

Figure 2: Effects of a selective leptin receptor antagonist on breast cancer stem cell activity. MFE evaluated in MCF-7-M1 and MCF-7-M2 (**A**) and in MDA-MB-231-M1 and MDA-MB-231-M2 (**B**) treated with CAF-CM and Adipo-CM with/without peptide LDFI (1 μg/ml). The values represent the means ± s.d. of three different experiments each performed in triplicate. *$p < 0.05$.

the direct involvement of this cytokine in the regulation of mammosphere formation/self-renewal in MCF-7 cells. In agreement with previous data demonstrating that leptin receptor plays a crucial role in maintaining cancers in a stem cell-like state [23–26], we found that MCF-7 mammosphere cultures exhibited increased *OBR* mRNA expression and in a greater extent the long isoform, compared to monolayer cells (Figure 3A). Accordingly, leptin treatment of mammosphere cultures resulted in a significant increase in MFE/self-renewal and in an enhanced percentage of $CD44^{+}/CD24^{-}$ population compared with untreated cells (Figure 3B, 3C and 3D). Accordingly, in MDA-MB-231 mammosphere cultures, we observed a significant increase in the long isoform of *OBR* mRNA expression compared to monolayer cells, and an enhanced MFE/self-renewal after leptin exposure (Supplementary Figure S3), demonstrating that this cytokine can directly regulate BCSC activity.

Since BCSCs display increased cell motility and invasion, we tested the effects of leptin on the migratory potential of MCF-7 mammospheres. Our data clearly showed that leptin exposure increased the number of migrated cells suggesting that this cytokine can facilitate the invasive behavior of BCSCs (Figure 3E). Next, *OBR* expression was stably knocked-down using lentiviral delivered short hairpin RNA (*OBR* sh) in MCF-7 cells (Figure 3F-*left panel*). Suppression of *OBR* expression led to a significant inhibition of MFE (Figure 3F-*right panel*), implying that this gene is necessary for maintaining cancer stem-like properties in breast cancer cells. In addition, we observed that leptin treatment induced the phosphorylation of specific OBR downstream signaling molecules such as STAT3, Akt and p42/44 MAPK (Figure 3G). As expected, the increase in MFE induced by leptin was reversed by the JAK2-STAT3 inhibitor AG490, the MEK1 inhibitor PD98059 and the PI3K/AKT inhibitor LY294002 (Figure 3H), suggesting

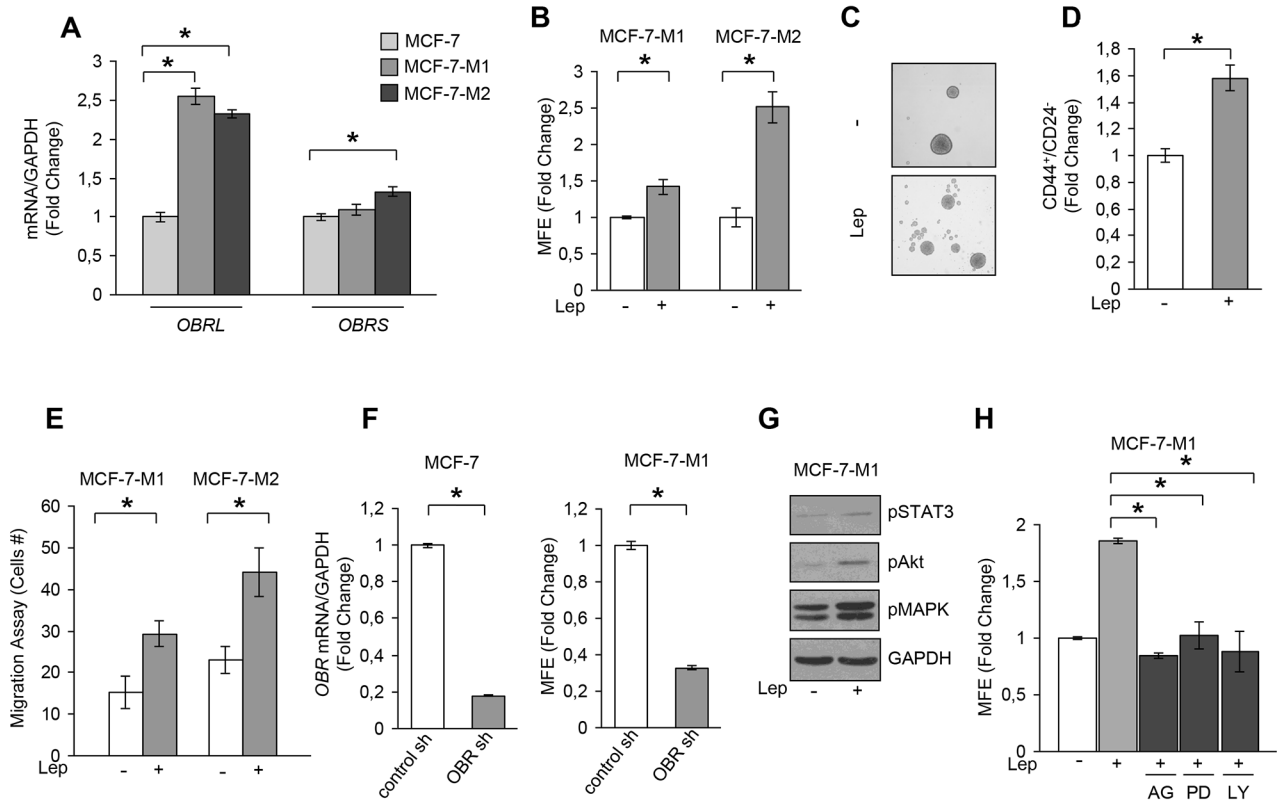

Figure 3: Leptin induces MFE in breast cancer cells. A. Leptin receptor long (*OBRL*) and short (*OBRS*) isoform mRNA levels, evaluated by real time RT-PCR, in MCF-7, MCF-7-M1 and MCF-7-M2 cells. Each sample was normalized to its *GAPDH* mRNA content. **B.** MFE in MCF-7-M1 and MCF-7-M2 in the presence or absence (−) of leptin 500 ng/ml (Lep). **C.** Representative phase-contrast images of mammospheres treated as in panel (B) are shown. **D.** $CD44^{+}/CD24^{-}$ population in MCF-7-M2 cells treated or not (−) with Lep. **E.** Transmigration assays in MCF-7-M1 and MCF-7-M2-derived cells treated or not (−) with Lep. **F.** MCF-7 cells were stably transfected with either a scrambled shRNA (control-sh) or OBR shRNA (OBR-sh). *OBRL* mRNA content was evaluated by real time RT-PCR (*left panel*). Each sample was normalized to its *GAPDH* mRNA content. MFE in MCF-7-M1 derived from either control-sh or OBR-sh clones (*right panel*). **G.** Immunoblotting of phosphorylated (p), STAT3 (Tyr^{705}), Akt (Ser^{473}), and MAPK (Thr^{202}/Tyr^{204}) at the indicated residues measured in cellular extracts from MCF-7-M1 cells treated or not (−) with Lep. GAPDH, loading control. **H.** MFE in MCF-7-M1 treated with Lep and AG490 (AG-20 μmol/L), PD98059 (PD-10 μmol/L) or LY294002 (LY-10 μmol/L). The values represent the means ± s.d. of three different experiments each performed in triplicate. *$p < 0.05$.

that leptin promotes stem cell properties *via* activation of classical leptin signaling pathways. In agreement with these observations, we also found an up-regulation of well-known leptin target genes as *OBR* and the heat shock protein 90 (HSP90) [20] in MCF-7 cells treated with leptin (Supplementary Figure S4A and 4B)

Gene expression profiling in leptin or stromal CM-treated mammosphere-derived cells

To determine whether leptin, CAF- and adipocyte-CM may similarly affect gene expression profile in mammosphere-derived cells, we performed gene expression profiling analysis on total RNA extracted from the second generation spheres. Microarray results highlighted several RNAs differentially expressed in treated *vs* untreated MCF-7 mammospheres. Venn diagram analysis was used to compare the gene lists and to identify those genes that are unique and in common among the three treatments (Figure 4A). A total of 2270 transcripts were commonly regulated in all treated samples (808 up- and 1462 down-regulated transcripts, respectively). It should be noted that the global overlap among genes expressed in treated samples includes a number of genes known to play a role in stem cell biology such as *BMI1*, *SUZ12*, *YES1*, *SOX4* (Figure 4B, *left panel*, Supplementary Table S2). Similar trends were also observed for the expression of other genes involved in cell cycle control (Figure 4B, *middle panel*, Supplementary Table S3). Moreover, treated samples displayed up-regulation of some transcripts related to the heat shock protein family, that recently have been suggested to be crucial in sustaining proliferation and self-renewal of stem cells [29] (Figure 4B, *right panel,* Supplementary Table S4). To validate our microarray study MCF-7 mammospheres treated with leptin were evaluated for the expression of a

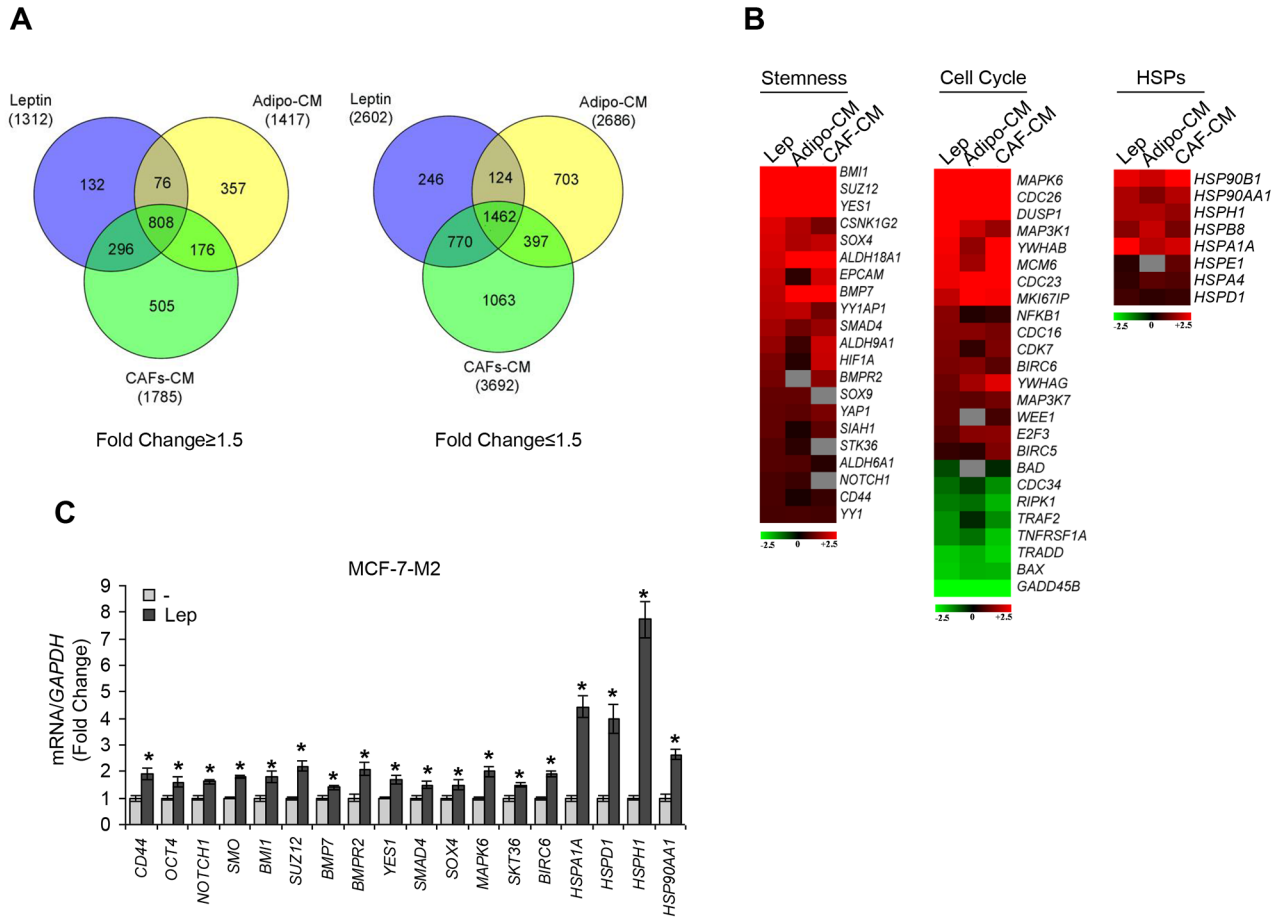

Figure 4: Gene expression profiling in mammosphere cultures treated with stromal cell-CM or leptin. A. Venn diagram of up-(*left panel*) and down-(*right panel*) regulated transcript identified by microarray analysis in MCF-7-M2 cells treated with CAF-CM, Adipo-CM or Lep compared to untreated samples. **B.** Heat-maps of stemness related-genes, cell cycle related-genes and HSP family genes from microarray data. Gene expression changes were calculated in treated cells with respect to the untreated controls. Transcript showing a DiffScore ≤ − 30 and ≥ 30, corresponding to a *p*-value of 0.001, and significant fold change in treated vs untreated ≥ 1.5 were considered. **C.** Real-time RT-PCR validation of a subset of genes in MCF-7-M2 cells treated or not (−) with Lep. Each sample was normalized to its *GAPDH* mRNA content. The values represent the means ± s.d. of three different experiments each performed in triplicate. **p* < 0.05 *vs* untreated (−) sample.

panel of genes by using real-time PCR (Figure 4C). Taken together, gene expression profile analyses strongly support the role of leptin as a crucial paracrine molecule able to mediate the microenvironment effects on BCSC activity.

Leptin increases patient-derived mammosphere formation/self-renewal activity

The role of leptin in the regulation of BCSC activity was then evaluated by using patient-derived breast cancer cells isolated from metastatic ascites or pleural effusions. Tumor histology, grade, hormone receptors and HER2 status of the primary tumors were reported in Table 1. Mammosphere cultures treated with leptin resulted in a significant increase in MFE compared to untreated samples (n = 10, Figure 5A). Secondary mammosphere formation was observed only in four samples and treatment with leptin significantly increased self-renewal in three of them (Figure 5B). Besides, four human metastatic samples taken from patients with breast cancer were also treated with peptide LDFI. MFE induced by leptin was significantly decreased with the addition of LDFI (Figure 5C). Interestingly, treatment with peptide LDFI alone reduced the mammosphere formation, underlying how this peptide negatively interferes with leptin autocrine loop (Figure 5C). Then, to investigate the direct involvement of OBR in the regulation of mammosphere formation, *OBR* gene expression was analyzed in cells from metastatic ascites and pleural effusion fluids using microarray data. There was a significant direct correlation between the expression of *OBR* mRNA in cells from the metastatic fluids and MFE (r = 0.68; p = 0.05, Figure 5D). In agreement with the microarray data obtained in MCF-7 mammospheres, a significant correlation between MFE and *HSP90* gene expression in the same metastatic patient-derived samples (r = 0.71; p = 0.036) was also observed (Figure 5E). These data suggest that patients with higher levels of *OBR* and *HSP90* mRNAs in cells of metastatic fluids have greater *ex vivo* CSC activity.

OBR expression correlates with reduced overall survival in breast carcinomas

To investigate the clinical significance of *OBR* gene expression in human breast cancers the relationship between *OBR* levels and overall survival (OS) of breast cancer patients (n = 781) was estimated by Kaplan–Meier analysis. Survival curves indicated that women with high *OBR* expression exhibited a lower rate of OS than those with low *OBR* expression (HR = 1.9, p = 0.022) (Figure 6A). Similarly, breast carcinoma patients with high *HSP90*

Table 1: Summary of metastatic patients-derived cancers

SAMPLE ID	AGE	SOURCE	Histology	GRADE	ER	PR	HER2
BB3RC29	70	ASC	UN	UN	POS	POS	NEG
BB3RC46	68	ASC	ILC	2	POS	POS	NEG
BB3RC50	46	ASC	IDC	2	POS	POS	NEG
BB3RC59[1]	69	ASC	ILC	2	POS	POS	NEG
BB3RC60	66	ASC	ILC	2	POS	POS	NEG
BB3RC65[2]	62	ASC	ILC	2	POS	POS	NEG
BB3RC66[1]	69	ASC	ILC	2	POS	POS	NEG
BB3RC70[2]	62	ASC	ILC	2	POS	POS	NEG
BB3RC71	48	PE	UN	3	POS	POS	POS
BB3RC79	UN	PE	IDC	3	NEG	NEG	NEG
BB3RC81	55	ASC	IDC	2	POS	POS	NEG
BB3RC84	UN	PE	UN	3	NEG	NEG	NEG
BB3RC90	66	PE	IDC/ILC	2	P0S	POS	NEG
BB3RC92	61	ASC	IDC	1	POS	POS	NEG
BB3RC93	UN	ASC	UN	UN	POS	POS	NEG
BB3RC94	41	ASC	UN	UN	POS	POS	NEG

[1, 2]These samples were obtained at different time points from the same patients
Sixteen patient-derived breast cancer samples were used in this study. Tumor histology and grade for metastatic samples (ASC and PE) relates to the primary cancer. Abbreviation: **UN** unknown, **PE** pleural effusion, **ASC** ascites sample, **ILC** invasive lobular carcinoma , **IDC** invasive ductal carcinoma, **POS** positive, **NEG** negative, **ER** Estrogen Receptor, **PR** Progesterone Receptor, **HER2**, epidermal growth factor receptor 2.

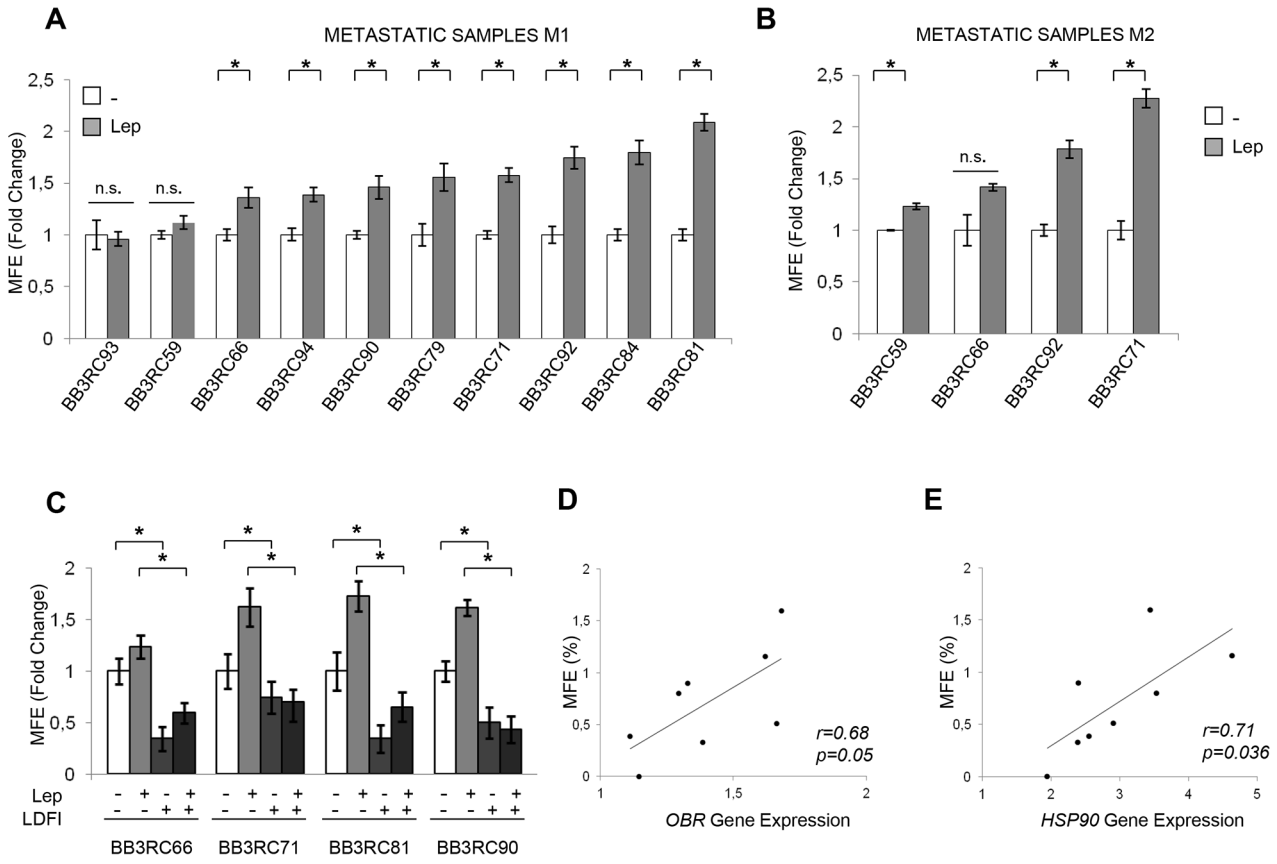

Figure 5: Leptin enhances mammospheres formation/self-renewal activity in patient-derived metastatic cells. 10 metastatic fluid samples obtained from breast cancer patients (BB3RC59/BB3RC66/BB3RC71–94) undergoing palliative drainage of symptomatic ascites or pleural effusions were used (Table 1). MFE in metastatic patient-derived cells grown as primary (Metastatic samples M1) (**A**) or secondary (Metastatic samples M2) (**B**) mammospheres in the presence or absence (−) of Lep. (**C**) MFE in 4 Metastatic sample M1 untreated (−) or treated with Lep, peptide LDFI (1 μg/ml), and Lep+LDFI. The values represent the means ± s.d. of three different experiments each performed in triplicate. *$p < 0.05$. n.s.:nonsignificant. Correlation between *OBR* (**D**) or *HSP90* mRNA expression (**E**) in cells of the metastatic fluids and MFE (8 patients/BB3RC29–70) (Pearson correlation coefficient, $r = 0.68$, $p = 0.05$; $r = 0.71$, $p = 0.036$, respectively).

expression had decreased OS compared with those with low *HSP90* expression (*HR = 2.2, p = 0.00017*) (Figure 6B).

Basal-like breast cancer is an aggressive tumor subtype, composed by primitive undifferentiated cells. Indeed, basal-like breast tumors, which are enriched for $CD44^{+}/CD24^{-}$ cells, exhibit epithelial–mesenchymal transition features and express high levels of stem cell-regulatory genes [30–34]. In agreement with these observations, the results of the Kaplan-Meier analysis indicated a more relevant discrimination in terms of overall survival between high and low expression of *OBR* and *HSP90* in basal breast cancer patients ($n = 143$) (*HR = 4.4, p = 0.011; HR = 5.2, p = 0.013* respectively) (Figure 6C and 6D).

DISCUSSION

The heterotypic signals arising in the tumor-associated stroma have been shown to be important in inducing and maintaining a stem-like state in the tumor cells through either the secretion of soluble molecules or cell–cell communication [35, 36]. Particularly, in the case of breast carcinoma, it has been reported that various types of stromal cells *via* growth factors and cytokines may enhance the proliferation and survival of BCSCs, induce angiogenesis, and recruit tumor-associated macrophages and other immune cells, which in turn secrete additional factors promoting tumor cell invasion and metastasis [8].

Here we demonstrated, for the first time, that leptin and its receptor play a crucial role in mediating the interaction between stromal cells (CAFs and adipocytes) and BCSCs. The initial conditioned media experiments indicated that the entire complement of secretory proteins released by CAFs and adipocytes significantly increase MFE/self-renewal in breast cancer cells. An important role is played by leptin as a fundamental environmental regulator of CSCs in the cancer stem niche. Indeed, either leptin immunodepletion from CAF- and adipocyte-derived CM or inhibition of leptin signaling by using peptide LDFI, a small-molecule that acts as a full leptin

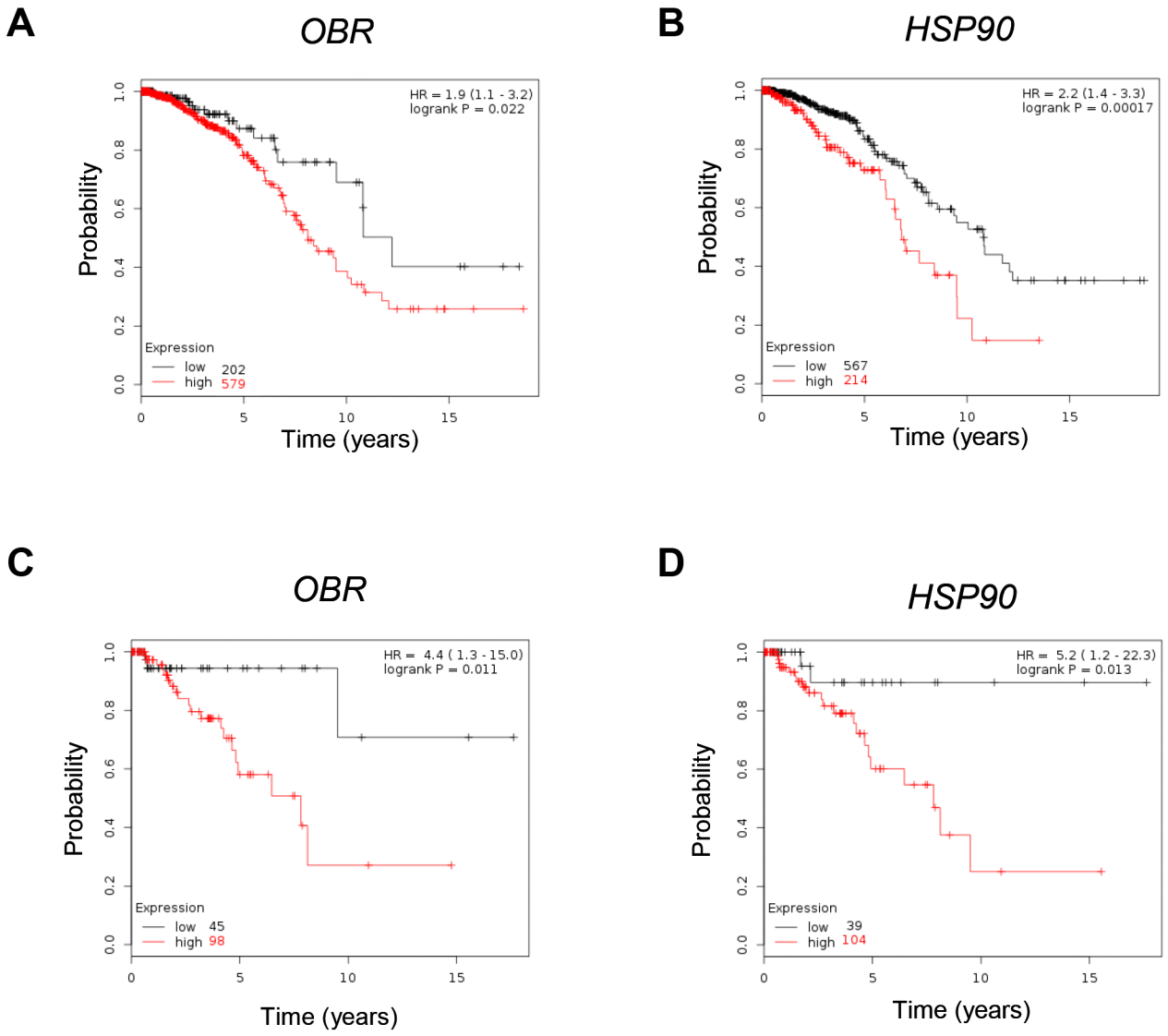

Figure 6: Correlation between *OBR* and *HSP90* mRNA levels and overall survival in breast cancer. Kaplan–Meier survival analysis in breast carcinoma patients (n = 781) with high and low *OBR* (**A**) or *HSP90* (**B**) expression analyzed as described in *Materials and Methods*. Kaplan–Meier survival analysis in basal breast cancer patients (n = 143) with high and low *OBR* (**C**) or *HSP90* (**D**) expression. Kaplan-Meier survival graph, and hazard ratio (HR) with 95% confidence intervals and logrank P value.

receptor antagonist [28], reduced the effects of CM on mammosphere formation. Gene expression profiling revealed a significant overlap of regulated genes in mammosphere cells following treatment with CAF-, adipocyte-derived CM or leptin. Of particular interest was the observation that genes commonly expressed in all treated-samples include several of those involved in stemness. Among these, the polycomb gene *BMI1*, which has been reported to play an important role in self-renewal of stem cells and has a positive correlation with clinical grade/stage and poor prognosis [37], was one of the most highly induced in all treated cells. One of the features of CSCs is the uncontrolled proliferation, perhaps due to a reduced responsiveness to negative growth regulators or to the loss of contact inhibition and gap junction intercellular communication [38]. Our results clearly evidenced that a number of genes involved in cell cycle control showed a similar expression profile upon treatment with stromal-CM and leptin. Another family of genes, crucial in sustaining self-renewal of stem cells [29], is the heat shock protein family. We have previously demonstrated that the HSP90, a main functional component of this chaperone complex, is a target of leptin in breast cancer cells [20]. Our microarray data showed that some transcripts of the HSP family were upregulated in stromal-CM and leptin-treated samples. Thus, since the expression pattern of genes regulated by leptin and involved in stem cell biology closely mirrors those modulated by stromal cells, it is reasonable to speculate that leptin may represent a critical paracrine

molecule in mediating the microenvironment effects on BCSC activity.

The expression of the leptin receptor is a characteristic feature of CSCs and of a broad array of embryonic and induced pluripotent stem cells, which exhibit an increased response to leptin including phosphorylation and activation of STAT3 and induction of stem cell markers, as *OCT4* and *SOX2* [23]. Leptin receptor has also been reported as a marker for identification and *in vivo* fate of bone marrow mesenchymal stem cells (MSCs) [39] and leptin signaling represents an essential step for the enhanced survival, chemotaxis and therapeutic properties of MSCs induced by hypoxia [40, 41]. Moreover, it has been reported that leptin is able to regulate and activate several signaling pathways and oncogenes which are critically implicated in BCSCs [42–46] and leptin deficiency in MMTV-Wnt-1 transgenic mice results in functional depletion of BCSCs leading to less tumor outgrowth [24]. More recently, it has also been demonstrated that OBR is necessary for maintaining a CSC-like state in TNBC cells [25] and high OBR expression induced by the adiposity-leptin enriched environment generates a population with enhanced CSC properties and tumorigenic capacity [26]. Our studies extended these previous findings by demonstrating a direct involvement of leptin in sustaining breast cancer stem cell behavior using both breast cancer cell lines and metastatic breast cancer patient-derived cells. We found that MCF-7 mammospheres exhibited increased *OBR* mRNA expression, while OBR silencing caused a significant reduction in the sphere-forming efficiency. Treatment with leptin induced an increase in MFE, self-renewal and an enhanced percentage of $CD44^{+}/CD24^{-}$ cell population, through the activation of the classical signaling pathways. Importantly, we also showed that leptin is able to increase the mammosphere formation and self-renewal activity in metastatic breast cancer cells isolated from patients. Moreover, *OBR* mRNA expression, analyzed in cells from metastatic fluids, was directly correlated with mammosphere formation activity *ex vivo*. In agreement with our data of gene expression profile, a significant positive correlation between MFE and *HSP90* mRNA expression in the same metastatic patient-derived samples was observed.

It has been previously reported that high-grade tumors associated with poor prognosis display an enrichment of BCSCs [47, 48]. Here, using Kaplan-Meier analysis we found that *OBR* expression, which is crucial in maintaining stem cell phenotype, was associated with reduced overall survival in breast carcinomas suggesting its potential role as a prognostic factor. Interestingly, in basal-like breast cancer patients, a more relevant discrimination in terms of overall survival between high and low *OBR* expression could be observed. Finally, we demonstrated that blocking leptin signaling by using the peptide LDFI significantly reduced mammosphere formation in metastatic breast cancer patient-derived cells, suggesting that strategies aimed at inhibiting leptin signaling represent a rationale therapeutic approach to target cancer stem cells.

In conclusion, our findings identify, for the first time, leptin as an important paracrine molecule that mediates the interaction between stromal cells and BCSCs, providing novel insights into understanding how BCSCs are influenced by the tumor microenvironment. As clinical implications, these data suggest that targeting leptin/leptin receptor signaling generated in the microenvironment may be useful for BCSC eradication and eventually to prevent recurrence and metastasis in patients with breast carcinoma.

MATERIALS AND METHODS

Cell culture

Human MCF-7 and MDA-MB-231 breast cancer epithelial cells were acquired in 2010 and 2015 respectively, from American Type Culture Collection where they were authenticated, stored according to supplier's instructions, and used within 4 months after frozen aliquots recovery. Breast subcutaneous human female preadipocytes (Lot.#:BR071812B; BR070810) were from Zen-Bio. Adipocytes, obtained following differentiation procedure, were routinely maintained in Adipocyte maintenance medium (Zen-Bio). Every 4 months, cells were authenticated by single tandem repeat analysis at our Sequencing Core; morphology, doubling times, estrogen sensitivity, and mycoplasma negativity were tested (MycoAlert, Lonza).

Cancer associated fibroblast (CAF) isolation

Human breast cancer specimens were collected in 2013 from primary tumors of patients who signed informed consent following the procedures previously described [9]. Briefly, small pieces of fresh tumor excision were digested (500 IU collagenase in Hank's balanced salt solution; Sigma; 37°C for 2 h). After differential centrifugation (90 g for 2 min), the supernatant containing CAFs was centrifuged (500 g for 8 min), resuspended, and cultured in RPMI-1640 medium supplemented with 15% FBS and antibiotics. The fibroblastic nature of the isolated cells was confirmed by microscopic determination of morphology, and characterization by αSMA, vimentin, pan-Cytokeratin and fibroblast activation protein (FAP) expression. CAFs between 4 and 10 passages were used.

Immunofluorescence

Immunofluorescence assay was performed as described [9] using anti-α-SMA or ERα antibodies and

fluorescein isothiocyanate-conjugated secondary antibody (Santa Cruz Biothecnology).

Conditioned medium (CM) and Leptin-immunodepleted CM

CM from CAFs and adipocytes and leptin-immunodepleted CM were obtained as described [9]. Leptin levels were measured by ELISA (LDN).

Metastatic breast cancer patient-derived cells

Pleural effusion and ascites samples were obtained from patients with metastatic breast cancer undergoing palliative drainage at The Christie Hospital NHS Foundation Trust Manchester (UK). Metastatic breast sample details in Table 1. Ascites and pleural effusions were centrifuged at 1000 g for 10 min at 4°C and suspended in PBS. Erythrocytes and leucocytes were removed by centrifugation through Lymphoprep solution (Axis Shield), followed by removal of CD45-positive cells using anti-CD45 magnetic beads (Miltenyi Biotec). Single cell suspension of breast cancer epithelial cells was then used to perform mammosphere assay.

Mammosphere culture

MCF-7 and MDA-MB-231 monolayer cells were enzymatically and manually disaggregated to obtain single-cell suspension. Single cells were plated in ultralow attachment plates (Corning) at a density of 500 cells/cm^2 in a serum-free Human mammary epithelial cell growth medium (HUMEC), supplemented with B27, 20 ng/mL human epidermal growth factor (EGF), 4 µg/mL heparin, 5 µg/ml insulin, 1 ng/ml hydrocortisone, 1 mg/ml penicillin-streptomycin and 0,25 µg/ml amphotericin B (Life Technologies). Growth factors and treatments (leptin, Life Technologies; AG490 Sigma; PD98059/LY294002 Calbiochem) were added to the mammosphere cultures every 3 days. After 7 days mammospheres > 50 µm (primary mammospheres-M1) were counted using a microscope (x40 magnification), collected, enzymatically dissociated, plated at the same seeding density used in the primary generation to obtain secondary mammospheres-M2. Mammosphere cultures from metastatic breast patient-derived cells was assessed as described [49]. Mammospheres forming efficiency (MFE) was calculated as number of mammospheres per well/number of cells seeded per well and reported as fold versus control.

Flow cytometry

Mammospheres were dispersed to obtain single-cell suspension. Cells were washed in PBS with 2,5% BSA and stained with FITC anti-human CD44 and PE anti-human CD24 (BD Biosciences), according to the supplier's protocol. Flow cytometric analysis was performed on a FACScan and acquisition was performed with WinDI software (Becton Dickinson).

Reverse transcription and real-time reverse transcriptase PCR assays

PPARγ/OB/FAP/36B4 mRNA expression was evaluated by the RT–PCR method as described [50]. Real-time RT-PCR was assessed using SYBR Green Universal PCR Master Mix (Biorad). Each sample was normalized on its *GAPDH* mRNA content. Relative gene expression levels were calculated as previously described [50]. Primers in Supplementary Table S1.

Immunoblot analysis

Protein extracts were subjected to SDS-PAGE as described [50]. Immunoblots show a single representative of 3 separate experiments.

Transmigration assays

Mammosphere derived MCF-7 cells were placed in the upper compartments of Boyden chamber (8-µm membranes/Corning Costar) and transmigration assay was performed as described [9].

Lentiviral transfection

We established stable OBR sh MCF-7 cell line using the lentiviral expression system (GeneCopoeia; lentiviral plasmid sh-clone #HSH010584). 48 h after transfection with packaging plasmids and pLentiviral plasmids of target gene in HEK293 cells, supernatants containing lentiviral particles were filtered (0.45 µm PES), mixed with polybrene (8 µg/ml) and used to infect MCF-7 cells. 24 h after infection, cells were selected with 2 µg/mL puromycin overtime to eliminate un-infected cells. *OBR* mRNA expression in stable MCF-7 clones was evaluated by real-time RT-PCR.

Microarray and data analysis

Microarray analyses were carried out on total RNA from MCF-7-M2 mammosphere-derived cells treated with CAF-CM, Adipocyte-CM or Leptin by pooling equal amounts of nucleic acids extracted from three independent cell cultures. Gene expression profiling was performed in triplicate using 500ng of each RNA pool as described [51], cRNAs were hybridized for 18 h at 55°C on Illumina HumanHT-12 v4.0 BeadChips (Illumina Inc.) and scanned with an Illumina iSCAN. Data analyses were performed with GenomeStudio software version 2011.1 (Illumina Inc.). Data were normalized with the quantile algorithm and genes were considered if the detection *p*-value was < 0.01. Statistical significance was calculated

with the Illumina DiffScore, a proprietary algorithm that uses the bead standard deviation to build an error model. Transcripts showing a DiffScore ≤ -30 and ≥ 30, corresponding to a *p*-value of 0.001 and significant fold change in treated *vs* untreated ≥ 1.5 were considered. Venn diagram was generated using Venny 2.0 software. Heat-maps were generated with the Multiexperiment Viewer 4.9 software after performing one way hierarchical clustering of transcripts with the average linkage method and Euclidian distance.

Raw microarray data have been deposited, in a format complying with the Minimum Information About a Microarray Gene Experiment (MIAME) guidelines of the Microarray Gene Expression Data Society (MGED), in the EBI ArrayExpress database (http://www.ebi.ac.uk/arrayexpress) with Accession Number: E-MTAB-3641.

Total RNA from 8 different metastatic breast cancer samples was extracted using the RNeasy Plus Mini Kit (QIAGEN). The Exon Gene Array ST1 platform (Affimetrix) was used to assess gene expression. Data obtained were analysed using Bioconductor R Software. The mean of log2 gene expression values was calculated across all 8 patient derived samples for each individual gene.

Construction of RNA-seq database

RNA-seq data was obtained from the TCGA depository. We transferred the pre-processed level 3 data generated by the Illumina HiSeq 2000 RNA Sequencing Version 2 platform. Expression levels for these samples were computed using a combination of MapSplice and RSEM. Individual patient files were merged into a single database using the plyr R package [52].

Statistical analyses

Each datum point represents the mean ± s.d. of three different experiments. Data were analyzed by Student's *t* test using the GraphPad Prism 4 software. $P < 0.05$ was considered as statistically significant. Pearson correlation coefficient (r) was used to measure the correlation between *OBR* or Heat Shock Protein 90 (*HSP90*) gene expression of 8 metastatic breast cancer samples and mean MFE; a 2-tailed $p \leq 0.05$ was considered statistically significant.

Kaplan-Meier analysis was performed as described [53]. Kaplan-Meier survival graph, and hazard ratio with 95% confidence intervals and logrank *P* value were calculated and plotted in R using Bioconductor packages.

CONFLICTS OF INTEREST

The authors declare they have no conflict of interest.

GRANT SUPPORT

This work was supported by PRIN-MIUR (Programmi di Ricerca Scientifica di Rilevante Interesse Nazionale-Ministero dell'Istruzione dell'Università della Ricerca) 2010–2011 and Associazione Italiana per la Ricerca sul Cancro (AIRC) grants: IG-11595 and IG-13176. European Commission/FSE/Regione Calabria to FC and SP and Lilli Funaro foundation to SP.

REFERENCES

1. Jemal A, Siegel R, Xu J, Ward E. Cancer statistics, 2010. CA Cancer J Clin. 2010; 60:277–300.
2. Visvader JE, Lindeman GJ. Cancer stem cells in solid tumours: accumulating evidence and unresolved questions. Nat Rev Cancer. 2008; 8:755–768.
3. Clarke MF, Dick JE, Dirks PB, Eaves CJ, Jamieson CH, Jones DL, Visvader J, Weissman IL, Wahl GM. Cancer stem cells—perspectives on current status and future directions: AACR Workshop on cancer stem cells. Cancer Res. 2006; 66:9339–9344.
4. Li X, Lewis MT, Huang J, Gutierrez C, Osborne CK, Wu MF, Hilsenbeck SG, Pavlick A, Zhang X, Chamness GC, Wong H, Rosen J, Chang JC. Intrinsic resistance of tumorigenic breast cancer cells to chemotherapy. J Natl Cancer Inst. 2008; 100:672–679.
5. Phillips TM, McBride WH, Pajonk F. The response of CD24(-/low)/CD44+ breast cancer-initiating cells to radiation. J Natl Cancer Inst. 2006; 98:1777–1785.
6. Kakarala M, Wicha MS. Implications of the cancer stem-cell hypothesis for breast cancer prevention and therapy. J Clin Oncol. 2008; 26:2813–2820.
7. Liu S, Dontu G, Wicha MS. Mammary stem cells, self-renewal pathways, and carcinogenesis. Breast Cancer Res. 2005; 7:86–95.
8. Korkaya H, Liu S, Wicha MS. Breast cancer stem cells, cytokine networks, and the tumor microenvironment. J Clin Invest. 2011; 121:3804–3809.
9. Barone I, Catalano S, Gelsomino L, Marsico S, Giordano C, Panza S, Bonofiglio D, Bossi G, Covington KR, Fuqua SA, Andò S. Leptin mediates tumor-stromal interactions that promote the invasive growth of breast cancer cells. Cancer Res. 2012; 72:1416–1427.
10. Cirillo D, Rachiglio AM, la Montagna R, Giordano A, Normanno N. Leptin signaling in breast cancer: an overview. J Cell Biochem. 2008; 105:956–964.
11. Ishikawa M, Kitayama J, Nagawa H. Enhanced expression of leptin and leptin receptor (OB-R) in human breast cancer. Clin Cancer Res. 2004; 10:4325–4331.
12. Miyoshi Y, Funahashi T, Tanaka S, Taguchi T, Tamaki Y, Shimomura I, Noguchi S. High expression of leptin receptor mRNA in breast cancer tissue predicts poor prognosis for

patients with high, but not low, serum leptin levels. Int J Cancer. 2006; 118:1414–1419.

13. Andò S, Barone I, Giordano C, Bonofiglio D, Catalano S. The Multifaceted Mechanism of Leptin Signaling within Tumor Microenvironment in Driving Breast Cancer Growth and Progression. Front Oncol. 2014; 4:340.
14. Andò S, Catalano S. The multifactorial role of leptin in driving the breast cancer microenvironment. Nat Rev Endocrinol. 2011; 8:263–275.
15. Saxena NK, Sharma D. Multifaceted leptin network: the molecular connection between obesity and breast cancer. J Mammary Gland Biol Neoplasia. 2013; 18:309–320.
16. Catalano S, Marsico S, Giordano C, Mauro L, Rizza P, Panno ML, Andò S. Leptin enhances, via AP-1, expression of aromatase in the MCF-7 cell line. J Biol Chem. 2003; 278:28668–28676.
17. Catalano S, Mauro L, Marsico S, Giordano C, Rizza P, Rago V, Montanaro D, Maggiolini M, Panno ML, Andò S. Leptin induces, via ERK1/ERK2 signal, functional activation of estrogen receptor alpha in MCF-7 cells. J Biol Chem. 2004; 279:19908–19915.
18. Fiorio E, Mercanti A, Terrasi M, Micciolo R, Remo A, Auriemma A, Molino A, Parolin V, Di Stefano B, Bonetti F, Giordano A, Cetto GL, Surmacz E. Leptin/HER2 cross-talk in breast cancer: *in vitro* study and preliminary *in vivo* analysis. BMC Cancer. 2008; 8:305.
19. Soma D, Kitayama J, Yamashita H, Miyato H, Ishikawa M, Nagawa H. Leptin augments proliferation of breast cancer cells via transactivation of HER2. J Surg Res. 2008; 149:9–14.
20. Giordano C, Vizza D, Panza S, Barone I, Bonofiglio D, Lanzino M, Sisci D, De Amicis F, Fuqua SA, Catalano S, Andò S. Leptin increases HER2 protein levels through a STAT3-mediated up-regulation of Hsp90 in breast cancer cells. Mol Oncol. 2013; 7:379–391.
21. Saxena NK, Taliaferro-Smith L, Knight BB, Merlin D, Anania FA, O'Regan RM, Sharma D. Bidirectional crosstalk between leptin and insulin-like growth factor-I signaling promotes invasion and migration of breast cancer cells via transactivation of epidermal growth factor receptor. Cancer Res. 2008; 68:9712–9722.
22. Newman G, Gonzalez-Perez RR. Leptin-cytokine crosstalk in breast cancer. Mol Cell Endocrinol. 2014; 382:570–582.
23. Feldman DE, Chen C, Punj V, Tsukamoto H, Machida K. Pluripotency factor-mediated expression of the leptin receptor (OB-R) links obesity to oncogenesis through tumor-initiating stem cells. Proc Natl Acad Sci U S A. 2012; 109:829–834.
24. Zheng Q, Dunlap SM, Zhu J, Downs-Kelly E, Rich J, Hursting SD, Berger NA, Reizes O. Leptin deficiency suppresses MMTV-Wnt-1 mammary tumor growth in obese mice and abrogates tumor initiating cell survival. Endocr Relat Cancer. 2011; 18:491–503.
25. Zheng Q, Banaszak L, Fracci S, Basali D, Dunlap SM, Hursting SD, Rich JN, Hjlemeland AB, Vasanji A, Berger NA, Lathia JD, Reizes O. Leptin receptor maintains cancer stem-like properties in triple negative breast cancer cells. Endocr Relat Cancer. 2013; 20:797–808.
26. Chang CC, Wu MJ, Yang JY, Camarillo IG, Chang CJ. Leptin-STAT3-G9a Signaling Promotes Obesity-Mediated Breast Cancer Progression. Cancer Res. 2015; .
27. Dontu G, Abdallah WM, Foley JM, Jackson KW, Clarke MF, Kawamura MJ, Wicha MS. *In vitro* propagation and transcriptional profiling of human mammary stem/progenitor cells. Genes Dev. 2003; 17:1253–1270.
28. Catalano S, Leggio A, Barone I, De Marco R, Gelsomino L, Campana A, Malivindi R, Panza S, Giordano C, Liguori A, Bonofiglio D, Liguori A, Andò S. A novel leptin antagonist peptide inhibits breast cancer growth *in vitro* and *in vivo*. J Cell Mol Med. 2015; 19:1122–1132.
29. Isolani ME, Conte M, Deri P, Batistoni R. Stem cell protection mechanisms in planarians: the role of some heat shock genes. Int J Dev Biol. 2012; 56:127–133.
30. May CD, Sphyris N, Evans KW, Werden SJ, Guo W, Mani SA. Epithelial-mesenchymal transition and cancer stem cells: a dangerously dynamic duo in breast cancer progression. Breast Cancer Res. 2011; 13:202.
31. Ben-Porath I, Thomson MW, Carey VJ, Ge R, Bell GW, Regev A, Weinberg RA. An embryonic stem cell-like gene expression signature in poorly differentiated aggressive human tumors. Nat Genet. 2008; 40:499–507.
32. Honeth G, Bendahl PO, Ringner M, Saal LH, Gruvberger-Saal SK, Lovgren K, Grabau D, Ferno M, Borg A, Hegardt C. The CD44+/CD24- phenotype is enriched in basal-like breast tumors. Breast Cancer Res. 2008; 10:R53.
33. Park SY, Lee HE, Li H, Shipitsin M, Gelman R, Polyak K. Heterogeneity for stem cell-related markers according to tumor subtype and histologic stage in breast cancer. Clin Cancer Res. 2010; 16:876–887.
34. Sarrio D, Rodriguez-Pinilla SM, Hardisson D, Cano A, Moreno-Bueno G, Palacios J. Epithelial-mesenchymal transition in breast cancer relates to the basal-like phenotype. Cancer Res. 2008; 68:989–997.
35. Pattabiraman DR, Weinberg RA. Tackling the cancer stem cells - what challenges do they pose?. Nat Rev Drug Discov. 2014; 13:497–512.
36. Beck B, Blanpain C. Unravelling cancer stem cell potential. Nat Rev Cancer. 2013; 13:727–738.
37. Siddique HR, Saleem M. Role of BMI1, a stem cell factor, in cancer recurrence and chemoresistance: preclinical and clinical evidences. Stem Cells. 2012; 30:372–378.
38. Trosko JE, Chang CC, Upham BL, Tai MH. Ignored hallmarks of carcinogenesis: stem cells and cell-cell communication. Ann N Y Acad Sci. 2004; 1028:192–201.

39. Zhou BO, Yue R, Murphy MM, 1 Peyer JG, Morrison S J. Leptin-Receptor-Expressing Mesenchymal Stromal Cells Represent the Main Source of Bone Formed by Adult Bone Marrow. Cell Stem Cell. 2014; 15:154–168.

40. Hu X, Wu R, Jiang Z, Wang L, Chen P, Zhang L, Yang L, Wu Y, Chen H, Chen H, Xu Y, Zhou Y, Huang X, Webster KA, Yu H, Wang J. Leptin signaling is required for augmented therapeutic properties of mesenchymal stem cells conferred by hypoxia preconditioning. Stem Cells. 2014; 10:2702–13.

41. Chen P, Wu R, Zhu W, Jiang Z, Xu Y, Chen H, Zhang Z, Chen H, Zhang L, Yu H, Wang J, Hu X. Hypoxia Preconditioned Mesenchymal Stem Cells Prevent Cardiac Fibroblast Activation and Collagen Production via Leptin. PloS ONE. 2014; 9:e103587.

42. Zhou J, Wulfkuhle J, Zhang H, Gu P, Yang Y, Deng J, Margolick JB, Liotta LA, Petricoin E 3rd, Zhang Y. Activation of the PTEN/mTOR/STAT3 pathway in breast cancer stem-like cells is required for viability and maintenance. Proc Natl Acad Sci U S A. 2007; 104:16158–16163.

43. Pratt MA, Tibbo E, Robertson SJ, Jansson D, Hurst K, Perez-Iratxeta C, Lau R, Niu MY. The canonical NF-kappaB pathway is required for formation of luminal mammary neoplasias and is activated in the mammary progenitor population. Oncogene. 2009; 28:2710–2722.

44. Guo S, Gonzalez-Perez RR. Notch, IL-1 and leptin crosstalk outcome (NILCO) is critical for leptin-induced proliferation, migration and VEGF/VEGFR-2 expression in breast cancer. PLoS One. 2011; 6:e21467.

45. Knight BB, Oprea-Ilies GM, Nagalingam A, Yang L, Cohen C, Saxena NK, Sharma D. Survivin upregulation, dependent on leptin-EGFR-Notch1 axis, is essential for leptin-induced migration of breast carcinoma cells. Endocr Relat Cancer. 2011; 18:413–428.

46. Guo S, Liu M, Wang G, Torroella-Kouri M, Gonzalez-Perez RR. Oncogenic role and therapeutic target of leptin signaling in breast cancer and cancer stem cells. Biochim Biophys Acta. 2012; 1825:207–222.

47. Farnie G, Clarke RB, Spence K, Pinnock N, Brennan K, Anderson NG, Bundred NJ. Novel cell culture technique for primary ductal carcinoma *in situ*: role of Notch and epidermal growth factor receptor signaling pathways. J Natl Cancer Inst. 2007; 99:616–627.

48. Pece S, Tosoni D, Confalonieri S, Mazzarol G, Vecchi M, Ronzoni S, Bernard L, Viale G, Pelicci PG, Di Fiore PP. Biological and molecular heterogeneity of breast cancers correlates with their cancer stem cell content. Cell. 2010; 140:62–73.

49. Shaw FL, Harrison H, Spence K, Ablett MP, Simoes BM, Farnie G, Clarke RB. A detailed mammosphere assay protocol for the quantification of breast stem cell activity. J Mammary Gland Biol Neoplasia. 2012; 17:111–117.

50. Catalano S, Malivindi R, Giordano C, Gu G, Panza S, Bonofiglio D, Lanzino M, Sisci D, Panno ML, Andò S. Farnesoid X receptor, through the binding with steroidogenic factor 1-responsive element, inhibits aromatase expression in tumor Leydig cells. J Biol Chem. 2010; 285:5581–5593.

51. Nassa G, Tarallo R, Giurato G, De Filippo MR, Ravo M, Rizzo F, Stellato C, Ambrosino C, Baumann M, Lietzen N, Nyman TA, Weisz A. Post-transcriptional regulation of human breast cancer cell proteome by unliganded estrogen receptor beta via microRNAs. Mol Cell Proteomics. 2014; 13:1076–1090.

52. Wickham . The Split-Apply-Combine Strategy for Data Analysis. J Stat Softw. 2011; 40:1–29.

53. Gyorffy B, Lanczky A, Eklund AC, Denkert C, Budczies J, Li Q, Szallasi Z. An online survival analysis tool to rapidly assess the effect of 22,277 genes on breast cancer prognosis using microarray data of 1,809 patients. Breast Cancer Res Treat. 2010; 123:725–731.

Identification of Novel 2-(1*H*-Indol-1-yl)benzohydrazides CXCR4 Ligands Impairing Breast Cancer Growth and Motility

Fedora Grande[1]*[#], Ines Barone[1#], Francesca Aiello[1], Andrea Brancale[2], Michela Cancellieri[2], Mariateresa Badolato[1], Francesca Chemi[1], Cinzia Giordano[3], Valentina Vircillo[1], Daniela Bonofiglio[1], Antonio Garofalo[1], Sebastiano Andò[1], Stefania Catalano[1].

[1]Department of Pharmacy, Health and Nutritional Sciences, University of Calabria, Via P. Bucci, 87036 Rende (Cs), Italy.

[2]School of Pharmacy and Pharmaceutical Sciences, Cardiff University, King Edward VII Avenue, Cardiff, CF10 3NB, UK

[3]Centro Sanitario, University of Calabria, Via P. Bucci, 87036 Rende (Cs), Italy.

[#]Authors contributed equally.

*Author for correspondence:

Fedora Grande Tel.: +39 0984 493019; Fax: +39 0984 493118, E-mail: fedora.grande@unical.it

Background: Stromal-derived-factor-1 (SDF-1) and the G-protein-coupled-receptor CXCR4 are involved in several physiological and pathological processes including breast cancer spread and progression. Several CXCR4 antagonists have currently reached advanced development stages as potential therapeutic agents for different diseases. **Results**: A small series of novel CXCR4 ligands, based on a 2-(1*H*-indol-1-yl)-benzohydrazide scaffold, have been designed and synthesized. Their orientation into CXCR4 active site was predicted by molecular docking and confirmed by whole cell-based [^{125}I]-SDF-1 ligand competition binding assays. One of the synthesized compounds resulted particularly active in blocking SDF-1-induced breast cancer cell motility, proliferation and downstream signaling activation in different breast cancer cell models

and co-culture systems. **Conclusion**: The newly synthesized compounds represent suitable leads for the development of innovative therapeutic agents targeting CXCR4.

CXCR4 (C-X-C chemokine receptor type 4), also known as CD184 (cluster of differentiation 184) or fusin, is a seven transmembrane G-protein coupled receptor (GPCR) belonging to rhodopsin-like GPCR family [1,2]. CXCR4, first identified as one of the two co-receptors required for the fusion of HIV envelope with the membrane of the targeted cell, was found to be widely expressed in the hematopoietic and immune systems, where it is likely involved in several physiological and pathological processes [3,4].

The natural CXCR4 ligand was recognized to be the Stromal Derived Factor-1 (SDF-1), an eight-kDa homeostatic chemokine peptide also known as CXCL12, which promotes chemotaxis after binding the receptor [5]. The SDF-1/CXCR4 interaction plays a key role in pathological processes, such as HIV infection, inflammation and cancer onset and progression, thus representing an appealing target for the development of innovative broad-spectrum therapeutics [6,7].

The mounting evidence of the crucial role played by CXCR4 in several diseases has encouraged the development of compounds that are able to modulate its biological activity. In the past few years, numerous compounds belonging to different chemical classes, have been demonstrated capacity to block SDF-1/CXCR4 interaction (**Figure 1**). Some of these compounds are currently under clinical trials for the treatment of various diseases including cancers, hematologic and vascular diseases, HIV infection, and other immune system disorders involving the modulation of the SDF-1/CXCR4 axis, such as rheumatoid arthritis and lupus [8].

The first identified CXCR4 antagonists were peptide derivatives that, despite the unfavorable pharmacokinetics and metabolic instability, have been the starting point for building up a pharmacophore model subsequently adopted for the design of simpler non-peptide antagonists [8,9]

Among the non-peptide ligands, a macrocyclic "bicyclam" derivative, called AMD3100, also known as Plerixafor (**1**), has been the first CXCR4 antagonist approved by the FDA for diseases involving the mobilization of hematopoietic stem cells [10] and presently it is in advanced clinical trials for other pathological conditions [11-15].

Despite the noteworthy potency, the clinical applicability of this compound is yet limited by a poor bioavailability due to its high overall positive charge at physiologic pH.

Furthermore, the small molecule AMD070 (**2**), the lead of a series of compounds containing at the same time a benzimidazole and a tetrahydroquinoline moiety in their structure, demonstrated a remarkable antagonistic activity after oral administration and it is currently under advanced clinical investigation for the prophylaxis of HIV infection [16-18].

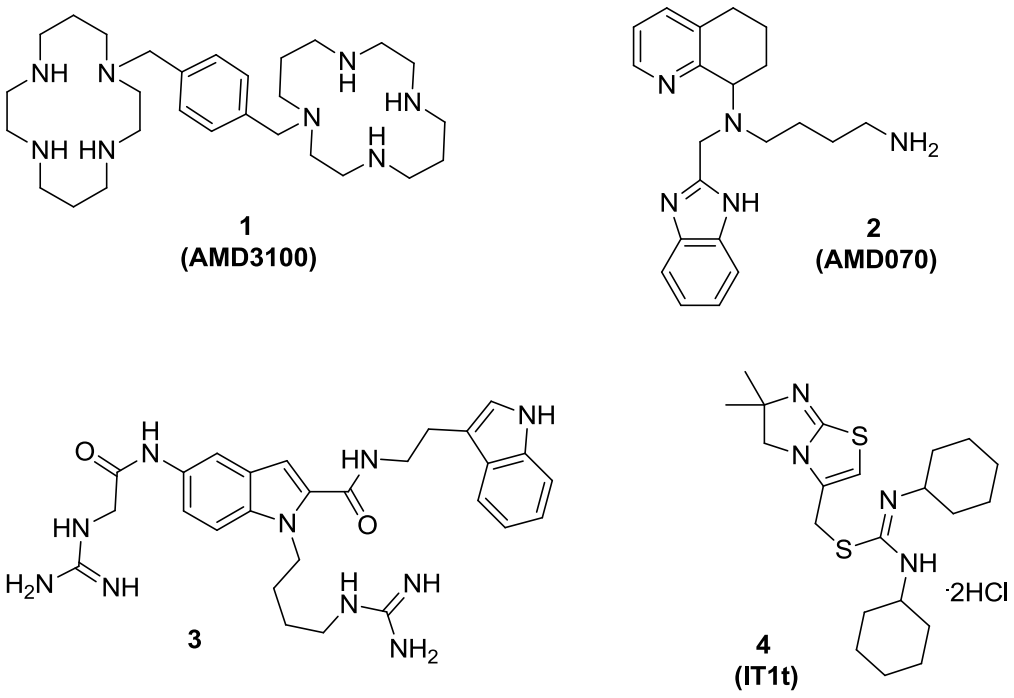

Figure 1. Chemical structures of known antagonists of CXCR4.

The evolution in the search of alternative structure for CXCR4 antagonists brought to the identification of poly-substituted indoles, among them compound **3** represents the most promising prototype active in human CXCR4 transfected Chinese hamster ovary (CHO) cells in a [^{125}I]-SDF-1 radio-ligand assay [19].

These compounds were abandoned due to their high protonation degree 'in vivo', which precludes an adequate tissues distribution. However, the structures of these compounds suggested that indole could serve as a valuable scaffold to be further explored, since molecular modeling showed that this nucleus, properly decorated, meets the spatial requirements for the key interactions in the previously reported pharmacophore model [20]. A further improvement in the definition of CXCR4 receptor was the discovery of the oraclly active isothiourea ligand IT1t (**4**), which was co-crystallized with the receptor [21,22].

Herein, we report the identification of a small series of CXCR4 antagonists based on a 2-(1*H*-indol-1-yl)-*N*'-arylbenzohydrazide moiety (FIL1-3, **Figure 2**) with typical small molecule drug characteristics reflecting potential favorable pharmacokinetics and many possibilities to be optimized.

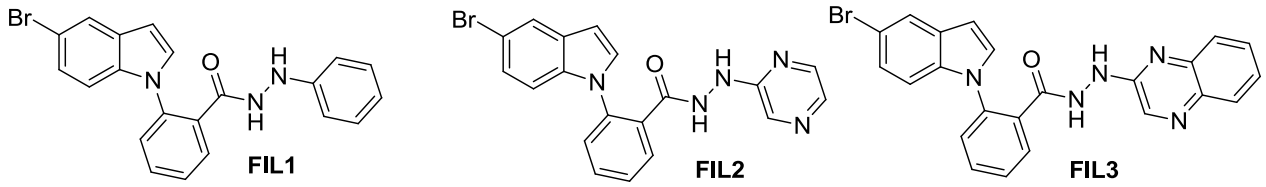

Figure 2. Structures of studied compounds.

Since the chemokine SDF-1α and its cognate receptor CXCR4 play a crucial role in breast cancer spread and progression [23,24], the effects of synthesized compounds have been tested in different breast cancer cell models and in co-culture systems by using specific biological assays, such as cell proliferation and wound-healing assays, where they revealed interesting anticancer properties.

In particular, one of the tested compounds, FIL2, resulted particularly active in blocking SDF-1α-dependent cell motility, proliferation and downstream signaling activation in estrogen-receptor negative and positive breast cancer cells as well as in experimental cell models for acquired endocrine resistance. A specific [^{125}I]-SDF-1α binding assay has confirmed that the above properties were unambiguously due to CXCR4 inhibition. This compound was also able to inhibit the effects of cancer-associated fibroblasts (CAFs), key players in the breast tumor microenvironment, on cancer progression.

Based on all the promising results we obtained, the newly synthesized compounds could be considered leads for the development of new selective CXCR4 antagonists as novel tools for the treatment of breast cancer and other CXCR4-related diseases.

MATERIALS AND METHODS

Molecular modelling and docking simulations

The molecular modelling simulations were performed on an Apple Mac pro 2.66 GHz Quad-Core Intel Xeon, Running Ubuntu 12.04. The CXCR4 protein was downloaded from the Protein Data Bank, accession code: 3ODU [20] and prepared using the Protein Preparation Wizard tool of Maestro [25]. Putative inhibitors were built and prepared in Maestro and docked with GLIDE, using the SP mode. Images were created using MOE [26].

Chemical synthesis

General experimental information is reported in ref. 27. The purity of FIL1-3 was > 96 %, as determined by HPLC.

2-(5-Bromo-1H-indol-1-yl)-N'-phenylbenzohydrazide (FIL1)

To a stirred solution of 2-(5-bromo-1*H*-indol-1-yl)benzoic acid **1** [27] (0.060 g; 0.190 mmol) in DMF (1 mL) CDI (0.031; 0.190 mmol) was added in 10 min. A solution of phenylhydrazine (0.020 g; 0.190 mmol) in DMF (1 mL) was slowly added in 15 min. The reaction mixture was heated to 60°C for 8 hours. The solvent was then evaporated and the solid residue obtained was taken up into ethyl acetate. The resulting solution was sequentially debated with 5% HCl solution and brine. After evaporation of the solvent, the crude product was purified by column chromatography (toluene/ethyl acetate/methanol/ammonium hydroxide, 10/1/1/0.25, as eluent). The title compound was separated as an orange amorphous solid in 22% yield. ^{1}H NMR (300 MHz, MeOD) δ 7.82 (s, 1H), 7.69-7.60 (m, 3H), 7.44-7.37 (m, 3H), 7.24-7.06 (m, 5H), 7.01-6.81 (m, 2H). ^{13}C NMR (75 MHz, MeOD) δ 164.0, 148.8, 144.7, 143.9, 142.8, 136.6, 135.9, 130.6, 130.2, 129.4, 129.0,

129.9, 128.8, 128.5, 128.2, 128.0, 127.9, 125.9, 120.4, 118.9, 112.6. HRMS calcd for $C_{21}H_{16}BrN_3O$ 405.0477, found 405.0420. IR (KBr) ν_{max}: 1676 cm^{-1}.

2-(5-Bromo-1H-indol-1-yl)-N'-(pyrazin-2-yl)benzohydrazide (FIL2)

This compound was prepared following the procedure applied for FIL1 starting from pyrazin-2-yl-hydrazine (0.021 g; 0.190 mmol). The pure compound was obtained as a brown amorphous solid in 50% yield. ^{1}H NMR (300 MHz, MeOD) δ 8.11 (s, 1H), 7.99-7.88 (m, 2H), 7.73-7.62 (m, 3H), 7.67 (t, 1H, *J* = 7.6 Hz), 7.44 (d, 1H, *J* = 7.9 Hz), 7.29 (d, 1H, *J* = 3.2 Hz), 7.20-7.09 (m, 1H), 6.97 (d, 1H, *J* = 4.7 Hz), 6.58 (d, 1H, *J* = 3.2 Hz). ^{13}C NMR (75 MHz, MeOD) δ 167.0, 140.8, 137.8, 135.9, 133.0, 131.3, 130.5, 130.2, 129.9, 128.7, 128.2, 128.0, 127.8, 127.7, 124.5, 124.2, 122.9, 110.9, 102.3. HRMS calcd for $C_{19}H_{14}BrN_5O$ 407.0382 found 407.0407. IR (KBr) ν_{max}: 1656 cm^{-1}.

2-(5-Bromo-1H-indol-1-yl)-N'-(quinoxalin-2-yl)benzohydrazide (FIL3)

This compound was prepared following the procedure applied for FIL1 starting from quinoxalin-2-yl-hydrazide (0.030 g; 0.190 mmol). The pure compound was obtained as a purple solid in 37% yield. ^{1}H NMR (300 MHz, MeOD) δ 8.32 (d, 1H, *J* = 7.5 Hz), 8.10 (d, 1H, *J* = 9.1 Hz), 7.82 (d, 1H, *J* = 9.1 Hz), 7.79-7.69 (m, 2H), 7.55 (t, 2H, *J* = 7.7 Hz), 7.42-7.35 (m, 3H), 7.20-7.05 (m, 3H), 6.59 (d, 1H, *J* = 3.2 Hz). ^{13}C NMR (75 MHz, MeOD) δ 159.5, 158.0, 137.3, 134.0, 133.3, 132.5, 129.0, 128.8, 128.0, 127.6, 127.0, 126.2, 125.4, 124.2, 123.0, 122.2, 121.5, 120.0, 118.8, 117.6, 111.3, 108.5, 102.1. HRMS calcd for $C_{23}H_{16}BrN_5O$ 457.0538 found 457.0525. IR (KBr) ν_{max}: 1693 cm^{-1}.

Biological materials and methods

Reagents and antibodies

SDF-1α and [^{125}I]-SDF-1α were obtained from Sichim and Perkin-Elmer, respectively. Antibodies used for immunoblotting were: total Akt, phosphoAkt^{Ser437} and GAPDH (Santa Cruz Biotechnology), MAPK and phosphoMAPK$^{Thr202/Tyr204}$ (Cell Signaling Technology). Peroxidase-coupled secondary antibodies goat anti-mouse or anti-rabbit were obtained from Santa Cruz Biotechnology and the enhanced chemiluminescence system was from Amersham Pharmacia. Collagenase, 3-[4,5-Dimethylthiazol-2-yl]-2,5-diphenyltetrazolium bromide reagent/MTT and Coomassie Brilliant Blue were obtained from Sigma. TRIZOL reagent was from Invitrogen. RETROscript kit was purchased from Promega.

Cell culture

MCF-10A normal breast epithelial cells were grown in Dulbecco's modified Eagle's medium-F12 plus glutamax containing 5% Horse Serum, 1 mg/ml penicillin–streptomycin, 0.5 mg/ml hydrocortisone, and 10mg/ml insulin. Human estrogen receptor (ER)-negative MDA-MB-231 breast cancer cells were cultured in DMEM medium supplemented with 10% Fetal Bovine Serum, 0.1 nmol/L nonessential amino acid, 2 mmol/L L-glutamine, and 50 units/ml penicillin/streptomycin. Human ER-positive MCF-7 breast cancer cells were cultured in DMEM/F-12 medium supplemented with 5% Newborn Calf Serum, 0.1 nmol/L nonessential amino acid, 2 mmol/L L-glutamine, and 50 units/ml penicillin/streptomycin. Tamoxifen-resistant (TR) cells derived from MCF-7 cultured with 4-OH-tamoxifen over a period of 12 months and long-term estrogen-deprived cells (LTED) were derived from MCF-7 after six-month estrogen deprivation were obtained as previously described [28]. Subconfluent cell cultures, synchronized for 48 hours in medium without phenol red and serum, were used for all experiments.

CAF isolation and conditioned medium systems

Human cancer-associated fibroblasts (CAFs) were obtained from three specimen of human primary breast cancers as described [29]. Briefly, following digestion of small tumor pieces (collagenase 500 U/mL in Hank's balanced salt solution, at 37°C for 2 hours) and differential centrifugation (90 g for 2 minutes), the supernatant containing CAFs was centrifuged (500 g for 8 minutes), resuspended, and cultured in RPMI-1640 medium supplemented with 15% Fetal Bovine Serum, and antibiotics. CAFs between 4-10 passages

were used, tested by mycoplasma-presence, authenticated by morphology and FAP and α-SMA expression. For generation of conditioned media, CAFs were incubated with medium without phenol red and serum for 48-72 hours. Conditioned media were collected, centrifuged to remove cellular debris and utilized in respective experiments.

RT-PCR assays

Total cellular RNA was extracted using TRIZOL reagent as suggested by the manufacturer. The purity and integrity were checked spectroscopically and by gel electrophoresis before carrying out the analytical procedures. Two microgram of total RNA were reverse transcribed in a final volume of 20 µL using a RETROscript kit as suggested by the manufacturer. The cDNAs obtained were amplified by PCR using the following primers: 5'-TTACCCGCAAAAGACAAGT-3' (SDF1-α forward) and 5'-AGGCAATCACAAAACCCAGT-3' (SDF1-α reverse), 5'-AATCTTCCTGCCCACCATCT-3' (CXCR4 forward) and 5'-GACGCCAACATAGACCACCT-3' (CXCR4 reverse), 5'-CTCAACATCTCCCCCTTCTC-3' (36B4 forward) and 5'-CAAATCCCATATCCTCGTCC-3' (36B4 reverse). Negative controls containing water instead of first strand cDNA were utilized.

Wound-healing assays

For the measurement of cell migration during wound healing, confluent cell cultures were incubated in phenol-red and serum-free medium for 24 hours before the beginning of the experiment. Cell monolayers were then scraped, washed to remove debris and treated as indicated in the respective experiments. Wound closure was monitored over 24 hours. Cells were then fixed, stained with Comassie Brillant Blue and photographed after wounding under phase contrast microscopy at 10X magnification. Pictures represent one of three-independent experiments.

Cell proliferation assays

MTT assays. Cells (2 x 10^4 cells/well) were plated in 24-well plates and treated as indicated for 3 days. The MTT assay was performed as the following: 100 µL MTT solution in PBS (2 mg/mL) was added into each

well and allowed to incubate at 37°C for 2 hours followed by media removal and solubilization in 500 µL dimethyl sulfoxide (DMSO). After shaking the plates for 15 minutes, the absorbance at 570 nm was measured in each well, including the blanks. Cell proliferation was expressed as fold change relative to vehicle-treated cells. A minimum of three experiments, containing eight different doses of FIL2 in triplicate, was combined for IC_{50} calculations. The absorbance readings were used to determine the IC_{50} using GraphPad Prism 4 (GraphPad Software). Briefly, values were log-transformed, normalized, and nonlinear regression analysis was used to generate a sigmoidal dose– response curve to calculate IC_{50} values.

Soft agar growth assays. Cells (10^4/well) were plated in 0.35% agarose with 5% charcoal stripped-FBS in phenol red-free media (4 mL), with 0.7% agarose base in six-well plates. After two days, media containing vehicle or indicated treatments were added to the top layer, and replaced every 2 days. After 14 days, 300 µL of MTT reagent was added to each well and incubated at 37°C for 4 hours. Plates were then placed at 4°C overnight and colonies > 50µm diameter from triplicate assays were counted. The data are representative of three independent experiments, each performed in triplicates.

Immunoblot analysis

Total protein lysates were subjected to SDS–PAGE as described [30]. Briefly, cells were harvested in cold PBS and resuspended in lysis buffer containing HEPES (20 mmol/L, pH 8), EGTA (0.1 mmol/L), $MgCl_2$ (5 mmol/L), NaCl (0.5M), glycerol (20%), Triton (1%), and protease inhibitors (0.1 mmol/L sodium orthovanadate, 1% phenylmethylsulfonylfluoride, and 20 mg/mL aprotinin). Equal amounts of total protein lysates were resolved on a 11% SDS–polyacrylamide gel, transferred to a nitrocellulose membrane, and probed with appropriate antibodies as indicated in the respective experiments. Band intensities representing relevant proteins were measured by Scion Image laser densitometry scanning program (Scion Corporation) and standard deviations along with associated P values for the biological replicates were determined by using GraphPad-Prism4 software (GraphPad Inc., San Diego, CA). Immunoblots show one representative image of three separate experiments.

[^{125}I]-SDF-1α competition binding assays

MDA-MB-231 cells were harvested with versene reagent and washed twice in PBS. Ligand binding experiments were performed using 1 nM of [^{125}I]-SDF-1α (specific activity, 2.200 Ci/mmol) in a final volume of 100 µL binding buffer (50 mM HEPES, pH 7.4, 1 mM $CaCl_2$, 150 mM NaCl, 5 mM $MgCl_2$, 5% bovine serum albumin) containing 5 x 10^5 cells/well in the presence of serially diluited concentrations of unlabeled SDF-1α or FIL2 compound. Nonspecific binding was determined by adding 150 nM of unlabeled SDF-1α. Samples were incubated for 60 minutes at 4°C. After incubation, cells were washed twice with 300 µL wash buffer (50 mM HEPES, pH 7.4, 1 mM $CaCl_2$, 500 mM NaCl, 5 mM $MgCl_2$). Bound ligands were determined by standard gamma counting techniques. At least three independent experiments were performed. The binding data were analyzed by nonlinear regression using the GraphPad PRISM program.

Statistical analysis

Data were analyzed for statistical significance using two-tailed student's Test, GraphPad-Prism4 software. Standard deviations (S.D.) were shown.

RESULTS AND DISCUSSION

Design and synthesis

The isothiourea ligand IT1t (**4**), [(E)-(6,6-dimethyl-5,6-dihydroimidazo[2,1-b]thiazol-3-yl)methyl N,N'-dicyclohexylcarbamimidothioate dihydrochloride], showing an IC_{50} = 48 nM in CXCR4 radioligand binding assay, was fruitfully used during the mapping of the active binding site of the protein, as already mentioned [20].

The rationale behind the design of the hereby-reported inhibitors was guided by two considerations: *in silico* analysis of the interactions between IT1t and CXCR4 in the crystal complex and the synthetic feasibility of the newly designed compounds using established procedures. In particular, we were interested in a chemical scaffold we could easily prepare using our recently reported method [27]. All the compounds designed using these criteria were docked and their binding mode analyzed to verify how well the new structures would mimic the IT1t binding mode (**Figure 3**). The first designed modification for the backbone of the new compounds was the replacement of the dihydroimidazo[2,1-*b*]thiazole system of IT1t with a flatter *N*-

substituted indole that could still result in favorable interactions with Trp94. The 6,6-dimethyl motif is replaced by a bromine atom directed towards the Tyr116 and filling the small hydrophobic cavity present in that position. The benzo group linked at position 1 of indole could at the same time establish additional hydrophobic interactions with Val112 and support the polar carbohydrazide moiety. This latter group is also establishing a hydrogen bond with Asp97, a residue that is involved in a strong interaction with the carbamimidic group of IT1t. The final modification was the removal of bulky cyclohexyl substituents of IT1t with the concomitant introduction of a cyclic system linked to the N'-atom of the benzohydrazide moiety. Among the attempted aryl substituents, the pyrazine gave best results probably due to the possibility to interact further with Arg183 (**Figure 3B**).

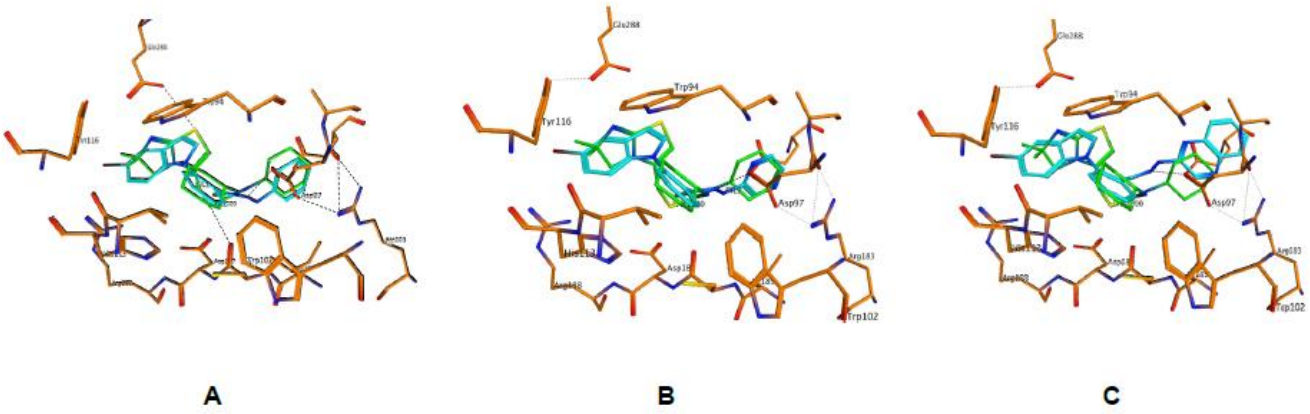

Figure 3. Docking simulation. Putative binding mode of **(A)** FIL1, **(B)** FIL2 and **(C)** FIL3 (represented in cyan) in the CXCR4 binding pocket. Co-crystallized ligand (IT1t) is represented in green.

The three studied compounds (FIL 1-3) were obtained in moderate yields starting from a common intermediate, the 2-(5-bromo-1*H*-indol-1-yl)benzoic acid **1,** whose preparation was recently described [27]. The acid **1** was coupled with a proper hydrazine by action of 1,1'-carbonyldiimidazole (CDI) in DMF to give compounds FIL1, FIL2 and FIL3 in 22, 50 and 37% yield, respectively (**Figure 4**).

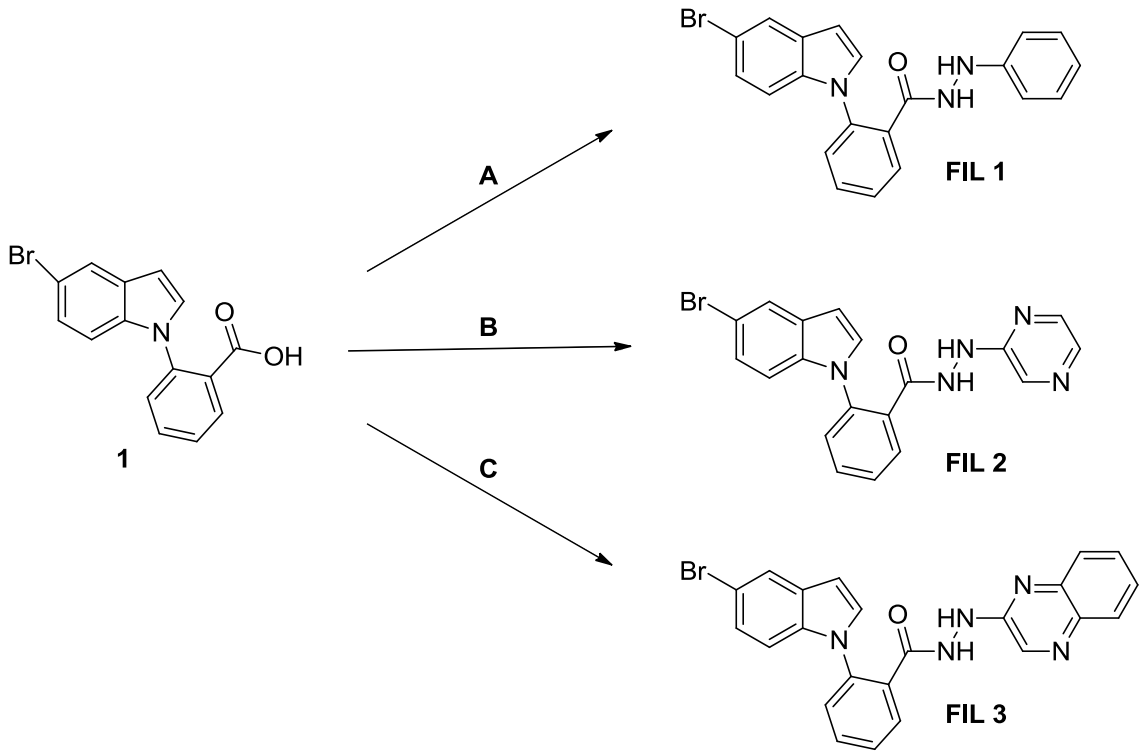

Figure 4. Synthesis of FIL 1-3. Reagents and Conditions: (**A**) CDI, DMF, phenylhydrazine, 60°C (22%); (**B**) CDI, DMF, 2-hydrazinylpyrazine, 60°C (50%); (**C)** CDI, DMF, 2-hydrazinylquinoxaline, 60°C (37%).

FIL2 compound blocks SDF-1α-dependent cell motility, proliferation and downstream signalling activation in MDA-MB-231 breast cancer cells

It has been reported that the chemokine SDF-1α and its cognate receptor CXCR4 are expressed in breast carcinoma tissues and in breast cancer cell lines, and that cell clones isolated from metastatic sites (e.g., bone or lungs) exhibit higher levels of CXCR4 than the parental cells [31-33]. Prior to evaluating the biological activity of the CXCR4 antagonists, we analyzed SDF-1α and CXCR4 expression in estrogen receptor (ER)-negative MDA-MB-231 breast cancer cells, which are well characterized in terms of their metastatic potential and properties. RT-PCR analysis revealed SDF-1α and CXCR4 expression in MDA-MB-231 breast cancer cells (**Figure 5A**). Given the crucial role of SDF-1α/CXCR4 signaling axis in modulating cancer cell migration [34], we first explored the ability of the CXCR4 antagonists that we synthesized to inhibit cell motility in wound-healing assays. MDA-MB-231 breast cancer cells were treated with three different CXCR4 antagonists (FIL1, FIL2, FIL3) at increasing concentrations (0.01, 0.1, 1, 10μM) for 24 hours. **Figure 5B** showed that FIL1 and FIL3 did non affect cell motility at all the doses tested, while FIL2 was

able to inhibit migration at concentrations as low as 10nM. Therefore, in agreement with the docking simulation, the *in vitro* evaluations of the CXCR4 inhibitory efficacy on cell motility also resulted in the selection of the antagonist FIL2 for the subsequent studies. Next, we assessed the effects of increasing concentrations of FIL2 compound on breast cancer cell proliferation (**Figure 5C**). We observed that FIL2 treatment for 72 hours significantly reduced cell viability in MDA-MB-231 cells at all the doses tested, with IC50 values of 49.4 µM (95% Confidence Intervals, 30.1-81.2 µM). The activity of FIL2 compound was also evaluated using soft agar anchorage-independent growth. Consistently with MTT assays, FIL2 treatment decreased colony formation in MDA-MB-231 cells (**Figure 5D**). In contrast, FIL2 did not elicit any significant growth inhibitory effects on MCF-10A non-tumorigenic breast epithelial cells (**Figure 5E**). Taken together, these results showed that the compound FIL2 inhibits cell growth and migratory potential of highly invasive MDA-MB-231 breast cancer cells, interfering with the autocrine effects of SDF-1α /CXCR4 system in these cells.

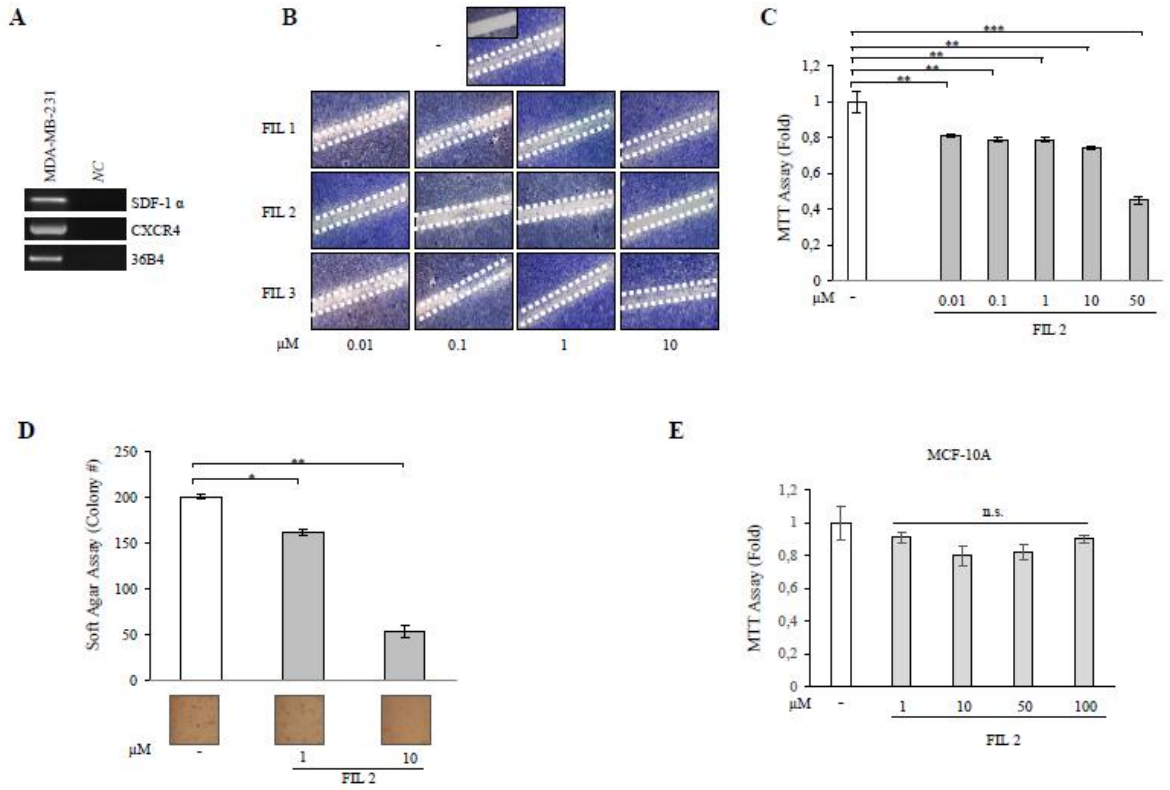

Figure 5. FIL2 compound inhibits motility and growth of MDA-MB-231 breast cancer cells. **(A)** RT-PCR for SDF-1α, CXCR4 and 36B4 (internal standard). *NC*, negative-control. **(B)** Wound-healing assay in cells treated with vehicle (-) or increasing concentrations of FIL1, FIL2 and FIL3 compounds (0.01, 0.1, 1, 10µM). *Small squares*, time 0. **(C)** MTT growth assay in cells treated with vehicle (-) or FIL2 compound (0.01, 0.1, 1, 10, 50 µM). **(D)** Soft agar

anchorage-independent growth assay in cells treated with vehicle (-) or FIL2 compound (1, 10µM). *Bottom panel*, a typical well for each condition is shown. **(E)** MTT growth assay in MCF-10A normal epithelial breast cells treated with vehicle (-) or FIL2 compound (1, 10, 50, 100 µM). n.s.= non significant. **P*<0.05, ***P*<0.005, ****P*<0.0005.

In order to verify that the CXCR4 antagonist FIL2 binds to the CXCR4 receptor, we established a whole cell-based [^{125}I]-SDF-1α ligand competition binding assay. A typical result is shown in **Figure 6**. In a homologous competition binding assay, we found that MDA-MB-231 cells bind SDF-1α in a dose dependent-manner with IC_{50} value of 26.1 ± 8 nmol/L (**Figure 6A**). The [^{125}I]-SDF-1α binding was replaced by cold SDF-1α, confirming the specificity of SDF-1 binding. FIL2 was able to inhibit [^{125}I]-SDF-1α ligand binding to MDA-MB-231 cells in a heterologous competition binding assay with IC_{50} value of 10.9 ± 4.2 nmol/L (**Figure 6B**). The binding curve was fitted to an one site binding model. These results indicate that FIL2 exhibits an increased affinity for the receptor compared to endogenous SDF-1α ligand and may act as a highly selective CXCR4 receptor antagonist.

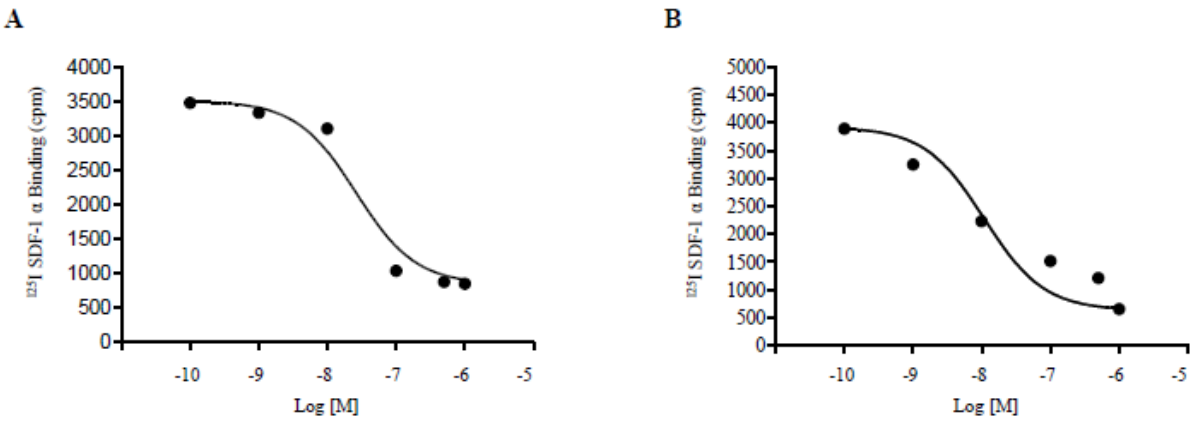

Figure 6. [^{125}I]-SDF-1α ligand binding by MDA-MB-231 cells. [^{125}I]-SDF-1 competition binding assay was performed as described in Materials and Methods section. [^{125}I]-SDF-1α bound to MDA-MB-231 cells was competed with either unlabelled SDF-1α **(A)** or FIL2 compound **(B)**. The specificity of [^{125}I]-SDF-1α binding was confirmed by a replacement experiment with cold SDF-1α (150-fold excess).

We, then, aimed to assess the ability of FIL2 compound to counteract SDF-1α-induced cell motility and growth. As expected, MDA-MB-231 breast cancer cells moved the farthest in either direction to close the 'gap' in the cell bed after treatment with SDF-1α (200 ng/mL) compared to basal vehicle-treated conditions (**Figure 7A**). Pretreatment with FIL2 at 0.01-1μM concentrations strongly reduced SDF-1α-mediated effects on cell motility (**Figure 7A**). Moreover, FIL2 exposure significantly reduced the increase in the colony numbers observed after SDF-1α treatment (**Figure 7B**).

Stimulation of CXCR4 by SDF-1 induces phosphorylation of Akt and p42/44 MAPK, promoting proliferation and migration of different types of cells [35]. Thus, we conducted time-course studies to analyze whether FIL2 compound was able to antagonize the effects of SDF-1α on activation of the above mentioned downstream signaling molecules (**Figure 7C&7D**). As expected, treatment with SDF-1α resulted in an increased phosphorylation of Akt and MAPK in MDA-MB-231 breast cancer cells. Interestingly, pretreatment with FIL2 abrogated the SDF-1α activation of these signaling pathways.

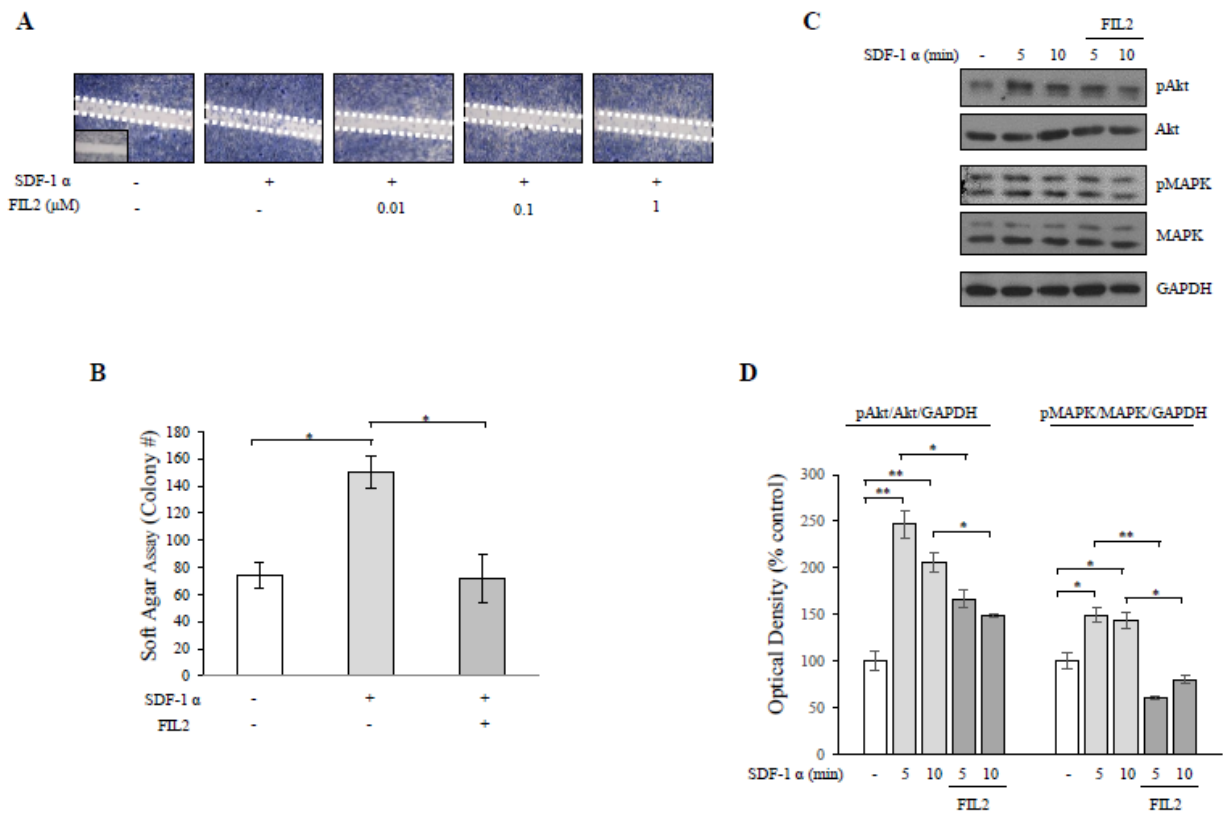

Figure 7. FIL2 compound antagonizes SDF-1α–mediated motility, growth and signalling activation in MDA-MB-231 breast cancer cells. **(A)** Wound-healing assay in cells treated with vehicle (-), SDF-1α (200 ng/mL) with or without FIL2 compound (0.01, 0.1, 1μM). *Small squares*, time 0. **(B)** Soft agar anchorage-independent growth assay in cells treated with vehicle (-), SDF-1α (200 ng/ml) in the presence or not of FIL2 compound (1μM). **(C)** Immunoblotting

of phosphorylated (p) Akt and MAPK and total proteins from cells treated with SDF-1 (200 ng/mL for 5 and 10 minutes) with or without FIL2 compound (1μM). **(D)** Histograms represent the mean ± SD of three separate experiments in which band intensities were evaluated in terms of optical density arbitrary units and expressed as percentage of control which was assumed to be 100%. **P*<0.05, ***P*<0.005.

Efficacy of FIL2 compound in antagonizing CXCR4 signaling in different breast cancer cell models and co-culture systems

To extend our results, as an additional model system for breast cancer we investigated the effects of FIL2 molecule in affecting growth, and motility of ER-positive MCF-7 breast cancer cells. First, we demonstrated SDF-1α and CXCR4 expression in these cells (**Figure 8A**). As previously shown for MDA-MB-231 cells, we found a significant decrease in both anchorage-independent proliferation and migration of MCF-7 breast cancer cells after FIL2 exposure (**Figure 8B**). Again, treatment with SDF-1 at 200 ng/mL concentration increased colony numbers and motility of cells, and pretreatment with FIL2 compound reduced SDF-1α-mediated activities (**Figure 8C**). Finally, we demonstrated that FIL2 was able to reverse the stimulatory effects induced by SDF-1α on the phosphorylation levels of Akt and MAPK (**Figure 8D&8E**), confirming that the FIL2 compound may act as a CXCR4 antagonist in different breast cancer cellular backgrounds.

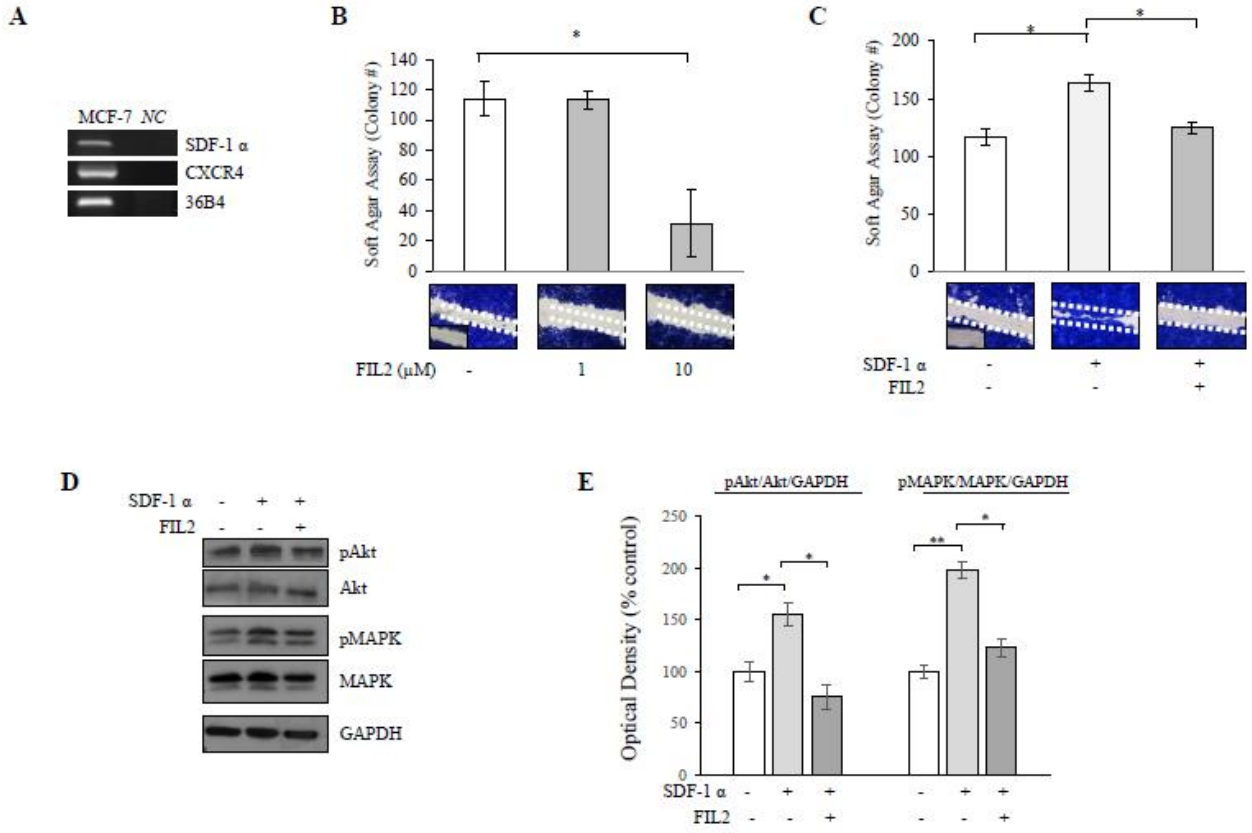

Figure 8. FIL2 effects in MCF-7 breast cancer cells. **(A)** RT-PCR for SDF-1α, CXCR4 and 36B4 (internal standard). *NC*, negative-control. **(B)** Soft agar anchorage-independent growth (*upper panel*) and wound-healing (*lower panel*) assays in cells treated with vehicle (-) or FIL2 compound (1, 10μM). *Small squares*, time 0. **(C)** Soft agar anchorage-independent growth (*upper panel*) and wound-healing (*lower panel*) assays in cells treated with vehicle (-), SDF-1α (200 ng/mL) with or without FIL2 compound (1μM). *Small squares*, time 0. **(D)** Immunoblotting of phosphorylated (p) Akt and MAPK and total proteins from cells treated with SDF-1α (200 ng/mL for 5 minutes) with or without FIL2 compound (1μM). Numbers below the blots represent the average fold change in phospho-proteins/total proteins/GAPDH ratio relative to vehicle (-)-treated cells. **(E)** Histograms represent the mean ± SD of three separate experiments in which band intensities were evaluated in terms of optical density arbitrary units and expressed as percentage of control which was assumed to be 100%. **P*<0.05, ***P*<0.005.

The behavior of tumor cells seems to be regulated not only by cell autonomous signals, but it also relies on heterotypic signals coming from surrounding myofibroblast stromal cells, able to create a specific and local microenvironment to tightly control breast cancer proliferation and differentiation. Indeed, fibroblasts adjacent to primary breast tumors have higher expression of SDF-1α than those of normal breast tissue and through this paracrine signaling, CXCR4 may promote local tumor cell proliferation, motility, and invasion [36,37]. Therefore, we examined the ability of FIL2 compound to inhibit breast cancer cell proliferation and motility promoted by cancer-associated fibroblasts (CAFs). To this aim, CAFs were isolated from biopsies of primary breast tumors and coculture experiments were performed to create 'in vitro' conditions that can

mimic the complex 'in vivo' microenvironment [29,38]. Both MDA-MB-231 and MCF-7 breast cancer cells were incubated with phenol-red and serum-free medium (-), or CAF-derived conditioned media (C.M.) in the presence or not of FIL2 compound and growth and motility were evaluated (**Figure 9**). As previously demonstrated [29], CAF C.M. significantly increased colony numbers and motility of breast cancer cells. Interestingly, treatment with FIL2 compound attenuated growth and migration-promoting activities of CAF C.M.

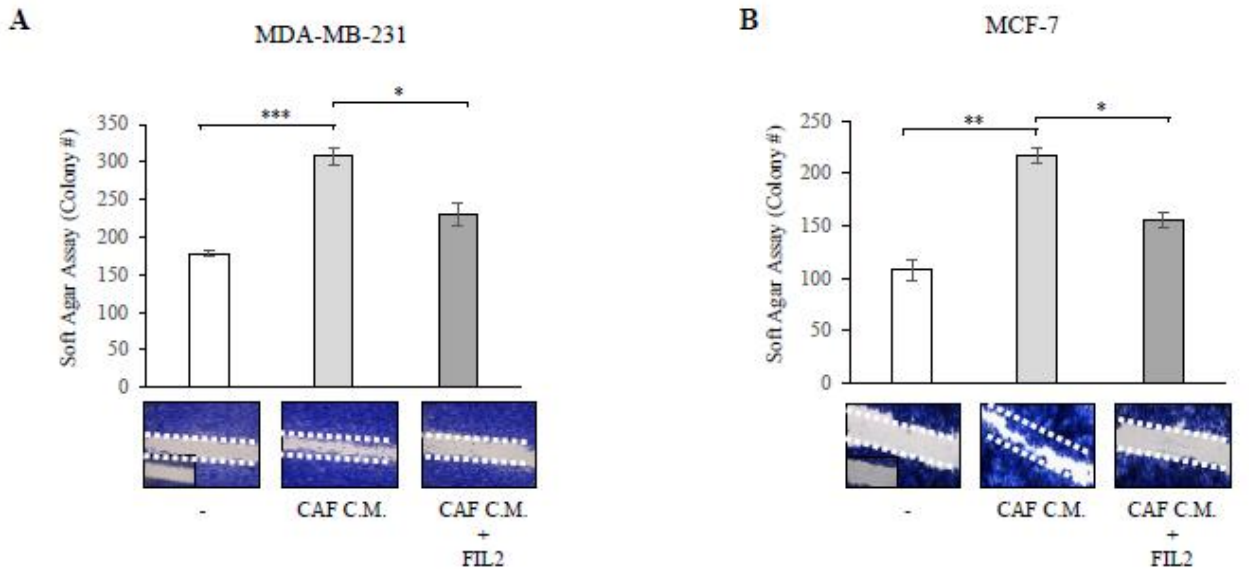

Figure 9. FIL2 reduces growth and migration induced by CAF-derived conditioned media in breast cancer cells. Soft agar anchorage-independent growth (*upper panel*) and wound-healing (*lower panel*) assays in MDA-MB-231 **(A)** and MCF-7 **(B)** cells treated with phenol-red and serum-free medium (-), conditioned media derived from CAFs (CAF C.M.) with/without FIL2 compound (1μM). *P<0.05, **P<0.01, ***P<0.0005. Small squares, time 0.

It has been recently reported that enhanced CXCR4 signaling is sufficient to drive ER-positive breast cancers to an endocrine therapy-resistant phenotype, highlighting CXCR4 signaling as a rational therapeutic target also for the treatment of ER-positive, estrogen-independent breast carcinoma [39,40]. Therefore, as a final step of this study, we evaluated whether FIL2 compound was able to affect the progression of hormone-independent and therapeutic-resistant breast cancer cell lines, using other two additional breast cancer cellular models. In particular, as experimental cell models for acquired resistance, we used: 1) tamoxifen-resistant (TR) cells obtained from MCF7 cells cultured with 4-OH tamoxifen over a period of 12 months; 2) MCF7 LTED cells, which gradually acquired aromatase inhibitor resistance upon culture in estrogen/steroid-

free conditions [28]. As shown in **Figure 10A&10B**, we found increased SDF-1α and CXCR4 expression in TR cells and LTED cells compared to parental MCF-7 breast cancer cells. In agreement with a previous study [30], resistant cells exhibited a higher basal non-stimulated growth and motility (**Figure 10C&10D**). Treatment with SDF-1α or CAF-derived conditioned medium resulted in an enhancement of growth and motility of TR and LTED cells and, again, FIL2 compound had a significant inhibitory effect in basal as well as SDF-1α and C.M.-stimulated conditions.

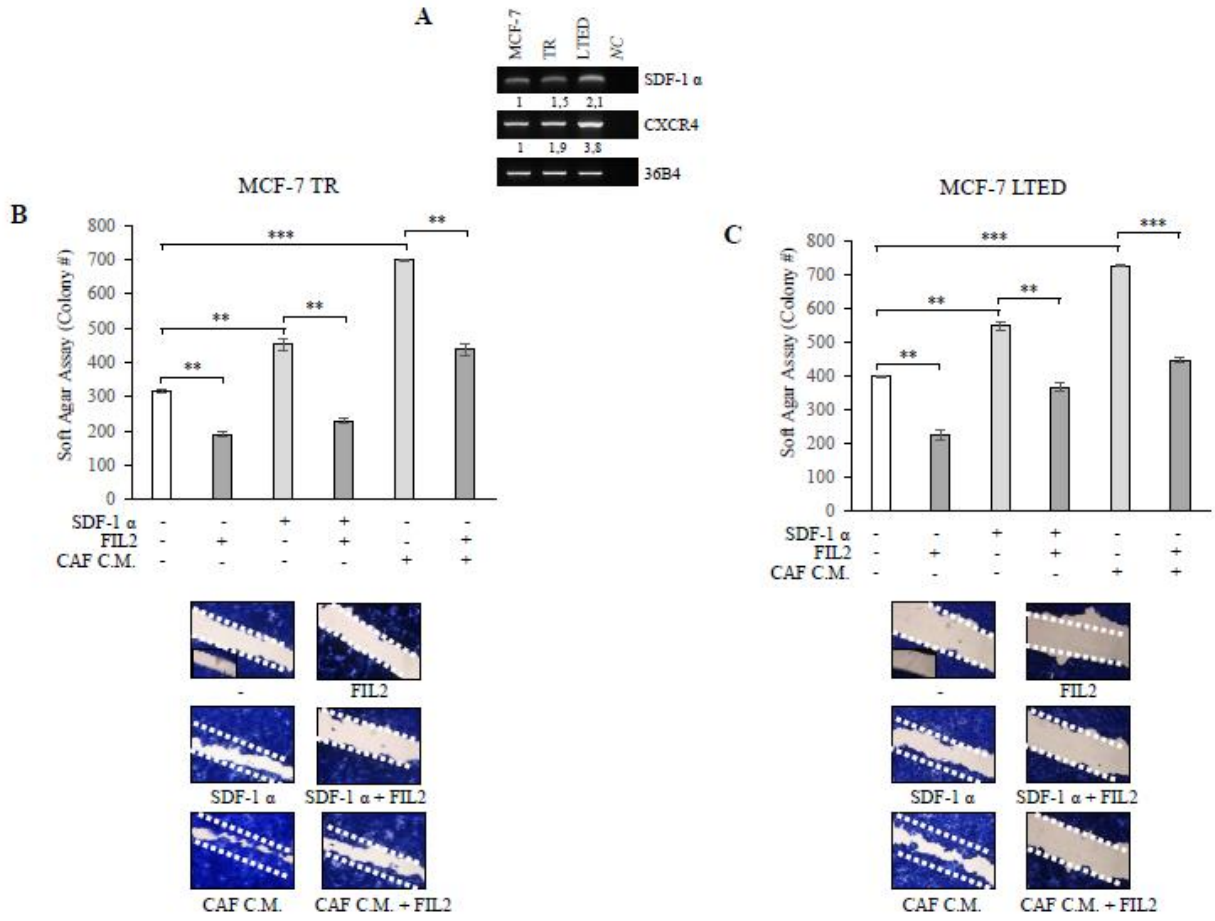

Figure 10. FIL2 compound reduces growth and migration in hormone-resistant breast cancer cells. **(A)** RT-PCR for SDF-1α, CXCR4 and 36B4 (internal standard). *NC*, negative-control. **(B)** Histograms represent the mean ± SD of three separate experiments in which band intensities were evaluated in terms of optical density arbitrary units and expressed as percentage of control, which was assumed to be 100%. Soft agar anchorage-independent growth (*upper panel*) and wound-healing (*lower panel*) assays in tamoxifen-resistant MCF-7 TR **(C)** and long term-estrogen deprived MCF-7 LTED **(D)** breast cancer cells treated with vehicle (-), SDF-1α (200 ng/mL), conditioned media derived from CAFs (CAF C.M.) with or without FIL2 compound (1μM). *P<0.05, **P<0.005, ***P<0.0005. *Small squares*, time 0.

CONCLUSION

CXCR4 plays a role in several pathophysiological conditions such as cancer, altered immune conditions and HIV infection, hence chemical agents able to prevent the interaction between this receptor and its endogenous ligand SDF-1 might result useful in the management of a number of pathologies [5-9]. Despite the huge number of identified CXCR4 antagonists, most of them show inadequate bioavailability, that represents the bigger limit to a clinical application. Thus, only a few compounds have so far entered clinical trials [11-15]. Among the small-molecule antagonists, indole based compounds, suitably modified, seem to meet pharmacokinetic requirements and optimal features to interact with the target.

In the present study, we describe the design and the synthesis of three novel molecules namely FIL1-3 investigated for their capability to interact with CXCR4. In particular, one of the derivatives shows the ability to bind to CXCR4 as revealed by molecular docking and whole cell-based [^{125}I]-SDF-1α ligand competition binding assays. This compound is able to inhibit SDF-1α-mediated cell motility, proliferation and downstream signaling activation in different breast cancer cell lines as well as to prevent tumor microenvironment stimulatory effects in co-culture studies. This activity assumes a great importance in hormone-resistant breast cancer cell lines, as resistance to endocrine therapy still remains a major clinical concern.

Since breast cancer progression has been correlated to the SDF-1α-CXCR4 signaling axis, specific agents able to prevent this interaction, could result of great interest for the management of such a type of cancer.

Based on these findings, we may consider FIL-2 as a lead for the development of a new class of selective antagonist ligands of CXCR4 that may be useful in order to better assess the biological function of this receptor. In addition, the CXCR4 antagonism may represent a starting point for the development of novel therapeutics for the treatment of breast cancer and other diseases in which the receptor is involved.

FUTURE PERSPECTIVE

The role played by the interaction of CXCR4 and its natural ligand SDF-1α in several types of tumors, including breast cancer, as well as in other diseases is clearly recognized. This suggests that CXCR4

represents a promising target for the development of innovative therapeutics and the identification of FIL2, as a selective targeting CXCR4 lead compound, may help the discovery of effective CXCR4 antagonists to be proposed to clinical practice. Moreover, the possibility to prepare a FIL2 ^{79}Br- or ^{81}Br-radiolabeled derivative to be used as functional biomarkers in early diagnosis, disease prevention, and drug response may represent a further applicative development for the class of compounds herein described.

EXECUTIVE SUMMARY

CXCR4 Inhibition

Inhibition of CXCR4 represents a promising therapeutic approach in the treatment of breast cancer and other diseases involving this receptor.

Lead identification and synthesis

A new selective CXCR4 antagonist has been identified and could be useful for a rational design of broad-spectrum therapeutics.

Binding assay

A whole cell-based [^{125}I]-SDF-1α ligand competition binding assay was accomplished in order to verify that FIL2 binds to the CXCR4 receptor as hypothesized by molecular docking prevision.

DEFINED KEY TERMS

Docking simulation:

Computational simulation technique used to predict the binding orientation of a candidate ligand into the active site of the target protein.

Mapping of the active binding site:

The assignment of chemical features for the definition of topology in the interaction site of a receptor.

Poly-substituted indoles:

Molecules based on an indole scaffold bearing substituents capable to bind specific groups of the active site of a target molecule.

Acquired endocrine resistance:

Despite the significant advances in the treatment of breast cancer following the introduction of endocrine therapy (tamoxifen and aromatase inhibitors), in many estrogen receptor-positive breast tumors drug resistance develops during treatment leading to disease progression (acquired resistance).

Tumor microenvironment:

The behavior of malignant cells seems to be dependent not only on cell autonomous signals, but it also relies on heterotypic signalings deriving from surrounding stromal cells, able to generate a microenvironment to tightly control breast tumor progression. Among the stromal cells, cancer-associated fibroblasts (CAFs) play a crucial role in determining cancer proliferation and differentiation.

Soft agar growth assay:

The soft agar colony formation assay is a technique used to evaluate cellular anchorage-independent proliferation *in vitro*. This assay is considered to better reflect *in vivo* three-dimensional tumor growth.

Ligand binding assay:

Detection method used to evaluate the interactions that occur between two molecules, such as a receptor and its ligands.

Coculture experiments:

Coculture experiments were performed by incubation of breast cancer cells with CAF-derived conditioned media. This allows to create *in vitro* conditions that can mimic the complex *in vivo* microenvironment.

ACKNOWLEDGEMENTS

This work was supported by AIRC Grant (IG11595) to SA. European Commission/FSE/Regione Calabria to FC.

REFERENCES

1 Lefrancois M, Lefebvre MR, Saint-Onge G *et al*. Agonists for the chemokine receptor CXCR4. *ACS Med. Chem. Lett.* 2, 597-602 (2011).

2 Allen SJ, Crown SE, Handel TM. Chemokine: receptor structure, interactions, and antagonism. *Annu. Rev. Immunol.* 25, 787-820 (2007).

3 Bleul CC, Wu L, Hoxie JA, Springer TA, Mackay CR. The HIV coreceptors CXCR4 and CCR5 are differentially expressed and regulated on human T lymphocytes. *P. Natl. Acad. Sci. USA* 94, 1925-1930 (1997).

4 Bleul CC, Farzan M, Choe H *et al*. The lymphocyte chemoattractant SDF-1 is a ligand for LESTR/fusin and blocks HIV-1 entry. *Nature* 382, 829-833 (1996).

5 Raman D, Sobolik-Delmaire T, Richmond A. Chemokines in health and disease. *Exp. Cell. Res.* 317, 575-589 (2011).

6 Balkwill FR. The chemokine system and cancer. *J. Pathol.* 226, 148-157 (2012).

7 Didigu CA, Doms RW. Novel Approaches to Inhibit HIV Entry. *Viruses* 4, 309-324 (2012).

8 Grande F, Garofalo A, Neamati N. Small molecules anti-HIV therapeutics targeting CXCR4. *Curr. Pharm. Des.* 14, 385-404 (2008).

°Summarizes chemical classes of compounds able to prevent CXCR4-mediated HIV entry.

9 Debnath B, Xu S, Grande F, Garofalo A, Neamati N. Small molecule inhibitors of CXCR4. *Theranostics* 3, 47-75 (2013).

°°Summarizes all classes of compounds targeting CXCR4.

10 Burger JA, Stewart DJ. CXCR4 chemokine receptor antagonists: perspectives in SCLC. *Expert Opin. Investig. Drug.* 18, 481-490 (2009).

11 [Internet] NCT01339039. Plerixafor (AMD3100) and Bevacizumab for recurrent high-grade glioma. http://clinicaltrialsgov.

12 [Internet] NCT01141543. Feasibility and efficiency study of leukemic cell mobilization with Plerixafor injection. http://clinicaltrialsgov.

13 [Internet] NCT01373229. Lenalidomide + Plerixafor in previously treated chronic lymphocytic leukemia (CLL). http://clinicaltrialsgov.

14 [Internet] NCT01058993. AMD 3100 for treatment of myelokathexis. http://clinicaltrialsgov.

15 [Internet] NCT01018979. Safety, pharmacokinetics and stem cell mobilization of TG-0054 in multiple myeloma, non-Hodgkin lymphoma and Hodgkin disease patients. http://clinicaltrialsgov.

16 Harvey JR, Mellor P, Eldaly H, Lennard TW, Kirby JA, Ali S. Inhibition of CXCR4-mediated breast cancer metastasis: a potential role for heparinoids? *Clin. Cancer Res*. 13, 1562-1570 (2007).

17 Wilson LJ, Liotta DC. Emergence of small-molecule CXCR4 antagonists as novel immune and hematopoietic system regulatory agents. *Drug Develop. Res.* 72, 598-602 (2011).

18 [Internet] NCT00089466. Safety and activity of the oral HIV entry inhibitor AMD11070 in HIV infected patients. http://clinicaltrialsgov.

19 Ueda S, Kato M, Inuki S *et al*. Identification of novel non-peptide CXCR4 antagonists by ligand-based design approach. *Bioorg. Med. Chem. Lett.* 18, 4124-4129 (2008).

20 Wu B, Chien EY, Mol CD *et al*. Structures of the CXCR4 chemokine GPCR with small-molecule and cyclic peptide antagonists. *Science* 330, 1066-1071 (2010).

21 Thoma G, Streiff MB, Kovarik J *et al*. Orally bioavailable isothioureas block function of the chemokine receptor CXCR4 in vitro and in vivo. *J. Med. Chem*. 24, 7915-7920 (2008).

22 Hung TC, Lee WY, Chen KB, Chen CYC. Lead Screening for CXCR4 of the Human HIV Infection Receptor Inhibited by Traditional Chinese Medicine. *BioMed Research International* ID 809816 (2014).

23 Sobolik T, Su YJ, Wells S, *et al*. CXCR4 drives the metastatic phenotype in breast cancer through induction of CXCR2 and activation of MEK and PI3K pathways. *Mol. Biol. Cell* 25, 566-582 (2014).

24 Zhang Z, Ni C, Chen W *et al*. Expression of CXCR4 and breast cancer prognosis: a systematic review and meta-analysis. *BMC Cancer*, 14:49 (2014).

25 Maestro 9.3, Schrödinger, LLC, New York, NY, 2012. http://www.schrodinger.com.

26 Molecular Operating Environment (MOE 2012.10). Chemical Computing Group, Inc. Montreal, Quebec, Canada. www.chemcomp.com.

27 Grande F, Brizzi A, Garofalo A, Aiello F. Active manganese dioxide promoted cyclization of *ortho*-(1*H*-pyrrol-1-yl)aryl and heteroaryl carboxylic acids to 5*H*-pyrrolo[1,2-*a*][3,1]benzoxazin-5-one derivatives. *Tetrahedron* 69, 9951-9956 (2013).

28 Lombardo Y, Faronato M, Filipovic A, Vircillo V, Magnani L, Coombes RC. Nicastrin and Notch4 drive endocrine therapy resistance and epithelial to mesenchymal transition in MCF7 breast cancer cells. *Breast Cancer Res.* 16, R62 (2014).

29 Barone I, Catalano S, Gelsomino L *et al*. Leptin mediates tumor-stromal interactions that promote the invasive growth of breast cancer cells. *Cancer Res*. 72(6), 1416-1427 (2012).

°°Reinforces the concept that blocking cancer–stromal cell communication may represent an effective strategy for targeted therapy of breast cancer.

30 Gu G, Barone I, Gelsomino L *et al*. Oldenlandia diffusa extracts exert antiproliferative and apoptotic effects on human breast cancer cells through ERα/Sp1-mediated p53 activation. *J. Cell. Physiol.* 227(10), 3363-72 (2012).

31 Müller A, Homey B, Soto H *et al*. Involvement of chemokine receptors in breast cancer metastasis. *Nature* 410(6824), 50-56 (2001).

°Highlights the involvement of CXCR4 in breast cancer spread and progression.

32 Kang Y, Siegel PM, Shu W *et al*. A multigenic program mediating breast cancer metastasis to bone. *Cancer Cell* 3(6), 537-549 (2003).

33 Schmid BC, Rudas M, Resniczek GA, Leodolter S, Zeillinger R. CXCR4 is expressed in ductal carcinoma in situ of the breast and in atypical ductal hyperplasia. *Breast Cancer Res. Treat.* 84(3), 247-250 (2004).

34 Fernandis AZ, Prasad A, Band H, Klosel R, Ganju RK. Regulation of CXCR4-mediated chemotaxis and chemoinvasion of breast cancer cells. *Oncogene* 23, 157-167 (2004).

35 Kijowski J, Baj-Krzyworzeka M, Majka M *et al*. The SDF-1-CXCR4 axis stimulates VEGF secretion and activates integrins but does not affect proliferation and survival in lymphohematopoietic cells. *Stem Cells* 19, 453-466 (2001).

36 Allinen M, Beroukhim R, Cai L *et al*. Molecular characterization of the tumor microenvironment in breast cancer. *Cancer Cell*, 6, 17-32 (2004).

°Outlines SDF-1 overexpression in tumor myoepithelial cells and myofibroblasts and its ability to bind to receptors on epithelial cells and enhance their proliferation, migration, and invasion.

37 Orimo A, Gupta PB, Sgroi DC *et al*. Stromal fibroblasts present in invasive human breast carcinomas promote tumor growth and angiogenesis through elevated SDF-1/CXCL12 secretion. *Cell*, 121, 335-348 (2005).

°Adds more insights in the role of SDF-1 as an important paracrine molecule in breast cancer microenvironment.

38 Catalano S, Giordano C, Panza S *et al*. Tamoxifen through GPER upregulates aromatase expression: a novel mechanism sustaining tamoxifen-resistant breast cancer cell growth. *Breast Cancer Res. Treat.* 146(2), 273-285 (2014).

39 Rhodes LV, Short SP, Neel NF *et al*. Cytokine receptor CXCR4 mediates estrogen-independent tumorigenesis, metastasis, and resistance to endocrine therapy in human breast cancer. *Cancer Res.* 71, 603-613 (2011).

°**Underlines CXCR4 signaling as a rational therapeutic target for the treatment of estrogen-independent breast carcinomas**

40 Dubrovska A, Hartung A, Bouchez LC *et al*. CXCR4 activation maintains a stem cell population in tamoxifen-resistant breast cancer cells through AhR signalling. *Br. J. Cancer* 107(1), 43-52 (2012).

Title

Glucocorticoid receptor as a potential target to decrease aromatase expression and inhibit Leydig tumor growth

Authors

S Panza[1,3], R Malivindi[1,3], F Chemi[1], V Rago[1], C Giordano[2], I Barone[1], D Bonofiglio[1], L Gelsomino[1], S Andò[*,1,4] and S Catalano[*,1,4]

Affiliations

[1] Department of Pharmacy, Health and Nutritional Sciences, University of Calabria, Arcavacata di Rende, CS, Italy.

[2] Centro Sanitario, University of Calabria, Arcavacata di Rende CS, Italy.

[3] These authors contributed equally to this work.

[4] These authors are joint senior authors.

Running title: GR inhibits Leydig tumor growth

Key words: aromatase; Leydig cell tumor; Glucocorticoid Receptor

Abbreviations: GR, glucocorticoid receptor; Arom, aromatase; L-19, mitochondrial ribosomal protein L19; DEXA, dexamethasone; RU-486, mifepristone; NCoR, nuclear receptor corepressor protein; SMRT, silencing mediator of retinoid and thyroid hormone receptors; GAPDH, glyceraldehyde 3-phosphate dehydrogenase; DAPI, 2-(4 amidinophenyl)-6-indolecarbamidine dihydrochloride; MTT, 3-[4,5-dimethylthiaoly]-2,5-diphenyltetrazolium bromide

Correspondence and requests should be addressed to:

[*]Sebastiano Andò: Department of Pharmacy, Health and Nutritional Sciences, University of Calabria, 87036 Arcavacata di Rende (CS), Italy. Phone: + 39 0984 496201. e-mail: sebastiano.ando@unical.it .

[*]Stefania Catalano: Department of Pharmacy, Health and Nutritional Sciences, University of Calabria, 87036 Arcavacata di Rende (CS), Italy. Phone: + 39 0984 496207. e-mail: stefania.catalano@unical.it .

Abstract

Glucocorticoid receptor (GR), a member of the nuclear receptor superfamily, plays a crucial role on reproductive and endocrine functions of the gonads modulating steroid synthesis and spermatogenesis. It is well known that elevated glucocorticoid levels, resulting from diverse stressful conditions, lead to a decrease of serum testosterone. Conversely, the reduction of endogenous corticosterone levels is associated with an increased testosterone production by Leydig cells. In Leydig cells, glucocorticoid-induced inhibition of testosterone biosynthesis occurs through suppression of several cytochrome gene expression, involved in testicular steroidogenesis. However, information regarding the precise function of GR in Leydig tumor cells are still lacking.

In the present study we detected the expression of GR in R2C Leydig tumor cells and its activation, using the specific ligand dexamethasone (DEXA), is associated with a significantly decrease of the expression and the enzymatic activity of cytochrome P450 aromatase, enzyme responsible for the local conversion of androgens into estrogens. This inhibitory effect relies on the ability of activated GR to regulate the aromatase gene transcriptional activity through the recruitment of the corepressors NCoR and SMRT to a newly identified putative glucocorticoid responsive element within the aromatase PII proximal promoter. Moreover, treatment with GR ligand significantly reduces both anchorage dependent an anchorage-independent growth in R2C cells. Finally, we evidenced using R2C xenografts models that treatment with DEXA markedly reduced Leydig tumor growth *in vivo*. Indeed, tumors from DEXA-treated mice exhibited a decrease in the expression of the proliferation marker Ki-67 and aromatase. Collectively, our data demonstrate that activated GR, decreasing aromatase expression, induces Leydig tumor regression both *in vitro* and *in vivo* highlighting GR as a new target for the therapy of Leydig tumors.

Introduction

Estrogen dependence is a feature of testicular tumor which is the most common malignant neoplasm in young men (20-40 years old) accounting for up to 20% of all malignancies diagnosed at this age. More than 90% of testicular tumors originate from germ cells whereas Leydig cell tumors (LCTs) are the most common tumors of the male gonadal interstitium and represent about 3% of all testicular neoplasia.[1] Several observations on both rodents and humans suggest that local estrogen synthesis plays a significant role in sustaining Leydig cell tumorogenesis. Transgenic mice overexpressing aromatase, the enzyme responsible for the conversion of androgens to estrogens, and exhibiting an enhancement of circulating 17β-estradiol (E2) levels show Leydig cell hyperplasia and tumors.[2,3] In a previous study, we observed that rat tumor Leydig cells (R2C) release a conspicuous amount of E2, as a consequence of aromatase over-expression in these cells, that stimulates a short autocrine loop determining cell proliferation.[4] In humans, elevated aromatase expression with subsequent high plasma estradiol levels has been reported in patients with testicular LCTs[5-8] further supporting the crucial role played by the aromatase enzyme on the pathogenesis of leydigiomas. All these experimental and clinical observations suggest that a reduction of local estrogen production by inhibiting aromatase expression may open new opportunities for therapeutic intervention in Leydig cell tumor.

In this context, we have previously shown that a decrease of aromatase expression induced by farnesoid X receptor (FXR) plays an important role in inhibiting Leydig tumor growth cell.[9-10] Particularly, we have demonstrated that FXR is able to compete with the steroidogenic factor 1 (SF-1) in binding to a common nuclear response element within the PII aromatase promoter, interfering negatively with its activity.[9] More recently, we also have identified the existence of a functional cross-talk between the androgen receptor, the orphan nuclear receptor DAX-1 and aromatase involved in the inhibition of the estrogen-dependent Leydig cancer cell proliferation.[11]

Glucocorticoid receptor (GR), another member of the nuclear receptor superfamily, highly expressed in Leydig cells[12-14] plays a physiological role in the control of male sexual maturation and adult reproductive functions modulating gonadal steroid synthesis and spermatogenesis.[15] It is well recognized that elevated glucocorticoid levels resulting from diverse stressful conditions, whether physical or psychological, lead to suppression of serum testosterone levels.[16] Conversely, reduction of endogenous corticosterone levels (the main glucocorticoid in rodents) leads to increased testosterone production by Leydig cells, thus further supporting the repressive role of glucocorticoids on testosterone production.[17] These observations well fit with the evidences that activation of GR suppresses, in Leydig cells, expression of several steroidogenic enzyme-encoding genes, including Star, Cyp11a1, Cyp17a1, Hsd3b1, Hsd17b3 and Cyp19a1.[18-24] In addition to repressing gene expression, glucocorticoids also induce apoptosis in rat Leydig cells.[25] However, informations regarding the precise function of GR in Leydig tumor cells are still lacking.

Here, we investigated in rat tumor Leydig cells R2C whether GR activation by specific agonist dexamethasone (DEXA) may modulate aromatase expression and thus inhibit testicular tumor growth. We report the identification of a novel glucocorticoid-mediated mechanism that controls the expression of aromatase in Leydig tumor cells by negatively regulating aromatase transcript and protein levels. Transcriptional repression of aromatase gene by GR appears to be consequent to the recruitment of nuclear receptor corepressor protein (NCoR) and silencing mediator of retinoid and thyroid hormone receptors (SMRT) corepressors to the GRE-containing region of the aromatase promoter.

Results

GR is expressed in R2C Leydig tumor cells.

We first aimed to evaluate, by immunoblot analysis, the expression of GR receptor in R2C cells, a well-documented experimental model for Leydigioma. Immunoblot analysis revealed the presence of a GR-immunoreactive protein band in R2C cells, and expression levels are comparable to TM3 cells, an immortalized Leydig cell line derived from normal mouse testis (Supplementary Figure 1a). These results were further confirmed by immunofluorescence analysis detecting GR immunoreactivity in the cytoplasm region of R2C cells. No reaction was noticed in the cells processed without primary antibody (NC) (Supplementary Figure 1b).

Inhibitory effects of GR agonist dexamethasone on aromatase expression in R2C cells.

On the basis of previous data demonstrating that GR activation down-regulates the aromatase enzyme in testes[26] we explored the possibility that GR agonist dexamethasone (DEXA) might modulate aromatase gene expression in R2C cells. Treatment with 0.01, 0.1 and 1 μM DEXA was able to reduce the cellular content of the enzyme, in a concentration-dependent manner, at both mRNA and protein levels, as determined by RT-PCR and immunoblot analysis (Figure 1a and b). The reduction of aromatase expression upon DEXA administration was also reflected by a change in its enzymatic activity, as evaluated by the tritiated water release assay (Figure 1c). A direct involvement of GR in modulating aromatase expression was provided by the evaluation of aromatase mRNA, protein content, and its enzymatic activity after administration of the GR inhibitor RU-486 (Figure 1d-f). R2C cells were treated with DEXA in the presence or absence of the inhibitor compound. The addition of RU-486 completely reversed the down-regulatory effects induced by DEXA suggesting that activated GR directly regulates the aromatase expression in R2C cells.

Ligand-activated GR decreases the transcriptional activity of aromatase PII-proximal promoter.

Next we tested whether the down-regulatory effects of DEXA on aromatase expression could be due to a negative influence on aromatase gene transcriptional activity. Aromatase activity is regulated primarily at the level of gene expression by tissue-specific promoters and is present in testicular somatic cells and along the maturative phases of male germ cells.[27,28] A promoter proximal to the translation start site, called promoter II (PII) regulates aromatase expression in fetal and adult testis, R2C and H540 rat Leydig tumor cells, and in purified preparations of rat Leydig, Sertoli, and germ cells.[29,30]

Thus, R2C cells were transiently transfected with a luciferase reporter construct containing the PII aromatase promoter (PII-Arom) sequence (-1037/+94; p-1037) and treated with increasing concentrations of DEXA. We found a significant dose-dependent inhibition of aromatase promoter activity after treatment with DEXA (Figure 2a). To identify the region within the aromatase promoter that are functionally important for transcriptional regulation by DEXA, transient transfection experiments were performed by using constructs containing different 5'-deleted regions of rat PII aromatase promoter, as schematically reported in Figure 2b (*upper panel*). Similarly to what observed for the PII-Arom (-1037/+94), the transcriptional activity of the PII-Arom constructs (-688/+94, p-688 and -475/+94, p-475) was decreased in response to DEXA stimulation whereas in the presence of the PII-Arom construct encoding the sequence from -183 to +94 (p-183) we evidenced the loss of the inhibitory effect exerted by DEXA (Figure 2b, *lower panel*). This latter result highlights that the region from -475 to -183 was essential for the down-regulation induced by DEXA on aromatase promoter activity. The nucleotide sequence analysis of this region revealed a putetive GRE binding motif located at position -470/-460, suggesting that P450 aromatase regulation by DEXA requires GRE motif.

GR reduces aromatase promoter activity at GRE site through Corepressor Recruitment

The interaction of GR with the aromatase gene promoter was further investigated by chromatin immunoprecipitation, ChIP assay. Using specific antibody against GR and RNA-Pol II, protein-chromatin complexes were immunoprecipitated from R2C cells cultured with or without DEXA 0.1 and 1 μM. GR occupancy to the GRE site containing sequence of aromatase promoter was induced in a ligand-dependent manner, since GR recruitment was enhanced by DEXA (Figure 2c *left panel*). The inhibitory role of GR on aromatase promoter, is evidenced by the dynamic of RNA Pol II recruitment onto the aromatase promoter, that appears to be drastically reduced upon DEXA treatment (Figure 2c *right panel*). To assess whether the decrease in aromatase promoter transcriptional activity might be caused by the cooperative interaction between GR and negative transcriptional regulators, we investigated the involvement of NCoR and SMRT, which interact with and function as negative coregulators of GR.[31] Re-ChIP assays demonstrated increased NCoR and SMRT occupancy of the GRE-containing region of the aromatase promoter after DEXA (0.1 and 1 μM) exposure (Figure 2d).

DEXA inhibits R2C cell proliferation through GR activation.

We previously demonstrated that local estradiol production by highly expressed aromatase represents a major feature involved in the positive control of R2C cell proliferation.[4] Thus, we examined the effects of DEXA on R2C cell proliferation. As shown in Figure 3a, treatment with DEXA 0.01, 0.1 and 1 μM for 24 and 48 h reduced cell growth in R2C cells in a dose dependent manner. The specific involvement of GR in the antiproliferative response of R2C cells to DEXA was demonstrated by the evidence that such inhibitory effects were completely reversed in the presence of the GR inhibitor RU-486 (Figure 3b). A second approach we employed was to evaluate the inhibitory growth effects mediated by GR-activated using anchorage-independent soft agar growth assays (Figure 3c). Consistently with MTT assays, DEXA treatment significantly reduced colony formation in R2C cells. To extend our results we also investigated the effects of DEXA in

affecting growth of Leydig normal cell lines, TM3. As reported in supplementary Figure 2 DEXA exposure did not elicit any significant inhibitory effects in TM3 cells at all the doses tested.

Activation of GR inhibits R2C tumor xenograft growth

As a final step of the current study, we used the R2C tumor xenograft model to examine the effects of DEXA on Leydig tumor growth *in vivo*. To this aim, we injected R2C cells into the intrascapular region of male nude mice and followed tumor growth after administration of DEXA at 1 and 10 mg/Kg/day. This administration was well tolerated because no change in body weight or in food and water consumption was observed along with no evidence of reduced motor function. In addition, no significant differences in the mean weights or histological features of the major organs (liver, spleen, and kidney) after sacrifice were observed between vehicle-treated mice and those that received treatment, indicating a lack of toxic effects at the dose given. As shown in Figure 4a, DEXA (1 and 10 mg/kg/day) induced a regression in tumor growth. This effect was evident as early as day 12 of treatment, and tumor volumes continued to reduce over control for the duration of experiment. 30 days after injection, tumor weigth as well as tumor size were markedly smaller in animals treated with DEXA respect to vehicle-treated mice (Figure 4b). In agreement with our *in vitro* findings, we observed in R2C xenograft tumors from mice treated with DEXA a significant decrease of aromatase expression, evaluated by both western blotting and immunohistochemistry analysis (Figure 5a and b). This was concomitant with a reduction in the expression of Ki-67, a well-known marker for cell proliferation, in R2C xenograft tumors from mice treated with DEXA than in tumors from vehicle-treated controls (Figure 5c).

It is worth to underline that the hystopathological features of seminiferous tubules from DEXA-treated mice showed a normal cellularity and morphology, very similar to those of the control group (Supplementary Figure 3).

Discussion

Leydigioma is a rare testicular tumor that affects males at any age with two peaks of incidence, during prepuberty, between 5 and 10 years, and in adulthood between 25 and 35 years of age.[32] Although usually benign, about 10% of LCTs in adult patients reveal a malignant phenotype metastasizing to retroperitoneal lymph nodes, liver, lungs and bone.[33] Unfortunately, malignant LCTs respond poorly to chemotherapy or radiation,[34,35] rendering it necessary to identify new therapeutic target for Leydig cell tumor treatment.

In this study, we have shown that glucocorticoid receptor (GR) is a potential new target to reduce Leydig tumor proliferation. In fact, GR is expressed in this type of cancer and its activation is associated with a drastic reduction of cell proliferation resulting from the inhibition of aromatase expression and activity.

Glucocorticoid hormones control a wide variety of biological processes, such as metabolic homeostasis, inflammation, immune response, development and reproduction.[36] Moreover, glucocorticoids are key regulators of cell growth and proliferation in many cell types. Indeed, glucocorticoids can induce a G1 cell cycle arrest and programmed cell death of immature thymocytes, several leukemic cell lines, and mature peripheral T lymphocytes.[37,38] They also inhibit the proliferation of mammary epithelial cells,[39,40] fibroblasts[41] and hepatoma cells.[42] The antiproliferative effect exerted by glucocorticoids has prompted their use clinically as a part of anticancer therapy for a diverse range of dysplasias, including lymphoproliferative disorders and several solid tumors.[43-47]

We identified a novel glucocorticoid-mediated mechanism that controls cell growth in Leydig tumor cells. We found that a synthetic glucocorticoid receptor agonist dexamethasone is able to significantly reduce proliferation rate in a well-documented *in vitro* model for Leydig cell neoplasms, such as rat Leydig tumor cells R2C, as a consequence of a reduction of local estrogen production. Indeed, in R2C cells, DEXA treatment negatively impacts on the enzyme aromatase by

decreasing its expression at both mRNA and protein levels, together with the inhibition of its enzymatic activity. Our results indicate that the down-regulation of aromatase expression induced by DEXA administration is strictly dependent on GR activation since it was completely reversed in the presence of the GR inhibitor RU-486. All these findings suggest that GR-mediated inhibition of aromatase involves regulation of aromatase gene transcriptional activity and thus we focused on the molecular mechanisms by which GR mediates repression of the aromatase enzyme.

Distinctive tissue-specific aromatase promoters are employed to control the expression of aromatase mRNA. The promoter located immediately upstream of the transcriptional initiation site (PII) regulates aromatase expression in rat Leydig, Sertoli, and germ cells and in R2C Leydig tumor cells.[29,30] In this report we provided evidences that activated GR is a transcriptional repressor of the aromatase gene in Leydig tumor cells. Specifically, we have demonstrated by functional studies and ChIP assay that GR-mediated inhibition of the aromatase is consequent to direct binding of the GR to a newly identified putative glucocorticoid responsive site within the aromatase proximal promoter.

It is well known that glucocorticoids exert their effects by activating the GR, a ligand-dependent transcriptional regulator that transduces the hormonal signal into the nucleus to alter the expression of target genes. Upon glucocorticoid binding, GR undergoes conformational changes, dissociates from the HSPs, homodimerizes and translocates into the nucleus, where it binds to GREs into DNA in the promoter of target genes, resulting in stimulation or suppression of the transcription of response genes (known as transactivation or transrepression effect, respectively).[36] GR can regulate transcription by several distinct mechanisms, and its function, as shown for other corticosteroid receptors, seem to depend not only on ligand binding, which is known to regulate receptor conformation, but also on the context of the gene and associated promoter factors that contribute to create a gene-specific topography, achieving specific profiles of gene expression. Indeed, the liganded-GR can interact with many components of the transcriptional machinery, including

coactivators, corepressors, chromatin remodeling proteins, components of the mediator complex as well as RNA polymerase II and components of the basal transcriptional machinery.[48]

Data from ChIP analysis revealed that GR occupancy to the GRE containing promoter region is concomitant with a decrease in RNA Pol II recruitment, consistent with the reduced aromatase transcriptional activity. GR-mediated repression of the aromatase gene involves the recruitment of the corepressors NCoR and SMRT, which share the same molecular architecture, interact with many of the same transcription factors, and assemble into similar corepressor complexes.[49] Indeed, NCoR and SMRT are recruited by GR to regulate the transcription of different genes.[50]

The physiological relevance of the inhibitory effects exerted by glucocorticoids on Leydig tumor cells is pointed out by our *in vivo* studies showing that DEXA significantly decreases the growth of R2C xenografts. Our results evidenced in tumor sections from DEXA-treated mice a marked reduction in the expression of the nuclear proliferation antigen Ki-67 as well as of the estrogen-producing enzyme aromatase. Importantly, DEXA administration did not affect the normal testis structure. Indeed, no significant differences were found on the hystopathological features of seminiferous tubules between vehicle-treated and DEXA-treated mice.

In conclusion, our findings suggest the possibility that targeting the glucocorticoid receptor could be helpful in improving new molecular and pharmacological approaches for Leydig cell tumor treatment.

Materials and Methods

Reagents and Antibodies

Nutrient Mixture F-12 Ham, Dulbecco's modified Eagle's medium/Ham's F-12, penicillin, streptomycin, fetal bovine serum, horse serum, dexamethasone (DEXA), mifepristone (RU-486), aprotinin, leupeptin, phenylmethylsulfonyl fluoride, sodium orthovanadate, formaldehyde, NP-40, MTT, dimethyl sulphoxide, proteinase K were from Sigma (Milan, Italy). TRIzol was provided by Invitrogen. FuGENE HD Transfection Reagent, TaqDNA polymerase, RETROscript kit, Dual Luciferase kit by Promega (Madison, WI). SYBR Green Universal PCR Master Mix was from Bio-Rad. Antibodies against GR, β-Actin, GAPDH, RNA polymerase II, ki-67, NCoR, SMRT and ECL system were by Santa Cruz Biotechnology (Santa Cruz, CA); antibody against Aromatase was by Serotec (Raleigh, NC). [1β-3H]androst-4-ene-3,17-dione, from PerkinElmer (Wellesley, MA). Salmon sperm DNA/protein A-agarose was from UBI (Chicago, IL).

Cell cultures

Rat Leydig tumor cells (R2C) were acquired in 2011 from American Type Culture Collection (LGC Standards, Tedding-ton Middlesex, UK) where they were authenticated, stored according to supplier's instructions and used within 4 months after frozen aliquots resuscitations. R2C were cultured in Ham's F-12 supplemented with 15% horse serum, 2.5% FBS, and antibiotics. Mouse Leydig cells (TM3) were cultured in Dulbecco's modified Eagle's medium/Ham's F-12 supplemented with 5% horse serum, 2.5% FBS, and antibiotics.

Immunoblot Analysis

R2C and TM3 cells were lysed in 500 µl of 50 mM Tris-HCl, 150 mM NaCl, 1% Nonidet P-40, 0.5% sodium deoxycholate, 2 mM sodium fluoride, 2 mM EDTA, 0.1% SDS, containing a mixture of protease inhibitors (aprotinin, phenylmethylsulfonyl fluoride, and sodium orthovanadate) for protein extraction. Protein extracts from tumor tissues were homogenized in lysis buffer

supplemented with 10% glycerol. Equal amounts of total protein were resolved on 10% SDS-polyacrilamide gels electrophoresis (PAGE), as described.[51]

Immunofluorescence

R2C cells seeded on glass coverslips, washed with PBS, and then fixed with 4% paraformaldehyde in PBS for 20 min at room temperature. Next, cells were permeabilized with 0.2% Triton X-100 in PBS for 5 min, blocked with 5% bovine serum albumin for 30 min, and incubated overnight with anti-GR antibody (1:100) in PBS overnight at 4 °C. The day after the cells were washed three times with PBS and incubated with the secondary antibody anti-rabbit IgG-fluorescein isothiocyanate (1:200) for 1 h at room temperature. To check the specificity of immunolabeling the primary antibody was replaced by normal rabbit serum (negative control). Fluorescence was photographed using OLYMPUS BX51 microscope using a 40x objective.

Total RNA Extraction and Reverse Transcription-PCR Assay

Total RNA was extracted from R2C using TRIzol reagent and evaluation of gene expression was performed by the reverse transcription-PCR method using a RETROscript kit. The cDNAs obtained were amplified by PCR using the following primers: forward 5'-CAGCTATACTGAAGGAATCCACACTGT-3' and reverse 5'-AATCGTTTCAAAAGTGTAACCAGGA-3' (P450 aromatase); forward 5'-GAAATCGCCAATGCCAACTC-3' reverse 5'-ACCTTCAGGTACAGGCTGTG-3' (L19). The PCR was performed for 25 cycles for P450 aromatase (94°C for 1 min, 58°C for 1 min, and 72°C for 2 min), and 20 cycles for L19 (94°C for 1 min, 60°C for 1 min, and 72°C for 2 min) in the presence of 1µl of first strand cDNA, 1µM each of the primers, 0.5 mM dNTP, Taq DNA polymerase (2 units/tube), and 2.2 mM magnesium chloride in a final volume of 25 µl. DNA quantity in each lane was analyzed by ImageJ, NIH, USA.

Aromatase Activity Assay

The aromatase activity in sub-confluent R2C cells culture medium was measured by the tritiated water release assay using 0,5 μM [1β-3H]androst-4-ene-3,17-dione as substrate.[10] The incubations were performed at 37°C for 2 h under an air/CO2 (5%) atmosphere. The results obtained were expressed as picomole/h and normalized to mg of protein (pmol/h/mg of protein).

Plasmids, transfections and luciferase reporter assays

R2C cells were transiently transfected using FuGENE HD reagent with the plasmids containing different segments of the rat aromatase PII sequence ligated to a luciferase reporter gene (-1037/+94 (p-1037), -688/+94 (p-688), -475/+94 (p-475), -183/+94 (p-183) previously described.[52] After transfection, R2C cells were treated with DEXA (0.01, 0.1, 1 μM) for 24 h. Thymidine kinase *Renilla* luciferase plasmid was used to normalize the efficiency of the transfection. Firefly and *Renilla* luciferase activities were measured by the Dual Luciferase kit. The firefly luciferase data for each sample were normalized based on transfection efficiency measured by *Renilla* luciferase activity.

Chromatin immunoprecipitation and Re-ChIP assay

R2C cells were treated with 0.1 and 1μM DEXA for 1 h and then cross-linked with 1% formaldehyde and sonicated. Supernatants were immunocleared with salmon sperm DNA/protein A-agarose for 1 h at 4°C. The precleared chromatin was immunoprecipitated with specific anti-GR or anti-polymerase II antibodies and re-immunoprecipitated with anti-NCoR, or anti-SMRT antibodies. A normal mouse serum IgG was used as negative control. Pellets were washed as reported, eluted with elution buffer (1%SDS, 0.1M NaHCO3), and digested with proteinase K. DNA was obtained by phenol/chloroform/isoamyl alcohol extractions and precipitated with ethanol. A 5 μl volume of each sample and input were used for real-time PCR using the primers flanking GRE sequence in the P450arom PII promoter region: 5'-GTAGAAGGGTACAGTTCTCGG-3' and 5'-CCTAGGACACACATGCTCAC-3'. PCR were performed in the iCycler iQ Detection System

(Bio-Rad), using 0.1 µM of each primer, in a total volume of 30 µl of reaction mixture following the manufacturer's recommendations. SYBR Green Universal PCR Master Mix with the dissociation protocol was used for gene amplification. Negative controls contained water instead of DNA. Final results were calculated using the ΔΔCt method as previously reported[4], using input Ct values. The basal sample was used as calibrator.

Cell proliferation assays

MTT anchorage-dependent growth assay. Cell viability was determined by using the 3-(4,5-dimethylthiazol-2-yl)-2,5- diphenyltetrazolium (MTT) assay as previously described.[53] Results are expressed as fold change ± SD relative to vehicle treated cells, and are representative of three different experiments each performed in triplicate.

Soft agar anchorage-independent growth assays. Cells (10^4/well) were plated in 2 ml of 0.5% agarose with 5% charcoal stripped-FBS in phenol red-free media, with a 0.7% agarose base in six well plates. Two days after plating, media containing vehicle, or treatments as indicated were added to the top layer, and replaced every 2 days. After 14 days, colonies were counted as described.[54] Data shown are the mean colony numbers of three plates and are representative of three independent experiments, each performed in triplicate.

In vivo experiments

The *in vivo* experiments were done in 35-day-old male nude mice (nu/nu Swiss; Charles River, Milan, Italy). At day 0, mice were inoculated with R2C cells ($1.0x10^5$/mouse) into the intrascapular region. Dexamethasone (DEXA) treatment was started at day 14 later and delivered daily to the animals by i.p. injection. Tumor growth was monitored as described.[55] At the time of killing, 30 days after injection, tumors were dissected out from the neighboring connective tissue, frozen in nitrogen and stored at -80°C. All animals were maintained and handled in accordance with the

recommendation of the Guidelines for the Care and Use of Laboratory Animals and were approved by the Animal Care Committee of University of Calabria.

Histopathological analysis

Tumor, testis, livers, spleen, and kidneys were fixed in 4% formalin, sectioned at 5 μm and stained with hematoxylin and eosin Y (H&E), as suggested by the manufacturer (Bio-Optica, Milan, Italy). H&E was photographed using OLYMPUS BX51 microscope using a 20x objective.

Immunohistochemical analysis

Paraffin-embedded section, 5 μm thick, were mounted on slides precoated with poly-lysine, and then they were deparaffinized and dehydrated (seven to eight serial sections). Immunohistochemical (IHC) experiments were performed as described[56], using rabbit polyclonal Ki-67 and mouse monoclonal anti-aromatase primary antibody at 4°C over-night. Then, a biotinylated goat-anti-rabbit and goat-anti-mouse IgG was applied for 1 h at room temperature, followed by the avidin biotin-horseradish peroxidase complex (Vector Laboratories, CA). Immunoreactivity was visualized by using the diaminobenzidine chromogen (Sigma-Aldrich). The primary antibody was replaced by normal rabbit and normal mouse serum negative control section. IHC was photographed using OLYMPUS BX51 microscope using a 40x objective.

Statistical analyses

Each datum point represents the mean ± S.D. (Standard Deviation) of three different experiments. Data were analyzed by Student's t test using the GraphPad Prism 4 software program. $p < 0.05$ was considered as statistically significant.

Acknowledgements

This work was supported by Associazione Italiana Ricerca sul Cancro (AIRC) grant IG 11595 European Commission, European Social Fund and the Calabria of region and Lilli Funaro Foundation to S.P.

Conflicts of interest

The author declare no conflicts of interest

References

1. Hawkins C, Miaskowski C. Testicular cancer: a review. *Oncol Nurs Forum* 1996; **23**:1203-11.
2. Fowler KA, Gill K, Kirma N, Dillehay DL, Tekmal RR. Overexpression of aromatase leads to development of testicular leydig cell tumors: an *in vivo* model for hormone-mediated Testicular Cancer. *Am J Pathol* 2000; **156**:347-53.
3. Li X, Strauss L, Kaatrasalo A, Mayerhofer A, Huhtaniemi I, Santti R, *et al*. Transgenic mice expressing p450 aromatase as a model for male infertility associated with chronic inflammation in the testis. *Endocrinology* 2006; **147**:1271-7.
4. Sirianni R, Chimento A, Malivindi R, Mazzitelli I, Andò S, Pezzi V. Insulin-like growth factor-I, regulating aromatase expression through steroidogenic factor 1, supports estrogen-dependent tumor Leydig cell proliferation. *Cancer Res* 2007; **67**:8368-77.
5. Carpino A, Rago V, Pezzi V, Carani C, Andò S. Detection of aromatase and estrogen receptors (ERalpha, ERbeta1, ERbeta2) in human Leydig cell tumor. *Eur J Endocrinol* 2007; **157**:239-44.
6. Brodie A, Inkster S, Yue W. Aromatase expression in the human male. *Mol Cell Endocrinol* 2001; **178**:23-8.
7. Bulun SE, Rosenthal IM, Brodie AM, Inkster SE, Zeller WP, DiGeorge AM, *et al*. Use of tissue-specific promoters in the regulation of aromatase cytochrome P450 gene expression in human testicular and ovarian sex cord tumors, as well as in normal fetal and adult gonads. *J Clin Endocrinol Metab* 1994; **78**:1616-21.
8. Straume AH, Løvås K, Miletic H, Gravdal K, Lønning PE, Knappskog S. Elevated levels of the steroidogenic factor 1 are associated with over-expression of CYP19 in an oestrogen-producing testicular Leydig cell tumour. *Eur J Endocrinol* 2012; **166**:941-9.
9. Catalano S, Malivindi R, Giordano C, Gu G, Panza S, Bonofiglio D, *et al*. Farnesoid X receptor, through the binding with steroidogenic factor 1-responsive element, inhibits aromatase expression in tumor Leydig cells. *J Biol Chem* 2010; **285**:5581-93.
10. Catalano S, Panza S, Malivindi R, Giordano C, Barone I, Bossi G, *et al*. Inhibition of Leydig tumor growth by farnesoid X receptor activation: the *in vitro* and *in vivo* basis for a novel therapeutic strategy. *Int J Cancer* 2013; **132**:2237-47.
11. Maris P, Campana A, Barone I, Giordano C, Morelli C, Malivindi R, *et al.* Androgens inhibit aromatase expression through DAX-1: insights into the molecular link between hormone balance and Leydig cancer development. *Endocrinology* 2015; **156**:1251-62.

12. Ortlip SA, Li SA, Li JJ. Characterization of specific glucocorticoid receptor in the Syrian hamster testis. *Endocrinology* 1981; **109**:1331-8.
13. Stalker A, Hermo L, Antakly T. Covalent affinity labeling, radioautography, and immunocytochemistry localize the glucocorticoid receptor in rat testicular Leydig cells. *Am J Anat* 1989; **186**:369-77.
14. Schultz R, Isola J, Parvinen M, Honkaniemi J, Wikström AC, Gustafsson JA, *et al*. Localization of the glucocorticoid receptor in testis and accessory sexual organs of male rat. *Mol Cell Endocrinol* 1993; **95**:115-20.
15. Bartke A. Effects of growth hormone on male reproductive functions. *J Androl* 2000; **21**:181-8.
16. Hardy MP, Gao HB, Dong Q, Ge R, Wang Q, Chai WR, *et al*. Stress hormone and male reproductive function. *Cell Tissue Res* 2005; **322**:147-153.
17. Gao HB, Shan LX, Monder C, Hardy MP. Suppression of endogenous corticosterone levels *in vivo* increases the steroidogenic capacity of purified rat Leydig cells *in vitro*. *Endocrinology* 1996; **137**: 1714-1718.
18. Schwarzenbach H, Manna PR, Stocco DM, Chakrabarti G, Mukhopadhyay AK. Stimulatory effect of progesterone on the expression of steroidogenic acute regulatory protein in MA-10 Leydig cells. *Biol Reprod* 2003; **68**:1054-1063.
19. Martin LJ, Tremblay JJ. Glucocorticoids antagonize cAMP-induced Star transcription in Leydig cells through the orphan nuclear receptor NUR77. *J Mol Endocrinol* 2008; **41**:165-175.
20. Hales DB, Payne AH. Glucocorticoid-mediated repression of P450scc mRNA and de novo synthesis in cultured Leydig cells. *Endocrinology* 1989; **124**:2099-2104.
21. Payne AH, Sha LL. Multiple mechanisms for regulation of 3 beta-hydroxysteroid dehydrogenase/delta 5-delta 4-isomerase, 17 alpha hydroxylase/C17-20 lyase cytochrome P450, and cholesterol side-chain cleavage cytochrome P450 messenger ribonucleic acid levels in primarycultures of mouse Leydig cells. *Endocrinology* 1991; **129**:1429–1435.
22. Badrinarayanan R, Rengarajan S, Nithya P, Balasubramanian K. Corticosterone impairs the mRNA expression and activity of 3beta- and 17beta-hydroxysteroid dehydrogenases in adult rat Leydig cells. Biochem Cell Biol 2006; **84**:745-754.
23. Xiao YC, Huang YD, Hardy DO, Li XK, Ge RS. Glucocorticoid suppresses steroidogenesis in rat progenitor Leydig cells. *J Androl* 2010; **31**:365-71.

24. Ing NH, Forrest DW, Riggs PK, Loux S, Love CC, Brinsko SP, *et al.* Dexamethasone acutely down-regulates genes involved in steroidogenesis in stallion testes. *J Steroid Biochem Mol* Biol 2014; **143**:451-9.
25. Gao HB, Tong MH, Hu YQ, Guo QS, Ge R, Hardy MP. Glucocorticoid induces apoptosis in rat leydig cells. *Endocrinology* 2002; **143**:130-8.
26. Ing NH, Forrest DW, Riggs PK, Loux S, Love CC, Brinsko SP, *et al*. Dexamethasone acutely down-regulates genes involved in steroidogenesis in stallion testes. *J Steroid Biochem Mol Biol* 2014; **143**:451-9.
27. Aquila S, Sisci D, Gentile M, Carpino A, Middea E, Catalano S, *et al.* Towards a physiological role for cytochrome P450 aromatase in ejaculated human sperm. *Hum Reprod* 2003; **18**:1650-9.
28. Inkster S, Yue W, Brodie A. Human testicular aromatase: immunocytochemical and biochemical studies. *J Clin Endocrinol Metab* 1995; **80**:1941-7.
29. Young M, Lephart ED, McPhaul MJ. Expression of aromatase cytochrome P450 in rat H540 Leydig tumor cells. *J Steroid Biochem Mol Biol* 1997; **63**:37-44.
30. Lanzino M, Catalano S, Genissel C, Ando S, Carreau S, Hamra K, *et al.* Aromatase messenger RNA is derived from the proximal promoter of the aromatase gene in Leydig, Sertoli, and germ cells of the rat testis. *Biol Reprod* 2001; **64**:1439-43.
31. Ronacher K, Hadley K, Avenant C, Stubsrud E, Simons SS Jr, Louw A, *et al.* Ligand-selective transactivation and transrepression via the glucocorticoid receptor: role of cofactor interaction. *Mol Cell Endocrinol* 2009; **299**:219-231.
32. Ahmed HU, Arya M, Muneer A, Mushtaq I, Sebire NJ. Testicular and paratesticular tumours in the prepubertal population. *Lancet Oncol* 2010; **11**:476-483.
33. McCluggage WG, Shanks JH, Arthur K, Banerjee SS. Cellular proliferation and nuclear ploidy assessments augment established prognostic factors in predicting malignancy in testicular Leydig cell tumours. *Histopathology* 1998; **33**:361-8.
34. Woolveridge I, Taylor MF, Rommerts FF, Morris ID. Apoptosis related gene products in differentiated and tumorigenic rat Leydig cells and following regression induced by the cytotoxin ethane dimethanesulphonate. *Int J Androl* 2001; **24**:56-64.
35. Azer PC, Braunstein GD. Malignant Leydig cell tumor: objective tumor response to o,p'-DDD. *Cancer* 1981; **47**:1251-5.
36. Vandevyver S, Dejager L, Libert C. Comprehensive overview of the structure and regulation of the glucocorticoid receptor. *Endocr Rev* 2014; **35**:671-93.

37. Alnemri ES, Fernandes TF, Haldar S, Croce CM, Litwack G. Involvement of BCL-2 in glucocorticoid-induced apoptosis of human pre-B-leukemias. *Cancer Res* 1992; **52**:491-5.
38. Thompson EB, Thulasi R, Saeed MF, Johnson BH. Glucocorticoid antagonist RU 486 reverses agonist-induced apoptosis and c-myc repression in human leukemic CEM-C7 cells. *Ann N Y Acad Sci* 1995; **761**:261-75.
39. Buse P, Woo PL, Alexander DB, Cha HH, Reza A, Sirota ND, *et al.* Transforming growth factor-alpha abrogates glucocorticoid-stimulated tight junction formation and growth suppression in rat mammary epithelial tumor cells. *J Biol Chem* 1995; **270**:6505-14.
40. Goya L, Maiyar AC, Ge Y, Firestone GL. Glucocorticoids induce a G1/G0 cell cycle arrest of Con8 rat mammary tumor cells that is synchronously reversed bysteroid withdrawal or addition of transforming growth factor-alpha. *Mol Endocrinol* 1993; **7**:1121-32.
41. Frost GH, Rhee K, Ma T, Thompson EA. Expression of c-Myc in glucocorticoid-treated fibroblastic cells. *J Steroid Biochem Mol Biol* 1994; **50**:109-19.
42. Sánchez I, Goya L, Vallerga AK, Firestone GL. Glucocorticoids reversibly arrest rat hepatoma cell growth by inducing an early G1 block in cell cycle progression. *Cell Growth Differ* 1993; **4**:215-25.
43. Coleman RE. Glucocorticoids in cancer therapy. *Biotherapy* 1992; **4**:37-44. Review.
44. Gaynon PS, Lustig RH. The use of glucocorticoids in acute lymphoblastic leukemia of childhood. Molecular, cellular, and clinical considerations. *J Pediatr Hematol Oncol* 1995; **17**:1-12. Review.
45. Pirotte B, Levivier M, Goldman S, Brucher JM, Brotchi J, Hildebrand J. Glucocorticoid-induced long-term remission in primary cerebral lymphoma: case report and review of the literature. *J Neurooncol* 1997; **32**:63-9.
46. Karmakar S, Jin Y, Nagaich AK. Interaction of glucocorticoid receptor (GR) with estrogen receptor (ER) α and activator protein 1 (AP1) in dexamethasone-mediated interference of ERα activity. *J Biol Chem* 2013; **288**:24020-34.
47. Yemelyanov A, Czwornog J, Chebotaev D, Karseladze A, Kulevitch E, Yang X, *et al.* Tumor suppressor activity of glucocorticoid receptor in the prostate. *Oncogene* 2007; **26**:1885-96.
48. Kumar R, Thompson EB. Gene regulation by the glucocorticoid receptor: structure:function relationship. *J Steroid Biochem Mol Biol* 2005; **94**:383-94.

49. Ghisletti S, Huang W, Jepsen K, Benner C, Hardiman G, Rosenfeld MG, *et al.* Cooperative NCoR/SMRT interactions establish a corepressor-based strategy for integration of inflammatory and anti-inflammatory signaling pathways. *Genes Dev* 2009; **23**:681-693.

50. Wang Q, Blackford JA Jr, Song LN, Huang Y, Cho S, Simons SS Jr. Equilibrium interactions of corepressors and coactivators with agonist and antagonist complexes of glucocorticoid receptors. *Mol Endocrinol* 2004; **18**:1376-1395.

51. Catalano S, Barone I, Giordano C, Rizza P, Qi H, Gu G, Malivindi R, *et al.* Rapid estradiol/ERalpha signaling enhances aromatase enzymatic activity in breast cancer cells. *Mol Endocrinol* 2009; **23**:1634-45.

52. Young M, McPhaul MJ. A steroidogenic factor-1-binding site and cyclic adenosine 3',5'-monophosphate response element-like elements are required for the activity of the rat aromatase promoter in rat Leydig tumor cell lines. *Endocrinology* 1998; **139**:5082-93.

53. Barone I, Cui Y, Herynk MH, Corona-Rodriguez A, Giordano C, Selever J, *et al.* Expression of the K303R estrogen receptor-alpha breast cancer mutation induces resistance to an aromatase inhibitor via addiction to the PI3K/Akt kinase pathway. *Cancer Res* 2009; **69**:4724-32.

54. Giordano C, Cui Y, Barone I, Ando S, Mancini MA, Berno V, *et al.* Growth factor-induced resistance to tamoxifen is associated with a mutation of estrogen receptor alpha and its phosphorylation at serine 305. *Breast Cancer Res Treat* 2010; **119**:71-85.

55. Catalano S, Leggio A, Barone I, De Marco R, Gelsomino L, Campana A, *et al.* A novel leptin antagonist peptide inhibits breast cancer growth in vitro and in vivo. *J Cell Mol Med.* 2015; **19**:1122-32.

56. Catalano S, Pezzi V, Chimento A, Giordano C, Carpino A, Young M, *et al.* Triiodothyronine decreases the activity of the proximal promoter (PII) of the aromatase gene in the mouse Sertoli cell line, TM4. *Mol Endocrinol* 2003; **17**:923-34.

Figure Legends

Figure 1 Effects of DEXA on aromatase expression and activity in R2C cells.

(**a**) Total RNA was extracted from R2C cells treated with vehicle (-), or 0.01, 0.1 and 1µM DEXA for 24 h and reverse transcribed. cDNA was subjected to PCR using primers specific for P450 aromatase or L19. NC, negative control, RNA sample without the addition of reverse transcriptase. (**b**) Total proteins extracted from R2C cells treated with vehicle (-), or 0.01, 0.1 and 1µM DEXA for 24 h were used for immunoblot analysis of aromatase. GAPDH was used as a loading control. The histograms represent the mean ± S.D. of three separate experiments in which band intensities were evaluated in terms of optical density arbitrary units and expressed as percentages of the control, which was assumed to be 100%. *, $p < 0.05$; ns non-significant. (**c**) R2C were cultured in the presence of vehicle (-) or 0.01, 0.1 and 1µM DEXA for 24 h. Aromatase activity was performed as described under "*Material and Methods*" The results obtained were expressed as picomole of $[^3H]H_2O$/h of release and were normalized for milligrams of protein (pmol/mg of proteins/h). The values represent the mean ± S.D. of three different experiments each performed with triplicate samples. *, $p < 0.05$;. ns non-significant. R2C cells were treated with DEXA 1µM with or without RU-486 5 µM, for 24 h and RT-PCR (**d**), immunoblot analysis (**e**) and aromatase activity (**f**) were performed.

Figure 2 DEXA decreases transcriptional activity of aromatase PII-proximal promoter.

(**a**) R2C cells were transiently transfected with a luciferase reporter plasmid containing the PII aromatase promoter (-1037/+94, p-1037) and treated for 24 h with vehicle (-) or 0.01, 0.1 and 1µM DEXA. (**b**) Schematic map of the P450arom proximal promoter PII constructs used in this study (*upper panel*). All of the promoter constructs contain the same 3' boundary (+94). The 5' boundaries of the promoter fragments varied from -688 to -183 (p-688, p-475, p-183). R2C cells were transfected with constructs p-688, p-475 and p-183 and treated with vehicle (-) or 0.01, 0.1

and 1μM DEXA, for 24 h (*lower panel*). The results represent the mean ± S.D. of three different experiments performed in triplicate. *, p< 0.05. ns non-significant. (**c**) R2C cells were treated in the presence of vehicle (-) or 0.1 and 1 μM DEXA for 1 h, then cross-linked with formaldehyde, and lysed. The precleared chromatin was immunoprecipitated with anti-GR, and anti-RNA Pol II antibodies. (**d**) Chromatin immunoprecipitated with the anti-GR antibody was re-immunoprecipitated with anti-NCoR and SMRT antibodies. The PII promoter sequence including the GRE site was detected by real time PCR with specific primers, as described under "*Material and Methods*". *, p < 0.05.

Figure 3 DEXA effects on R2C cell proliferation.

(**a**) R2C cells were treated with vehicle (-) or 0.01, 0.1 and 1 μM DEXA, or (**b**) treated with DEXA 1μM in the presence or absence of RU-486 5 μM, for 24 and 48 h, before testing cell viability using MTT assay. The results results are expressed as fold change ± SD relative to vehicle treated cells, and are representative of three different experiments each performed in triplicate. (**c**) R2C cells were seeded (10,000/well) in 0.5% agarose and treated as described above. Cells were allowed to grow for 14 days and then the number of colonies >50 μm were quantified and the results graphed. *, p <0.05; ns non-significant.

Figure 4 DEXA treatment inhibits Leydig tumor growth *in vivo*.

(**a**) R2C cells were injected in male nude mice. After 14 days, mice were assigned randomly in groups of five to receive 1 mg/kg/day DEXA, 10 mg/kg/day DEXA or vehicle (C) as control, and tumor growth was monitored over time. *, p < 0.05, DEXA-treated groups versus control group. (**b**) *Upper panel*: average tumor weight from untreated (C) and DEXA-treated mice (n=5 per each condition). *Lower panel*: images of a representative individual tumor from each treatment group. (**c**) hematoxylin and eosin stained histologic images of R2C xenograft tumors. Scale bars: 25 μm.

Figure 5 DEXA treatment decreases aromatase expression and reduces proliferation in R2C tumor xenografts.

(**a**) Protein extracts from xenografts excised from vehicle (C) and DEXA-treated mice were tested for aromatase expression by immunoblot analysis. β-Actin was used as a loading control. The histograms represent the mean ± S.D. of three separate experiments in which band intensities were evaluated in terms of optical density arbitrary units and expressed as percentages of the control, which was assumed to be 100%. *, $p < 0.05$. (**b**) Representative pictures of aromatase or, in (**c**) Ki-67 immunohistochemical staining of R2C xenograft tumors. Small squares, negative control. Scale bars: 12,5 μm.

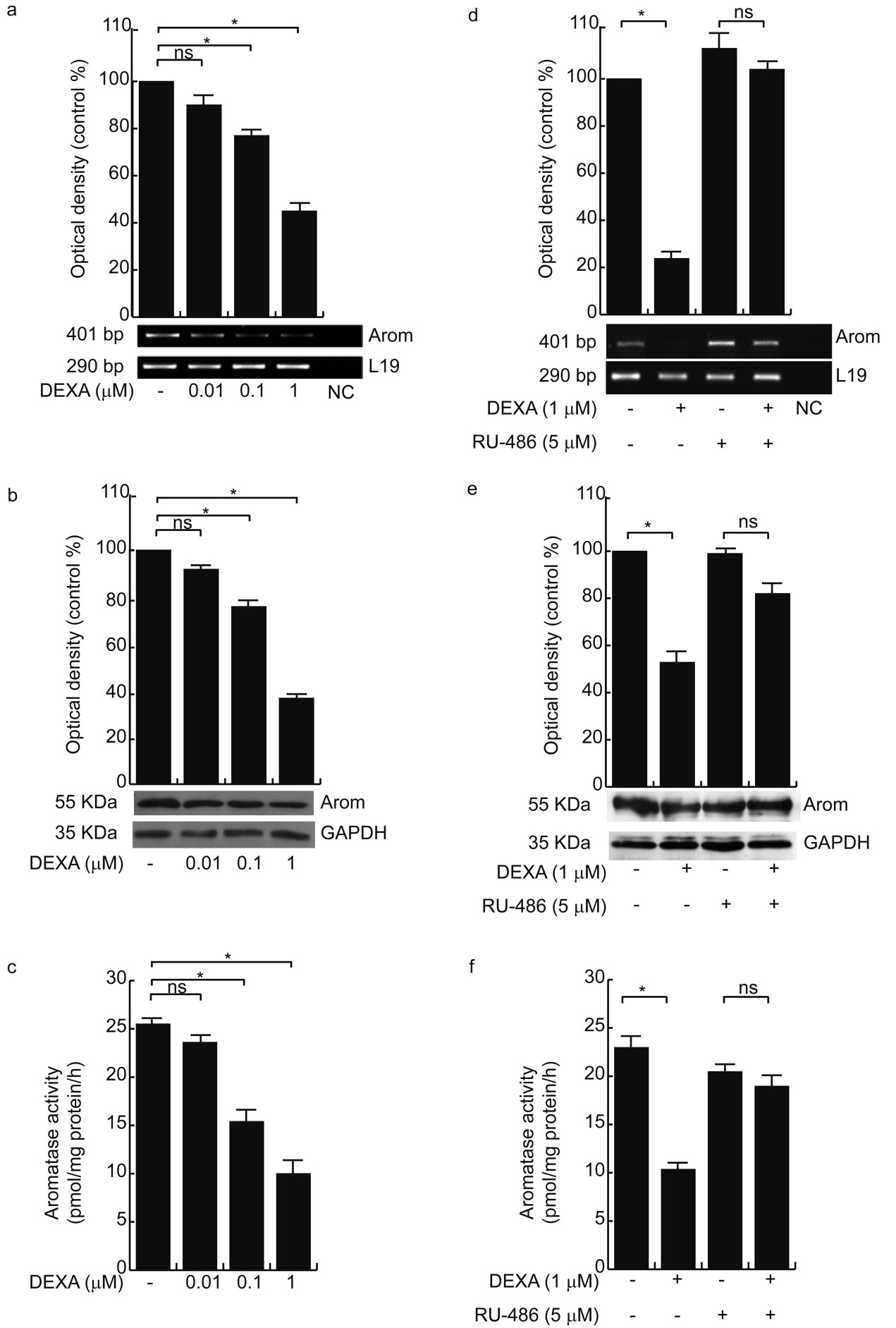
a
Optical density (control %)
110
100
80
60
40
20
0
*
ns
*
401 bp
290 bp
Arom
L19
DEXA (μM) - 0.01 0.1 1 NC
b
Optical density (control %)
55 KDa
35 KDa
Arom
GAPDH
DEXA (μM) - 0.01 0.1 1
c
Aromatase activity (pmol/mg protein/h)
30
25
20
15
10
5
0
DEXA (μM) - 0.01 0.1 1
d
Optical density (control %)
ns
DEXA (1 μM) - + - + NC
RU-486 (5 μM) - - + +
e
DEXA (1 μM) - + - +
RU-486 (5 μM) - - + +
f
DEXA (1 μM) - + - +
RU-486 (5 μM) - - + +

Figure 1

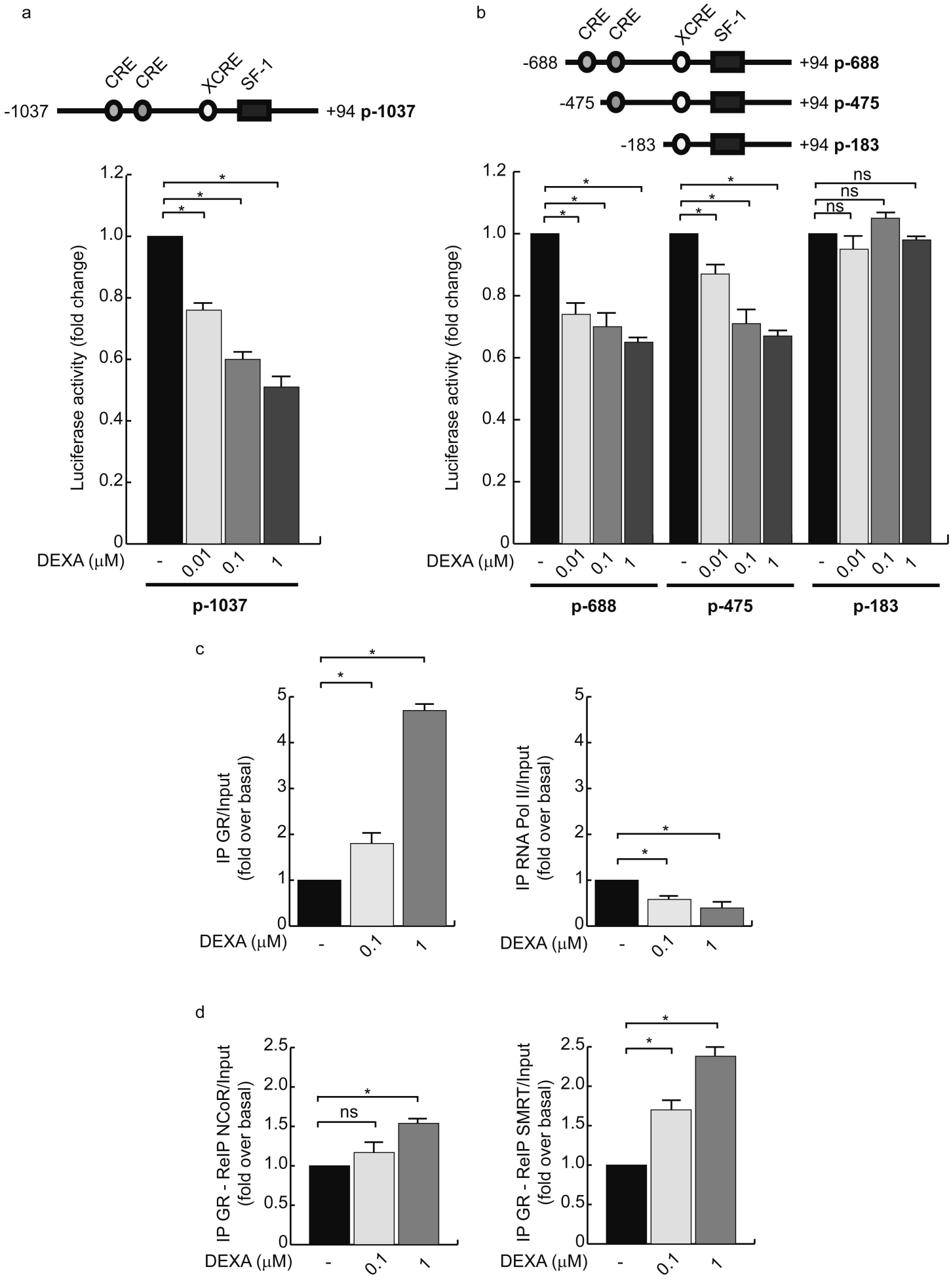
a
CRE
CRE
XCRE
SF-1
-1037
+94 p-1037
Luciferase activity (fold change)
DEXA (μM)
p-1037
b
-688
+94 p-688
-475
+94 p-475
-183
+94 p-183
p-688
p-475
p-183
ns
c
IP GR/Input (fold over basal)
IP RNA Pol II/Input (fold over basal)
d
IP GR - ReIP NCoR/Input (fold over basal)
IP GR - ReIP SMRT/Input (fold over basal)

Figure 2

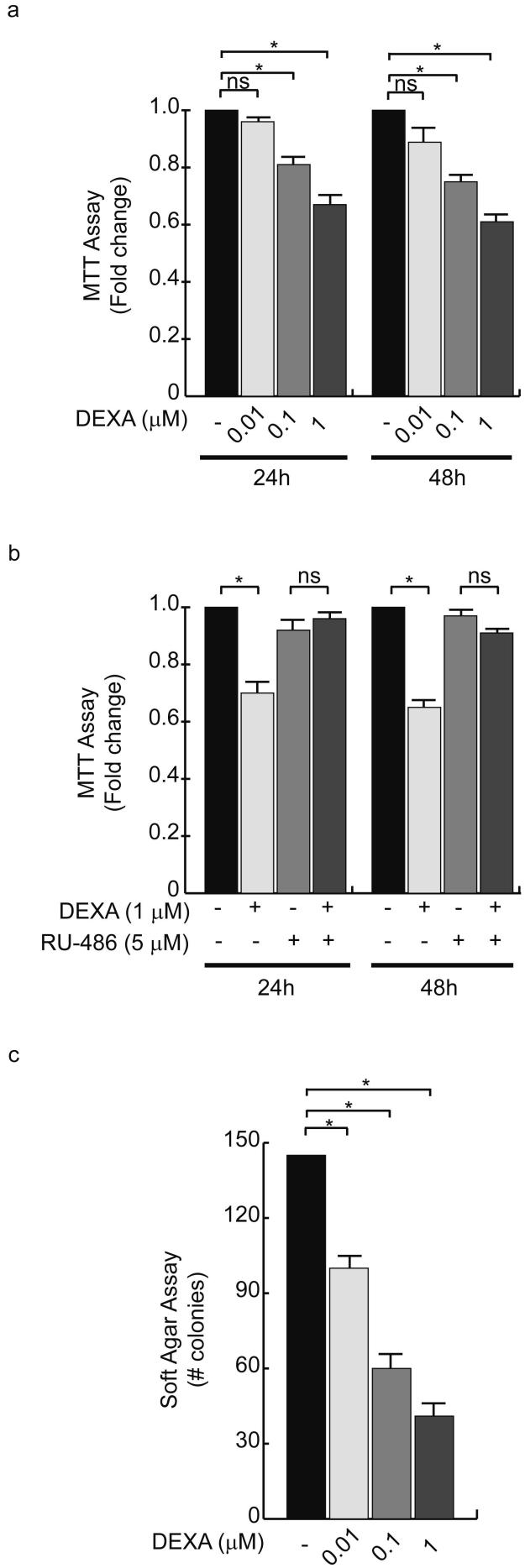
a
MTT Assay
(Fold change)
1.0
0.8
0.6
0.4
0.2
0
*
*
ns
*
*
ns
DEXA (μM)
-
0.01
0.1
1
-
0.01
0.1
1
24h
48h
b
MTT Assay
(Fold change)
1.0
0.8
0.6
0.4
0.2
0
*
ns
*
ns
DEXA (1 μM)
RU-486 (5 μM)
24h
48h
c
Soft Agar Assay
(# colonies)
150
120
90
60
30
0
*
*
*
DEXA (μM)
-
0.01
0.1
1

Figure 3

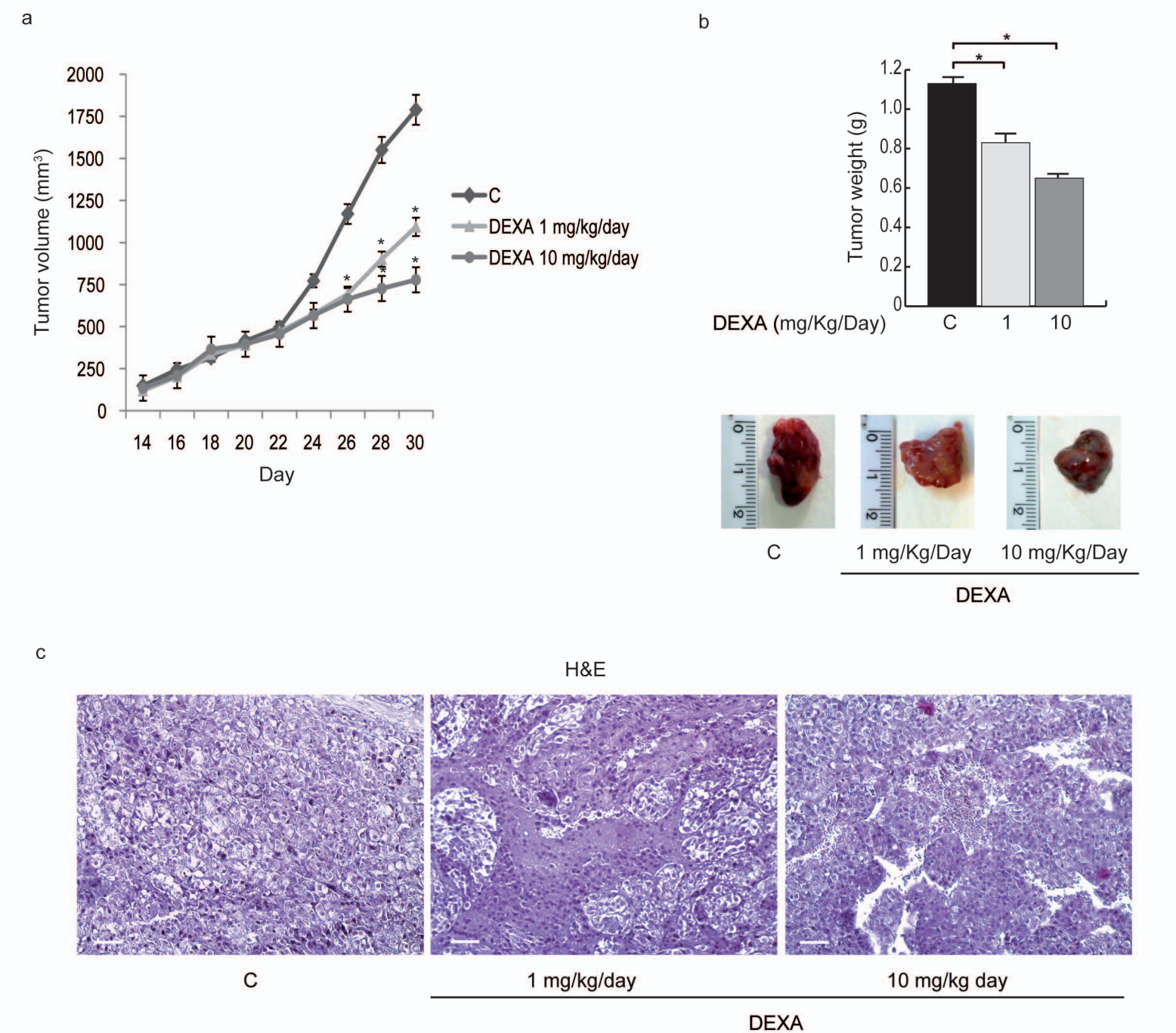
a
Tumor volume (mm3)
2000
1750
1500
1250
1000
750
500
250
0
14 16 18 20 22 24 26 28 30
Day
C
DEXA 1 mg/kg/day
DEXA 10 mg/kg/day
b
Tumor weight (g)
1.2
1.0
0.8
0.6
0.4
0.2
0
DEXA (mg/Kg/Day)
C 1 10
C
1 mg/Kg/Day
10 mg/Kg/Day
DEXA
c
H&E
C
1 mg/kg/day
10 mg/kg day
DEXA

Figure 4

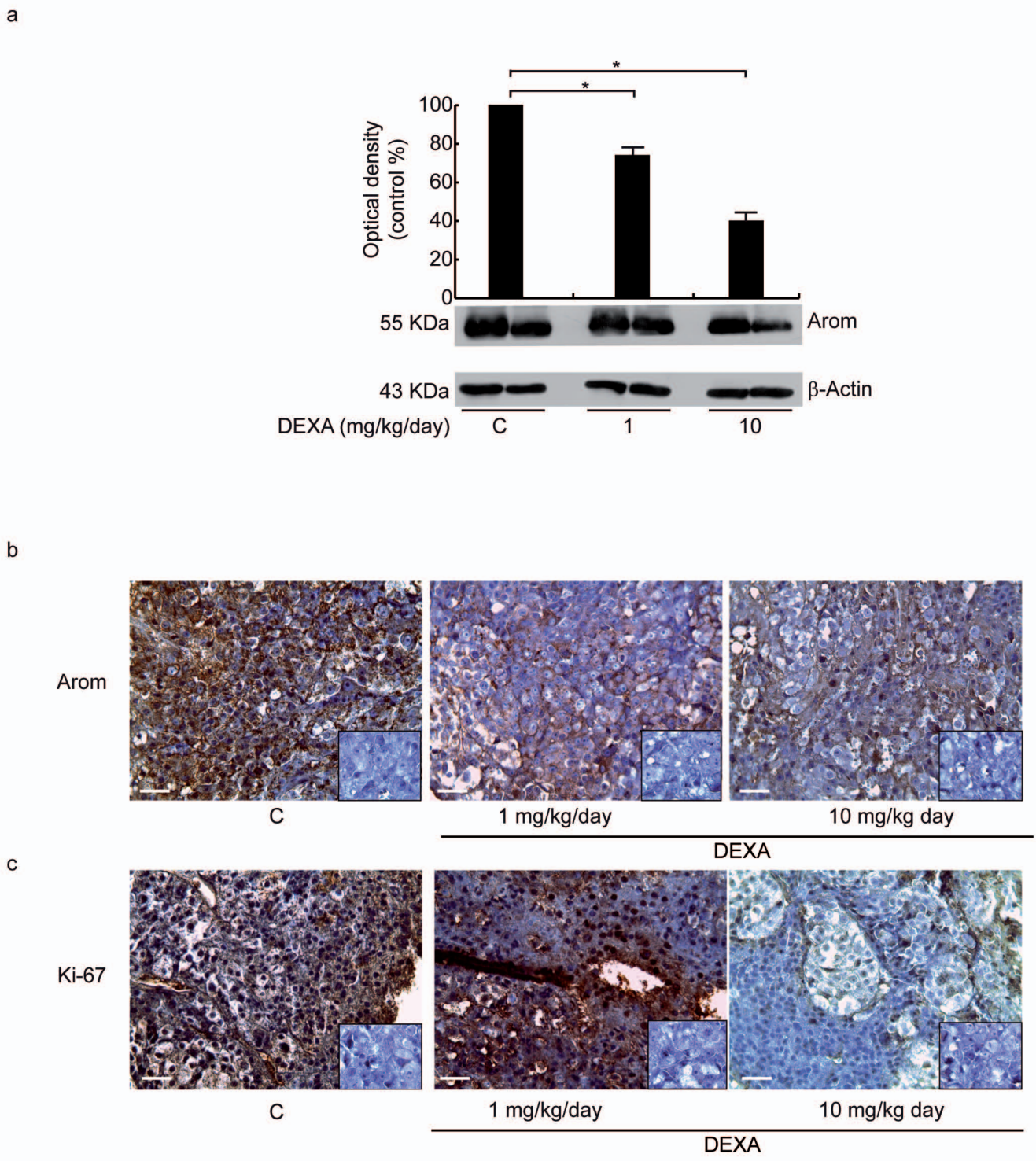
a
*
*
100
80
60
40
20
0
Optical density
(control %)
55 KDa
Arom
43 KDa
β-Actin
DEXA (mg/kg/day)
C
1
10
b
Arom
C
1 mg/kg/day
10 mg/kg day
DEXA
c
Ki-67
C
1 mg/kg/day
10 mg/kg day
DEXA

Figure 5

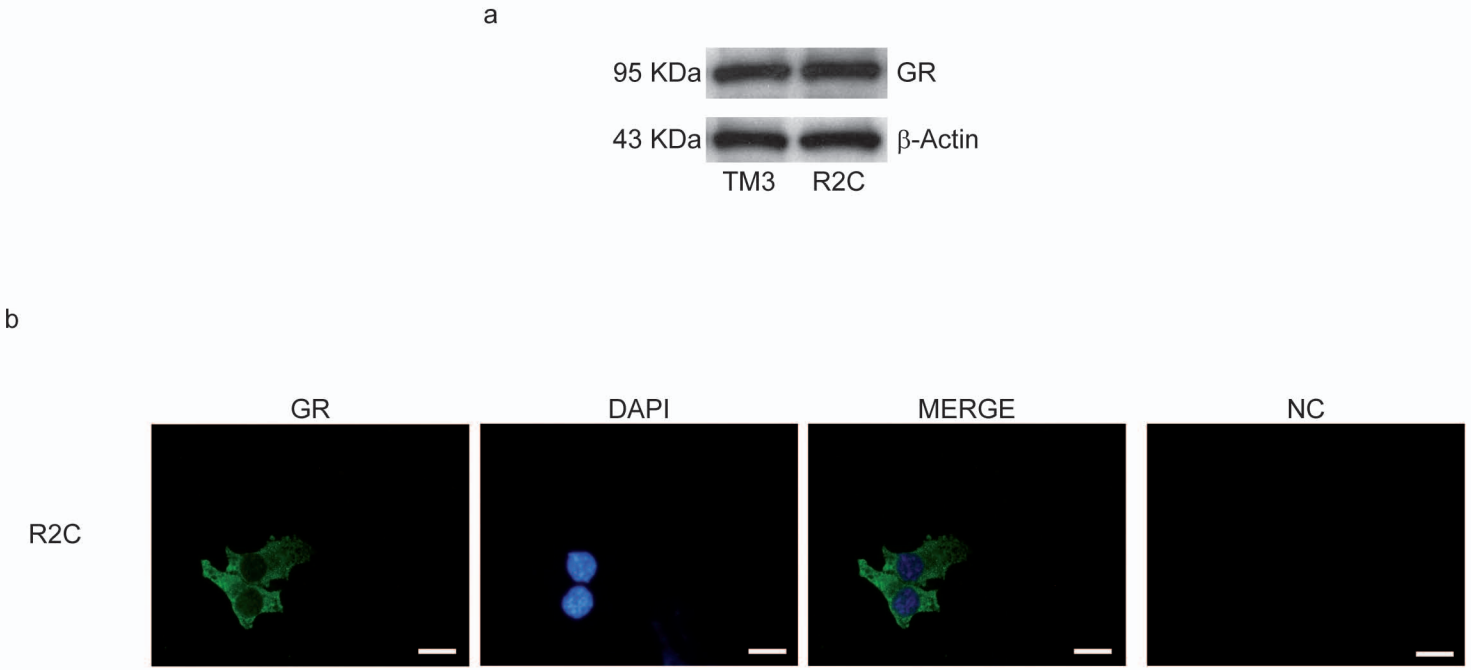

Supplementary Figure 1 GR expression in TM3 and R2C cells. (**a**) Immunoblot analysis of GR was done on 50 μg of total proteins extracted from normal (TM3) and tumor Leydig cells (R2C). β-Actin was used as a loading control. (**b**) GR expression was determined by immunofluorescence analysis in R2C cells. 4',6-Diamidino-2-phenylindole (DAPI) staining was used to visualize the cell nucleus. NC negative control. Scale bars: 12,5 μm

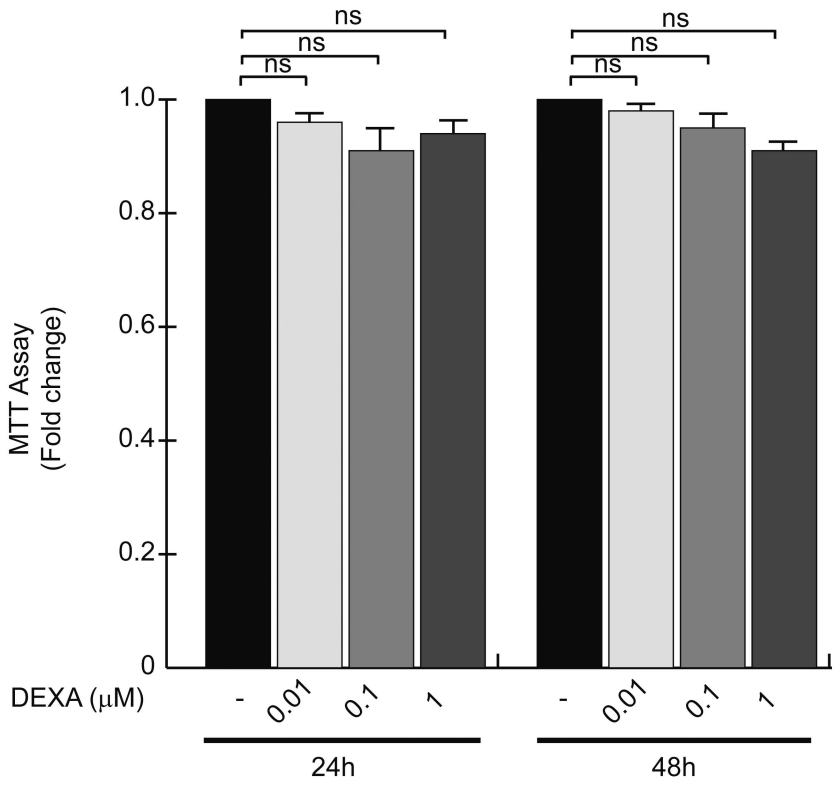

Supplementary Figure 2 DEXA effects on TM3 cell proliferation. TM3 cells were treated with vehicle (-) or 0.01, 0.1 and 1 μM DEXA for 24 and 48 h, before testing cell viability using MTT assay. The results represent the mean ± S.D. of three different experiments each performed with triplicate samples. ns non-significant.

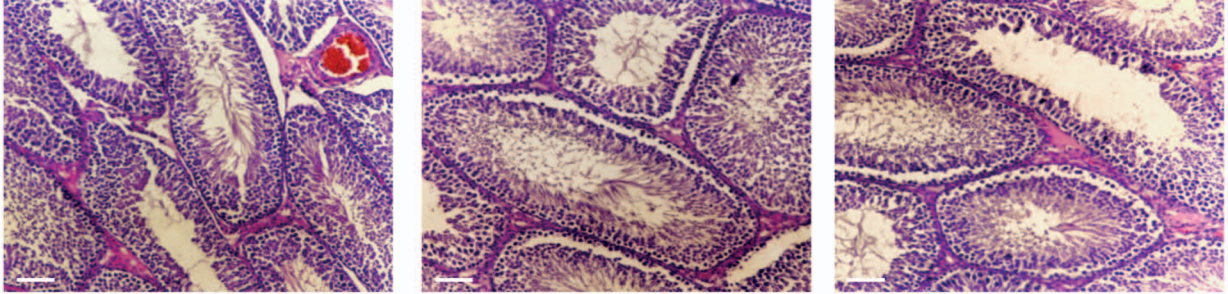

Supplementary Figure 3 Testicular morphology in DEXA-treated mice. Representative H&E performed on paraffin-embedded testis sections. The photomicrograph of the sections of the testes of control and DEXA-treated mice. In seminiferous tubules with normal aspect, germ cells are organized in concentric layers and tubular lumen is empty. Scale bars: 50 μm.